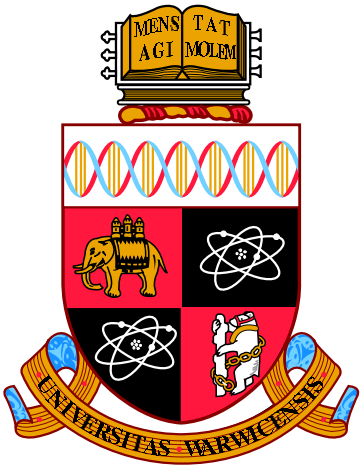

Proteomic Analysis of Drought & Oxidative Stress in *Arabidopsis thaliana* & *Zea mays*

by

Georgina Charlton

Thesis

Submitted to the University of Warwick

for the degree of

Doctor of Philosophy

Depatment of Chemistry

March 2020

Contents

List of Tables

List of Figures

Acknowledgments

This is gonna be a long one, bear with me.

To my supervisor Alex Jones, for all her support over the years, the learning curve was steep at first, but we got there in the end, and I believe I have grown as a scientist and a person under her guidance.

To my second supervisor Peter Kilby and John Sinclair thank you for all your support and guidance over the last 3 years. Thank you to Syngenta and the EPSRC for providing funding for the project for three years.

Andrew Bottrill, Juan Hernandez Fernaud and Cleidi Zampronio, thank you for all the wonderful work you have done and do running the proteomics facility. Thanks for helping me to run my samples and teaching me how to analyse my data.

Thanks to Jenny Goodman, for teaching so many new techniques when I first started in the lab. None of this would have been possible without her.

Thanks to Susan Breen, Fraz Hussain, Trupti Gaikwad and Natassa Kanali, for help with growing Arabidopsis plants for my experiments, and letting me use space in their growth room. I'd be missing a chapter without these guys. Thanks to Ryan Morrison, Rob Maple and Yang-Seok Lee, for providing me with maize seeds when I first started my PhD, for teaching me how to care for maize, and how to pollinate them and for looking after then when I was away on holiday. Thanks to Gary Grant

in PBF for looking after my plants and watering them in PBF, especially when I was on holiday. Thank you to Mingkee Achom for teaching me to use MapMan and other pathway mapping tools from the other side of the world. She was a life saver.

Thanks to all my friends in C30 and C46 past and present for all their support, through the good times and the bad.

Thanks to the MAS CDT for giving me this opportunity, funding me for over three years, and taking a chance on me, particularly Nikola Chmel who is the main reason I was given the PhD opportunity. Steven Brown, who supports all MAS students. Naomi Grew, who was always the first port of call with any issues and always put our welfare first.

Thanks to everyone in the 2015 MAS CDT cohort, especially Emily Corlett, who started this research as part of her masters, and who came to the gym with me every week and heard me complain about everything that was going wrong, and Nicole Kelly who always heard how I was from Emily and would never fail to have a chat with me when things were rough. Not forgetting Charlotte Fletcher, who I'm sure I've driven insane in the time we've known each other, she has given me the most support of any of my friends, giving me honest and helpful advice.

Thanks to my fiancé Charlie, for supporting me through the last 4 years, and putting my dream first, it's not always been easy. Also thanks to him for spending long days helping me to code.

To my Mum, thanks for all her support during my time at university, both morally and financially, especially during my masters year.

Finally, to my Dad. Although he can't be here to see this, I hope he would have been proud.

Declarations

This thesis is submitted to the University of Warwick in support of my application for the degree of Doctor of Philosophy. It has been composed by myself and has not been submitted in any previous application for any degree. The work presented (including data generated and data analysis) was carried out by the author.

Abstract

Stress in plants can be caused by a variety of factors and create changes to proteins in the form of post translational modifications (PTMs). Reactive oxygen species (ROS) mediate cell signalling pathways but under stress conditions, their quantities become too high and they cause oxidative damage to DNA, lipids and proteins. Oxidative damage causes irreversible damage to proteins, leading to loss or change in function. Carbonylation modifications are used as key biomarkers of oxidative stress in animals and plants due to their relative chemical stability. However, due to their low abundance, carbonyl modifications have been difficult to analyse. Therefore, a suitable tagging and enrichment process is needed to fully analyse carbonyl modifications. In this thesis, the effect of drought stress on protein abundance in maize B73 was analysed. Using the tandem mass tag (TMT) for quantitative analysis 271 proteins were identified in the leaves and 405 proteins in the silks which changed significantly during drought stress. Phosphorylation as downstream signalling of drought stress was also analysed. 61 phosphopeptides were identified in the leaves and 130 phosphopeptides in the silks which significantly changed in the drought treated samples. These were novel phosphorylation sites. The effect of methyl viologen (MV), a herbicide which kills plants by causing oxidative damage, on protein abundance in *Arabidopsis thaliana* and maize B73 was also analysed. Using TMT for quantitative analysis 397 proteins were identified in the Arabidopsis soluble fraction and 578 proteins in the Arabidopsis membrane fraction with significantly changed abundance during MV treatment. MV's effect on phosphorylation as downstream signalling was also analysed 84 phosphopeptides were identified in the Arabidopsis soluble fraction (five of which were novel phosphopeptides) and

42 phosphopeptides in the Arabidopsis membrane fraction (fourteen of which were novel phosphopeptides) which significantly changed in the methyl viologen treated samples. The effect of MV on maize was analysed, whilst there was no change in proteins identified using TMT quantification, 19 phosphopeptides were identified which significantly changed in the MV treatment, all of which were novel phosphopeptides. An attempt to enrich for carbonyl modifications in BSA was also made, for the purpose of enriching for carbonyl modifications in complex mixtures, however due to time constraints, this was not achievable.

Abbreviations

1D —One-Dimensional

2D —Two-Dimensional

AA —Amino Acid

ABA —Abscisic Acid

ABC —Ammonium Bicarbonate

AcN —Acetonitrile

ADH —Alcohol Dehydrogenases

ADP —Adenosine Diphosphate

ALDH —Aldehyde Dehydrogenase

APX —Cytosolic Ascorbate Peroxidase

ARP —Aldehyde Reactive Probe

ATP —Adenosine Triphosphate

BLAST —Basic Local Alignment Search Tool

BSA —Bovine Serum Albumin

C —Celsius

Ca^{2+} —Calcium Ion

CAA —Chloroacetamide

CAT —Peroxisomal Catalase

CDK —Cyclin Dependent Kinase

CDPK —Calcium Dependent Protein Kinase

CID —Collision-Induced Dissociation

cm —Centimetre

CO_2 —Carbon Dioxide

Col-0 —Columbia-0

Da —Dalton

DHB —2.5-Dihydroxybenzoic Acid

DIGE —Difference in Gel Electrophoresis

DMSO —Dimethylsulfoxide

DNA —Deoxyribonucleic Acid

DNPH —2,4-Dinitrophenylhydrazine

DPS —Dependent Peptide Search

DTT —Dithiothreitol

ECL —Electrochemiluminescence

EDTA —Ethylenediaminetetraacetic Acid

EGTA —Ethylene Glycol-Bis(β-Aminoethyl Ether)-N,N,N;N´Tetraacetic Acid

ELISA —Enzyme-Linked Immunosorbent Assay

ER —Endoplasmic Reticulum

ESI-MS —Electrospray Ionisation-Mass Spectrometry

ETD —Electron Transfer Dissociation

ETS —Error Tolerant Search

FA —Formic Acid

FASP —Filter Aided Sample Preparation

FDR —False Discovery Rate

FT-ICR —Fourier-Transform Ion Cyclotron Resonance

g —Gram

g —G-Force

GO —Gene Ontology

GPx —Glutathione Peroxidase

HCD —Higher-energy Collision Dissociation

HCl —Hydrochloric Acid

HEPES —4-(2-hydroxyethyl)-1-piperazineethanesulfonic acid

HNE —4-Hydroxynonenal

HPLC —High Performance Liquid Chromatography

HRP —Horse Radish Peroxidase

HSP —Heat Shock Protein

H_2O_2 —Hydrogen Peroxide

IAA —Iodoacetamide

ICAT —Isotope Coded Affinity Tags

iTRAQ —Isobaric Tag for Absolute and Relative Quantification

K^+ —Potassium Ion

KCl —Potassium Chloride

kDa —Kilodalton

KEGG —Kyoto Encyclopedia of Genes and Genomes

KH_2PO_4 —Monopotassium Phosphate

LC —Liquid Chromatography

LEA —Late Embryogenesis Abundant

LFQ —Label Free Quantification

M —Molar

m/z —Mass to Charge Ratio

MALDI —Matrix Assisted Laser Desorption/Ionization

MAPK —Mitogen-Activated Protein Kinase

MAPKKK —Mitogen-Activated Protein Kinase Kinase Kinase

MCO —Metal Catalysed Oxidation

MES —2-(N-morpholino) Ethanesulfonic Acid

mg —Milligram

MGF —Mascot Generic Format

mL —Milliliter

mM —Millimolar

MMFPh —Maximal Motif Finder for Phosphoproteomics Datasets

MQ —Max Quant

mRNA —Messenger Ribonucleic Acid

MS —Mass Spectrometry

MS1 —Parent Ion Scan

MS2 —Fragment Ion Scan

MS^2PIP —MS2 Peak Intensity Prediction

MS3 —Fragment Ion Scan of MS2 Fragment

MS/MS —Tandem Mass Spectrometry

MV —Methyl Viologen

Na_2HPO_4 —Disodium Phosphate

NaCl —Sodium Chloride

NADP —Nicotinamide Adenine Dinucleotide Phosphate

NADPH —Nicotinamide Adenine Dinucleotide Phosphate Reduced

NaF —Sodium Flouride

nM —Nanomolar

nm —Nanometer

NP40 —Nonidet-P40

NPQ —Non-Photochemical Quenching

$\cdot O_2^-$ —Superoxide Anion

$\cdot OH$ —Hydroxyl Radical

PBS —Phosphate-buffered Saline

PBST —Phosphate-buffered Saline Tween

PCA —Principle Component Analysis

PEG —Polyethylene Glycol

PIC —Protein Inhibitor Cocktail

PKC —Protein Kinase C

PMSF —Phenylmethylsulfonyl Fluoride

PP2C —Protein Phosphatase 2C

ppb —Parts Per Billion

ppm —Parts Per Million

PRIDE —Proteomics Identifications Database

PSI —Photosystem I

PSII —Photosystem II

PTMs —Post Translational Modifications

PVP —Polyvinylpyrrolidone

PYL —Pyrabactin Resistance-Like

PYR —Pyrabactin Resistance

RCAR —Regulatory Component of Abscisic Acid Receptor

RLK —Receptor Like Kinase

RNA —Ribonucleic Acid

ROS —Reactive Oxygen Species

rpm —Revolutions Per Minute

SAX —Strong Anion Exchange

SDS —Sodium Dodecyl Sulfate

SDS-PAGE —Sodium Dodecyl Sulfate Polyacrylamide Gel Electrophoresis

SnRK —Sucrose Non-Fermenting Related Protein Kinase

SLK —STE20 Like Kinase

SOD —Superoxide Dismutase

TBS —Tris-buffered Saline

TBST —Tris-buffered Saline Tween

TCA —Trichloroacetic acid

TECP —Tris(2-carboxyethyl)phosphine

TFA —Trifluoroacetic acid

Th —Thomson

TiO_2 —Titanium Dioxide

TMT —Tandem Mass Tag

TOF —Time of Flight

UPAX —Strong Anion Exchange Chromatography

UV —Ultraviolet

μL —Microliter

μM —Micromolar

V —Volts

Chapter 1

Introduction

1.1 Stress in Plants

1.1.1 *Arabidopsis thaliana* & *Zea mays*

Arabidopsis thaliana is a small dicotyledonous plant which is often used as a model plant in biology due to its small size, fast reproduction rate, high seed production and high transgenic efficiency. Arabidopsis is a member of the brassica or mustard family, which also includes broccoli and turnips. Arabidopsis was the first plant to be genome sequenced in 2000 and initial estimates of encoded genes was 25,498 (Kaul *et al.*, 2000). The updated genome contains 27,466 genes and encodes for 39,361 proteins. Whilst it is used intensively for research as a model plant, it has no economical importance and is genetically far removed from crop plants present in agriculture, meaning studies in Arabidopsis aren't easily translatable to crop plants.

Maize (*Zea mays*) is a cereal grain often used in agriculture and is used to produce food for animals and humans and as biofuels. Between 2008 and 2010 global maize production was 750 million metric tons, making maize the world's third largest crop for food production, after wheat and rice (Shiferaw *et al.*, 2011). Maize along with wheat and rice provide around 30% of the calories for more than 4.5 billion people in developing countries around the world (Shiferaw *et al.*, 2011). By 2050 it is predicted that the world's population will increase to 9.3 billion, meaning demand for maize production will rise (Rosegrant *et al.*, 2009). The inbred maize B73 was the first maize line to be genome sequences in 2009 and contains 39,400 genes (Schnable *et al.*, 2009). The maize B73 proteome UP000007305 contains 99,254 proteins.

1.1.2 What is Plant Stress?

In recent years the average temperature of the earth has increased, leading to more extreme weather, and this increase is expected to continue. The earth's temperature is expected to rise in the next 50-100 years by 3-5^{o}C (Schnable *et al.*, 2009). This will reduce food availability across the world, possibly leading to human starvation. The factors affected by climate change cause plants to become stressed which leads to loss of yield.

Plant stress occurs when a plant is growing in non-ideal conditions, which put an increased demand on its ability to function. There are many different types of stress such as salt, temperature, drought, pests, herbicides and so on. These stresses will affect metabolism, root development, reproduction or growth.

Abiotic stresses come from the environment the plant is growing in and cause major crop loss worldwide (Gull *et al.*, 2019). The environment can cause osmotic stress, malfunction of ion distribution and plant cell homeostasis (Gull *et al.*, 2019). If stress is mild (or short in duration) then plants can recover, with minimal effects to its growth or reproduction cycle, however severe stress (or long duration) leads to plant death, and will prevent reproduction from taking place (Verma *et al.*, 2013). The most common abiotic cause of stress is water, as plants need a certain amount of water for optimal growth, too much can cause plant cells to swell, and rotting of the roots, whereas too little can cause loss of moisture from tissues leading to drought stress and cell death.

In general, different stress factors affect several cell signalling pathways in plants, and cause changes in: reactive oxygen species (ROS), protein kinases, protein phosphorylation, the plant hormone abscisic acid (ABA) and the secondary messenger calcium ions (Ca^{2+}) (Nievola *et al.*, 2017). How plants sense stress and respond is an important biological question and improving stress tolerance is vital for agricultural productivity. Plants have putative sensors which recognise changes in the environment and allow the plant to respond to various stresses. OSCA1 (reduced hyperosmolality-induced calcium increase 1) is a sensor for hypoosmotic stress, which is a signal of salt and drought stress (Yuan *et al.*, 2014) and COLD1 mediates cold response signalling (Ma *et al.*, 2015). Stress responses largely depend on the sucrose non-fermenting related protein kinase (SnRK) family of protein kinases (Hardie *et al.*, 2016). SnRK2s are important in osmotic stress and ABA signalling, however SnRK3s are regulators of ion homeostasis required to cope with

salt and nutrient stress in soil (Zhu, 2016). Many stress signalling pathways also involve the calcium-dependent protein kinase (CDPK), which are closely related to SnRKs. Nearly all stress pathways involve mitogen-activated protein kinases (MAPKs), which is a shared feature of stress signalling in organisms from plants to animals (Zhu, 2016). The widespread use of calcium, ROS, nitric oxide, and lipid molecules as second messengers, are also common to stress responses in plants and animals (Zhu, 2016).

Salt stress decreases crop yield and crop productivity in areas which are affected (Maas and Grattan, 1999). Salt stress causes osmotic stress and ion toxicity which reduces plant growth. The increased amount of salt in the soil means the osmotic pressure in the soil is higher than the osmotic pressure in the plant cells. This limits the plant's ability to take up water and minerals such as K^+ and Ca^{2+}, which leads to assimilate production, reduced cell expansion and decreased cytosolic metabolism (Isayenkov and Maathuis, 2019). High salt levels cause ion toxicity, hyperosmotic stress and secondary stresses such as oxidative stress.

Drought stress is caused by a decrease in the water available in the soil and causes loss of yield and, in severe cases, plant death. Plants respond to drought by decreasing shoot growth to reduce metabolic demand and by synthesising protective compounds, such as abscisic acid (ABA) (Gargallo-Garriga *et al.*, 2014). Plants response to drought stress and salt stress are closely related with many of the mechanisms overlapping. During salt and drought stress response ABA accumulates and SnRK2 family proteins are activated and auto phosphorylate (Zhu, 2002). SnRK2 signals for stomata to close, reducing gas exchange and increasing stress tolerance.

Cold stress decreases crop productivity by affecting the quality of the crops (Barlow *et al.*, 2015). Due to plants' inability to move from their environment they must adapt. Cold and freezing temperature conditions will cause stress to plants, freezing temperatures cause ice crystals to form in cell walls. As the ice crystals grow, they puncture the cell wall causing changes to cell structure. Plants need to acclimatise to the changes in temperature, however, many crop plants' mechanism of adaptation is insufficient to deal with cold acclimatisation (Gull *et al.*, 2019). Cold stress generally affects plants transcriptomics and metabolism, rising from inhibition of enzymes due to low temperatures and changes in gene expression (Chinnusamy *et al.*, 2007). Cold stress causes calcium influx and activation of calcium response proteins and the MAPK cascade which regulates cold response gene expression (Zhu,

2016).

Increases in global temperatures have led to an increase in heat stress, which affects plant growth and productivity in agriculture. Heat stress reduces the percentage of seeds which germinate and the efficiency of photosynthesis (Sonjaroon *et al.*, 2018). Heat stress is particularly harmful during plants reproductive stage (Wang *et al.*, 2016-2). Heat stress induces expression of heat shock proteins (HSP), which prevent protein denaturing and maintain protein homeostats. During heat stress, transcription factors are released and activate heat stress response (Wang *et al.*, 2016-2). Heat stress activates MAPKs which is thought to be linked to heat-induced changes in membrane fluidity and calcium signalling which are important for HSP gene expression and heat tolerance (Sangwan *et al.*, 2002).

Biotic stresses come from attack by various pathogens, fungi, bacteria and herbivores which cause disease, infection and damage to plants. Biotic stresses deprive plants of essential nutrients which can lead to the plant's death. Disease causes the majority of crop loss worldwide (Verma *et al.*, 2013). Soil is full of fungi and bacteria and, whilst some are beneficial to plants, others are damaging. After the plant is infected, reactive oxygen species (ROS) are generated to limit pathogen spread (Atkinson and Urwin, 2012). A ROS burst causes the activation of mitogen-activated protein kinases (MAPKs), which control ethylene production (Thao *et al.*, 2015). Ethylene signalling during biotic stress has a negative effect on plant growth and development (Maksymiec, 2011). Plants do not have the adaptive immune system which vertebrates have, meaning they cannot adapt to new diseases or become resistant to past infections (Andolfo and Ercolano, 2015). Plants respond to pathogens, bacteria and fungi via an immune response. After the plant is infected ROS are generated and oxidative bursts limit pathogen spread (Atkinson and Urwin, 2012), cell lignification is also increased, blocking parasite invasion and reducing susceptibility of the host.

1.2 Post Translational Modifications of Proteins

1.2.1 Types of Post Translational Modification

Post translational modifications (PTMs) are biochemical modifications which occur on amino acids (AA) after the protein has been synthesised (Carter and Shieh, 2015). PTMs change the function of proteins by adding a functional group, proteolytic cleavage of regulatory subunits, or degradation of proteins (Duan and Walther,

2015). PTMs include phosphorylation, carbonylation, ubiquitination, nitrosylation, methylation, glycosylation and acetylation to name but a few (Duan and Walther, 2015). PTMs play an important role in cell function. Phosphorylation modifications are involved in intercellular signalling, ubiquitination is involved in regulation of protein stability, methylation is necessary for transcription regulation and glycosylation is important for cell surface signalling, to name a few.

PTMs can occur at any time in the protein's life cycle. Many proteins are modified soon after being translated, for example glycosylation occurs in the endoplasmic reticulum (ER) in order to mediate protein folding, stability and protein localisation (Darling and Uversky, 2018). Other modifications happen after folding and localisation, these are to activate or inhibit enzyme activity, or biological activity of the protein (Barber and Rinehart, 2018). PTMs can also be used to signal a protein for degradation, most commonly ubiquitination (Wang *et al.*, 2013-1).

Depending on the nature of the modification, PTMs can be reversible (Carter and Shieh, 2015). Phosphorylation of kinases is reversible through the action of phosphatases. Phosphorylation regulates kinase activity, where proteins are phosphorylated at specific AA residues and is important for enzyme activity and inhibition (Ardito *et al.*, 2017). Phosphatases can hydrolyse the phosphorylation modification, thus reversing the modification and the biological activity (Hunter, 2012). Phosphorylation causes a conformational change to many enzymes and receptors, leading to a change to the structure, causing them to become activated or deactivated. For example, phosphorylation of glycogen phosphorylase b converts it to the active glycogen phosphorylase a, this is known as glycogen phosphorylase. Phosphorylation of the enzyme GSK-3 regulates the insulin signalling pathway. Phosphorylation of serine, threonine and tyrosine were initially thought to be the main mode of phosphorylation mediated signalling. However, more recently it has become clear that histidine phosphorylation also plays an important role in cell signalling (Besant and Attwood, 2012; Fan *et al.*, 2012).

Carbonylation is an irreversible modification caused by ROS (Stadtman and Levine, 2003). ROS are a byproduct of aerobic metabolism, and play an important role in signalling and development, but are also very reactive towards proteins, and cause oxidative damage. Carbonylation is the most stable form of oxidative damage, and therefore is used as a biomarker for oxidative damage (Fedorova *et al.*, 2014).

1.2.2 Affinity Enrichment Techniques for Modified Peptides

Protein phosphorylation is one of the most important post translational modifications (PTM), which causes loss, gain or change in function of proteins (Mann and Jensen, 2003). Serine, threonine and tyrosine amino acid residues are the most common sites for phosphorylation. Other sites such as histidine can also be phosphorylated but these are harder to isolate due to their instability under acidic solutions commonly used in LC-MS/MS (Hardman *et al.*, 2017). Protein phosphorylation is reversible and plays an important role in cell signalling (Cohen, 2002). Sequential phosphorylation of proteins plays an important part in the signalling cascade such as the canonical MAPK signalling module. However, due to the modification's low levels in the proteome, phosphorylation modifications have proved difficult to analyse directly and some form of enrichment is needed.

The most common method for phosphopeptide enrichment involves metal ion chelation, which uses the metal ions' positive charge to interact with the negatively charged phosphate group, allowing phosphate groups to be enriched from complex mixtures (Figure 1.1A). Initially Fe^{3+} or Ga^{3+} ions were used for phosphopeptide enrichment. However, it was observed that these ions weren't specific enough for phosphopeptide enrichment due to the chelating ligands also binding to carboxylic and amino groups on peptides (Ficarro *et al.*, 2002). To increase specificity of binding, methyl-esterification of the carboxyl was performed before enrichment (2002) (Ficarro *et al.*, 2002). However, this caused side reactions which would complicate spectra (Han *et al.*, 2008). Later it was found that more specificity could be obtained using TiO_2 or ZrO_2 beads (2006) (Sugiyama *et al.*, 2008; Kweon and Håkansson, 2006). The use of TiO_2 beads for enrichment has become a standard method for use in protein mixtures (Benschop *et al.*, 2007; Fan *et al.*, 2014; Stecker *et al.*, 2014; Yang *et al.*, 2013).

When analysing phosphopeptides, label free quantification (LFQ) is a viable method of analysis. The alternative of using isobaric tags for quantification increases the search space, making false positives more likely, as well as adding more handling steps, increasing variation and potential loss of low abundance samples (Vu *et al.*, 2016). One limitation of phosphoproteomic studies is the inability to differentiate between changes in phosphorylation stoichiometry from changes in protein abundance. Phosphorylation stoichiometry is the ratio of the amount of protein phosphorylated on a particular site to the amount of protein. Phosphopeptide levels need to be normalised to overall protein abundance, to differentiate between

changes in protein abundance and stoichiometry. This can be done by analysing non-phosphorylated peptides within the same sample, i.e. before enrichment.

Standard methods of phosphopeptide enrichment are unsuitable for some amino acid (AA) phosphorylation sites because acidic conditions cause dephosphorylation. Therefore, a technique dubbed strong anion exchange (SAX) chromatography (UPAX) is often used to study these acid labile phosphorylation modifications. UPAX is an Unbiased Phosphopeptide enrichment strategy which allows enrichment of acid labile phosphopeptides under near neutral conditions (Hardman *et al.*, 2017). Hardman *et al.* (2017) were able to identify phosphorylation sites on histidine, arginine, lysine, asparagine and glutamine using UPAX, the latter four of which were not considered to phosphorylate in vertebrate cells.

Carbonylation is the result of oxidative damage to proteins and is an irreversible modification (Madian and Regnier, 2006). Carbonylation is a form of oxidative stress which has been linked to several diseases. In the cell, an increase in reactive oxygen species (ROS) causes oxidation to occur. Once the stress period is over, disulfides are reduced to sulfhydryls and the redox potential of the cell is restored (Madian and Regnier, 2006). Enzymes have evolved to repair oxidatively modified proteins, proteasomes and lysosomes destroy proteins which are too badly damaged (Jung and Grune, 2008).

Several enrichment techniques have been used for carbonyl modifications, but these generally use a carbonyl reactive probe to attach to the carbonyl group, then different enrichment strategies can be used. Some authors used ion exchange chromatography or affinity purification using the corresponding antibody to the tag conjugated to beads (Figure 1.1B) (Mirzaei and Regnier, 2006; Lee *et al.*, 2006; Chavez *et al.*, 2006). The analysis of the enrichment is either performed by western blot or mass spectrometry (MS).

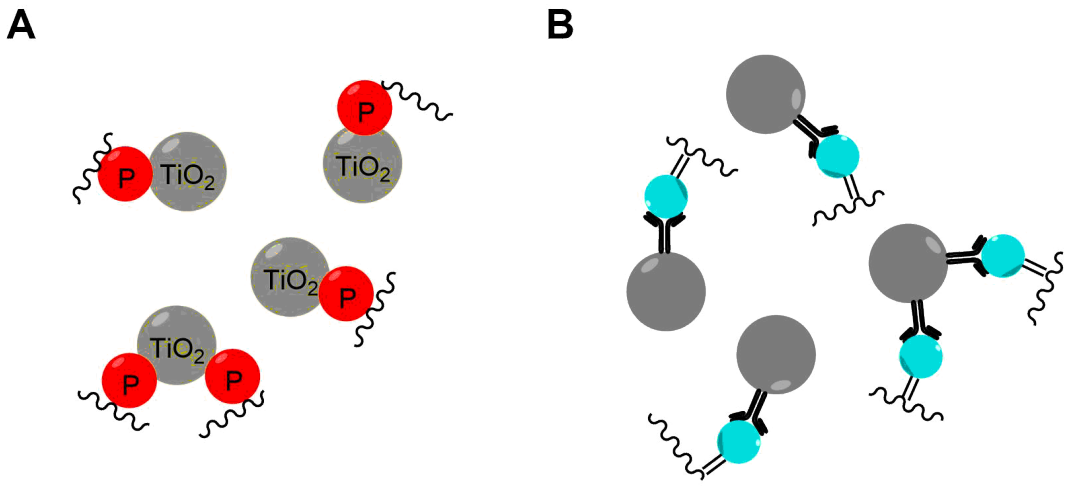

Figure 1.1: (A) Phosphopeptide enrichment using TiO_2 beads. (B) Affinity purification of carbonyl modifications using a carbonyl reactive tag and an antibody conjugated to beads.

1.3 Proteomic Techniques

1.3.1 Proteomics

The term proteomics was first used by Wilkins *et al.* (1996) in September 1994 and denotes the study of proteins expressed by cell genomes. The increase in sequenced genomes, genome annotations and the number of functional proteins in an organism has led to an increase in the number of organisms which can be analysed using proteomics (Reeves *et al.*, 2009). There are many more proteins in the proteome than genes in the genome due to splice variants and PTMs (Aebersold *et al.*, 2018). Proteomics is used to give us an increased understanding of function and regulation of an organism, information which the genes do not give (Graves and Haystead, 2002). Proteins also correspond to function and phenotypes of cells (Okazawa *et al.*, 2011). In order to control biological function of cells, proteins must first become modified, and form PTMs (Barber and Rinehart, 2018). PTMs are defined as a "series of chemical reactions whereby a newly synthesized polypeptide chain is converted into a functional protein" (Han and Martinage, 1992; Appel and Bairoch, 2004). Currently there are over 100 PTMs known, and there are likely to be many more yet to be discovered (Kersten *et al.*, 2006).

1.3.2 Quantitative Proteomics

Quantitative MS is used in proteomics to determine the amount of each individual protein in a sample. MS has been used for decades for qualitative analysis, but more recently there has been an increase in the ability for MS to provide quantitative data analysis. Several factors affect the quantitative capabilities of MS, these factors are either instrument-related, i.e. the detection efficiency and the MS calibration, or sample related, i.e. sample preparation, sample separation and sample homology (Urban, 2016).

From the mid-90s 2D gel electrophoresis was used to separate proteins before proteomic analysis using peptide mass fingerprinting techniques (Saraswathy and Ramalingam, 2011). 2D electrophoresis works by separating proteins by isoelectric point followed by molecular mass. However, this method is highly variable and can be difficult to reproduce, making it difficult to perform quantitative analysis between different gels (Lilley *et al.*, 2002). To enable direct comparison between two samples 'difference in gel electrophoresis' (DIGE) was developed, which involves labelling lysine residues on each protein with different fluorophores, the samples are then mixed and separated on a gel, allowing analysis of two different samples on the same gel (Drabik *et al.*, 2016). This increases identification sensitivity of proteins, by separating the proteins before MS analysis, but it also increases the complexity of proteins in the gel.

Later as tandem mass spectrometers became more available, non-gel separation techniques such as liquid chromatography (LC) allowed for higher throughput proteomics. LC uses a column of tightly packed C18 particles to separate peptides by their hydrophobicity (Otter, 2003). The chromatogram of peptides coming off the LC column can be used for label free quantification (LFQ), this method involves taking the retention time of a peptide from the LC column, and its peak area. Once the peptides have been identified by mass spectrometry, the retention time and peak area are then compared between samples and can be used to quantify the same peptide between different samples (Zhu *et al.*, 2009). Spectral counting can also be used to gain quantitative information, data depended acquisition softwares select peptides for MS/MS fragmentation based on their abundance and charge state, which typically leads to greater identification of more abundant peptides and proteins (Gokce *et al.*, 2011). Therefore, a dynamic exclusion is applied which excludes a peptide for a certain amount of time once it's been fragmented from being fragmented again, allowing lower abundant peptides to be analysed. Spectral counts must be normalised

to reduce variation observed between samples and replicates (Gokce *et al.*, 2011). However, over time columns retention times will change, so samples need to be run consecutively to get reliable LFQ data (Lai *et al.*, 2013). To combat this variability, isobaric tags for quantification were developed.

Isobaric labelling began with reacting specific amino acids and functional groups with the tags, such as cysteine groups with the isotope coded affinity tags (ICAT) (Applied Biosystems) (Gygi *et al.*, 1999). The tags consist of three parts, a reactive group, an isotopic coded linker and a tag, so labelled peptides can be isolated (Gygi *et al.*, 1999). Samples are tagged then combined and digested, before the tagged peptides can be pulled out of the mixture, then they can be separated and analysed by LC-MS, the ratios of the tags in the samples is used to quantify the relative amount of each protein in the sample. However, ICAT can only be used on two samples at a time, limiting analysis (Bachor *et al.*, 2019). Since ICAT tagged cysteine residues, and not all peptides contain a cysteine, the tagged samples were not necessarily representative of the dataset as a whole and whilst it could have been developed for use on more samples, high resolution mass spectrometers were not readily available at that time, meaning development wasn't economically viable then.

The two most widely used isobaric tags currently commercially available are isobaric tag for relative and absolute quantification (iTRAQ) (Applied Biosystems) and the tandem mass tag (TMT) (Thermo Scientific). They are both amine reactive and available in as multiple masses to allow for analysis of several samples at once (iTRAQ in 4 and 8plex, TMT in 2, 6, 10, 11 and 16plex) (Rauniyar and Yates, 2014).

TMT consists of an amine reactive group, which reacts with the N terminus of peptides, a mass normaliser region, and a reporter ion, which fragments during MS2 giving diagnostic peaks which can be used for quantification (Figure 1.2) (Thompson *et al.*, 2003). The amine reactive group also reacts with basic amino acids, such as lysine residue, as well as the N terminus of tryptic peptides. There are currently 16 different TMT tags which add up to the same overall molecular weight but have heavy isotopes (C^{13} and N^{15}) in different ratios within the reporter and mass normaliser regions of the molecule, so will have different mass reporter ions (Itzhak *et al.*, 2017). Proteins are digested and the peptides are tagged with TMT, each sample reacted with a different TMT molecule can then be combined and analysed using LC-MS/MS, the ratios of the reporter ions in each spectrum give quantitative

information on the proteins in the samples (Cheng *et al.*, 2016). Because the tags have the same overall mass and hydrophobicity they cannot be distinguished until MS2.

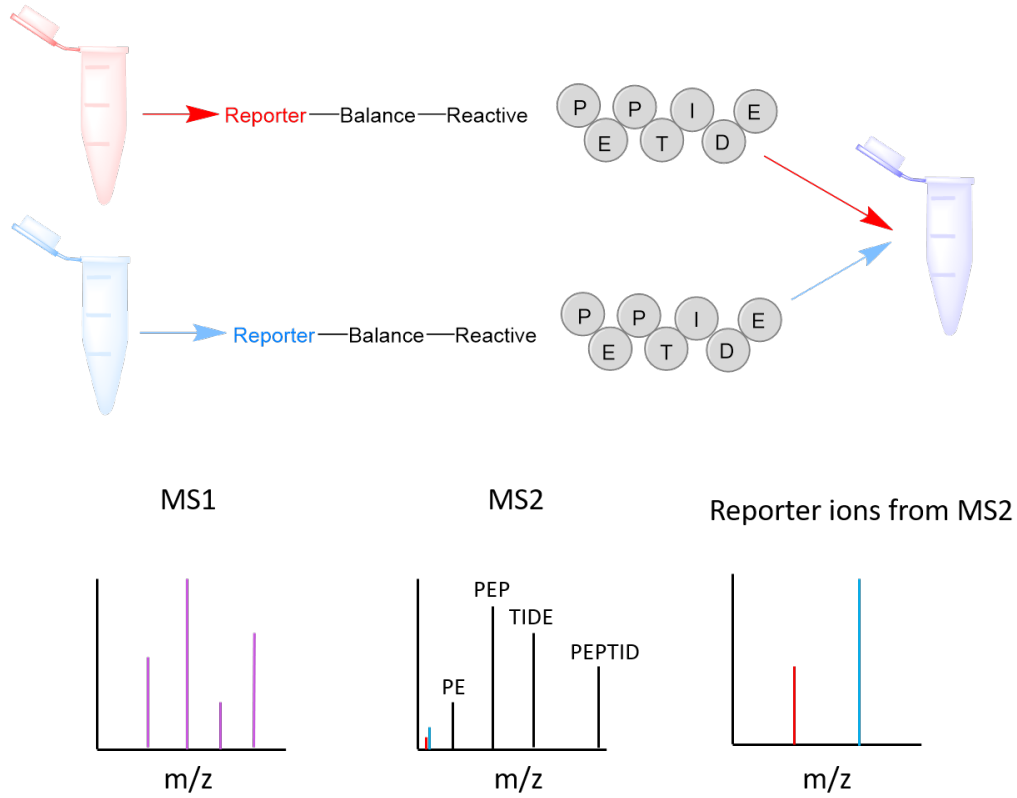

Figure 1.2: Isobaric tags consist of reporter ions, mass normalisers and reactive regions. This gives the tag the same overall mass in MS1; it is only when MS2 is performed and the reporter ion breaks off that the different masses can be seen, and the reporter ions can be used for quantification.

Isobaric tags such as TMT have their limitations. When TMT tagged peptides are analysed in the MS, peptides are isolated for MS2 within a 1 Da window (Savitski *et al.*, 2013). This means other lower abundant peptides, which are also tagged with TMT, are isolated along with the desired peptide, and the reporter ions of the lower abundant peptides also break off during MS2, affecting the TMT reporter ion ratios, causing a ratio suppression, making peptides which are significantly changing show as not significantly changing. To combat this MS3 analysis should be used, however, this is slower than MS2 analysis, decreasing the number of proteins which will be identified in the same length analysis (Ting *et al.*, 2011). Isobaric tagging also increasing sample handling and increases sample complexity,

leading to less peptides being identified.

1.3.3 Mass Spectrometers

The first mass spectrometer was developed in 1913 and was used to prove the existence of nonradioactive isotopes (Thomson, 1913). The mass spectrometer worked by using a local magnetic and electrostatic field to detect positive ions from vaporised samples. In 1946 time of flight (TOF) MS was developed which works by accelerating ions using an electric field, ions with the same charge will have the same kinetic energy, and the velocity depends on the mass to charge ratio (m/z) (Stephans, 1946). Quadrupole mass filter and quadrupole ion trap were developed in 1953 (Paul and Steinwedel, 1953). Quadrupole ion traps use dynamic electric fields to trap ions. In 1974 Fourier-transform ion cyclotron resonance (FT-ICR) MS was developed (Comisarow and Marshall, 1974). FT-ICR involves trapping ions using electrical trapping plates which are then excited at their resonant cyclotron frequency to a larger cyclotron radius. The excitation field is then removed, and ions are rotated at their cyclotron frequency in phase, this induces a charge on a pair of electrodes, the signal is Fourier transformed to give a mass spectrum. Triple quadrupole mass analysers were developed in 1978 (Yost and Enke, 1978). A triple quadrupole consists of two quadrupoles in series which act as mass analysers, with a quadrupole in between them which acts as a collision cell for fragmentation. In 2000 the Orbitrap was developed (Makarov, 2000) and traps ions in an orbital motion around a spindle electrode.

By the 1980s MS was commonly used for small organic molecules, but proteins and other large molecules proved more challenging. In 1988 matrix assisted laser desorption ionisation (MALDI) and electrospray ionisation (ESI) were developed which are softer ionisation techniques than previously developed and made analysis of larger molecules possible because they do not break apart during ionisation (Fenn *et al.*, 1989; Karas and Hillenkamp, 1988). MALDI involves using laser energy absorbing matrix to create ions. This creates little fragmentation and often produces singly charged ions. In ESI a high voltage is applied to a liquid, creating a plume of ions. Unlike MALDI, ESI produces multiply charged ions.

Mass spectrometry is widely used in the fields of biology, chemistry and physics to analyse samples. Tandem mass spectrometry (MS/MS) is a key technique for determining the peptide sequence and identifying the proteins present in complex mixtures and identifying any PTMs (Karpievitch *et al.*, 2010). MS/MS in-

volves breaking down selected precursor ions (peptides) (MS1) into fragments which reveal the chemical structure of the precursor ion (MS2). Selected ions from the MS2 scan can be further fragmented (MS3) and so on (MSn) (Ulintz *et al.*, 2009).

The Orbitrap Fusion (Thermo Scientific) contains three mass analysers, a quadrupole, an Orbitrap and a dual linear ion trap (Figure 1.3). The quadrupole consists of four cylinders which oscillate their charge in order to trap ions of a particular mass to charge ratio (m/z) (March *et al.*, 1989). The Orbitrap mass spectrometer is an ion trapping mass analyser consisting of an inner spindle shaped electrode and an outer barrel shaped electrode which traps ions (Hu *et al.*, 2005). Ions move backwards and forwards across the inner electrode whilst also circling it, a Fourier transform of this movement is used to calculate the m/z of the ion. A dual linear ion trap contains a high-pressure cell and a low-pressure cell. The high-pressure cell is where ions are trapped, and ions are detected in the low-pressure cell (Makarov *et al.*, 2006). This allows higher accuracy on trapping and higher resolution of ions.

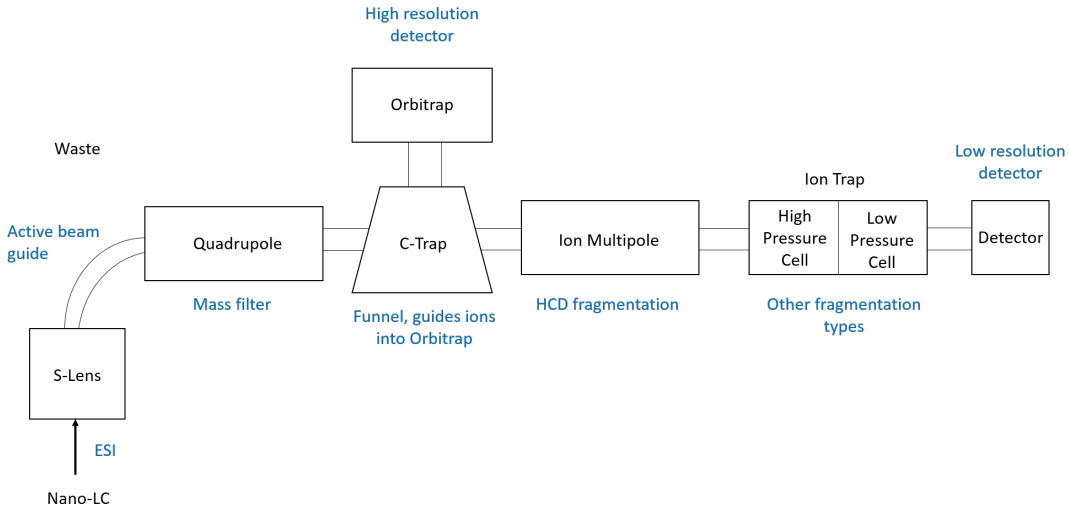

Figure 1.3: Schematic of the Orbitrap Fusion. The S-lens is used to focus the ion beam from the LC column. The bend is used to remove neutral particles and reduce background signal. The quadrupole selects precursor mass based on a pre-set mass range. MS1 analysis can be performed in the Orbitrap or ion trap. Peptides are fragmented in the ion multipole for higher-energy collisional dissociation (HCD) fragmentation or the pressure cell of the ion trap for collision-induced dissociation (CID) fragmentation.

Proteins can be analysed using MS either as whole proteins or as smaller peptides. However, typically peptides are analysed using MS because proteins are

often insoluble in the acidic MS buffers, so detergents are needed in order to solubilise them which are not MS compatible (because they ionise well and are in a large excess in the sample) (Steen and Mann, 2004). Fragmenting large proteins, especially in complex mixtures gives fragments which are difficult to assign back to proteins, whereas peptide fragments are much easier to interpret, and this has been highly automated with various algorithms. The sensitivity of the MS for proteins is also much lower than for peptides. However, analysis at the peptide level also creates problems, due to PTMs. If multiple peptides from the same protein are found to be modified, if the protein exists as one molecule is it modified in multiple places or present in multiple forms each modified in a subset of the modification sites.

In order to break a protein down into peptides it must be digested with an enzyme, the most common of which is trypsin, which cuts proteins C-terminal to lysine and arginine AA residues (Olsen *et al.*, 2004). Peptides can then be separated by reverse phase liquid chromatography (LC). This uses a column packed with C18 coated silica particles to which peptides will interact differently depending on their hydrophobicity (Shire, 2015). Once peptides elute off at a specific concentration of organic solvent, typically acetonitrile (AcN), they are ionised by electrospray ionisation (ESI), to give them a positive charge and then injected into the MS (Ho *et al.*, 2003). The gradual introduction of peptides to the MS from the LC allows more to be identified. In the MS an electric field is used to guide charged particles, any neutral particles are unaffected by the electric field and lost. Precursor MS1 scans are performed in the Orbitrap, which has a high mass accuracy, but low sensitivity (Hu *et al.*, 2005). A peptide is then selected from the MS1 to be fragmented, then analysed in the ion trap, which has a lower mass accuracy, but it more sensitive than the Orbitrap (Makarov *et al.*, 2006). From here the data are Fourier transformed to obtain a spectrum.

There are multiple possible fragmentation methods available in the Orbitrap Fusion. During collision induced dissociation (CID) ions are excited by applying an electrical potential, which increases their kinetic energy. The excited ions then collide with an inert gas present in the cell (often helium or argon), these collisions cause bonds to break along the peptide backbone creating B and Y ions (Frese *et al.*, 2011). Higher-energy collisional dissociation (HCD) uses higher-energy than CID fragmentation, allowing for better fragmentation (Jedrychowski *et al.*, 2011). Electron transfer dissociation (ETD) originally used anthracene ($C_{14}H_{10}$) to generate radical ions for electron transfer (Syka *et al.*, 2004), but now fluoranthene is

favoured (Hunt *et al.*, 2014). ETD allows for better fragmentation of larger peptides with higher charges (Kim and Pandey, 2012). The transfer of an electron causes the peptide backbone to fragment giving C and Z ions.

1.3.4 Data Analysis

To assign peptide sequences to MS/MS spectra, the spectra can be pattern matched against a database of peptides taking into account the predicted fragmentation pattern. During this project MASCOT and Max Quant (MQ) were used for data analysis.

MASCOT (Matrix Science) is a commercial software; the exact algorithm for identification is not published. However, the basic principle of the algorithm is known. FASTA files contain a database of proteins in a particular organism. Because digestion enzymes cleave proteins at specific AA residues (trypsin; arginine and lysine), and fragmentation methods give particular ions (HCD and CID give B and Y ions), this information is used to predict the peptide which will appear in the sample. A tolerance is set for the MS1 scan, so that only peptides in the FASTA file with an m/z within that tolerance are able to be assigned to a peptide. From here MASCOT will match the observed spectrum to the predicted spectrum (Perkins *et al.*, 1999). False positives are when a spectrum is incorrectly matched to a peptide. This can happen because of enzymes cleaving at unspecific sites, missed cleavages by an enzyme, the charge state of a peptide being misinterpreted or a protein modification being misinterpreted (Chen *et al.*, 2009). MASCOT generates its false discovery rate (FDR) by using a reverse database, where any hits to it are known to be wrong, so it can be inferred that the number of hits to the reverse database corresponds to the number of false positives in the dataset (Chen *et al.*, 2009).

The MASCOT error tolerant search (ETS) is used to decrease the search space when trying to identify multiple modifications within a dataset, and thus bring down the FDR (Creasy and Cottrell, 2002). It works by first matching peptides to proteins within the database, it then does a second search where it will look for modifications to proteins identified in the first search among the unassigned peptides. However, if a protein is not identified in the initial search then it cannot be identified as modified in the second search (Creasy and Cottrell, 2002).

MQ uses the Andromeda algorithm, and works in a similar way to the MAS-

COT algorithm in that it uses probability to match peptides to the database and assigns a score (Cox *et al.*, 2011). The probability score (p-score) is calculated by working out the B and Y ion series as in the MASCOT algorithm and determining the number matched to a spectrum. The probability of obtaining random matches between the predicted and measured MS2 spectra is used to give the FDR (Olsen *et al.*, 2004). This method is also used to assign the amino acid location of PTMs. MQ also allows label free quantification (LFQ) which MASCOT does not. LFQ uses the intensity of the peak coming off the LC column and matches it to assigned peptides, it then compares the size of this peak between samples to quantitatively analyse the amount of that peptide in each sample (Bantscheff *et al.*, 2012). The match between runs function in MQ means that if a peak from the LC column did not trigger an MS2 in one sample, but the corresponding peak was assigned to a peptide in another sample, it can assign the peak to a peptide based on their accurate masses and alignment of the chromatograms (Cox *et al.*, 2014).

MQ dependent peptide search (DPS) like the ETS search is used to bring down the FDR when searching for many modifications in a database. It does an initial search to identify unmodified peptides and then does a second search to match these peptides with a mass shift against unassigned peptides (Cvetesic *et al.*, 2016). However, if a peptide is not identified in the initial search then it cannot be identified as modified in the second search (Cvetesic *et al.*, 2016).

When analysing PTMs a site localisation score is given in order to identify which AA the modification is present on. When peptide fragments are in low abundance in an MS/MS spectrum, it is difficult to assign the exact AA the modification is present on (Ferries *et al.*, 2017). High sequence coverage is therefore needed to confidently assign PTM positions, this is especially important for doubly or triply modified peptides (Dephoure *et al.*, 2013).

Perseus was designed by the Cox and Mann groups to quantitatively interpret protein data and PTMs (Cox and Mann, 2012). It was codeveloped with MQ, allowing it to easily analyse data from MQ searches. The software contains a series of tools to analyse data statistically and computationally (Tyanova *et al.*, 2016). Tyanova *et al.* (2016) offers a comprehensive review of the many algorithms used by Perseus for data analysis. In order to quantify peptides between samples, the peptide must be present in all samples, when this is not the case Perseus can impute missing values from the normal distribution (Tyanova and Cox, 2018). This

assumes the peptide was present in the sample, but below the level of detection. It is therefore important to filter out peptides which are not present in multiple samples, as these are more likely to be false positives. Testing thousands of proteins for differential expression between samples is limited by the multiple hypothesis-testing problem which leads to an increase in the likelihood of identifying a protein as significantly changing, when in fact it is not differentially expressed (Tyanova and Cox, 2018). The appropriate correction method used depends on a balance between wrongly assigned significant hits and wrongly rejected significant hits (Tusher *et al.*, 2001; Benjamini and Hochberg, 1995).

MapMan is used to display large protein datasets as metabolic pathways and other processes (Thimm *et al.*, 2004). MapMan uses Scavenger modules, which collects and classifies the data received into function hieratical groups and an Image-Annotator which presents this data in graphical form (Thimm *et al.*, 2004; Usadel *et al.*, 2005). It is used specifically for *Arabidopsis thaliana*, but can also be used for crop plants (Usadel *et al.*, 2005).

Phosphat is a database of MS identified phosphorylation sites in *Arabidopsis thaliana* (Heazlewood *et al.*, 2008). The database is a repository of predicted and experimental phosphorylation sites. The database allows the user to search multiple experimental phosphorylation sites simultaneously and gives a summary of the predicted phosphorylation sites (Heazlewood *et al.*, 2008). Maximal motif finder for phosphoproteomics datasets (MMFPh) is used to find motifs in phosphorylation datasets (Wang *et al.*, 2014). It works by identifying amino acid residues which are overrepresented positions.

1.4 Aims of the Project

- Identify proteins which change due to different stresses in *Zea mays* and *Arabidopsis thaliana*. (Chapters 3 and 4)
- To determine how protein phosphorylation is affected by different stresses in *Zea mays* and *Arabidopsis thaliana*. (Chapters 3 and 4)
- To develop a method of tagging and enriching for carbonyl modifications caused by oxidative stress. (Chapter 5)

Chapter 2

Materials & Methods

2.1 Plant Growth

2.1.1 Arabidopsis Growth

Arabidopsis thaliana exotype Columbia-0 (Col-0) plants were grown in the Phytobiology facility at Warwick, at 21^{o}C, with an 8-hour day, 16-hour night cycle.

2.1.2 Maize Growth

Maize, *Zea mays*, B73 plants were grown in the Phytobiology facility at Warwick, at 28^{o}C during the day and 25^{o}C during the night, with a 16-hour day 8-hour night cycle.

2.2 Treatments

2.2.1 Drought Treatment of Maize Plants

Plants were droughted by withholding water, when they began to produce pollen, at approximately 65 days after emergence. Drought lasted for 1 week before normal watering was resumed. Soil moisture readings were taken using an SM150T soil moisture sensor (Delta-T Devices) from the first leaf stage until plants were dried for seed harvesting. The second leaf from the bottom of each plant was harvested at the end of the drought period, flash frozen in liquid nitrogen and stored at -80^{o}C until further use.

2.2.2 Methyl Viologen Treatment of Arabidopsis Leaves

Leaves were cut from 6-7 week old plants and placed in 25 mL of water in Petri dishes. Methyl viologen (MV) (Sigma Aldrich) in 0.1% Tween (Sigma Aldrich) was added to a concentration of 500 nM (Xu *et al.*, 2016). The same volume of 0.1% Tween was added to controls. Petri dishes were then sealed with Nescofilm and left gently shaking, at 21^{o}C, under constant light for 16 hours, after which proteins were extracted.

2.2.3 Methyl Viologen Treatment of Maize Leaves

Fresh maize leaves from 5-6 week old plants were cut into 1 cm pieces and placed in 25 mL of water in Petri dishes. MV in 0.1% Tween was added to a concentration of 1 μM or 10 mM (Kingston-Smith and Foyer, 2000). The same volume of 0.1% Tween was added to controls. Silwet L-77 (De Sangosse Ltd) was added in a 10,000 times dilution. Petri dishes were sealed with Nescofilm and left gently shaking under constant light, at 28^{o}C, for 16 hours or 2 hours, after which proteins were extracted.

2.2.4 Metal Catalysed Oxidation of Bovine Serum Albumin

Bovine Serum Albumin (BSA) (Fisher Scientific) samples were made up to a protein concentration of 10 mg mL^{-1} in phosphate buffered saline (PBS) pH 7.4 (144 mM sodium chloride (NaCl), 2.6 mM potassium chloride (KCl), 8 mM disodium phosphate (Na_2HPO_4), 1.5 mM monopotassium phosphate (KH_2PO_4)). Ferrous sulphate (II) (Sigma Aldrich) and Ascorbic acid (Sigma Aldrich) were added to concentrations of 0.75 mM and 1.25 mM, respectively, and the samples were incubated at 37^{o}C for 3 days (Bollineni *et al.*, 2011-1).

2.3 Carbonyl Tagging

2.3.1 2,4-Dinitrophenylhydrazine Tagging

Proteins were tagged with 2,4-Dinitrophenylhydrazine (DNPH) according to Protein Carbonyl Content Assay Kit (ab126287) Abcam. Extracted plant proteins in PBS were incubated with 10% Streptozocin solution (Abcam) for 15 minutes to remove DNA, lipids and other unwanted material which would interfere with the assay, this step was not performed on BSA samples. Samples were incubated with 2M DNPH hydrochloric acid (HCl) solution (Abcam) for 10 minutes at room temperature. 100% Trichloroacetic acid solution (TCA) (Abcam) was added to precipitate the proteins and samples were incubated on ice for 5 minutes, after which they were

spun for 2 minutes at maximum speed in a Sigma 1-14 centrifuge (16.163 g) and the supernatant was removed. Acetone (Sigma Aldrich) chilled to -20^{o}C was used to remove any free DNPH, samples were sonicated for 30 seconds and then left at -20^{o}C for 5 minutes before centrifuging at maximum speed for 2 minutes then removing acetone. Samples were then resuspended in PBS or 6 M guanidine hydrochloride (Abcam).

2.3.2 Aminoxy Tandem Mass Tag Tagging

BSA samples in PBS were diluted to 1 mg mL^{-1} in PBS and labelled with 1 mM aminoxy tandem mass tag (TMT) (Thermo Scientific) in 2-(N-morpholino) ethanesulfonic acid (MES) buffer (Sigma Aldrich) at pH 5 for 2 hours at room temperature (Afiuni-Zadeh *et al.*, 2016). Acetone precipitation was used to remove excess aminoxyTMT (details below).

2.3.3 Biotin Hydrazide Tagging

BSA was diluted to 3.5 mg mL^{-1} in PBS. Following metal catalysed oxidation (MCO) treatment as above, buffer was removed using 10 kDa spin filters (Merck) by centrifuging at 8,000 g for 10 minutes. Sample was washed three times with 500 μL of 2.5% acetonitrile (AcN) 0.1% Trifluoroacetic acid (TFA), washed through by centrifuging at 8,000 g for 10 minutes. Proteins were recovered by inverting the filter in a new tube and centrifuging at 1,000 g for 2 minutes. 5 mM biotin-LC-hydrazide (Thermo Scientific) dissolved in dimethylsulfoxide (DMSO) (Sigma Aldrich) and 1% sodium dodecyl sulfate (SDS) (Fisher Scientific) were added to tag the protein and left for 2 hours at 37^{o}C with shaking. The hydrazone bond was reduced with 60 mM sodium cyanoborohydride (Fisher Scientific) in ice cold PBS and incubated at 4^{o}C for 30 minutes (Havelund *et al.*, 2017). Excess tag was removed by centrifuge filtering using 10 kDa spin filters.

2.3.4 Alkoxyamine Biotin Tagging

BSA was diluted to 1 mg mL^{-1} in PBS. The pH was adjusted to pH 4, 1.25 mM alkoxyamine-PEG$_4$-biotin/alkoxyamine-PEG$_4$-SS-PEG$_4$-biotin (Thermo Scientific) was added to the BSA and left binding at room temperature for 2 hours (Bollineni *et al.*, 2013). The unreacted tag was removed with methanol chloroform precipitation (details below).

2.3.5 Acetone Precipitation

Four times sample volume of acetone was added to samples and they were left overnight at -20^{o}C to precipitate. Samples were then centrifuged at max speed in a Sigma 1-14 centrifuge (16.163 g) for 2 minutes and the acetone was removed, samples were resuspended in 50 mM 4-(2-hydroxyethyl)-1-piperazineethanesulfonic acid (HEPES) (Alfa Aesar).

2.3.6 Methanol Chloroform Precipitation

Four sample volumes of methanol (Fisher Scientific) followed by one sample volume of chloroform (Sigma Aldrich) and three sample volumes of water were added to samples. Samples were left at -20^{o}C for 10 minutes to precipitate. Samples were then centrifuged at max speed in a Sigma 1-14 centrifuge (16.163 g), for 1 minute and the top phase was removed being careful not to disturb the interface. Samples were washed with four sample volumes of methanol and centrifuged at maximum speed for 5 minutes, liquid was removed. Samples were resuspended in 50 mM HEPES.

2.4 Protein Extraction

2.4.1 Soluble Protein Extraction

Maize material was ground in liquid nitrogen to a fine powder. Buffer (PBS, 500 mM sucrose, 10% glycerol, 20 mM ethylenediaminetetraacetic acid (EDTA), 20 mM ethylene glycol-bis(β-aminoethyl ether)-N,N,N;N-tetraacetic acid (EGTA), 50 mM sodium flouride (NaF), 5 mM β-glycerphosphate, 0.6% polyvinylpyrrolidone (PVP), 10 mM ascorbic acid, 1 mM phenylmethylsulfonyl fluoride (PMSF), 1 mM dithiothreitol (DTT), 1x protease inhibitor cocktail (PIC)) was added and samples were vortexed and filtered through Miracloth (Merck). Samples were then centrifuged at 20,000 g in a Heraeus Fresco 21 centrifuge (Thermo Scientific) for 30 minutes at 4^{o}C (Santoni, 2007). Protein concentration was established using a Bradford assay (Bradford, 1976) and protein quality was checked by running 20 μg of protein on a 12% sodium dodecyl sulfate polyacrylamide gel electrophoresis (SDS-PAGE) gel.

2.4.2 Soluble & Membrane Protein Separation

Leaf samples from Arabidopsis and maize were ground fresh on ice in buffer (PBS, 500 mM sucrose, 10% glycerol, 20 mM EDTA, 20 mM EGTA, 50 mM NaF, 5 mM β-glycerphosphate, 0.6% PVP, 10 mM ascorbic acid, 1 mM PMSF, 1 mM DTT,

1xPIC). Samples were spun at 20,000 g in a Heraeus Fresco 21 centrifuge (Thermo Scientific) for 30 minutes at 4^oC to spin down cell debris. The liquid was then spun at 84,000 g in a Beckman Coulter Optims^{TM} MAX–XP ultracentrifuge in a TLA 100.3 rotor in polycarbonate tubes for 30 minutes at 4^oC, the liquid was collected as the soluble fraction and the pellet was resuspended in membrane buffer (PBS, 150 mM NaCl, 1 mM EDTA, 20 mM NaF, 1 mM PMSF, 1 mM DTT, 1xPIC) (Santoni, 2007). A Bradford assay was performed to establish the protein concentration, and an SDS-PAGE gel was run with 20 μg of protein to check protein quality.

2.5 Colourimetry Assays & Western Blotting

2.5.1 2,4-Dinitrophenylhydrazine Colourimetry Assay

DNPH tagged proteins were resuspended in 6 M guanidine and transferred to a 96 well plate which does not absorb in the ultraviolet (UV) range (Abcam). Absorbance was read at 360 nm on a Tecan Genios FL Fluorescence Plate Reader.

2.5.2 2,4-Dinitrophenylhydrazine Western Blotting

6 μg of BSA or 20 μg of a complex mixture was loaded to a 12% SDS-PAGE gel and run for 15 minutes at 100V then for 1 hour at 140V. Proteins were then transferred overnight at 30V at 4^oC to an Immobilon-FL membrane (Pall Corporation, Pensacola, FL) in transfer buffer (Sigma Aldrich). Blots were blocked with 5% milk solution in 0.1% Phosphate-buffered saline Tween (PBST) for 1 hour, and then incubated with rabbit anti-DNPH (1:10,000) (Sigma Aldrich) in 5% milk 0.1% PBST solution for 3 hours. After which membranes were washed 3 times for 5 minutes with 0.1% PBST. The membrane was then treated with anti-rabbit horse radish peroxidase (HRP) (1:10,000) (Abcam) in 5% milk 0.1% PBST for 1 hour, then washed 3 times with 0.1% PBST. Membranes were incubated in Electrochemiluminescence (ECL) (GH healthcare) and were visualised using an Image Quant LAS 4000 (GH healthcare).

2.5.3 Tandem Mass Tag Western Blotting

6 μg of BSA was loaded to a 12% SDS-PAGE gel and run for 15 minutes at 100V then for 1 hour at 140V. Proteins were transferred from the gel overnight at 30V at 4^oC to an Immobilon-FL membrane in transfer buffer. Blots were blocked with 5% milk solution in 0.1% tris-buffered saline Tween (TBST) for 1 hour, and then incubated with anti-TMT mouse (1:1,000) (Thermo Scientific) in 5% milk 0.1% TBST solution

for 1 hour. After which membranes were washed 3 times for 5 minutes with 0.1% TBST. The membrane was then treated with anti-mouse HRP (1:5,000) (Sigma Aldrich) in 5% milk 0.1% TBST for 1 hour, then washed 3 times with 0.1% TBST. Membranes were incubated in ECL and were visualised using an Image Quant LAS 4000.

2.5.4 Biotin Western Blotting

6 μg of BSA was loaded to a 12% SDS-PAGE gel and run for 15 minutes at 100V then for 1 hour at 140V. Proteins were transferred from the gel overnight at 30V at 4^{o}C to an Immobilon-FL membrane in transfer buffer. Blots were blocked with 5% milk solution in 0.1% TBST for 1 hour, and then incubated with anti-biotin HRP (1:10,000) (Cell Signalling Technology) in 5% milk 0.1% TBST solution for 1 hour. After which membranes were washed 3 times for 5 minutes with 0.1% TBST. Membranes were incubated in ECL and were visualised using an Image Quant LAS 4000.

2.6 Affinity Purification

2.6.1 2,4-Dinitrophenylhydrazine Enrichment

DNPH tagged samples were either enriched at the protein level or the peptide level. Dynabeads (Sigma Aldrich) (10 μL for 100 μg of protein) were combined with anti-DNPH in 0.02% Tween in PBS (PBST). This was left to bind for 10 minutes, then washed once with PBST. Sample was then added to beads and left to bind for 10 minutes with gentle shaking. Beads were washed three times with PBST and eluted by boiling the beads (Kristensen *et al.*, 2004).

2.6.2 Aminoxy Tandem Mass Tag Enrichment

AminoxyTMT tagged samples were enriched either at the protein level or the peptide level. TMT resin (Thermo Scientific) (250 μL for 100 μg of protein) was washed 3 times with 50 mM tris-buffered saline (TBS) pH 6.8. Sample in TBS was added to TMT resin and incubated overnight with end over end mixing at 4^{o}C. Supernatant was removed, and resin was washed five times with TBS, three times with distilled water and once with 4 M urea (Fisher Scientific). Samples were eluted with four washes of TMT elution buffer (Thermo Scientific) (Afiuni-Zadeh *et al.*, 2016). Washes were pooled and dried using a Concentrator plus speed vac (Eppendorf) before further analysis.

2.6.3 Biotin Hydrazide Enrichment

Biotin-LC-hydrazide tagged samples were enriched either at the protein level or the peptide level. Samples were resuspended in PBS pH 7.4. Samples were enriched using Streptactin resin (Fisher Scientific) (20 μL for 1 mg of protein). Beads were washed once with distilled water and twice with PBS. Sample in PBS was added to resin and left for 5 minutes to allow binding. Beads were washed five times with PBS and once with distilled water. The tagged sample was then rapidly eluted with two washes of distilled water heated to 95^{o}C (Havelund *et al.*, 2017). These washes were pooled and dried using a Concentrator plus speed vac before further analysis.

2.6.4 Alkoxyamine Biotin Enrichment

Alkoxyamine biotin tagged samples were either enriched at the protein level or the peptide level. Samples were resuspended in 50 mM HEPES. 400 μL of monomeric avidin resin (Thermo Scientific) were packed into a Pierce spin column (Thermo Scientific), and the column was washed with PBS and water. Samples were added to column and left binding at room temperature for 1 hour. Samples were flushed through column and column was washed 5 times with PBS. Samples were eluted 5 times with 1 M D-biotin (Sigma Aldrich), and column was regenerated with 1 M glycine (Fisher Scientific) pH 2.8. Elution's were pooled for analysis.

2.6.5 Phosphopeptide Enrichment

After samples were filter aided sample preparation (FASP) digested, phosphopeptides were enriched using Titanospere titanium dioxide (TiO_2) beads (GL Sciences Inc. Japan). Peptides in 50 mM HEPES were diluted to 5 mM HEPES with 80% AcN and 5% TFA. TiO_2 beads were diluted to 1 mg in 10 μL of 2.5-dihydroxybenzoic acid (DHB) (Sigma Aldrich) solution at 20 mg mL^{-1} and mixed for 10 minutes at 650 rpm. 2 mg of beads was added for every 1 mg of peptides and were mixed gently with end over end mixing for 1 hour. This was repeated once. Beads were centrifuged at 2,000 g for 2 minutes and the supernatant was removed. A C8 membrane was packed into a 200 μL pipette tip to make a column to support the beads. The beads were added on top of the C8 membrane and washed with 10% AcN, this was centrifuged through at 2,000 g for 10 minutes. Beads were then washed with 40% AcN and spun at 2,000 g for 6 minutes. Beads were finally washed with 60% AcN and spun at 2,000 g for 4 minutes. Peptides were eluted from the beads using 5% ammonium hydroxide (Sigma Aldrich) followed by 15% ammonium hydroxide, 25% AcN and centrifuged at 2,000 g for 2 minutes (Benschop *et al.*, 2007).

The ammonium hydroxide and AcN were removed by Concentrator plus speed vac (Eppendorf) for 20 minutes. Samples were resuspended in 2% AcN 0.1% TFA and sonicated for 15 minutes before clean up via C18-stage tip (details below).

2.7 Mass Spectrometry

2.7.1 In Solution Digest

Ammonium bicarbonate (ABC) (Sigma Aldrich) was used to change the pH of samples to pH 8, pH was measured with universal indicator paper. 10 mM tris(2-carboxyethyl)phosphine (TCEP) (Sigma Aldrich) and 40 mM Chloroacetamide (CAA) (Sigma Aldrich) were added to reduce disulfide bonds and alkylate cysteines with incubation at 70^{o}C for 5 minutes. 1 μg of trypsin (Promega) was added for every 100 μg of protein in sample, and samples were left digesting overnight at 37^{o}C. To stop the reaction, TFA was added to bring the pH down to pH 2, pH was measured using universal indicator paper (Medzihradszky, 2005). Samples underwent clean up via C18-stage tip (details below) before MS analysis.

2.7.2 In Gel Digest

Bands from gels were cut into cubes and transferred to 1.5 mL Eppendorf tubes. Coomassie stain (Sigma Aldrich) was removed with 3 washes of 50% ethanol in 50 mM ABC incubated for 20 minutes at 55^{o}C with shaking. Gel pieces were dehydrated with ethanol for 5 minutes with shaking. Proteins were reduced and alkylated with 10 mM TCEP and 40 mM CAA for 5 minutes at 70^{o}C. The gel pieces were then washed 3 times with 50% ethanol in 50 mM ABC for 20 minutes with shaking. Ethanol was added to dehydrate gel pieces, ethanol was removed before 1 μg of trypsin in ABC was added per tube, and samples were left digesting overnight at 37^{o}C. Peptides were extracted from gel pieces with 25% AcN and sonicated for 10 minutes three times (Goodman *et al.*, 2018). Peptides were dried with Concentrator plus speed vac and resuspended in 50 μL of 2% AcN 0.1% TFA and sent for MS analysis.

2.7.3 On Bead Digest

All enrichment beads were spun down, and the supernatant was removed, 50 μL of ABC was added, bringing the pH of samples to pH 8. 10 mM TCEP and 40 mM CAA were added to reduce disulfide bonds and alkylate cysteines with incubation at 70^{o}C for 5 minutes. 1 μg of trypsin was added for every 100 μg of protein in

sample, and samples were left digesting overnight at 37^{o}C. To stop the reaction, TFA was added to bring the pH down to pH 2, pH was measured using universal indicator paper (Medzihradszky, 2005). Samples underwent clean up via C18-stage tip (details below) before MS analysis.

2.7.4 Filter Aided Sample Preparation Digest

Protein samples at 1 mg mL^{-1} in PBS pH 7.4 were moved into 0.5 mL 10 kDa cut off filter columns (Millipore), and spun at 8,000 g for 20 minutes. Samples were washed 3 times with 6 M urea (Sigma Aldrich), centrifuging at 8,000 g for 20 minutes each time. Samples were washed 3 times with 50 mM ABC. Samples were incubated with 10 mM TCEP and 40 mM CAA to reduce disulphide bonds and alkylate cysteines, for 30 minutes at room temperature. TCEP and CAA were spun through the filter at 8,000 g for 20 minutes. Filter was washed 3 times with 50 mM HEPES. 1 μg of trypsin per 100 μg of protein was added, and samples were left digesting overnight at 37^{o}C. The peptides were then centrifuged through the column for 20 minutes at 8,000 g. The filter was washed with water to collect any residual peptides left on the filter (Wisniewski *et al.*, 2009). Peptides were concentrated using a Concentrator plus speed vac (Eppendorf).

2.7.5 Tandem Mass Tag Tagging

TMT tags (Thermo Scientific) were removed from the freezer and allowed to defrost for 15 minutes before opening. 0.2 mg of TMT tags were dissolved in 20 μL of anhydrous AcN (Sigma Aldrich), and each tag was added to 100 μg of peptide and left reacting at room temperature for 2 hours. 1 μL of Hydroxylamine (Sigma Aldrich) was added to stop the reaction. 1 μL of each sample were combined (Biringer *et al.*, 2011). Samples were speed vacuumed using a Concentrator plus speed vac to remove AcN and clean up was performed using C18-stage tipping (details below) before MS analysis to check reporter ion ratios before fractionation.

Samples were combined and dried via a Concentrator plus speed vac to remove AcN. Samples were resuspended in 0.1% TFA and high pH fractionation was performed using Pierce C-18 spin columns. Each column was equilibrated twice with AcN and once with 0.1% TFA and each spun for 1 minute at 5,000 g. The column was loaded with sample and spun at 3,000 g for 5 minutes, this loading was repeated to improve binding. Each column was washed with ethyl acetate 1% TFA, followed by 0.1% TFA, water twice and HpH solution (5% AcN 0.1% Triethylamine (Thermo

Scientific)), each time spun at 3,000 g for 3 minutes. Fractions were collected in separate tubes for MS analysis. Each elution contained an increasing amount of AcN (10%, 12.5%, 15%, 17.5%, 20%, 22.5%, 25%, 35%, 50%) and was spun at 5,000 g for 4 minutes. Column was washed with HpH solution between elutions (Sinclair and Timms, 2011).

5 μL of sample was loaded. Samples were separated with an UltiMate 3000 series high performance liquid chromatography (HPLC) using Nano Series Standard Columns. Samples were analysed by nano liquid chromatography-electrospray ionisation-tandem mass spectrometry (LC-ESI-MS/MS) using the Ultimate 3000/Orbitrap Fusion instrumentation (Thermo Scientific), with higher-energy collision dissociation (HCD) fragmentation in data dependent mode, liquid chromatography (LC) run of 120 minutes on a 50 cm column. Quantification was performed either using MS2 or MS3 fragmentation. For MS2 quantification analysis, MS1 and MS2 scans were performed in the Orbitrap with HCD fragmentation. For MS3 quantification MS1 scan was performed in the Orbitrap, MS2 scan in the ion trap with collision-induced dissociation (CID) fragmentation and MS3 analysis in the Orbitrap with HCD fragmentation.

2.7.6 C18-Stage Tipping

All samples were cleaned up before MS analysis using 2 C18 membranes compacted into a p200 pipette tip. The membranes were equilibrated with methanol and centrifuged at 2,000 g for 2 minutes, followed by AcN, then 2% AcN 0.1% TFA which was centrifuged for 4 minutes, prior to sample loading. 10 μg of peptides in a maximum of 150 μL was loaded onto the stage tip before centrifuging at 2,000 g for 10 minutes. Membranes were washed with ethyl acetate to remove detergent, and 2% AcN 0.1% TFA and spun at 2,000 g for 4 minutes. Peptides were eluted with 20 μL of 80% AcN and centrifuged at 2,000 g for 2 minutes (Rappsilber *et al.*, 2007). AcN was removed with a Concentrator plus speed vac for 10 minutes, after which the samples were resuspended in 40 μL of 2% AcN 0.1% TFA for MS analysis.

2.7.7 Phosphopeptide Detection

Samples underwent phosphopeptide enrichment after FASP digest. 20 μL of sample was loaded onto the LC column. Peptides were separated with an UltiMate 3000 series HPLC using Nano Series Standard Columns. Samples were analysed by nano LC-ESI-MS/MS using the ultimate 3000/Orbitrap Fusion instrumentation, with

HCD fragmentation in data dependent mode, LC run of 60 or 120 minutes on a 50 cm column.

2.7.8 Carbonylation Detection

5 μL of peptide sample was loaded onto the LC column. Peptides were separated with an UltiMate 3000 series HPLC using Nano Series Standard Columns. Samples were analysed by nano LC-ESI-MS/MS using the UltiMate 3000/Orbitrap Fusion instrumentation, with HCD fragmentation in data dependent mode, LC run of 60 minutes on a 50 cm column.

2.7.9 Ion Targeted Mass Spectrometry for Biotin Tagged Samples

5 μL of sample was loaded on to the LC column. Peptides were separated with an UltiMate 3000 series HPLC using Nano Series Standard Columns. Samples were analysed by nano LC-ESI-MS/MS using the UltiMate 3000/Orbitrap Fusion instrumentation, with HCD fragmentation in data dependent mode, LC run of 60 minutes on a 50 cm column. MS1 and MS2 analysis was performed in the Orbitrap, if reporter ions were seen at m/z 227.1350 or m/z 340.1801 then the peptide was collected again, and a higher fragmentation energy was used.

2.7.10 Electron Transfer Dissociation Fragmentation

5 μL of sample was loaded on to the LC column. Peptides were separated with an UltiMate 3000 series HPLC using Nano Series Standard Columns. Samples were analysed by nano LC-ESI-MS/MS using the UltiMate 3000/Orbitrap Fusion instrumentation, with HCD fragmentation for 2-3+ ions and electron transfer dissociation (ETD) fragmentation for 3-6+ ions in data dependent mode, LC run of 60 minutes on a 50 cm column.

2.8 Data Analysis

2.8.1 Peptide Assignment Using MASCOT

Mascot generic format (MGF) files were generated from Xcalibur RAW files, in order to search in MASCOT (Matrix Science) (Perkins *et al.*, 1999). All samples were searched against a database of common contaminants (http://www.thegpm.org/cRAP/index.html) as well as the database for that organism. Mascot searches were performed with trypsin as the digestion enzyme with up to 3 missed cleavages, a fragment ion mass tolerance of 1.2 Da and a parent ion tolerance of 20 ppm.

Oxidation of Met was set as a variable modification and Carbamidomethyl of Cys were set as a fixed modification for all searches. Targeted searches where performed, where the m/z of specific modifications of interest were added as additional variable modifications to the standard search parameters (glutamic semialdehyde on arginine and proline, allysine of lysine and 2-amino-3-ketobutyric acid of threonine, plus tags, phosphorylation on S, T, Y).

2.8.2 Peptide Assignment & Label Free Quantification Using MaxQuant

Xcalibur RAW files were used for searches. Max Quant (MQ) searches (Cox and Mann, 2008) were performed with trypsin as the digestion enzyme, with up to 2 missed cleavages, and a parent ion mass tolerance of 4.5 ppm. Oxidation of Met was set as a variable modification and Carbamidomethyl of Cys as a fixed modification for all searches. Targeted searches where performed, where the m/z of specific modifications of interest were added as additional variable modifications to the standard search parameters (phosphorylation on S, T, Y). Label free quantification (LFQ) was used for phosphopeptide samples and quantification via MS2 using TMT10plex was used for TMT tagged samples.

2.8.3 Analysis of Tandem Mass Tags Using Perseus

The protein groups text file from the MQ search was loaded into Perseus (Tyanova *et al.*, 2016), and the reporter ion intensities were loaded into the main column. Potential contaminant hits, reverse database hits and only identified by site hits were filtered out of the data. Single peptide hits were removed from the dataset. Samples were grouped into the treated and control and log2X transformed. Any peptides which did not have reporter ions for at least three samples in one group were removed, and any missing values were replaced from the normal distribution. The data was then transformed 2^X and the median of the reporter ion intensities was established. All reporter ion intensities were normalised to the strongest reporter ion, and the data was transformed log2X. PCA plots, volcano plots and heat maps could then be generated.

2.8.4 Label Free Quantification Using Perseus

The protein groups text file from the MQ search was loaded into Perseus, and the LFQ intensities were loaded into the main column. Potential contaminant hits, reverse database hits and only identified by site hits were filtered out of the data.

Single peptide hits were removed from the dataset. Samples were grouped into the treated and control and log2X transformed. Any peptides with missing values in at least three samples in one group were removed, and any missing values were replaced from the normal distribution. PCA plots, volcano plots and heat maps could then be generated.

2.8.5 Quantification of Phosphopeptides Using Perseus

The Phospho (STY) Sites text file from the MQ search was loaded into Perseus, and intensity 1, 2 and 3 for each sample was loaded into the main column. Potential contaminant hits and reverse database hits were filtered out of the data. The modification table was expanded, samples were grouped into treated and control, and the data was transformed log2X. Peptides with missing values in at least 3 samples in one group were removed from the dataset and missing values were replaced from the normal distribution. PCA plots, volcano plots and heat maps could then be generated.

Chapter 3

Quantitative Protein Analysis of Drought Stressed Maize Material

3.1 Introduction

3.1.1 Drought Stress & Maize

Plant growth is limited by several different abiotic stress factors which can cause both physiological symptoms (wilting, browning of leaves etc.) and subcellular biochemical responses (protein response) in plants (Rejeb *et al.*, 2014). Stress factors include drought, salt and temperature. The effects of climate change mean longer spells without rain are expected in the future, increasing drought conditions in certain areas of the world (Easterling *et al.*, 2000). This combined with the worlds growing population (in 2019 growing at a rate of 1.08% or 82 million per year) means food availability will decrease in the near future (Wallace, 2000).

Drought is caused by insufficient water availability. Drought stress occurs when the soil moisture content falls and the environmental conditions are unable to replenish the water supply (Jaleel *et al.*, 2009). All plants show a certain level of drought tolerance, but this varies substantially between and within species. Plants respond initially to drought stress by closing stomata on leaves to limit gas exchange (Yan *et al.*, 2017). Photosynthesis continues for a short time after stomatal closure, causing build up of CO_2 in cells. During this time sunlight causes the leaf to heat up, but because stomata are closed the leaf cannot transpire to cool down. Stomata closure also increases the build-up of reactive oxygen species (ROS). Continued

drought stress leads to disruption of cell metabolism, cell structure and enzyme activity (Osmolovskaya *et al.*, 2018). Severe stress results in inhibition of growth, photosynthesis, respiration, metabolism disruption and finally cell death (Wang *et al.*, 2018). Between 2001 and 2013 globally drought caused the loss of enough food to feed 81 million people per day according to the World Bank (Richard; *et al.*, 2017).

Maize (*Zea mays*) is a cereal crop in the grass family which produces kernels of seed which are used for food for humans and livestock as well as biofuels. Maize plants usually develop 20-21 leaves during their lifetime, flower (silk) 65 days after sprouting and the cobs are fully mature after 120 days (Cello *et al.*, 1997; Montgomery and Brown, 2008) (Figure 3.1). These time scales and number of leaves can vary depending on variety, environment and the time of year the crop is planted. Global maize production between 2008 and 2010 was 750 million metric tons making maize the world's third largest crop for food production, after wheat and rice, and any effect on its growth cycle leading to loss of yield can be devastating to the food industry especially in developing countries (Shiferaw *et al.*, 2011).

The maize lifecycle consists of two growth stages, the vegetative stage, which takes place from sowing seed to tassel (male flower) production (55-65 days after emergence) and reproductive stage which takes place from silking (female flower) and pollen production to maturity (50-65 days after silking) (Salvador and Pearce, 1995) (Figure 3.1). Maize is particularly susceptible to drought stress because water is needed for cell elongation and the reproductive stage cannot be delayed. Therefore, drought at any point in the maize life cycle can cause loss of yield. The amount of yield loss depends on the stage of growth of the plant and the severity of the drought, but the most water is needed when the plant begins to produce pollen (55-65 days after emergence), therefore yield loss due to drought is most acutely felt when the plant is producing pollen (Doorenbos, 1979). Drought at this time can reduce silk length, inhibit embryo growth, cause emerging silks to become unreceptive to pollen, and interfere with synchronisation between pollen production and silking, causing silks to emerge after pollen production has finished (Herrero and Johnson, 1981).

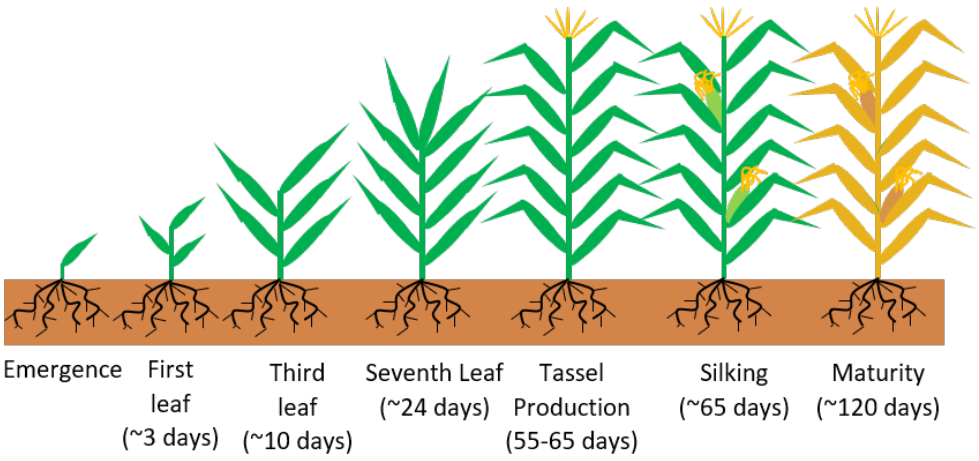

Figure 3.1: The lifecycle of maize, beginning with emergence where the vegetative stage begins, and continues until tassel production between 55 and 65 days when the reproductive stage begins. Maize silks after tassel production at ∼65 days, and plants reach full maturity at ∼120 days.

Abscisic acid (ABA) is known to regulate drought responsive stomatal closure (Osakabe *et al.*, 2014) (Figure 3.2). ABA is a plant hormone produced under drought stress conditions that causes physiological responses and activates signalling networks. Once ABA is produced it binds to ABA receptors, pyrabactin resistance (PYR), pyrabactin resistance-like (PYL) and regulatory component of ABA receptor (RCAR). These ABA receptors undergo a conformational change that allows binding of protein phosphatase 2C (PP2C), in order to inhibit it (Cutler *et al.*, 2010). Under non stress conditions PP2C is bound to sucrose nonfermenting 1 related protein kinase 2 family (SnRK2), preventing it from performing its function of phosphorylating targets (Boudsocq *et al.*, 2007). Mutants with SnRK2 knocked out do not close stomata under drought stressed conditions, causing the plant to wilt (Kulik *et al.*, 2011). SnRK2 is therefore considered an important protein in drought stress response in plants. Mitogen-activated protein kinases (MAPKs) are also stimulated by ABA which modulates their transcription, protein accumulation, and kinase activity (Liu, 2012; Danquah *et al.*, 2014). In the absence of ABA, SnRK2s autophosphorylation is inhibited by binding to PP2C, but in the presence of ABA, PP2C binds to ABA receptors, freeing up SnRK2 to be auto phosphorylated. MAPKs are phosphorylated and regulate an ABA response, though the mechanism by which MAPKS become phosphorylated is unknown. It is thought SnRK2 is involved in the phosphorylation process (Matsuoka *et al.*, 2015; Mitula *et al.*, 2015).

Mitochondria are well known to be involved in cell adaptation to abiotic stress (Pastore *et al.*, 2007). Mitochondria transfer redox equivalents to chloroplasts and peroxisomes in the photorespiratory cycle (Raghavendra *et al.*, 1998). Mitochondria are also involved in the metabolism of proline, which accumulates during drought, and acts as an osmotolerant (Ashraf and Foolad, 2007). Mitochondria are the cell's main source of ROS, a by-product of respiration, which cause oxidative damage, under abiotic stress conditions. Mitochondria help to defend the cell against the ROS produced by firstly keeping the electron transport chain oxidised, thus avoiding ROS production, but once ROS have accumulated, antioxidant enzymes such as super oxide dismutase (SOD), peroxisomal catalase (CAT) and glutathione peroxidase (GPx) are produced for ROS detoxification and mitochondria help to repair of ROS mediated damages (Moller, 2001). Chloroplasts also play a vital role in stress response, and act as sensors for environmental changes thus optimising different cell functions to allow the cell to adapt (Tamburino *et al.*, 2017). Chloroplasts synthesise metabolites which protect plants from abiotic stresses (Yoo *et al.*, 2019).

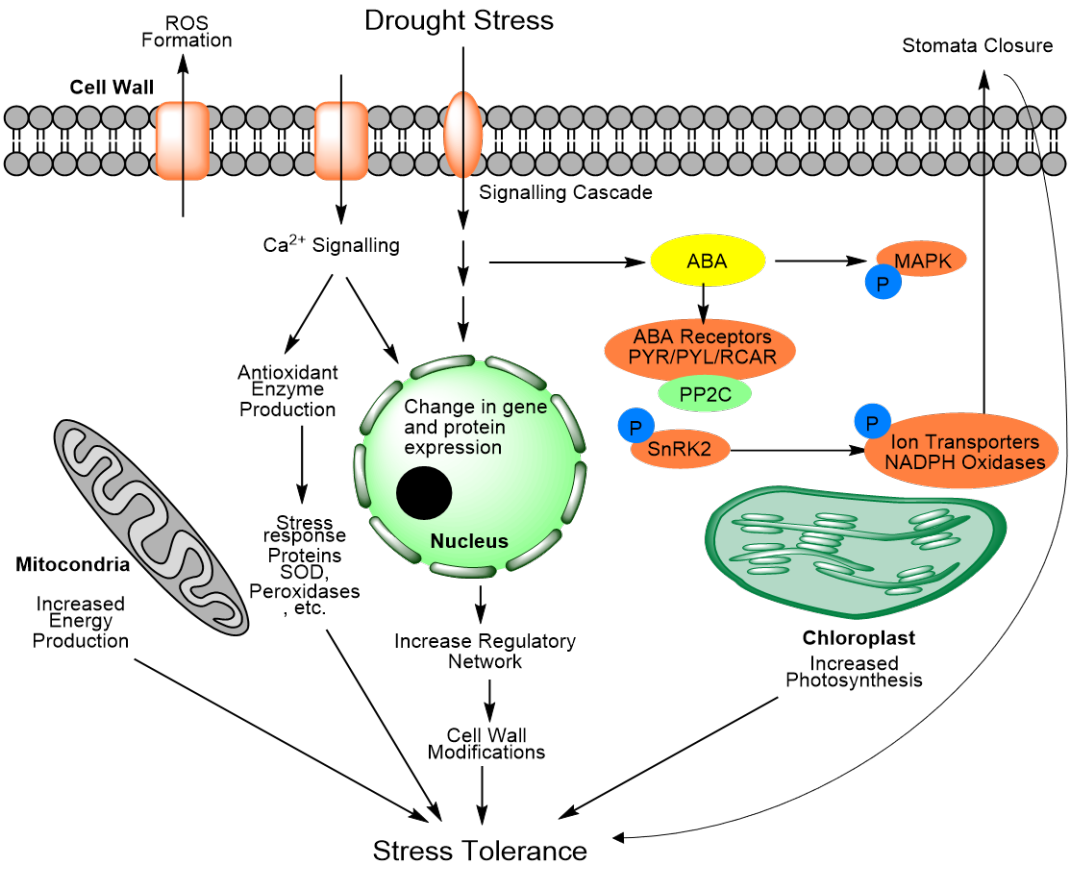

Figure 3.2: Cell response to drought stress and how it improves stress tolerance. Within cells key processes are upregulated during drought stress, which contribute to stress tolerance. These include ABA response pathways which cause stomata closure, increased photosynthesis in the chloroplasts, increased respiration in the mitochondria, calcium signalling which causes antioxidant enzyme production and changes to gene and protein expression.

In the literature different methods have been used to induce drought conditions. These include; withholding water, air drying and chemicals such as polyethylene glycol (PEG). PEG is known to affect the water potential of cells, thus mimicking drought stress caused by air drying (Hohl and Schopfer, 1991; Dami and Hughes, 1997).

3.1.2 Proteomics of Drought Stressed Plants

Arabidopsis thaliana was established as the model plant due to its short lifespan, small size, high seed production and high transgenic efficiency and was the first plant to be fully genome sequenced in 2000. Arabidopsis encodes 25,498 genes (Kaul *et al.*, 2000), and other plant genomes were completed soon after. The availability of these

databases allowed proteome analysis to become easier by enabling high throughput assignment of peptide sequences to tandem mass spectra. Mass spectrometry-based proteomics allows qualitative and quantitative analysis of high numbers of proteins from organisms. Mass spectrometry (MS) also allows information to be gained on post translational modifications (PTMs), protein-protein interactions, and protein function.

Because Arabidopsis is a commonly used model plant, a vast amount of proteomic work ranging from profiling of tissues and organelles to response to stress conditions has been published in the last decade. In Arabidopsis, aldehyde dehydrogenases (ALDHs) have been found to increase in abundance under drought conditions (Ndimba *et al.*, 2005; Seki *et al.*, 2002), and lines which over expressed ALDH genes, were shown to cope better with drought conditions (Rodrigues *et al.*, 2006). ALDHs are a family of enzymes which catalyse the oxidation of reactive aldehydes to carboxylic acids (Stiti *et al.*, 2011). Though they are important for metabolic processes, build-up of aldehydes can become toxic to the cell, meaning ALDHs are important for regulating aldehyde homeostasis, and improving abiotic stress tolerance (Stiti *et al.*, 2011). Studies in Arabidopsis have shown that cytosolic ascorbate peroxidase (APX) significantly increase in abundance under drought conditions (Koussevitzky *et al.*, 2008; Harb *et al.*, 2010). APX plays an important role in regulating levels of H_2O_2 and H_2O_2 signalling (Asada, 1999; Apel and Hirt, 2004; Davletova *et al.*, 2005). Under drought stress conditions in Arabidopsis, ribosomal and oxidative phosphorylation proteins are shown to increase in abundance, showing that plants respond structurally and functionally to drought (Alqurashi *et al.*, 2018; Wang *et al.*, 2016-1). Proteins associated with endocytosis also increase in abundance under drought conditions, which is consistent with stress responses of increased active transport and recycling of membrane proteins, showing that physiological and structural changes are essential for plant survival under drought conditions (Alqurashi *et al.*, 2018). However, Arabidopsis has its limitations in studies of drought stress and its translation to crop studies, because it is dicotyledonous and so far removed from the monocotyledonous crops used in agriculture, studies are not easily translatable from Arabidopsis to crop plants such as maize, wheat, rice and barley (Wijk, 2001).

Wheat (*Triticum aestivum*) is a major food crop in temperate regions of the world and its seeds are rich in glutens and storage proteins (Gill *et al.*, 2004). There have been many proteomic studies into drought response in wheat, and sev-

eral proteins have been identified as changing under drought conditions. Heat shock protein (HSP) 70 is associated with stress response. In wheat HSP 70 was found to increase in abundance under drought conditions (Hajheidari *et al.*, 2006; Alvarez *et al.*, 2014; Qin *et al.*, 2014; Cheng *et al.*, 2015; Hao *et al.*, 2015). Adenosine triphosphate (ATP) synthase is a mitochondrial membrane protein associated with respiration. ATP synthase subunits were found to increase in abundance during drought in wheat (Qin *et al.*, 2014; Budak *et al.*, 2013; Liu *et al.*, 2015; Faghani *et al.*, 2015). Late embryo abundant (LEA) proteins are key biomarkers for drought stress and decrease aggregation of proteins to increase stress tolerance. LEA proteins were found to increase in abundance in several studies (Hajheidari *et al.*, 2006; Alvarez *et al.*, 2014; Mostafa *et al.*, 2010; Jiang *et al.*, 2012; Yang *et al.*, 2011). Rubisco subunits are enzymes involved in carbon fixation during photosynthesis and are key biomarker for drought stress which have been shown to increase in abundance in various studies (Cheng *et al.*, 2015; Hao *et al.*, 2015; Wang *et al.*, 2014; Caruso *et al.*, 2009). Drought causes an increase in ROS activity, which cause irreversible oxidative damage. To combat this there is an increase in antioxidant enzymes such as CAT, SOD and GPx (Qin *et al.*, 2014; Peremarti *et al.*, 2014; Ford *et al.*, 2011).

Rice (*Oryza sativa*) is a staple food for much of the world's population. It is a commonly used cereal crop, and a model system for molecular biology and genetic research. The first large scale proteomic study of rice was performed by Koller *et al.* (2002). They looked at different rice tissues, leaf, root and seeds and were able to identify 2528 proteins between the three tissues. Since then there have been several studies using proteomics to analyse drought stressed rice material. Dehydrogenases are enzymes that catalyse the removal of hydrogen atoms from particular molecules and have been shown to be more abundant under drought stress conditions in rice (Ke *et al.*, 2009; Agrawal *et al.*, 2016; Mirzaei *et al.*, 2014). HSPs are involved in abiotic stress response and are important for stress tolerance in plants. Many studies have shown an increase in HSPs under drought conditions (Mirzaei *et al.*, 2014; Pandey *et al.*, 2009; Wu *et al.*, 2015; Shu *et al.*, 2011; Mirzaei *et al.*, 2012), and overexpression of HSPs in rice has shown to improve drought tolerance (Xiang *et al.*, 2018). Similar to wheat, there is an increase in antioxidant enzymes under drought conditions in rice (Mirzaei *et al.*, 2012; Ji *et al.*, 2012; Ali and Komatsu, 2006; Rabello *et al.*, 2008).

Barley (*Hordeum vulgare*) is a crop typically grown in dry climates, and therefore has a high tolerance for drought and other abiotic stresses because the

plant reduces growth to maintain cellular homeostasis during drought conditions (Rollins *et al.*, 2013). Like in wheat ATP synthase is shown to increase in abundance under drought stress (Ashoub *et al.*, 2013; Wang *et al.*, 2015; Kausar *et al.*, 2013). HSPs were also shown to increase in abundance during drought in barley like in wheat and rice (Ashoub *et al.*, 2013; Kausar *et al.*, 2013). Glutathione peroxidase (GPx) which is an antioxidant enzyme, was shown to increase during drought (Vitamvas *et al.*, 2015).

Maize (*Zea mays*) is one of the most cultivated cereal crop worldwide, alongside wheat and rice. ABA response proteins are key biomarkers for drought stress, but are also important for plant growth, development and fruit ripening. Many studies in maize have shown an increase in abundance of ABA response proteins (Riccardi *et al.*, 1998; Zhao *et al.*, 2016-1; Yang *et al.*, 2014; Riccardi *et al.*, 2004). Dehydrins are produced by plants in response to drought stress, and many papers which studied drought stress in maize identified dehydrins as increasing in abundance (Zhao *et al.*, 2016-1; Yang *et al.*, 2014; Benesova *et al.*, 2012). Malate dehydrogenase is a key enzyme in the citric acid cycle which catalyses the oxidation of malate to oxaloacetate during the reduction of NADP to NADPH during respiration. The levels of malate dehydrogenase increase in maize during drought stress (Riccardi *et al.*, 1998, 2004; Huang *et al.*, 2012). Like wheat, rice and barley, antioxidant enzymes specifically SOD, which helps to break down harmful ROS molecules, were found to increase in abundance in maize during drought (Yang *et al.*, 2014; Huang *et al.*, 2012).

3.1.3 Protein Phosphorylation of Droughted Plant Material

Environmental stresses are known to cause changes to phosphorylation in plant proteins. In response to drought stress, many protein kinases are activated in order to regulate protein activity, including SnRK2, MAPK and calcium related kinases (Du *et al.*, 2011).

Many phosphoproteomic plant studies have been performed in different species in response to stress factors. Phosphorylation of ABA response proteins has been directly linked to drought stress in Arabidopsis (Hu *et al.*, 2015-2), many of these proteins are phosphorylated by SnRK2 (Umezawa *et al.*, 2013). Salt stress inhibits plant growth and development by causing water stress similar to drought. Photosystem II (PSII) reaction centre protein H PsbH is a core complex of PSII which is used for photosynthesis and was found to be phosphorylated in rice during salt

stress treatment (Chang *et al.*, 2012). Betaine-aldehyde dehydrogenase is an enzyme involved in the production of glycine betaine, and the expression of betaine-aldehyde dehydrogenase increases under stress conditions to improve tolerance to abiotic stress (Fitzgerald *et al.*, 2009), as well as phosphorylation levels (Lv *et al.*, 2016). Phosphorylated SOD was also found to increase in abundance in wheat during salt stress, making it a possible salt stress marker in wheat (Lv *et al.*, 2016). 2-Cys peroxiredoxin BAS1 catalyses the reduction of hydrogen peroxide and organic hydroperoxides to water and alcohols and play a role in protecting the cell from oxidative stress. 2-Cys peroxiredoxin BAS1 phosphorylation levels are shown to increase during abiotic stress in wheat (Lv *et al.*, 2016). MAPK plays a role in signalling during drought response. It is phosphorylated during this pathway, so levels of phosphorylation on this protein increase in abundance (Vu *et al.*, 2016). Levels of phosphorylation on PP2C is shown to decrease in abundance (Vu *et al.*, 2016). PP2C inhibits SnRK2 under normal conditions, however under stress conditions SnRK2 is released, so it can phosphorylate other proteins (Figure 3.2). It has been suggested that root proteins in barley need to be phosphorylated by a staurosporine sensitive kinase in order to transport water during salinity stress (Horie *et al.*, 2011).

3.1.4 Aims & Objectives

The aim of this chapter was to identify changes to the proteome of maize during drought stress. To achieve this aim maize plants which had been droughted when they started to produce pollen were used, because they are most susceptible to yield loss at this stage. From these samples proteins were extracted for proteomic analysis. Then label free and isobaric tagging approaches were used as quantitative methods to measure protein abundance. Three different types of maize tissue were used; leaf, silk and tassel. The silk and tassel tissues were of particular interest because they are the reproductive tissues, and so could give insight into the effect drought has on the proteins, and how they cause yield loss. Drought also causes modifications to the proteome and because many signalling pathways use phosphorylation, and phosphorylation occurs at sub stoichiometric levels, enrichment of phosphopeptides was used to determine likely signalling events during drought responses.

3.2 Results

3.2.1 Drought Treatment of Maize

Maize B73 plants were used for all experiments, because it has been fully genome sequenced and the proteome predicted, so peptides can be easily assigned to maize proteins from the MS analysis. *Zea mays* proteome UP000007305 was used which contains 39,400 genes and 99,254 predicted proteins.

To determine if maize plants were drought stressed under greenhouse conditions, soil moisture readings were taken using an SM150T soil moisture sensor and converted from voltage to percentage, based on the peat soil type used to grow the plants. Three biological replicates were used for leaf experiments, and a total of five replicates for each treatment were used. The soil moisture content readings (Figure 3.3) show the percentage of moisture in the soil used for the experiments. The drought period can be seen for each replicate at 18/04/17, 09/05/17 and 19/06/17 respectively for a seven-day period, during which time the percentage moisture in the soil dropped. There is a slight drought period of the control plants in batch 4, this is due to issues with watering over the weekend. Leaves were harvested at the end of this period, after which water was reapplied to droughted plants and they were left to grow and set seed. Once seeds were fully grown, they were harvested and measured.

To determine the impact of applied drought stress on yield, the seeds were weighed once harvested, and then dried for 3 days, to remove moisture and weighed again (Figure 3.4). Drought stressed plants had a lower yield than the control plants. In batch 5 the fresh weight of the control and droughted cobs are very similar, however when they were dried there was a far bigger difference, and the droughted cobs had a much lower yield.

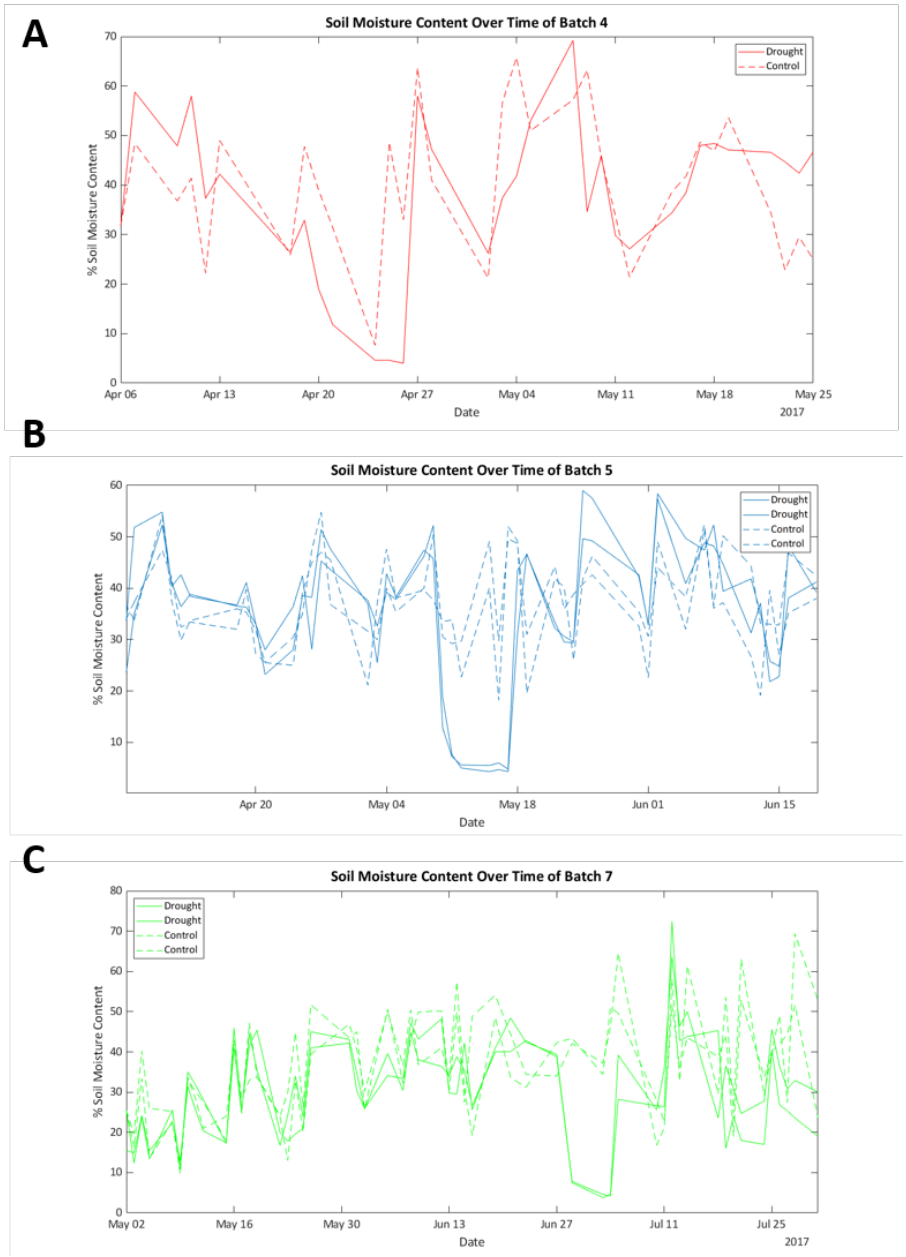

Figure 3.3: Soil moisture content of the plants used for the experiments. A is the percentage soil moisture content of plants from batch 4, B batch 5 and C batch 7. The plants were droughted for one week when they began to produce pollen and harvested at the end of the drought period. Leaves were harvested on (A) 26/04, (B) 18/05, and (C) 04/07.

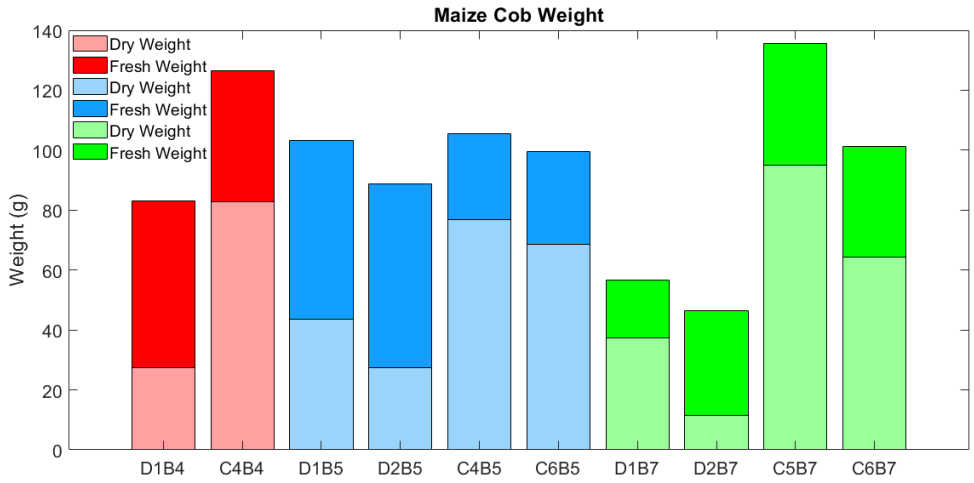

Figure 3.4: The effect of drought on cob yield. The weight of the cobs before and after drying for 3 days at 37^oC is shown. D is drought, C is control and B is batch. The droughted cobs weigh less than the control cobs, both before and after drying, but the effect is seen more after drying.

Once an effective treatment had been established, protein was extracted from harvested leaves (second leaf from bottom of plant) and digested with trypsin. Three different MS methods were used to analyse proteins; tandem mass tag (TMT) quantification, label free quantification (LFQ) and phosphopeptide enrichment (Figure 3.5). From here proteins were quantified and signalling events identified.

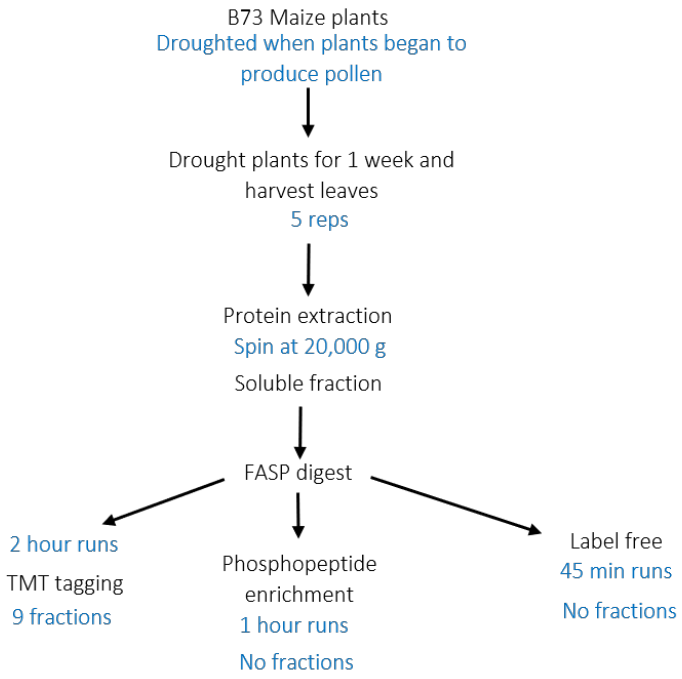

Figure 3.5: Plants were grown until they began to produce pollen, then half the plants were droughted for one week, after which the second leaf from the bottom was harvested from each plant and flash frozen in liquid nitrogen. Proteins were extracted using a PBS buffer and centrifugation. Proteins were then filter aided sample preparation (FASP) digested. 0.2 mg of protein from each sample was tagged with TMT, these were then combined and fractionated via high pH fractionation into 9 fractions and each was analysed via MS for 2 hours. Each sample was also analysed separately in an LFQ experiment for 45 mins. The rest of the samples were enriched for phosphopeptides and analysed for an hour each on the MS.

3.2.2 Tandem Mass Tag Analysis of Droughted Leaf Material

To identify proteins which changed in abundance in maize leaves after drought stress, bottom up proteomics was used, using liquid chromatography-tandem mass spectrometry (LC-MS/MS) (Orbitrap Fusion). Proteins were quantified using the Tandem Mass Tag (TMT) 10plex and data analysed using MaxQuant (MQ) and Perseus. TMT 10plex allows for direct comparison between samples. Samples were tagged with different TMT 10plex molecules and then combined for analysis. Each tag has the same isobaric mass and chemical structure, however the position of various heavy isotopes within the molecule creates different masses during MS2 fragmentation. The mass of the reporter ion will be different for each sample and is used to quantitatively measure protein abundance during peptide fragmentation

for ten multiplex samples.

To determine if the proteome changed during drought stress, a principal component analysis (PCA) was performed (Figure 3.6A). The PCA groups samples according to their main components; samples with similar protein compositions are grouped together. The droughted and control samples separate along component one in the PCA which amounts to 44.2% of the sample, showing that the drought treatment is changing the proteins abundances. Whilst the samples do not separate along component two this is 26.6% of the sample and therefore less significant than component one.

Volcano plots are produced using a two-sided t-test. The false discovery rate (FDR) is the negative log of the student t-test p-value and is the proportion of proteins which are incorrectly assigned as significant. In the volcano plot s0 is the minimum fold change, which filters out proteins which have low p-values and low fold changes, not showing them as significant. Proteins with low p-values and a fold change higher than the s0 are shown as significant on the volcano plot (Tusher *et al.*, 2001). In this work an FDR of 0.05 and an s0 of 0.1 were used, there is no accepted norm for reporting statistical significance levels for proteomic data according to the Molecular and Cellular Proteomic guidelines, and an FDR of 0.05 is generally accepted as being the usual cut off for student t-tests. The s0 should be small, and increasing the s0 puts a greater emphasis on the mean of the data, therefore unless the data is unusual in some way a small s0 value should be used.

In total, 1114 proteins were identified and quantified, of which 271 proteins were identified as significantly changing under the drought stress conditions (Figure 3.6B). 94 proteins were found to be significantly increasing in abundance under drought stress and 177 proteins were significantly decreased in abundance under drought stress. The proteins that increased significantly in abundance by more than log2 of one (to keep the table to a manageable size) under drought stress are presented in Table 3.1 and the proteins that decrease under drought stress are shown in Table 3.2. The proteins which significantly increased in abundance were generally associated with ABA response, dehydrins and stress response proteins. The proteins which significantly decreased in abundance were predominantly associated with stress response, ATP binding and ABA response.

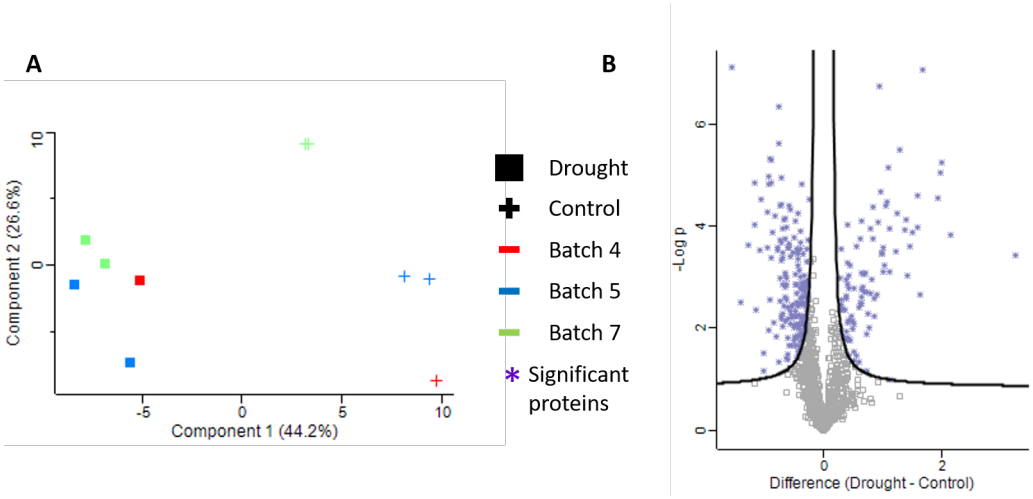

Figure 3.6: (A) PCA plot of the TMT tagged leaf samples. The PCA plot shows separation between the drought and the control samples. (B) The volcano plot shows the proteins which are significantly different between the drought and the control samples, log2 fold change is plotted against -logp value. 1114 proteins were identified of which 271 proteins (purple stars) have significant changes in their abundance. FDR: 0.05 s0: 0.1.

Table 3.1: Proteins that significantly increased in abundance with a log2 fold change of more than 1 under drought conditions.

Protein Name	**Gene Number**	**Log2 Fold Change**	**-Log P Value**	**MQ Score**	**Function/Pathway**
Dehydrin DHN1 (RAB17 protein)	rab17 ZEAMMB73_ Zm00001d037894	3.26	3.43	59.50	Cold acclimation, response to abscisic acid, response to water deprivation
Dehydrin3	542251 ZEAMMB73_ Zm00001d051420	2.15	3.84	76.00	Cold acclimation, response to abscisic acid, response to water deprivation
Abscisic acid stress ripening3	ZEAMMB73_ Zm00001d0037124	2.01	5.25	79.15	Response to water deprivation and fruit ripening
PEBP (Phosphatidyl ethanolamine-binding protein) family protein	100279044 ZEAMMB73_ Zm00001d010586	1.98	5.04	94.36	Lipid binding, neuronal development, serine protease inhibition, the control of the morphological switch between shoot growth and flower structures, and the regulation of several signalling pathways such as the MAP kinase pathway
Abscisic acid stress ripening1	542304 ZEAMMB73_ Zm00001d023529	1.94	4.54	18.27	Response to water deprivation and fruit ripening

Continued on next page

Table 3.1 – *Continued from previous page*

Protein Name	**Gene Number**	**Log2 Fold Change**	**-Log P Value MQ Score**	**Function/Pathway**	
Sucrose synthase	542365 ZEAMMB73_ Zm00001d045042	1.69	7.06	121.06	Sucrose metabolic process
17.4 kDa class I heat shock protein 3	100274593 ZEAMMB73_ Zm00001d028555	1.64	2.65	34.99	Protein complex oligomerization, protein folding, response to heat, response to hydrogen peroxide, response to reactive oxygen species, response to salt stress
Alkyl transferase	ZEAMMB73_ Zm00001d019629	1.60	4.60	77.04	Polyprenol biosynthetic process
Malate synthase	ZEAMMB73_ Zm00001d003247	1.60	3.98	19.67	Glyoxylate cycle, tricarboxylic acid cycle
Alkaline alpha galactosidase 2	ZEAMMB73_ Zm00001d037480	1.51	3.88	18.88	Raffinose family oligosaccharide biosynthetic process, response to cold, response to karrikin, response to oxidative stress
Late embryogenesis abundant protein, group 3	542216 ZEAMMB73_ Zm00001d038870	1.47	3.61	25.09	Response to water deficiency

Continued on next page

Table 3.1 – *Continued from previous page*

Protein Name	**Gene Number**	**Log2 Fold Change**	**-Log P Value MQ Score**	**Function/Pathway**	
ABA-responsive protein	100285725 ZEAMMB73_ Zm00001d023664	1.42	3.04	37.04	Embryo development ending in seed dormancy, maintenance of seed dormancy by absisic acid, regulation of seed germination, seed germination
4-hydroxyphenylpyruvate dioxygenase	ZEAMMB73_ Zm00001d015356	1.40	4.14	45.40	Tyrosine catabolic process
Glutathione transferase19	ZEAMMB73_ Zm00001d036951	1.38	3.93	39.04	Glutathione metabolic process
Cylicin-1	103648259 ZEAMMB73_ Zm00001d007901	1.30	5.48	14.02	
Asparagine synthetase [glutamine-hydrolyzing]	100192350 ZEAMMB73_ Zm00001d028750	1.25	4.26	45.91	Asparagine biosynthetic process, glutamine metabolic process
Non-specific lipid-transfer protein	ZEAMMB73_ Zm00001d044686	1.24	3.50	14.58	Lipid transport

Continued on next page

Table 3.1 – *Continued from previous page*

Protein Name	**Gene Number**	**Log2 Fold Change**	**-Log P Value MQ Score**	**Function/Pathway**	
Hydroxyproline-rich glycoprotein family protein	100274292 ZEAMMB73_ Zm00001d040190	1.13	3.94	57.25	Structural protein in plant cell walls
V-type proton ATPase catalytic subunit A	ZEAMMB73_ Zm00001d015427	1.13	3.10	6.22	ATP metabolic process
Nucleosome assembly protein 1	100279994 ZEAMMB73_ Zm00001d011130	1.12	1.00	7.07	Nucleosome assembly
Glutathione transferase23	ZEAMMB73_ Zm00001d020780	1.10	5.14	58.38	Glutathione metabolic process
Sucrose synthase	103634623 ZEAMMB73_ Zm00001d029087	1.09	4.48	48.06	Sucrose metabolic process
MtN19-like protein	100281705 ZEAMMB73_ Zm00001d031677	1.06	4.41	14.03	

Continued on next page

Table 3.1 – *Continued from previous page*

Protein Name	**Gene Number**	**Log2 Fold Change**	**-Log P Value MQ Score**	**Function/Pathway**
Glycine-rich protein	100191540 ZEAMMB73_ Zm00001d037239	1.03	3.24	31.46	Involved in cellular response and signalling
V-type proton ATPase subunit G	100282544 ZEAMMB73_ Zm00001d005253	1.01	3.11	29.30	Proton-exporting ATPase activity, phosphorylative mechanism
17.4 kDa class III heat shock protein	100191598 ZEAMMB73_ Zm00001d018298	1.01	3.58	20.14	Protein complex oligomerization, protein folding. response to heat, response to high light intensity, response to hydrogen peroxide, response to reactive oxygen species, response to salt stress

Table 3.2: Proteins that significantly decreased in abundance with a log2 fold change of more than 1 under droughted conditions.

Protein Name	**Gene Number**	**Log2 Fold Change**	**-Log P Value**	**MQ Score**	**Function/Pathway**
Phosphoenolpyruvate carboxykinase1	541622 ZEAMMB73_ Zm00001d028471	-1.55	7.11	177.80	ATP binding, kinase activity, phosphoenolpyruvate carboxykinase (ATP) activity, gluconeogenesis
Pyruvate, phosphate dikinase 1, chloroplastic	PPDK1 C4PPDKZM1 CYPPDKZM1 PPDK2	-1.40	2.51	8.39	Chloroplast, ATP binding, kinase activity, metal ion binding, pyruvate, phosphate dikinase activity, photosynthesis, pyruvate metabolic process
Catalase	ZEAMMB73_ Zm00001d054044	-1.26	3.63	88.75	Cytoplasm, plasma membrane, catalase activity, heme binding, metal ion binding, circadian rhythm, hydrogen peroxide catabolic process, response to abscisic acid, response to bacterium, response to heat, response to hydrogen peroxide, response to light stimulus, response to salt, response to water deprivation
Lipoxygenase	100037805 ZEAMMB73_ Zm00001d002000	-1.16	4.04	323.31	Metal ion binding, oxidoreductase activity, acting on single donors with incorporation of molecular oxygen, incorporation of two atoms of oxygen, oxylipin biosynthetic process

Continued on next page

Table 3.2 – *Continued from previous page*

Protein Name	**Gene Number**	**Log2 Fold Change**	**-Log P Value**	**MQ Score**	**Function/Pathway**
OSIGBa0147B06.5 protein	100192993 ZEAMMB73_ Zm00001d004452	-1.16	4.84	38.44	
Tryptophan aminotransferase-related protein 4	ZEAMMB73_ Zm00001d043650	-1.14	2.35	20.53	Integral component of membrane, carbon-sulfur lyase activity, transaminase activity
Catalase	542230 ZEAMMB73_ Zm00001d027511	-1.07	3.52	28.13	Peroxisome, plasma membrane, catalase activity, heme binding, metal ion binding, cell redox homeostasis, circadian rhythm, hydrogen peroxide biosynthetic process, hydrogen peroxide catabolic process, nitric oxide homeostasis, protein nitrosylation, response to abscisic acid, response to bacterium, response to cadmium ion, response to hydrogen peroxide, response to light stimulus, response to salt, response to water deprivation
Putative 2-oxoglutarate-dependent dioxygenase AOP1	100272363 ZEAMMB73_ Zm00001d003311	-1.06	4.52	61.08	Dioxygenase activity, indole-3-acetaldehyde oxidase activity, metal ion binding, auxin catabolic process, auxin homeostasis

Continued on next page

Table 3.2 – *Continued from previous page*

Protein Name	**Gene Number**	**Log2 Fold Change**	**-Log P Value**	**MQ Score**	**Function/Pathway**
Oxygen evolving complex2	ZEAMMB73_Zm00001d021703	-1.02	1.50	7.61	Chloroplast, extrinsic component of membrane, photosystem II oxygen evolving complex, calcium ion binding, electron transporter, transferring electrons within the cyclic electron transport pathway of photosynthesis activity, photosynthetic electron transport chain
Methionine–tRNA ligase chloroplastic/mitochondrial	ZEAMMB73_Zm00001d028038	-1.01	1.15	12.67	ATP binding, methionine-tRNA ligase activity, methionyl-tRNA aminoacylation

3.2.3 Identification of Drought Related Signalling Using Phosphoproteomics in Maize Leaves

Phosphorylation is a post translational modification (PTM) used for signalling in plants and animals. To identify drought related signalling events, mediated by phosphorylation, phosphopeptides were enriched for using TiO_2 beads under acidic conditions and eluted from the beads by raising the pH. LC-MS/MS data was analysed using MQ and Perseus, missing values were imputed from the normal distribution. If samples had a significantly lower number of peptides identified than other samples in the same experiment they were discounted from the analysis.

Phosphopeptide enrichment was performed on soluble proteins extracted from leaf material. A PCA plot was used to establish a difference between data from the droughted and control leaves, and shows samples separate along component one (33.9%), they do not separate by component two (24.6%) (Figure 3.7A). Two control and one drought samples were removed from the analysis because they had significantly fewer peptides than the other samples (less than 1000 peptides, compared to 1500 peptides in other samples) and were therefore affecting the quantification measurements for the analysis. 589 phosphopeptides were identified which mapped to 387 proteins, of which 61 phosphopeptides had statistically significant differences between the drought and the control (Figure 3.7B). A heat map was used to compare the significantly changing phosphopeptides between the control and the drought treatment (Figure 3.8). The phosphopeptides which significantly increased in abundance in the droughted over the control, with a log2 fold change of more than three (to make the size more manageable) are shown in Table 3.3 and the phosphopeptides which significantly decreased in abundance with a log2 fold change of more than three are shown in Table 3.4.

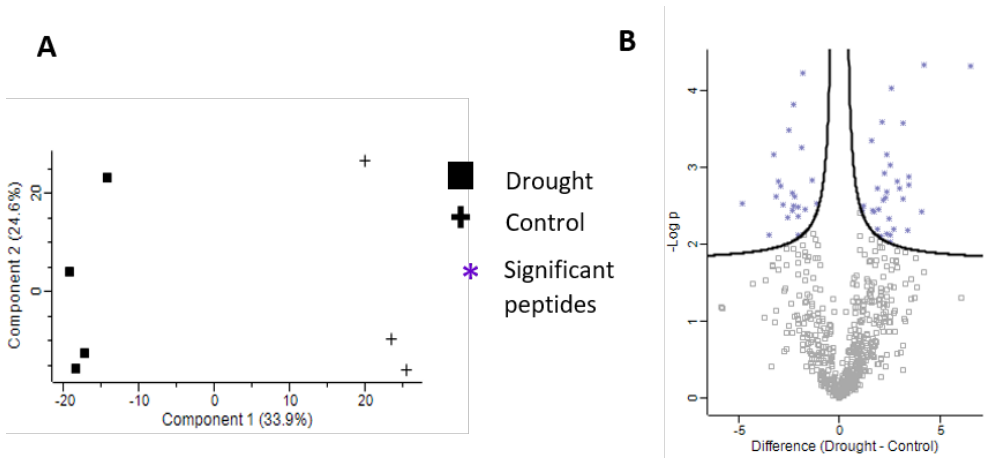

Figure 3.7: (A) PCA plot of the phosphopeptides identified from maize leaf samples. The PCA plot shows separation between the drought and the control samples. (B) The volcano plot shows the peptides which are significantly different between the drought and the control samples, log2 fold change is plotted against -logP value. 589 phosphopeptides were identified of which 61 had significantly changed ratio. FDR: 0.05 s0: 0.1.

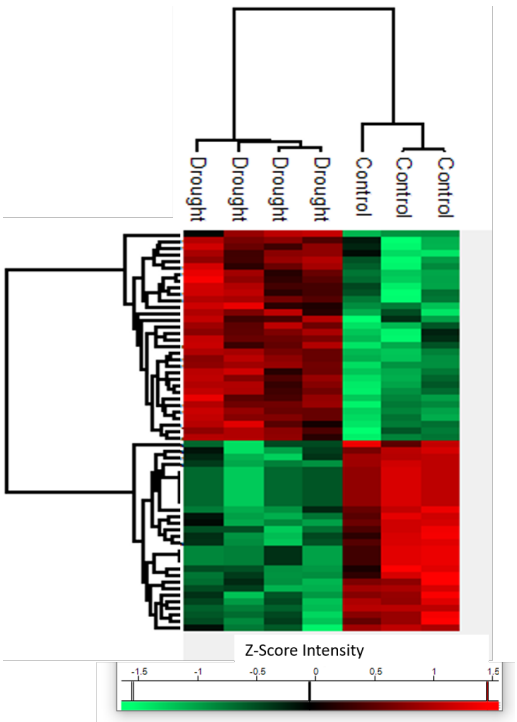

Figure 3.8: Heat map of the 61 significantly changing phosphopeptides in the maize drought treated leaves. Significant phosphopeptides log2 values have been z-scored for graphical representation.

In the phosphoproteomics data obtained from droughted maize leaves, the majority of phosphopeptides identified were mono phosphorylated (89.8%), 8.1% carried two phosphorylated residues and 2.0% carried three. There were 79.6% phosphoserine, 20.2% phosphothreonine and 0.2% phosphotyrosine identified in this study which is similar to proportions found in previous studies (Wu *et al.*, 2015; Vu *et al.*, 2016; Marcon *et al.*, 2015). To the best of my knowledge none of the significantly changing phosphorylation sites identified in the drought leaf study have previously been identified (as of February 2020 these modifications were not in UNIPROT).

Table 3.3: Phosphopeptides which significantly increase in abundance in the droughted leaf samples with a log2 fold change of more than 3 which map to proteins.

Protein Name	**Peptide AA Sequence**	**Gene Number**	**Log2 Fold Change**	**-Log P Value**	**MQ Score**	**Function/Pathway**	**Site & Position**
p-loop containing nucleoside triphosphate hydrolase superfamily protein	SI**S**ETTLER	103634999 ZEAMMB73_Zm00001d008983	6.52	4.31	159.83	Hydrolase activity	S162
Blue-light receptor phototropin 2	NRL**S**ENTELQSAK	ZEAMMB73_Zm00001d032353	4.19	1.63	191.63	ATP binding; blue light photoreceptor activity; FMN binding; identical protein binding; protein serine/threonine kinase activity	S530

Continued on next page

Table 3.3 – *Continued from previous page*

Protein Name	**Peptide AA Sequence**	**Gene Number**	**Log2 Fold Change**	**-Log P Value**	**MQ Score**	**Function/Pathway**	**Site & Position**
S-adenosyl-L-methionine-dependent methyltransferase superfamily protein	SSE**S**MSNLTK	100274302 ZEAMMB73_Zm00001d043827	4.17	4.32	123.01	Methyltransferase activity	S205
Sucrose synthase2	SIAADSW**S**VR	ZEAMMB73_Zm00001d029091	4.09	2.42	109.72	Sucrose synthase activity	S53
ABC-2 type transporter family protein	SS**S**IGNGVQFLNR	100216600 ZEAMMB73_Zm00001d027723	3.78	1.81	154.67	ATPase activity; ATPase-coupled transmembrane transporter activity; ATP binding	S152
Neutral/alkaline invertase	AK**S**DHLAPSLSLSR	100281530 ZEAMMB73_Zm00001d051666	3.47	2.88	166.03	Glycopeptide alpha-N-acetylgalactosaminidase activity; sucrose alpha-glucosidase activity	S25

Continued on next page

Table 3.3 – *Continued from previous page*

Protein Name	**Peptide AA Sequence**	**Gene Number**	**Log2 Fold Change**	**-Log P Value**	**MQ Score**	**Function/Pathway**	**Site & Position**
Sister chromatid cohesion 1 protein 4	ASSQA**S**LADPDDFDLTR	103636402 ZEAMMB73_Zm00001d012156	3.43	2.76	101.15	Sister chromatid cohesion	S14
DNA binding protein	VHE**S**PVLSPQR	100283408 ZEAMMB73_Zm00001d006034	3.41	2.18	183.99	AT DNA binding	S12
ATP binding protein	TPA**T**PPSSGGTQGLR	103633160 ZEAMMB73_Zm00001d021473	3.25	1.89	106.32	ATP binding; protein kinase activity	T27
Uncharacterized protein	AQSGVM**T**AETGTYR	ZEAMMB73_Zm00001d043736	3.17	2.58	107.69		T182
Ferredoxin–NADP reductase, chloroplastic (FNR) (EC 1.18.1.2)	VH**S**VLESEPR	100282643 ZEAMMB73_Zm00001d011833	3.14	3.57	129.00	Ferredoxin-NADP+ reductase activity; nucleotide binding	S114

Table 3.4: The phosphopeptides which significantly decrease in abundance in the leaf with at least a log2 fold change of 3, mapped to proteins.

Protein Name	**Peptide AA Sequence**	**Gene Number**	**Log2 Fold Change**	**-Log P Value**	**MQ Score**	**Function/Pathway**	**Site & Position**
Phosphoenol pyruvate carboxykinase1	GGAH**S**PFAVAI**S**EEER	541622 ZEAMMB73_ Zm00001d028471	-4.79	2.53	188.00	ATP binding; kinase activity; phosphoenolpyruvate carboxykinase (ATP) activity	S59; S66
VQ domain-containing protein	YSPGDLDSGAAAQGL**S**PR	ZEAMMB73_ Zm00001d027824	-3.48	2.12	94.19	Positive regulation of DNA-binding transcription factor activity	S84
Phosphoenol pyruvate carboxylase 3	A**S**TKAPGPGEK	ZEAMMB73_ Zm00001d024980	-3.32	1.72	176.87	Phosphoenolpyruvate carboxylase activity	S3
Phosphoenol pyruvate carboxykinase1	SAP**ST**PKRSAPTTPIK SAP**ST**PKRSAPT**T**PIK	541622 ZEAMMB73_ Zm00001d028471	-3.31	1.71	129.29	ATP binding; kinase activity; phosphoenolpyruvate carboxykinase (ATP) activity	S51; T52; T60
AAA-type ATPase family protein	SPLQNSP**T**FNR	100273408 ZEAMMB73_ Zm00001d045483	-3.26	3.16	210.95	ATP binding	T168

Continued on next page

Table 3.4 – *Continued from previous page*

Protein Name	**Peptide AA Sequence**	**Gene Number**	**Log2 Fold Change**	**-Log P Value**	**MQ Score**	**Function/Pathway**	**Site & Position**
Pyruvate orthophosphate dikinase2	GGM**T**SHAAVVAR	ZEAMMB73_Zm00001d010321	-3.15	2.62	171.26	ATP binding; kinase activity; pyruvate, phosphate dikinase activity	T308
Uncharacterized protein	SY**S**ASYERPTTAAPSTVQR	100273352 ZEAMMB73_Zm00001d053568	-3.04	1.66	118.21		S31
Bifunctional protein FolD 2	ADATVSVVH**S**R	100272563 ZEAMMB73_Zm00001d010867	-3.04	1.82	143.55	Methylenetetrahydrofolate dehydrogenase (NADP+) activity	S61
Phosphoenol pyruvate carboxykinase homolog2	**S**AP**TT**PIKGGAHSPFAVAISEEER	ZEAMMB73_Zm00001d047893	-3.02	2.81	128.04	ATP binding; kinase activity; phosphoenolpyruvate carboxykinase (ATP) activity	S55; T58; T59

3.2.4 Phosphosite Motif Analysis of Drought Stressed Maize Leaves

Motifs are common patterns around a modification site. Phosphopeptides from the drought leaf experiment were analysed for motifs using Maximal Motif Finder for Phosphoproteomics datasets (MMFPh) and linear motif analysis in Perseus. The motifs identified in the leaf dataset are shown in Table 3.5.

The linear motif analysis in Perseus maps motifs to peptides but uses human data to do this. Of the phosphopeptides which significantly increased in abundance 11 were found to have MAPK substrate motifs, including sister chromatid cohesion 1 (S14, log2 fold change -3.43), DNA binding protein (S12, log2 fold change 3.41) and Serine/arginine-rich splicing factor (S191, log2 fold change 2.86). One of the phosphopeptides identified as having a MAPK motif was an uncharacterised protein (T182, log2 fold change 3.17), this could give an insight into the function of this protein. 8 phosphopeptides which significantly decreased in abundance with MAPK substrate motifs were identified, including phosphoenolpyruvate carboxykinase 1 (S51 S52 T60, log2 fold change -3.31), bifunctional protein FolD 2 (S61, log2 fold change -3.04) and phosphoenolpyruvate carboxykinase homolog2 (S47, log2 fold change -2.51). 18 phosphopeptides which increased in abundance with a casein kinase II substrate were also identified. Casein kinase is serine/threonine kinase which regulates cell cycle control.

The MMFPh motif analysis of the whole dataset showed 8 significant motifs present in the dataset (Table 3.5), of which three were found to be significant in just the significant data, these were RxxS, sP and tP. Peptides which contain sP and tP motifs are thought to be substrates for MAPK, SnRK2, receptor like kinases (RLKs), AGC protein family kinases, cyclin dependent kinases (CDKs), calcium dependent protein kinases and (CDPKs) and STE20 like kinases (SLKs) (van Wijk *et al.*, 2014). Most of the motifs identified in my dataset were the proline directed motifs associated with kinase activity. The RxxS motif which is also present in the dataset is also recognised by MAPKs (Vu *et al.*, 2016).

Table 3.5: Motif analysis of the drought leaf phosphopeptide experiment.

Motif	Foreground Matches	Background Matches	Occurrence Threshold	Score
————SPP————-	29	18341	29	3.69
————TP————	35	119007	29	2.40
————-P-SP————	46	17636	44	4.41
————S—-P———-	53	208776	44	1.05
————S-P———-	68	214243	58	1.37
————-P-S————	58	206526	58	1.20
————R–S————	117	217450	87	2.13
————SP————	175	205541	87	2.80

3.2.5 Comparison of Tandem Mass Tag & Label Free Quantification Methods

TMT is used for protein quantification; samples can be combined to be directly compared quantitatively. Pooling samples decreases MS time but increases sample complexity, with the increased complexity in order to get the depth of analysis, samples were fractionated using high pH columns. The labelled sample was fractionated into 9 fractions which were each analysed for 2 hours, giving a total of 18 hours of MS analysis time.

LFQ MS runs are another way to gain quantitative information from samples. LFQ has disadvantages, in that samples all need to be run immediately sequentially, in order to rule out changes to the column affecting retention time, thus interfering with quantitative data. Samples need to be run for the same amount of time, which can lead to a lot of MS time being needed, which is expensive and time consuming. 10 samples were analysed with an LC gradient time of 45 mins each giving a total of 7.5 hours of MS analysis time.

TMT and LFQ experiments were performed on the same samples in order to interpret which is more effective at identifying proteins and those that significantly change. 1114 proteins were identified in the TMT analysis and 906 in the LFQ analysis of which 639 proteins were identified in both (Figure 3.9). 94 were identified to significantly increase in abundance in the TMT analysis and the LFQ identified 141 proteins of which 47 proteins were seen in both (Figure 3.9). 177 proteins were identified to significantly decrease in abundance using TMT and 77 proteins were identified in the LFQ analysis, of which 58 proteins were seen in both (Figure 3.9).

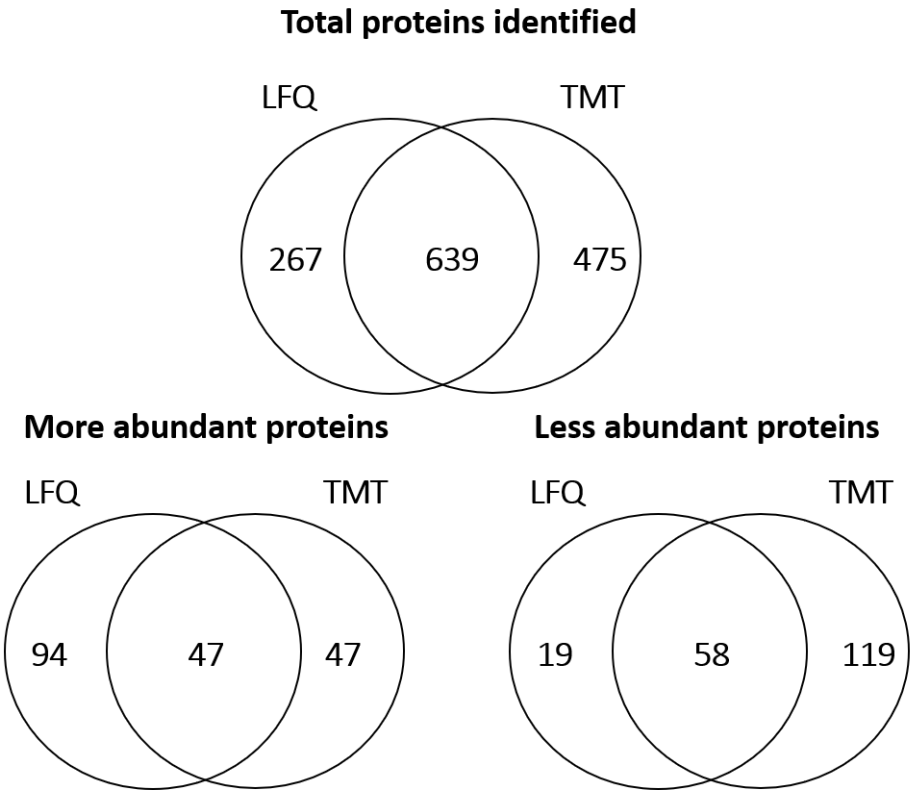

Figure 3.9: Proteins identified in the LFQ and TMT analysis and their overlap, and the overlap between the proteins which significantly increased and decreased in abundance.

When comparing the TMT and LFQ experiments, the proteins identified were mostly the same, with 267 proteins being identified in the LFQ experiment and not in the TMT experiment, whereas 475 proteins were identified in the TMT experiment and not in the LFQ. Therefore, the TMT gave more insight into the proteins present than the LFQ experiment. TMT can cause suppression of ratios between samples because the 1 Th window of isolation of peptides will isolate more than one peptide, therefore the reporter ions used for quantification will also be from other less abundant peptides isolated within this 1 Th window (Savitski *et al.*, 2013). This can be combatted by doing MS3 (Ting *et al.*, 2011), however, this will slow down the MS run because the Orbitrap is performing both the MS1 and MS3 runs and needs to be emptied each time, and whilst an MS3 run is being done, peptides coming off the LC column are not being analysed, therefore less proteins are identified (Sonnett *et al.*, 2018). Later in chapter 4 the use of MS3 when analysing TMT data will be looked at.

There are issues associated with LFQ analysis as well. Firstly, it relies on the retention time of the LC column being stable. However, retention times vary in LC columns, usually by up to 3 minutes (Lai *et al.*, 2011). This makes peptide alignment an issue for data analysis, and whilst algorithms will do this alignment, issues arise as to whether this alignment should be done before or after peptide assignment, and how the alignment should be performed (Lai *et al.*, 2013), there are many different approaches, such as OpenMS/TOPP which aligns peptides from different samples by plotting them as a 2D image, SuperHirn builds on this method by adding peptide identities to improve alignment (Kohlbacher *et al.*, 2007; Mueller *et al.*, 2007).

The TMT ratio suppression can be seen in all the data, particularly in the proteins which increased in abundance, where the LFQ experiment identified 94 proteins to be significantly increased in abundance in the droughted samples which the TMT experiment did not identify, which included ABA response proteins and stress response proteins. 100 of the proteins identified as significantly increasing in abundance in the LFQ experiment had a log2 fold change of more than 1, whereas only 26 proteins had a log2 fold change of more than 1 and only three were above 2, whereas the LFQ experiment showed 37 proteins with a log2 fold change of more than 2 (Figure 3.10).

The LFQ experiment showed 31 proteins which significantly decreased in abundance with a log2 fold change of more than 1, whereas the TMT experiment only showed 10 proteins with a log2 fold change of more than 1 and no proteins with a log2 fold change of more than 2, further showing the ratio supression seen in the TMT experiment (Figure 3.10). Three of the most significant proteins identified in the TMT experiment were not identified as significant in the LFQ experiment, and ten of the most significant proteins seen in the LFQ experiment were not seen in the TMT experiment, including the most significant protein, which was ferredoxin-thioredoxin reductase, which is involved in photosynthesis and oxidative stress responses (Keryer *et al.*, 2004). Many proteins are still identified as significant using TMT, but the fold change is lower due to ratio suppression.

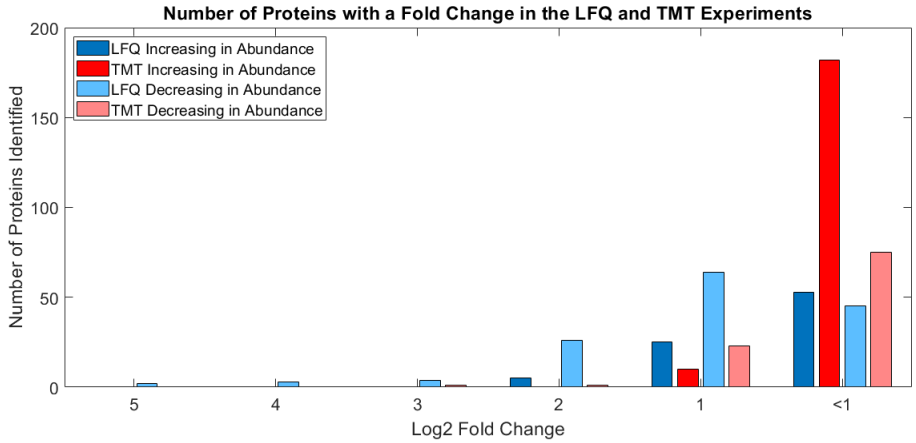

Figure 3.10: The number of proteins with each fold change in the LFQ and TMT experiments. In the higher fold changes only, proteins identified with LFQ are seen. There are also more proteins identified in the LFQ experiment with a log2 fold change of 1 than the TMT experiment. It's only in the proteins with a fold change of less than 1 where the TMT experiment identifies more than the LFQ experiment. This is showing the ratio supression in the TMT experiment.

Whilst TMT and LFQ experiments did identify the same proteins, there is a difference in the significant proteins identified. This should be noted before performing any experiments using TMT, but there are also issues with LFQ experiments. TMT experiments are not going to make proteins which are not significant show up as significant, so if the ratio suppression issue can be solved, perhaps with MS3, then there is no reason not to use TMT analysis.

3.2.6 Label Free Analysis of Droughted Silk Material

Since yield loss due to drought was being analysed, the reproductive tissues in maize and the changes to the proteins caused by drought were used for experiments.

To identify changes to the proteome of maize silks under drought stress, silks were harvested from maize B73 plants and proteins were extracted and digested with trypsin for global LFQ analysis, the rest of the sample was enriched for phosphopeptides and run on the Orbitrap Fusion mass spectrometer (Figure 3.11). TMT tagging was not performed on these samples.

A PCA plot was used to establish if the proteins changed between the drought and control silks (Figure 3.12A). 1338 proteins were identified, of which 405 were shown to be significantly different between the drought and the control (Figure

3.12B). 215 proteins significantly increased in abundance and 190 were significantly decreased in abundance under drought conditions. The proteins that increased with a log2 fold change of more than two (to keep the table to a manageable size) are shown in Table 3.6 and the proteins which significantly decreased in abundance with a log2 fold change of more than two (to keep the table to a manageable size) are shown in Table 3.7. The proteins which increased in abundance were mostly transferase activity proteins. The proteins which decreased in abundance were mostly ABA response proteins and drought stress associated proteins.

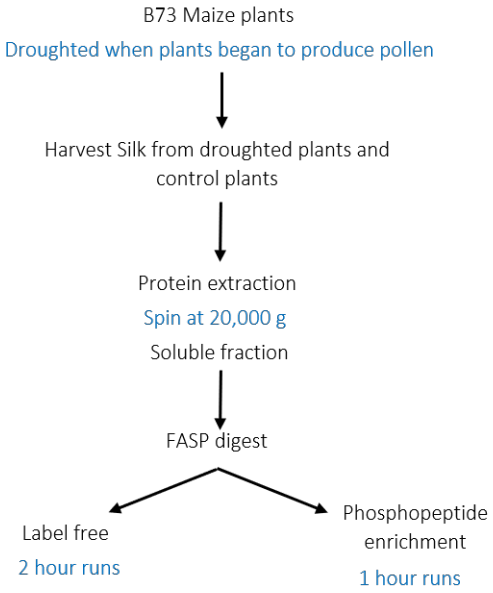

Figure 3.11: Plants were grown till they began to produce pollen and then half the plants were droughted for one week. Plant material was flash frozen in liquid nitrogen and protein was extracted using a PBS buffer and centrifugation. Proteins were digested using FASP digest, and samples were either analysed global LFQ on a 2-hour LC gradient or enriched for phosphopeptides then run on a 1-hour LC gradient before MS analysis.

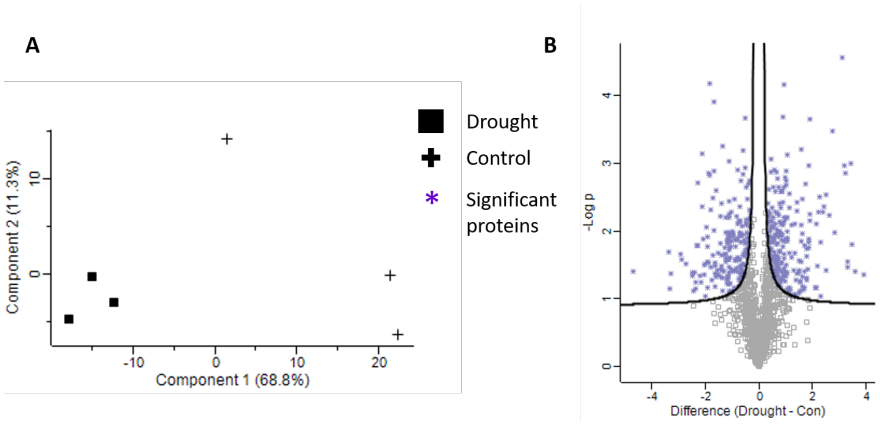

Figure 3.12: (A) PCA plot of the LFQ protein abundance of droughted silk material. The PCA plot shows separation between the drought and the control samples. (B) The volcano plot shows the proteins which are significantly different between the drought and the control samples, log2 fold change is plotted against -logP value. 1338 proteins were identified of which 405 were significantly changed at FDR: 0.05 s0: 0.1.

Table 3.6: Proteins that significantly increase in abundance during drought stress in maize silks with a log2 fold change of more than 2.

Protein Name	**Gene Number**	**Log2 Fold Change**	**-Log P Value**	**MQ Score**	**Function/Pathway**
Beta-D-glucoside glucohydrolase (EC 3.2.1.21)	GLU1	3.94	1.35	69.41	Beta-glucosidase activity; cellulose 1,4-beta-cellobiosidase activity; DIMBOA glucoside beta-D-glucosidase activity; fucosidase activity; galactosidase activity; mannosidase activity; scopolin beta-glucosidase activity; xylanase activity
Chaperone protein ClpB1	541780 ZEAMMB73_ Zm00001d038806	3.62	1.40	61.07	ATP binding
OSJNBb0091E11.19-like protein	100279506 ZEAMMB73_ Zm00001d044455	3.47	1.80	28.25	
Xyloglucan endotransglucosylase/hydrolase (EC 2.4.1.207)	ZEAMMB73_ Zm00001d052651	3.43	3.01	10.06	Hydrolase activity, hydrolysing O-glycosyl compounds; xyloglucan: xyloglucosyl transferase activity
Jacalin-type lectin domain-containing protein	100192837 ZEAMMB73_ Zm00001d047252	3.34	1.54	22.32	Carbohydrate binding

Continued on next page

Table 3.6 – *Continued from previous page*

Protein Name	**Gene Number**	**Log2 Fold Change**	**-Log P Value**	**MQ Score**	**Function/Pathway**
AIR12	ZEAMMB73_ Zm00001d031556	3.32	1.46	42.91	Auxin activated signalling pathway, oxidation reduction process
Major latex protein 22 (Pathogenesis-related protein 2)	ZEAMMB73_ Zm00001d003379	3.24	2.85	8.91	Abscisic acid binding; protein phosphatase inhibitor activity; signalling receptor activity
Arginine decarboxylase (EC 4.1.1.19)	100193626 ZEAMMB73_ Zm00001d051194	3.22	2.97	82.21	Arginine decarboxylase activity
Non-specific lipid-transfer protein	LTP3 100280743 ZEAMMB73_ Zm00001d043049	3.13	4.56	112.35	Lipid binding
Chalcone-flavonone isomerase family protein	ZEAMMB73_ Zm00001d044683	2.86	1.97	85.98	Intramolecular lyase activity
Pyrophosphate-dependent 6-phosphofructose-1-kinase	PFP-ALPHA ZEAMMB73_ Zm00001d017830	2.77	3.48	29.22	6-phosphofructokinase activity; ATP binding; diphosphate-fructose-6-phosphate 1-phosphotransferase activity; metal ion binding
Orf protein	ZEAMMB73_ Zm00001d002353	2.62	2.24	110.93	Transferase activity, transferring acyl groups other than amino-acyl groups

Continued on next page

Table 3.6 – *Continued from previous page*

Protein Name	**Gene Number**	**Log2 Fold Change**	**-Log P Value**	**MQ Score**	**Function/Pathway**
Acyltransferase (Hydroxycinnamoyltransferase12)	100191512 ZEAMMB73_ Zm00001d031893	2.51	2.54	78.57	Transferase activity, transferring acyl groups other than amino-acyl groups
Putative inactive linolenate hydroperoxide lyase	542163 ZEAMMB7_ Zm00001d054067	2.50	1.42	10.03	Heme binding; iron ion binding; lyase activity; monooxygenase activity; oxidoreductase activity, acting on paired donors, with incorporation or reduction of molecular oxygen
(+)-neomenthol dehydrogenase	ZEAMMB73_ Zm00001d025924	2.43	2.36	14.40	Oxidation reduction process
Uncharacterized protein	103650536 ZEAMMB73_ Zm00001d041578	2.40	2.28	65.45	
60S ribosomal protein L18a	100286074 ZEAMMB73_ Zm00001d009579	2.31	1.04	44.15	Structural constituent of ribosome
Basic endochitinase B	100191592 ZEAMMB73_ Zm00001d027524	2.30	1.84	113.58	Chitinase activity

Continued on next page

Table 3.6 – *Continued from previous page*

Protein Name	**Gene Number**	**Log2 Fold Change**	**-Log P Value**	**MQ Score**	**Function/Pathway**
Uncharacterized protein	100284786 ZEAMMB73_ Zm00001d006010	2.28	2.50	21.81	
Abscisic acid stress ripening2 (Abscisic stress ripening protein 2)	100281622 ZEAMMB73_ Zm00001d004843	2.22	2.29	9.83	Response to water deprivation and fruit ripening
Anthocyanidin 3-O-glucosyltransferase	100281608 ZEAMMB73_ Zm00001d037383	2.18	1.48	245.60	Transferase activity, transferring hexosyl groups; UDP-glycosyltransferase activity
Putative cinnamyl-alcohol dehydrogenase family protein	ZEAMMB73_ Zm00001d024314	2.17	2.11	47.99	Cinnamyl-alcohol dehydrogenase activity; oxidoreductase activity, acting on the CH-OH group of donors, NAD or NADP as acceptor; zinc ion binding
Transferase	ZEAMMB73_ Zm00001d034925	2.16	1.17	54.90	Transferase activity, transferring acyl groups other than amino-acyl groups
Dihydroflavonol-4-reductase (NADPH-dependent reductase)	A1 100286107 ZEAMMB73_ Zm00001d044122	2.11	1.16	202.51	Coenzyme binding; oxidoreductase activity; oxidoreductase activity, acting on the CH-OH group of donors, NAD or NADP as acceptor

Table 3.7: The proteins that significantly decreased in abundance in the droughted silks with a log2 fold change of more than 2.

Protein Name	**Gene Number**	**Log2 Fold Change**	**-Log P Value**	**MQ Score**	**Function/Pathway**
Lichenase-2	100282076 ZEAMMB73_ Zm00001d038049	-4.71	1.40	71.53	Anchored component of plasma membrane; hydrolase activity, hydrolysing O-glycosyl compounds; carbohydrate metabolic process
Protease inhibitor	pis7 542408 MPI ZEAMMB73_ Zm00001d011080	-3.36	1.69	16.65	Peptidase activity; serine-type endopeptidase inhibitor activity; response to wounding
Pathogenesis-related protein 10	100192117 ZEAMMB73_ Zm00001d028814 ZEAMMB73_ Zm00001d028815	-3.33	1.15	221.77	Cytoplasm; intracellular; nucleus; abscisic acid binding; protein phosphatase inhibitor activity; ribonuclease activity; RNA binding; signalling receptor activity; abscisic acid-activated signalling pathway; regulation of protein serine/threonine phosphatase activity; response to abscisic acid; response to stress
Pathogenesis-related protein 1	103636577 ZEAMMB73_ Zm00001d029558	-3.28	1.36	9.82	Extracellular space
Malate synthase (EC 2.3.3.9)	ZEAMMB73_ Zm00001d003247	-2.92	1.66	46.15	Cytoplasm; malate synthase activity; glyoxylate cycle; tricarboxylic acid cycle

Continued on next page

Table 3.7 – *Continued from previous page*

Protein Name	**Gene Number**	**Log2 Fold Change**	**-Log P Value**	**MQ Score**	**Function/Pathway**
Abscisic acid stress ripening5	100127507 ZEAMMB73_ Zm00001d025401	-2.90	1.57	307.05	Response to water deprivation and fruit ripening
Carboxypeptidase (EC 3.4.16.-)	ZEAMMB73_ Zm00001d048690	-2.71	1.51	34.05	Serine-type carboxypeptidase activity; proteolysis involved in cellular protein catabolic process
Early nodulin-like protein 9	100273206 ZEAMMB73_ Zm00001d014463	-2.49	1.38	30.77	Anchored component of plasma membrane; integral component of membrane; electron transfer activity
Soluble epoxide hydrolase	100191966 ZEAMMB73_ Zm00001d012909	-2.49	1.34	19.01	Hydrolase activity
Ras-related protein RABD2c	100191848 ZEAMMB73_ Zm00001d011162	-2.45	1.12	13.20	GTP binding; GTPase activity
Peptide methionine sulfoxide reductase	100283982 ZEAMMB73_ Zm00001d003271	-2.39	1.39	30.12	Cytoplasm; L-methionine-(S)-S-oxide reductase activity; peptide-methionine (S)-S-oxide reductase activity; cellular response to oxidative stress

Continued on next page

Table 3.7 – *Continued from previous page*

Protein Name	**Gene Number**	**Log2 Fold Change**	**-Log P Value**	**MQ Score**	**Function/Pathway**
ATP-dependent DNA helicase (EC 3.6.4.12)	ZEAMMB73_ Zm00001d004573	-2.38	1.15	40.60	ATP binding; DNA helicase activity; rRNA N-glycosylase activity; DNA recombination; DNA repair; negative regulation of translation; telomere maintenance
2-isopropylmalate synthase 1 chloroplastic	ZEAMMB73_ Zm00001d023243	-2.38	1.24	19.58	2-isopropylmalate synthase activity; leucine biosynthetic process
Glutathione transferase19	ZEAMMB73_ Zm00001d036951	-2.33	1.78	15.71	Cytoplasm; glutathione transferase activity; glutathione metabolic process
Acidic leucine-rich nuclear phosphoprotein 32-related protein	100286286 ZEAMMB73_ Zm00001d033420	-2.28	2.71	8.03	Intracellular signal transduction, nucleocytoplasmic transport, regulation of mRNA stability
Dehydrin3	542251 ZEAMMB73_ Zm00001d051420	-2.26	1.79	212.76	Cytosol; membrane; cold acclimation; response to abscisic acid; response to water deprivation
Aldose reductase (NAD(P)-linked oxidoreductase superfamily protein)	AR4 ZEAMMB73_ Zm00001d003524	-2.18	1.33	33.15	Cytosol; alcohol dehydrogenase (NADP+) activity; alditol: NADP+ 1-oxidoreductase activity; oxidoreductase activity

Continued on next page

Table 3.7 – *Continued from previous page*

Protein Name	**Gene Number**	**Log2 Fold Change**	**-Log P Value**	**MQ Score**	**Function/Pathway**
Serine/threonine-protein phosphatase 2A 65 kDa regulatory subunit A beta isoform	732740 ZEAMMB73_ Zm00001d036031	-2.17	1.24	4.63	Cytoplasm; protein phosphatase type 2A complex; protein phosphatase regulator activity; protein dephosphorylation
4-coumarate–CoA ligase-like 7	100191850 ZEAMMB73_ Zm00001d027711	-2.12	2.36	13.40	Integral component of membrane; ligase activity
Alanine aminotransferase 2 mitochondrial	100193705 ZEAMMB73_ Zm00001d030557	-2.10	3.14	37.73	L-alanine:2-oxoglutarate aminotransferase activity; pyridoxal phosphate binding; biosynthetic process
Stachyose synthase	ZEAMMB73_ Zm00001d019163	-2.08	1.88	71.86	Raffinose alpha-galactosidase activity
Ubiquitin-conjugating enzyme E2 36	103651370 ZEAMMB73_ Zm00001d043905	-2.04	1.35	14.77	ATP binding; transferase activity
Exoglucanase1	100191390 ZEAMMB73_ Zm00001d034015	-2.04	1.49	18.43	Hydrolase activity, hydrolysing O-glycosyl compounds; carbohydrate metabolic process

3.2.7 Identification of Drought Related Signalling Using Phosphoproteomics in Silks

Phosphopeptide enrichment was performed on droughted silk material. A PCA plot was used to test if there was a difference between the droughted and control silks (Figure 3.13A). 1553 phosphopeptides were identified which mapped to 981 proteins, of which 130 phosphopeptides were statistically significant between the drought and the control (Figure 3.13B). A heat map was used to compare the significantly changing proteins between the control and the drought treatment (Figure 3.14). To produce the heat map, log2 fold changes of the significantly changing phosphopeptides were Z scored. The phosphopeptides which significantly increased in abundance in the drought treated, with a log2 fold change of more than three (to keep the table size manageable) are shown in Table 3.8 and the phosphopeptides which significantly decreased in abundance, with a log2 fold change of more than three (to keep the table size manageable) are shown in Table 3.9.

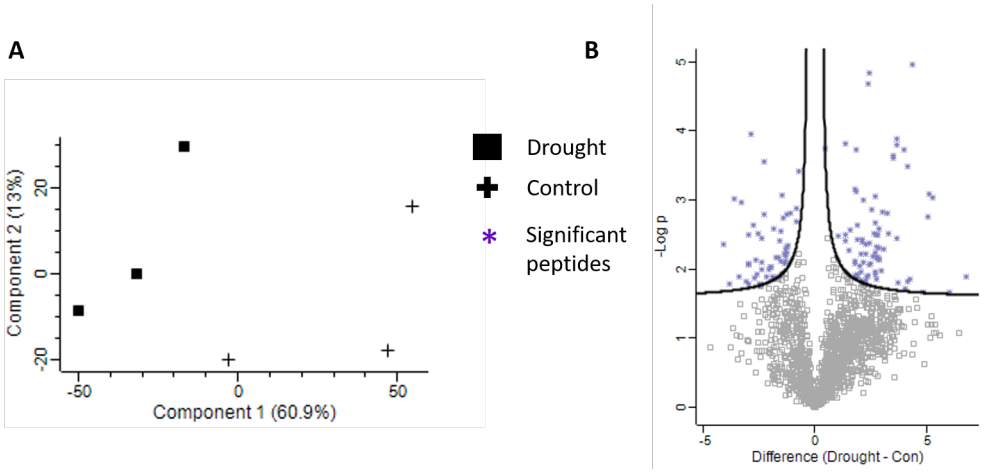

Figure 3.13: (A) PCA plot of the phosphopeptide enriched silk samples. The PCA plot shows separation between the drought and the control samples. (B) The volcano plot shows the peptides which are significantly different between the drought and the control samples, log2 fold change is plotted against -logP value. 1553 phosphopeptides were identified of which 130 were significant. FDR: 0.05 s0: 0.1.

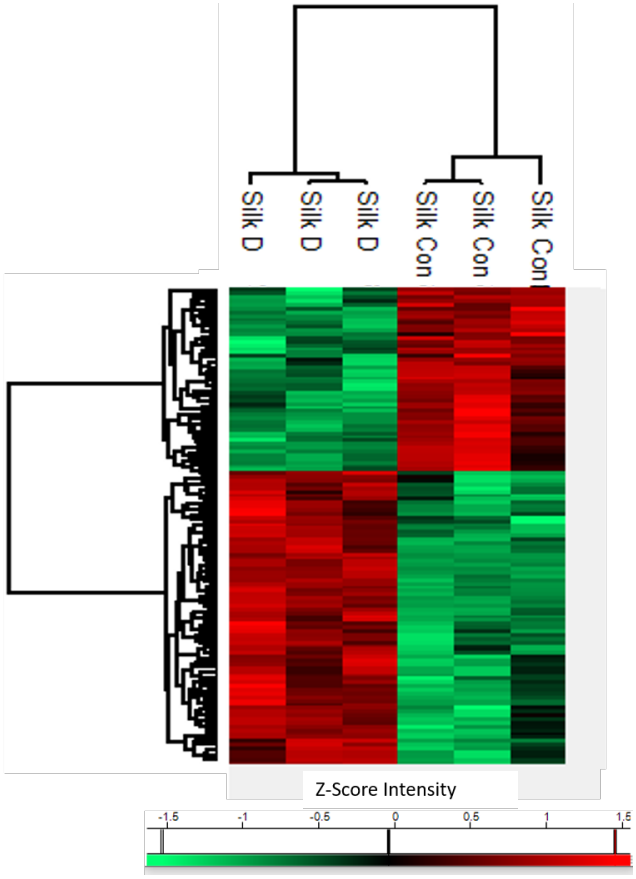

Figure 3.14: Heat map of the 130 significantly changing phosphopeptides in the maize drought treated silks. Significant phosphopeptides log2 fold change values have been z-scored for graphical representation.

In the droughted silk phosphopeptide data, the majority of proteins were mono phosphorylated (90.8%), 8.9% carried two phosphorylated residues and 0.3% carried three. There were 89.4% phosphoserine, 10.0% phosphothreonine and 0.6% phosphotyrosine identified in this study, which is similar to the proportions found in the leaves. To the best of my knowledge none of the phosphopeptide sites identified in this study have previously been identified in maize (as of February 2020 these modifications were not in UNIPROT).

Table 3.8: The phosphopeptides in the silks which significantly increased in abundance, with a log2 fold change of more than 3 mapped to proteins.

Protein Name	**Peptide AA Sequence**	**Gene Number**	**Log2 Fold Change**	**-Log P Value**	**MQ Score**	**Function/Pathway**	**Site & Position**
Universal stress protein PHOS34	LSAAAQAAAIQPS**S**PR	ZEAMMB73_Zm00001d043261	6.76	1.88	248.01	Stress response	S30
Tyrosinase_Cu-bd domain-containing protein	EYAGSFAVVPG**S**GAGK	103641120	5.26	3.04	133.96	Catechol oxidase activity; metal ion binding	S560
Uncharacterized protein	A**S**FSELVVGSPTR A**S**FSELVVG**S**PTR	ZEAMMB73_Zm00001d011478	5.08	3.08	178.67	Proteasome assembly	S9; S17
Tetratricopeptide repeat (TPR)-like superfamily protein	SLQNLFGTN**S**QR	100191827 ZEAMMB73_Zm00001d014961	5.07	2.75	250.81		S594

Continued on next page

Table 3.8 – *Continued from previous page*

Protein Name	**Peptide AA Sequence**	**Gene Number**	**Log2 Fold Change**	**-Log P Value**	**MQ Score**	**Function/Pathway**	**Site & Position**
ABC transporter C05D10.3 in chromosome III (ABC transporter G family member 11)	VGGDLQGDG**T**TPR	100281487 ZEAMMB73_Zm00001d002871	4.34	4.96	155.39	ATPase activity; ATPase-coupled transmembrane transporter activity; ATP binding	T13
Eukaryotic translation initiation factor 5A (eIF-5A)	**S**DSEEHHFESK	542601 542537 ZEAMMB73_Zm00001d006760 ZEAMMB73_Zm00001d022042	4.26	1.86	298.58	Ribosome binding; translation elongation factor activity; translation initiation factor activity	S2
Aquaporin PIP2-1	ALG**S**FRSNA ALGSFR**S**NA	541888 ZEAMMB73_Zm00001d019563	4.12	1.82	94.69	Channel activity	S149; S152
Multidrug resistance associated protein7	SFGGSS**S**LASGAK	100283662 ZEAMMB73_Zm00001d039653	4.12	3.49	120.63	Hydrolase activity	S8

Continued on next page

Table 3.8 – *Continued from previous page*

Protein Name	**Peptide AA Sequence**	**Gene Number**	**Log2 Fold Change**	**-Log P Value**	**MQ Score**	**Function/Pathway**	**Site & Position**
DNA glycosylase superfamily protein	**S**LSMPVYYDSNATAGAR SL**S**MPVYYDSNATAGAR	ZEAMMB73_Zm00001d012578	4.01	1.72	181.76	DNA-3-methyladenine glycosylase activity	S45; S47
Putative mediator of RNA polymerase II transcription subunit 26c	VSGFQY**S**PSPQR	100276791 ZEAMMB73_Zm00001d053189	3.96	3.73	65.65	Nucleus	S227
Vacuolar protein sorting-associated protein 9A	TAVD**S**SDDLEALGRPENA	100273143 ZEAMMB73_Zm00001d047863	3.73	1.81	190.57		S217
Protein BTR1	**S**PPQQQQSPSEEGDDKEKPTHLR **S**PPQQQQ**S**PSEEGDDKEKPTHLR	542422 ZEAMMB73_Zm00001d051881	3.67	3.88	161.26	RNA binding	S22; S29
Serine/arginine-rich splicing factor RSZ22	SY**S**R**S**PPLPPPPPR	100272442 ZEAMMB73_Zm00001d017177	3.67	2.44	59.87	RNA binding; zinc ion binding	S156; S158

Continued on next page

Table 3.8 – *Continued from previous page*

Protein Name	**Peptide AA Sequence**	**Gene Number**	**Log2 Fold Change**	**-Log P Value**	**MQ Score**	**Function/Pathway**	**Site & Position**
Calmodulin binding protein isoform 1	**S**PPQQQQSPSEEGDDKEKPTHLR	ZEAMMB73_Zm00001d038838	3.65	3.81	118.51		S22
Ethylene-responsive transcription factor ABR1	RH**S**LPSPNNGK	100275504 ZEAMMB73_Zm00001d010175	3.48	3.61	105.24	DNA binding; DNA-binding transcription factor activity	S531
Mitogen-activated protein kinase kinase kinase 3	MEGH**Y**SPTASAAEAGGER	ZEAMMB73_Zm00001d049080	3.48	3.64	234.63	ATP binding; protein serine/threonine kinase activity	Y5
Tetratricopeptide repeat (TPR)-like superfamily protein	LSETSV**S**PR	100191930 ZEAMMB73_Zm00001d051589	3.28	2.52	103.97		S173

Continued on next page

Table 3.8 – *Continued from previous page*

Protein Name	**Peptide AA Sequence**	**Gene Number**	**Log2 Fold Change**	**-Log P Value**	**MQ Score**	**Function/Pathway**	**Site & Position**
S-acyltransferase (EC 2.3.1.225) (Palmitoyl-transferase)	ASTEEGESEVSKPA**S**R	ZEAMMB73_Zm00001d038321	3.25	2.80	144.55	Protein-cysteine S-palmitoyltransferase activity	S76
SAND family protein	SA**S**DVIGR	100282740 ZEAMMB73_Zm00001d041948	3.07	2.30	139.46		S410
DUF4057 domain-containing protein	EAPEGLHDDDKDGDDV**S**QP-SPR	100276254 ZEAMMB73_Zm00001d047203	3.02	2.82	122.33		S81

Table 3.9: The phosphopeptides which significantly decreased in abundance in the drought treated silks, with a log2 fold change of more than 3 mapped to proteins.

Protein Name	**Peptide AA Sequence**	**Gene Number**	**Log2 Fold Change**	**-Log P Value**	**MQ Score**	**Function/Pathway**	**Site & Position**
Late embryogenesis abundant protein, group 3	A**S**HQDKASYQAGETK	542216 ZEAMMB73_Zm00001d038870	-4.06	2.36	213.69		S3
Dynein light chain	KPVG**S**GSPPPAATATAVAHK	100194301 ZEAMMB73_Zm00001d040291	-3.82	1.79	125.79	Dynein intermediate chain binding; dynein light intermediate chain binding; motor activity	S29
Putative mediator of RNA polymerase II transcription subunit 26c	VSGFQYSP**S**PQR	100276791 ZEAMMB73_Zm00001d053189	-3.57	3.01	240.37	Nucleus	S229

Continued on next page

Table 3.9 – *Continued from previous page*

Protein Name	**Peptide AA Sequence**	**Gene Number**	**Log2 Fold Change**	**-Log P Value**	**MQ Score**	**Function/Pathway**	**Site & Position**
ARM repeat superfamily protein (Eukaryotic initiation factor 5C CG2922-PF, isoform F)	**S**SKEKPTLGGTR S**S**KEKPTLGGTR	100284266 ZEAMMB73_Zm00001d004676	-3.36	1.88	152.00	Translation initiation factor activity	S2; S3
RPM1-interacting protein 4	GNE**T**PTRGSAVPK	ZEAMMB73_Zm00001d031580	-3.26	2.97	152.00	Plasma membrane; defence response signalling pathway, resistance gene-independent	T163
Remorin family protein	VE**T**EKRNSLIK	100304007 ZEAMMB73_Zm00001d002842	-3.05	1.82	116.90		T85

3.2.8 Motif Analysis of Drought Stressed Maize Silks

Motif analysis was performed on phosphopeptide enriched silk samples using MMFPh and the linear motif analysis in Perseus. The motifs identified in the silk dataset are shown in Table 3.10.

The motif analysis using the linear motif showed motifs identified on the phosphopeptides which significantly increased in abundance included MAPK substrate motifs on 12 phosphopeptides which mapped to proteins including serine/arginine-rich splicing factor (S156 S158, log2 fold change -3.67), s-acyltransferase (S76, log2 fold change -3.25) and DUF4057 domain-containing protein (S65, log2 fold change -2.94). 9 phosphopeptides which significantly decreased in abundance had MAPK substrate motifs including phosphopeptides which mapped to proteins myosin-6 (S774, log2 fold change 2.96), LEA protein group 3 (S68, log2 fold change 2.67) and patatin (S35 S41, log2 fold change 2.51). There were also 18 phosphopeptides identified with the casein kinase II motif which mapped to proteins including LEA protein group 3 (S3, log2 fold change 4.06), dynein light chain (S29, log2 fold change 3.82) and ARM repeat superfamily protein (S2/S3, log2 fold change 3.36).

The motif analysis using MMFPh identified 20 motifs in the drought silk dataset, of which one was found in just the significantly changing data, sP. The proline directed motifs which were also seen in the droughted leaf database, sP and tP, can be seen in the silk database, and are targets of various kinases (van Wijk *et al.*, 2014). RxxS and RSxS motifs were also identified which are basophilic motifs recognised by MAPKs (Vu *et al.*, 2016). xSxSx motif was identified in the dataset and is also a target for MAPKs, RLKs and CDKs (van Wijk *et al.*, 2014).

Table 3.10: Motif analysis of phosphopeptides identified in the drought silk experiment.

Motif	Foreground Matches	Background Matches	Occurrence Threshold	Score
————RS-S————	106	26332	75	3.49
————-L-R–S————	80	22786	75	3.30
————S———R———	143	213218	113	0.91
———R———S————	139	213531	113	0.87
————S————-R—-	135	213775	113	0.82
————R—S————	133	215398	113	0.79
————S———-R———-	131	212254	113	0.79
————R——S————	129	211413	113	0.77
————S—-P————-	127	208776	113	0.77
———-R———-S————	127	214328	113	0.73
————S——G———	148	251883	113	0.72
————S—-R————-	122	210856	113	0.70
————S-R————-	117	202755	113	0.69
————S-P————-	152	214243	150	0.99
————S———R———	150	215722	150	0.96
————GS————	184	268242	150	0.94
————-A-S————	157	293981	150	0.58
————SP————	475	205541	225	2.69
————R–S————	377	217450	225	2.28
————-S-S————	260	410148	225	0.83

3.2.9 Comparative Proteomics of Maize Leaf, Silk & Tassel Tissue

To identify tissue specific proteins found in maize leaf, silk and tassel materials the previous LFQ analysis of soluble proteins from leaves (TMT analysis was shown in Section 3.2.2, but LFQ analysis was also performed) and silks (Section 3.2.6) was extended to tassels. Droughted material was available for leaves and silks (as described in previous sections) but only well-watered tassel material was available. The proteins identified in control samples were compared and a total of 1,795 proteins were identified across the three tissues. 262, 625 and 105 proteins were identified as unique to the leaf, silk and tassels respectively (Figure 3.15A). The proteins unique to the leaf were mostly photosynthesis and chloroplast proteins. The proteins unique to the silk were mostly reproductive and metabolism proteins. The proteins unique to the tassel were mostly reproductive proteins. The proteins which were common to all tissues were predominantly core metabolism proteins.

Proteins identified in the droughted leaf and silk material were also compared. A total of 1,722 proteins were identified, of which 352 were unique to the leaf tissue and 843 proteins were unique to the silk tissue (Figure 3.15B). The proteins which were seen in both tissues were mostly core metabolism proteins and some stress response proteins. No data for drought in the tassels was obtained due to tassels becoming brittle during drought, and easily breaking when pollen was being collected.

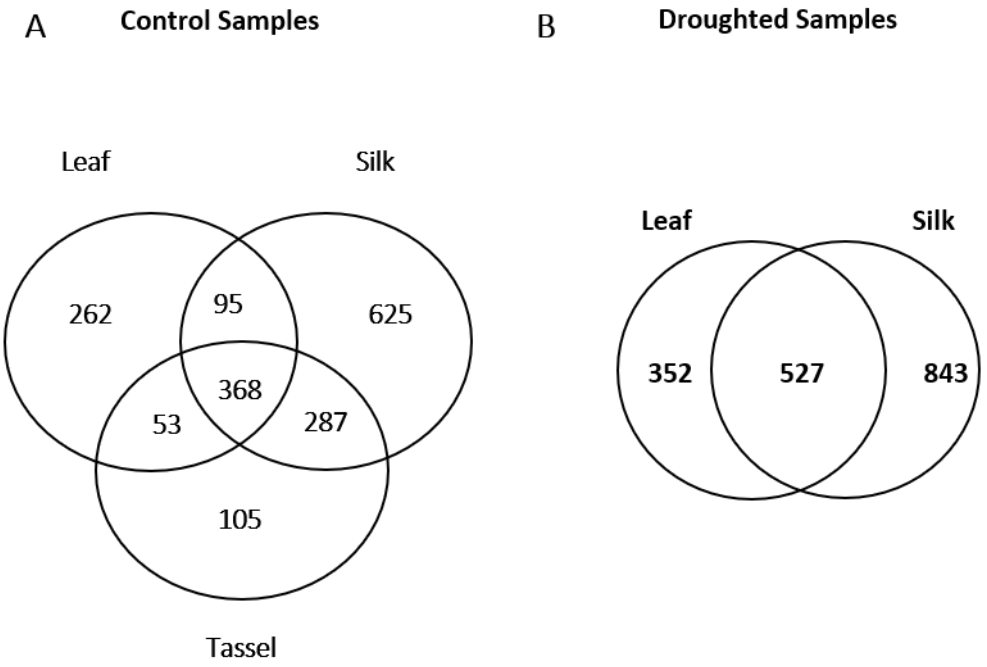

Figure 3.15: (A) Venn diagram of the control proteins identified in the 3 maize tissues and (B) Venn diagram of the proteins identified in the droughted leaf and silk materials.

Proteins from three different well-watered maize tissues; leaf, silk and tassel were compared. There were 368 proteins common to all three tissues and these were mostly core metabolism proteins such as ATP synthase subunit beta, which is a mitochondrial protein, profilin-5 which is involved in cytoskeleton structure and 40S ribosomal protein S8 which is involved in ribosome assembly and translation. This is as expected because these functions are common to all three tissues and needed for cells to perform their functions.

Proteins only identified in the leaf included sucrose-phosphate synthase, which is involved in photosynthesis and PsbP domain-containing protein 6, which is

found in chloroplasts and is involved in photosynthesis. This is as expected because leaves contain chloroplasts. The silks had the highest number of unique proteins. These included a lot of growth proteins; this is most likely because silks are a fast-growing tissue and are much younger than the other tissues. There were also some reproductive proteins such as elongation factor 1-beta and HOPM interactor 7 which are involved in pollen tube growth. Proteins only found in the tassels included proteins associated with sexual reproduction such as beta expansin1, beta expansin8, expansin-B11 and expansin-B9. Other proteins specific to the tassels were proteins associated with pollen production which is expected as tassels produce pollen. There were also several proteins which inhibited catalytic activity such as PMEI domain-containing protein and plant invertase/pectin methylesterase inhibitor superfamily protein.

Proteins in droughted leaf and silk tissue included benzoxazinone synthesis9, anamorsin homolog and profilin-5 which are all core metabolism proteins essential for cell function. Some stress related proteins and ABA response proteins were identified such as catalase, chaperonin CPN60-1 mitochondrial and ribulose bisphosphate carboxylase large chain. This is expected as the tissues were both droughted, so a response to this stress should be seen in both tissues. Proteins only identified in the leaf tissue included photosynthesis and chloroplast proteins such as, NAD(P)H-quinone oxidoreductase subuit H, ferredoxin–nitrite reductase and ferredoxin-thioredoxin reductase catalytic chain. There were also stress response proteins found to be unique to leaves, these included thiamine thiazole synthase 2, glycine-rich RNA-binding, abscisic acid inducible protein and HSP 70 kDa. These were most likely not seen in the silks because they are found in parts of the cell which are more common to leaves than silks. Proteins which were unique to the silks included metabolic proteins such as diphosphomevalonate decarboxylase, endoglucanase and dirigent protein. There were also some proteins involved in pollen production found such as pollen allergen Phl p 2 and phosphoserine phosphatase chloroplastic. This is unexpected as pollen production occurs in the tassels and not the silks. These proteins have most likely come from pollen on the silks. There were also some stress response proteins only found in the silks such as UPF0061 protein azo1574, annexin D4 and dehydrin COR410.

3.2.10 Comparison of the Phosphopeptides Identified in the Three Maize Materials

The phosphopeptides identified in the three tissues were compared. The phosphopeptides only identified in at least three replicates of the relevant control tissue were compared in between the leaf, silk and tassel (Figure 3.16). 2516 phosphopeptides were identified across the three tissues, of which 159, 816 and 1264 were identified only in the leaf, silk and tassel tissue respectively. Phosphopeptides identified in at least three replicates of the droughted leaf and silk material were compared. Overall 1555 phosphopeptides were identified in the droughted material of which 221 were common to both the leaf and silks, 293 were unique to the leaves and 1041 were unique to the silks.

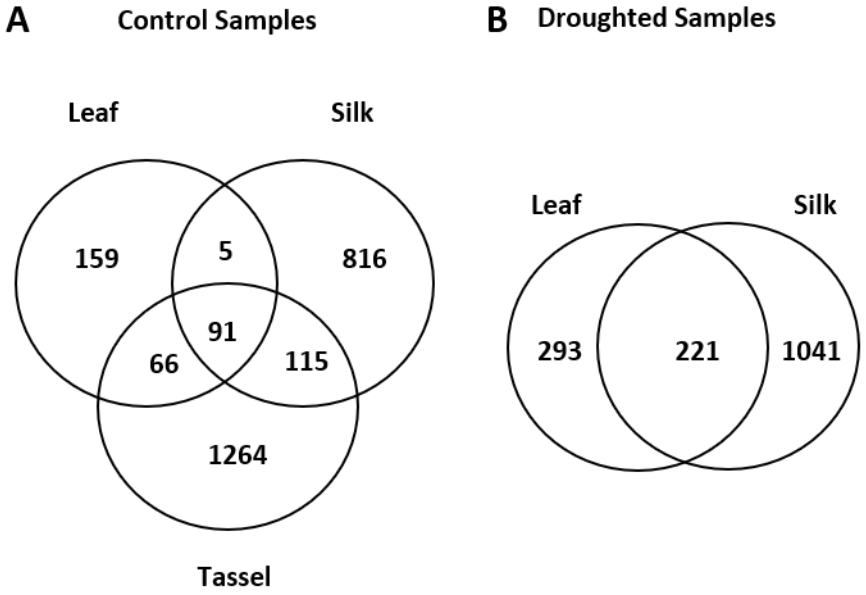

Figure 3.16: (A) Venn diagram of the overlap of the identified phosphopeptides in the control (well-watered) samples between the leaf, silk and tassel material. (B) Venn diagram showing the overlap between the phosphopeptides identified in the droughted samples of the leaf and silk samples.

In the tassel phosphoproteomic data, the majority of proteins were mono phosphorylated (88.9%), 10.3% carried two phosphorylated residues and 0.8% carried three. There were 87.5% phosphoserine, 11.8% phosphothreonine and 0.7% phosphotyrosine identified in this study, which is similar to the proportions found in the leaves and silks. 1436 phosphopeptides were identified in the tassels which mapped to 862 proteins.

In the leaf, silk and tassel control tissue 2516 phosphopeptides were identified in total, of which 91 were identified in all three tissues. These mapped to proteins which were mostly associated with core metabolism and signalling such as high mobility group family A 102 and calmodulin. Protein phosphatase 2C was also identified in all control tissues. Whilst PP2C is important in the drought response pathway, under non stress conditions it binds to SnRK2, which prevents it from phosphorylating itself and other proteins, so it is still present under non stress conditions, it is therefore not surprising that it is seen (Boudsocq *et al.*, 2007). There were 5 phosphopeptides only identified in the leaf and silk control material, these mapped to proteins associated with metal binding, DNA binding and tubulin binding. There were few phosphopeptides common to only these two tissues identified so analysis is difficult. The phosphopeptides which were common between the leaf and tassel mapped to proteins associated with photosynthesis, ATP binding and DNA binding. They are core metabolism proteins, which were not picked up in the silk analysis, possibly due to low abundance. The phosphopeptides found in the silk and tassel analysis could be mapped to proteins associated with transcription, silk and tassels are fast growing tissues, unlike leaves so this is expected, but there were also a lot of core metabolism proteins associated with ATP binding, metal ion binding and ribosomal structure. Whilst it is expected that these proteins will also be identified in the leaf analysis, far fewer proteins were identified in the leaf phosphopeptide analysis, so this absence may be because the levels were too low rather than they truly not being present in the sample. Interestingly no proteins associated with sexual reproduction were identified in the phosphopeptide data, these proteins most likely do not phosphorylate, and therefore were not observed. Phosphopeptides only identified in the leaves could be mapped to proteins associated with photosynthesis, because the leaves do most of the plants photosynthesis, mitochondrial proteins, other core metabolism proteins involved in ATP binding and metal ion binding were also identified. Proteins mapped from the phosphopeptides only identified in the silks included ATP binding proteins, ribosomal structure proteins and metal binding proteins. The only protein associated with sexual reproduction identified in the silks was putative nucleoside phosphatase GDA1, which is involved in pollen production, so most likely came from pollen on the silks rather than the silks themselves, it can only be assumed that these proteins do not phosphorylate. The phosphopeptides identified in the tassel samples mapped to proteins associated with sexual reproduction and pollen production, which is expected as the tassels produce pollen, and other core metabolism proteins with functions similar to those

identified in the other tissues.

In the droughted leaf and silk material phosphopeptides identified could be mapped to proteins associated with ABA response, such as dehydrin DHN1, nodulin-related protein 1 and dehydrin3. Stress proteins including peptide methionine sulfoxide reductase, universal stress protein PHOS34 and stress-response A/B barrel domain-containing protein UP3. Since drought stress was applied to both these tissues, stress response proteins are expected to be seen. There were also core metabolism proteins expected to be in all tissues identified. Phosphopeptides identified only in the leaves could be mapped to proteins associated with photosynthesis and other core metabolisms. There were also two proteins involved in drought stress which were not identified in the silks, abscisic Acid-Insensitive 5-like protein 5 and HSP 70. Phosphopeptides only identified in the silks could be mapped to proteins involved in core metabolism such as ATP binding, DNA binding and structural proteins. Proteins associated with stress only identified in the silks included DNAJ heat shock N-terminal domain-containing protein, heat stress transcription factor A-6b and late embryogenesis abundant protein, group 3. SnRK2 serine threonine protein kinase6 was also identified in the silks and not in the leaves, SnRK2 is known to play a role in the ABA response pathway, and phosphorylate during it, so it is unsurprising that it was identified. However, it was not identified in the leaf tissue, but the levels of phosphoproteins where much lower in the leaves than the silks, so it may have not been detected rather than not present. The only protein associated with reproduction was calmodulin-binding receptor-like cytoplasmic kinase 1 which is involved in pollen development, and most likely came from pollen on the silks rather than the silks themselves, because the silks are the female flowers and so do not produce pollen.

3.2.11 Comparison of Motifs Identified in Three Maize Materials

There were similar phosphopeptide motifs identified in the three well-watered maize materials. Proline directed motifs were identified in all three materials, and sP motifs were identified in the significantly changing phosphopeptides in the drought leaf and silk material. RxxS and tP were identified in the significantly changing phosphopeptides in the droughted leaf material, whilst these were not identified in the significantly changing phosphopeptides in the drought silks they were identified in the silk and tassel datasets. the motifs identified in the tassel dataset are shown in Table 3.11.

The motifs identified in the datasets included sP and tP motifs which are suggested substrates of MAPKs SnRKs, RLKs PKAs and CDKs (van Wijk *et al.*, 2014). RxxS and RSxs motifs were also identified in the datasets, which are also recognised by MAPKs (van Wijk *et al.*, 2014). Glycine rich motifs were only identified in the silk and tassel datasets, these motifs are known to be present in nucleus proteins and secreted proteins (van Wijk *et al.*, 2014).

Table 3.11: Motifs identified by MMFPh in the maize tassel phosphopeptide analysis.

Motif	Foreground Matches	Background Matches	Occurrence Threshold	Score
——————ASP——————	75	17105	70	0.756984
——————-P-SP——————	75	17636	70	0.712879
——————SPP——————-	73	18341	70	0.617336
——————RS-S——————	71	26332	70	0.055513
——————S——R———	135	215722	105	0.948297
——————S———-R—-	130	213775	105	0.90693
——————S——-R——-	126	212254	105	0.872143
——————S—-P———-	123	208776	105	0.861214
———R——S——————	121	211413	105	0.819454
——————S———R———	122	213218	105	0.819063
——————S—R———	118	217287	105	0.743696
——-R——-S——————	116	214328	105	0.738816
——————S—P———	114	215774	105	0.704024
——————S——G———	133	251883	105	0.703184
——————S–G———	128	253715	105	0.637446
——————-P-S——————	114	206526	105	0.767222
——————GS——————	157	268242	140	0.851741
——————S-P——————-	156	214243	140	1.166809
——————AS——————	157	305569	140	0.663778
——————-S-S——————	188	410148	175	0.499099
——————SP——————	443	205541	209	2.732392
——————R–S——————	263	217450	209	1.89889

3.3 Discussion

The proteins observed to increase in abundance under drought stress in the maize leaves were associated with ABA response, dehydrins and stress response. The two proteins which increased the most were dehydrin DHN1 (log2 fold change 3.26) and dehydrin3 (log2 fold change 2.15), other studies have also found an increase in de-

hydrin DHN1 under drought conditions, leading to better drought tolerance (Koag *et al.*, 2003). Abscisic acid stress ripening3 (log2 fold change 2.01) and abscisic acid stress ripening1 (log2 fold change 1.94) were also identified as significantly increasing in abundance under drought conditions, these are ABA response proteins and are therefore expected to increase in abundance. Late embryogenesis abundant (LEA) protein, group 3 (log2 fold change 1.47), LEA proteins are a type of dehydrin which many drought studies have noted as increasing in abundance under drought conditions (Hajheidari *et al.*, 2006; Mostafa *et al.*, 2010; Ghatak *et al.*, 2016).

The proteins which decreased in abundance most under drought stress in the maize leaves were phosphoenolpyruvate carboxykinase1 (log2 fold change -1.55) and pyruvate orthophosphate dikinase 1 (log2 fold change -1.40) which Hu *et al.* (2015-1) identified to increase in abundance in their maize drought studies. Abundance does not equal activity, and just because less of the protein was quantified does not mean it's less active. The protein could be being degraded at a higher rate than normal, which is affecting the abundance. Proteins which are highly modified will also not be identified in this search as only oxidation of methionine was included and no other variable modifications in the search parameters. These proteins were particularly prominent in Hu's phosphorylation studies due to there being many possible phosphorylation sites on these proteins. Lipoxygenase (log2 fold change -1.16) was also observed by Ghatak *et al.* (2016) to increase in abundance under drought conditions and is associated with water deprivation. Other proteins associated with stress and ABA response were also identified which included catalase (EC 1.11.1.6) (log2 fold change -1.26). Many studies show a large fold change in Rubisco under drought conditions, though this has been argued in other studies and contrasting results are shown (Demirevska *et al.*, 2009), however no significant change in the abundance of Rubisco was observed in this dataset. Photosynthesis is sensitive to stress conditions (Chaves *et al.*, 2009; Gururani *et al.*, 2015), and abiotic stresses are known to reduce photosynthesis (Gururani *et al.*, 2015), proteins such as oxygen evolving complex2 (log2 fold change -1.02) and plastocyanin (log2 fold change -0.94) were observed, which are involved in photosynthesis were shown to significantly decrease in abundance in the droughted samples. However the findings in this study are contradicted by Avramova *et al.* (2015) who found an upregulation of photosynthesis transcripts during drought.

In the drought leaf TMT dataset, there were 17 Kyoto encyclopedia of genes and genomes (KEGG) pathways identified as significantly enriched. Many of the

enriched pathways are involved in metabolism of pyruvate, amino acids and other small molecules, suggesting that drought causes an increase in production of these to cope with drought stress. Photosynthesis pathways were seen less in the drought material than the control, suggesting that the plants photosynthesis levels decreases during drought.

Two dehydrins, dehydrin DHN1 (T69, log2 fold change 1.12) and dehydrin3 (T196, log2 fold change 2.51) were identified as significantly increasing in phosphorylation levels dehydrins are markers of stress tolerance so are expected to increase in abundance (Hanin *et al.*, 2011).. Phosphorylation on serine/threonine-protein kinase SRK2A (S42, log2 fold change 2.67) was observed in the significantly increasing in abundance data. Little is known about this protein in maize, but when a Basic Local Alignment Search Tool (BLAST) search was performed, SRK2A was found to be 84.1% similar to the ABA response protein SnRK2 in Setaria viridis, SnRK2 is a key protein in the ABA response pathway which is known to auto phosphorylate. Ribulose bisphosphate carboxylase large chain (S359, log2 fold change -2.31) was identified as a phosphorylated protein, which is a Rubisco subunit and Rubisco was not observed as significantly changing in the TMT dataset but as previously stated, authors argue as to whether Rubisco shows a fold change under droughted conditions (Demirevska *et al.*, 2009). The data in this study shows that the total amount of Rubisco did not change under drought conditions, but its phosphorylation state did. Other proteins identified included kinases such as phosphoenolpyruvate carboxykinase1 (S59 S66 and S15 T52 T60, log2 fold change of -4.79 and -3.31) and pyruvate orthophosphate dikinase2 (S3, log2 fold change of -3.32), which are involved in signalling, which is contradicted by Ding *et al.* (2015); Wang *et al.* (2008) who found the expression levels of these phosphoproteins to be increased during abiotic stress.

There were 73 proteins which were observed in both the leaf TMT and leaf phosphoproteomics datasets, of which 10 were identified as significantly changing in both the TMT and phosphoproteomics datasets. These included two dehydrins, dehydrin3 and dehydrin DHN1, dehydrins are drought stress response proteins, both dehydrins increased in abundance in both datasets. PEP carboxylase (phosphoenolpyruvate carboxylase 1) and phosphoenolpyruvate carboxykinase1 decreased in abundance in both datasets. Phosphoenolpyruvate carboxykinase have been identified in other drought maize phosphorylation studies as increasing in abundance (Hu *et al.*, 2015-1). Heat shock proteins 70 significantly decreased in abundance in the phosphoproteomics dataset but did not significantly change in the TMT dataset.

HSPs are important stress response proteins, this data shows that they become dephosphorylated during the drought response pathway.

The fold changes for the droughted silk samples are much higher than for the leaf samples, this is because of the ratio suppression caused by the TMT therefore, as LFQ analysis was performed on the silk dataset, this ratio suppression is not seen. The silk proteome is also less complicated than the leaf proteome because there are no chloroplasts or chlorophyll, and in leaves half the proteins present are Rubisco which can mask other proteins. The significantly increasing proteins in the drought silks included, major latex protein 22 (pathogenesis-related protein 2) (log2 fold change 3.24) and abscisic acid stress ripening2 (log2 fold change 2.22), which are ABA response proteins. The proteins that significantly increased with the highest fold change was beta-D-glucosidase 1 (log2 fold change 3.94), which is an ABA metabolic protein, this is consistent with drought stress causing an increase in ABA metabolism. Chaperone protein ClpB1 (log2 fold change 3.62) also increased in abundance under drought conditions, this protein is specifically associated with a heat response, but may be a more general stress response protein.

The proteins which were significantly decreased in abundance included pathogenesis-related protein 10 (log2 fold change -3.33), abscisic acid stress ripening5 (Asr protein) (log2 fold change -2.90) and dehydrin3 (log2 fold change -2.26), which are all ABA response proteins associated with drought, which was found to increase in abundance by Alvarez *et al.* (2014); Mostafa *et al.* (2010); Ke *et al.* (2009); Riccardi *et al.* (1998); Zhao *et al.* (2016-1); Yang *et al.* (2013), it is therefore odd that in this data these proteins decreased in abundance. Protease inhibitor (proteinase inhibitor) (substilin /chymotrypsin-like inhibitor) (subtilisin-chymotrypsin inhibitor CI-1B) (log2 fold change -3.36) showed one of the largest fold changes in the dataset. This protein is associated with a wounding response, and whilst the plant was wounded by the removal of the silks, this was also the case for the droughts as well as the controls so there is no reason for a wounding response to be more prevalent in the control samples than the droughts. The protein with the highest fold change was lichenase-2 (log2 fold change -4.71), which is found in the plasma membrane and hydrolyses O-glycosyl compounds. It is interesting that this protein was seen as it is found in the plasma membrane and should be in a low abundance because the plasma membrane is a small component of cells, and plasma membrane proteins were not enriched for.

In the drought silk LFQ dataset there were 24 KEGG pathways identified as significantly enriched. Many of the enriched pathways are involved in metabolism of sugars, amino acids and other small molecules, which was also see in the leaf TMT dataset, further suggesting that drought causes an increase in production of these to cope with drought stress. Degradation pathways were enriched for in the control data including degradation of valine, leucine, isoleucine and lysine, suggesting that these amino acids are needed for stress tolerance. MAPK signalling pathway were also found to be significantly enriched for in the control data, MAPKs are known to be involved in the drought stress response pathway, therefore it would be expected that MAPK signalling pathways would be enriched for in the drought data.

The phosphoproteins which significantly increased in abundance identified in the silks included universal stress protein PHOS34 (S30, log2 fold change 6.76), which is associated with stress, so is expected to increase abundance in the silk material. Mitogen-activated protein kinase kinase kinase 3 (Y5, log2 fold change 3.48) was also a phosphopeptide which significantly increased in abundance, because MAPKKKs are involved in drought stress response and become phosphorylated. The proteins which significantly decreased in abundance identified in the phosphopeptide data for the droughted silks included the late embryogenesis abundant protein (S3, log2 fold change -4.06), which was identified as significantly increasing in abundance in phosphorylated protein in drought studies by Ke *et al.* (2009), and many other drought studies have noted LEA proteins as more abundant under drought conditions (Hajheidari *et al.*, 2006; Mostafa *et al.*, 2010; Ghatak *et al.*, 2016), so it is surprising that it decreased in abundance in this dataset. Protein kinases were also identified including serine/threonine-protein kinase STY46 (S249, log2 fold change -2.95) and serine/threonine-protein kinase TOR (S1256, log2 fold change -2.26), which are involved in signalling, the results in this study are contradicted by authors who found them to be increasing in abundance in droughted tissue (Hu *et al.*, 2015-2; Zhao *et al.*, 2016-2). However, abundance does not equal activity and the proteins may be being degraded faster than they are being produced. E3 ubiquitin-protein ligase UPL1 (S120, log2 fold change -1.72) was also identified, which is associated with ligase activity, and ubiquitin is known to be induced by drought stress, so would be expected to increase in abundance during drought. Mitogen-activated protein kinase kinase kinase 1 (S124, log2 fold change -1.91) was also identified as significantly decreased in abundance in the droughted silk material. MAPKKK proteins are known to play a role in the ABA response pathway though the mechanism is unknown, they are known to become phosphorylated most likely by SnRK2, and

Vu *et al.* (2016) found MAPK phosphoprotein targets to significantly increase in abundance under droughted conditions in maize, it is therefore odd that this MAPKKK was identified as decreasing in abundance.

There were 132 proteins which were observed in both the silk LFQ and silk phosphoproteomics datasets, of which 5 were identified as significantly changing in both the LFQ and phosphoproteomics datasets. These included dehydrin3, dehydrins are drought stress response proteins, and it decreased in abundance in both datasets, which is unexpected. Late embryogenesis abundant protein, group 3 also significantly decreased in abundance in both datasets. LEA proteins play an important role in stress tolerance, and therefore would be expected to increase in abundance in both datasets, it is therefore odd that it decreases in abundance. Heat shock 70 kDa protein 3 significantly decreased in abundance in the LFQ dataset but did not significantly change in the phosphoproteomics dataset. HSPs are important stress response proteins, this data shows that heat shock 70 kDa protein 3 does not become phosphorylated during the drought response pathway. Putative MAP kinase family protein also significantly decreased in abundance in the LFQ dataset but did not significantly change in the phosphoproteomics dataset. MAPKs are known to be involved in the drought response pathway and are known to become phosphorylated during drought, therefore it is surprising that this protein only significantly changes in the LFQ dataset and not the phosphoproteomics dataset.

Whilst experiments were performed on drought treated maize leaves and silk, they were not able to be performed on droughted tassels, due to time and issues with harvesting. More time would have allowed experiments to be performed on tassels, and since maize is most susceptible to drought when the tassels are producing pollen (Doorenbos, 1979), looking at the protein changes caused by drought in the tassels would have been ideal to gain an insight into the effects of drought on yield loss. In the data gathered, proteins which were related to pollen production in drought material were not identified, because these would be present in the tassels, but these proteins are likely to be affected by drought so would have been interesting to analyse.

To conclude drought response proteins were identified using TMT quantification in maize leaves. However, TMT causes suppression of ratios for quantification, so may not be the best method of quantification, but it would not make proteins which are not significant appear significant. TMT may cause significantly changed

proteins to be missed. Proteins which changed due to drought in silk material using LFQ were also identified. Proteins from three different maize tissues; leaf, silk and tassel were compared, the proteins common to all three tissues were core metabolism proteins, common to the silk and tassel were reproduction proteins. Proteins unique to the leaves were photosynthesis proteins, unique to the silks were growth proteins and unique to the tassels were proteins involved in pollen production. In the droughted material ABA response and stress response proteins were identified. In the phosphopeptide analysis drought stress associated proteins which were phosphorylated were identified. Phosphopeptides in the silk dataset were also identified which mapped to MAPKKK proteins which are associated with ABA response pathways, and other drought response proteins which were phosphorylated. When comparing phosphopeptides between the three maize tissues, the phosphopeptides could be mapped to proteins included in core function. Proteins associated with reproduction in the silk tissue were not identified. In the droughted tissue ABA and stress response proteins were identified in both tissues but also some only found in one of the tissues. In both tissues SnRK2 was identified, which is known to be involved in the ABA response pathways and is auto phosphorylated during this pathway.

Chapter 4

Damage Caused by Methyl Viologen Treatment to *Arabidopsis thaliana* & *Zea mays* Proteins

4.1 Introduction

4.1.1 Herbicides

Herbicides are used in many countries to combat invasive plants during crop growth. Nonselective herbicides target all plants whereas selective herbicides target specific groups, such as broadleaf plants (Davy and Perrow, 2002). Due to the toxicity of herbicides, they can also have an effect on the crops they are not targeting causing stress to the plant, which causes damage in the form of protein modifications (Wagner and Nelson, 2014).

Herbicides are classified on the basis of their mode of action. For example one class of herbicides acts as amino acid (AA) biosynthesis inhibitors and will target enzymes involved in AA biosynthesis (Duke, 1990). Another class inhibits photosynthesis by binding to the protein D1 in order to block electron transfer during photosynthesis (Fedtke and Trebst, 1987). Herbicides can also inhibit lipid biosynthesis, they work by inhibiting acetyl-CoA carboxylase, an enzyme present in most grasses (Duke and Kenyon, 1988; Wilkinson, 1988). Herbicides can also inhibit cell division, and work by attacking molecular sites which are essential for cell divi-

sion (Hess, 1987). Some herbicides work as carotenoid biosynthesis inhibitors, by blocking the terpenoid synthesis (Duke, 1990). Another class of herbicides act as photobleachers, and work by reacting with chlorophyll, causing bleaching of green tissue (Duke, 1990). Photobleachers include Paraquat and Diquat.

Herbicides affect monocots and dicots in different ways. Broadleaf herbicides are designed to kill dicots but leave monocots unaffected whereas grass herbicides kill monocots but generally leave dicots untouched (Bohan *et al.*, 2005), and non-selective herbicides will kill most plants regardless of them being monocots or dicots (Duke and Abbas, 1995). Monocots include crop plants such as wheat, rice, barley and maize. Dicots include soybeans and *Arabidopsis thaliana*. Four structural features separate dicots and monocots, relating to their leaves, stems, roots and flowers. These differences begin with the seed, in the embryo of a monocot, there is one cotyledon, whereas dicots have two (Zimmermann and Werr, 2005). This leads to different development processes of both plants. Monocots have fibrous roots, which branch extensively and do not go as deep as the taproot which dicots tend to have (McSteen, 2010). In the stem of a monocot, the vascular tissue is arranged sporadically, whereas in a dicot it is arranged in hollow circular structures (Scarpella and Meijer, 2004). Monocot leaves have parallel veins whereas dicots have branching veins (Nelson and Dengler, 1997). Monocot flower petals usually form in threes, whereas dicot flower petals form in groups of four or five (Rudall and Bateman, 2004).

Auxinic herbicides will kill dicot weeds, but not affect monocot crops, this is because monocots and dicots respond differently to synthetic auxin, which is a primary growth regulating plant hormone. There are many different theories as to why they respond differently such as limited translocation or rapid degradation of exogenous auxin (Gauvrit and Gaillardon, 1991), different vascular anatomy (Monaco *et al.*, 2002), or monocots perceiving auxin differently in monocots and dicots (Kelley and Riechers, 2007).

Sethoxydim and haloxyfop are toxic to monocots but leave dicots untouched (Buhler *et al.*, 1985; Swisher and Corbin, 1982). The absorption, translocation and metabolism of these herbicides is the same in both plant types, which suggests they are selective due to sensitivity at the primary site of action (Buhler *et al.*, 1985; Swisher and Corbin, 1982; Hendley *et al.*, 1985). Burton *et al.* (1987) found that the two herbicides inhibited fatty acid synthesis and acetyl-CoA carboxylase in the

chloroplasts of monocots but not dicots, concluding that the selectivity was due to differences in herbicide sensitivity of monocot and dicot acetyl-CoA carboxylase.

Methyl viologen (MV) is the active ingredient in Paraquat, a wide spectrum herbicide used for weed control in agriculture (Fan *et al.*, 2018) which kills plants by causing oxidative stress (Lascano *et al.*, 2012). MV exists in a 2+ charge state, allowing it to act as an electron acceptor, and it is the singlet charge state which reacts rapidly with oxygen causing the superoxide radical to be produced and following which hydrogen peroxide and the hydroxyl radical are produced (Figure 4.1) (Kröncke and Kolb-Bachofen, 1996). In plants, the reduction of MV mostly takes place within the chloroplasts and mitochondria. Under photosynthesising conditions, MV is a photobleacher and acts as an alternative electron acceptor to proteins in photosystem I (PSI), thus greatly hindering the ferredoxin reaction, NADPH regeneration and ascorbic acid production (Figure 4.2) (Lascano *et al.*, 2012). This prevention of the production of antioxidants and the increased production of reactive oxygen species (ROS) makes MV a very strong oxidative stress inducer (Lascano *et al.*, 2012), and causes bleaching of chlorophyll. There is another light independent mechanism, where MV induces ROS formation in the electron transfer chain in the mitochondria during respiration. However, the site of action within mitochondria is not currently known, but damage is still present in plants when kept in the dark, suggesting there is a mechanism of attack in the mitochondria (Cui *et al.*, 2018).

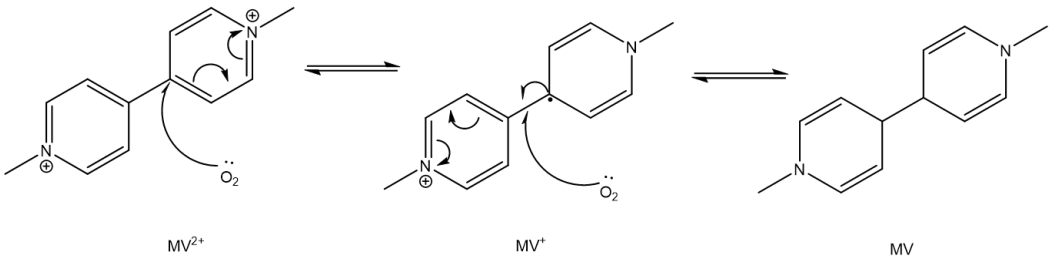

Figure 4.1: Mechanism of action for methyl viologen (MV). MV exists in the 2+ state, it accepts an electron and a free radical is generated for the intermediate product, another electron is accepted and the MV becomes neutral.

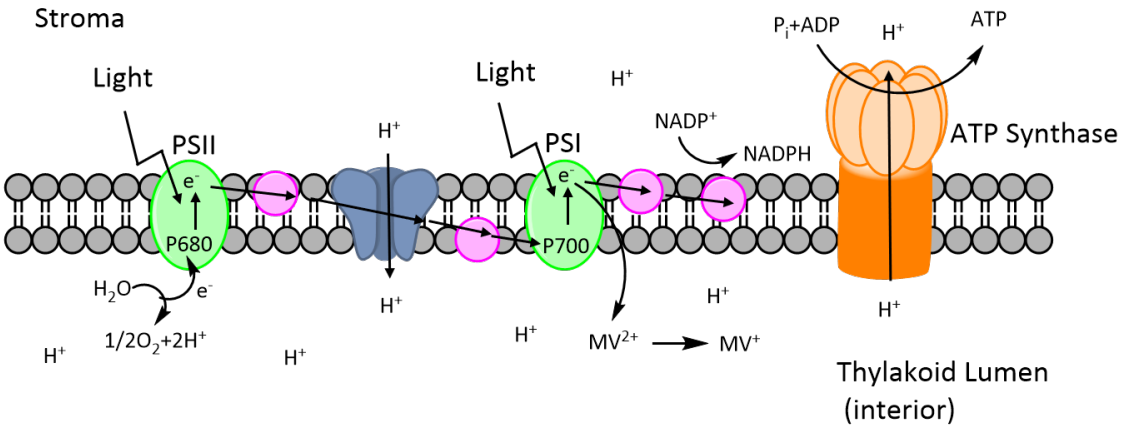

Figure 4.2: Mechanism of action for photosystem 1 and 2 during photosynthesis and the MV mechanism of action. MV^{2+} accepts an electron from PSI, inhibiting photosynthesis.

MV reactions take place in the chloroplasts of plant cells and cause a decrease in the amount of chlorophyll a and b in cells, decreasing leaf pigment and photosynthetic activity (Fan *et al.*, 2018). MV treatment causes down regulation of proteins involved in porphyrin, chlorophyll metabolism and photosynthesis, while proteins involved in respiration pathways are overexpressed, as well as proteins which regulate anti-oxidants in order to try and combat the increase in ROS activity (Fan *et al.*, 2018). MV causes increased expression of proteins involved in essential pathways including, carbon metabolism, biosynthesis of antibodies and amino acids, TCA cycle, glycolysis and pyruvate metabolism (Fan *et al.*, 2018). Expression of proteins associated with stress also increases under MV treatment (Fan *et al.*, 2018). Overall, there is an increase in stress, antioxidant enzymes and respiration associated proteins and a decrease in expression of proteins involved in photosynthesis.

MV induces ROS production, which causes oxidative damage to proteins. In unstressed Arabidopsis tissue, carbonylation naturally occurs at levels between 4 and 10 nmol mg^{-1} of protein (Debska *et al.*, 2013; Nguyen and Donaldson, 2005; Romero-Puertas *et al.*, 2002). Carbonylation increases in aging tissue but decreases in reproductive tissue (Johansson *et al.*, 2004). Arabidopsis cells respond to MV by increasing Non-Photochemical Quenching (NPQ), which decreases the plants sensitivity to light intensity and activates MV (Moustaka *et al.*, 2015). In lower concentrations, MV causes an increase in superoxide dismutase (SOD) activity and increases the plant's tolerance to oxidative damage, as the antioxidant enzymes are available at high enough levels to deal with the excess production of the superoxide

radical (Han *et al.*, 2014). However, with higher concentrations of MV SODs are unable to keep ROS levels under control allowing the uncontrolled production of the superoxide radical, leading to the production of the hydroxyl radical which is more toxic and causes rapid cell death (Han *et al.*, 2014).

4.1.2 Soluble & Membrane Proteins

In crop plants soluble proteins make up 20% of the proteome (Rosentrater and Evers, 2018). Soluble proteins are complex mixtures, with protein functions ranging from metabolic enzymes, hydrolytic enzymes and enzyme inhibitors (Rosentrater and Evers, 2018). Soluble proteins are found in the cytoplasm and other organelles like the nucleus and chloroplast (Rosentrater and Evers, 2018). The outer surface of soluble proteins contains hydrophilic amino acid (AA) residues which help to keep the protein solubilised (Yanagihara *et al.*, 1989). Hydrophobic AAs are contained within the protein, away from the surface (Yanagihara *et al.*, 1989). There are two types of membrane proteins, buried proteins and anchored proteins (Lodish *et al.*, 2000). Buried proteins are contained within membranes and they have hydrophobic AAs which interact with the membrane (Juretic *et al.*, 1998). Anchored proteins have lipid molecules which act as a linker to the membrane (Rossi and Chopineau, 2007).

Membrane proteins are more challenging to analyse than soluble proteins because of their hydrophobic nature, making them insoluble in samples which do not contain a solubilising agent such as detergent. Some membrane proteins have a low abundance (Ephritikhine *et al.*, 2004). This means they are often underrepresented in proteomic datasets, despite making up a third of the proteome in most eukaryotic cells (Ephritikhine *et al.*, 2004).

To isolate membrane proteins from soluble proteins, ultracentrifugation is often used (Reid and Williamson, 1974). Typically, nuclei are isolated at 600–1,000 g, chloroplasts at 2,000 g, mitochondria and peroxisomes at 3,000–15,000 g, and remaining membranes at 100,000 g (Graham *et al.*, 1994; Ozols, 1990). This final fraction is enriched for membrane proteins including plasma membranes, endoplasmic reticulum, Golgi apparatus, vascular membranes and various endosomal vesicles and compartments (Abas and Luschnig, 2010).

The plasma membrane separates the interior and exterior of the cell, which can also be isolated from other membranes by using phase separation after ultracen-

trifugation. Alexandersson *et al.* (2004) used reverse phase chromatography coupled to electrospray ionisation-mass spectrometry (ESI-MS) to identify over 200 plasma membrane proteins in Arabidopsis leaves. However, plasma membrane of monocots are difficult to isolate due to the differences in cell-wall polysaccharide composition between them and dicots, so there are few proteomic examples available in the literature (White and Broadley, 2003). Genomes for monocots have also not been available until recently, and even now they are often poorly annotated, which has limited proteomic studies.

4.1.3 Reducing Tandem Mass Tag Ratio Suppression with MS3 Analysis

Tandem mass tag (TMT) is used for quantitative analysis in MS. When analysing TMT tagged samples MS2 analysis involves MS1 scans in the Orbitrap, to get accurate peptide parent ion masses. MS2 analysis is performed in the Orbitrap with higher-energy collision dissociation (HCD) fragmentation, this allows the reporter ions to break under MS2 analysis and quantitative information can be established (Figure 4.3A) (Rauniyar and Yates, 2014). Since the ion trap is not accurate enough to distinguish between the reporter ions, the Orbitrap needs to be used for analysis. However, peptides are isolated from the MS1 within a 1 Da window, therefore more than one peptide is isolated for MS2 fragmentation, and these other peptides that are isolated also have reporter ions which will fragment during MS2, and these contribute to the ratios used for quantification, which can mask some significant proteins. To reduce the ratio suppression observed in complex samples when using isobaric tags (iTRAQ, TMT) Thermo Scientific recommend using MS3 when analysing TMT samples.

MS3 analysis involves MS1 scans in the Orbitrap, to get an accurate peptide parent ion mass. MS2 scans in the ion trap with collision-induced dissociation (CID) fragmentation, the CID fragmentation is lower energy than HCD fragmentation so should not break off the TMT reporter ions. MS3 in the Orbitrap with HCD fragmentation, the highest fragments from the MS2 are selected for MS3 analysis, the HCD fragmentation is higher energy than the CID fragmentation so will break off the reporter ions. The method is optimised for the bottom range so only the reporter ions are seen in the MS3. The MS3 reporter ion intensities are then averaged across the MS3s for the peptide and a ratio of reporter ions can be obtained for quantitative analysis (Figure 4.3B). The problem of ratio suppression is only seen in complex samples where isolation of near isobaric precursors can lead to ratio suppression

when using MS2 fragmentation only (Ting *et al.*, 2011), but MS3 analysis is much slower than MS2 analysis.

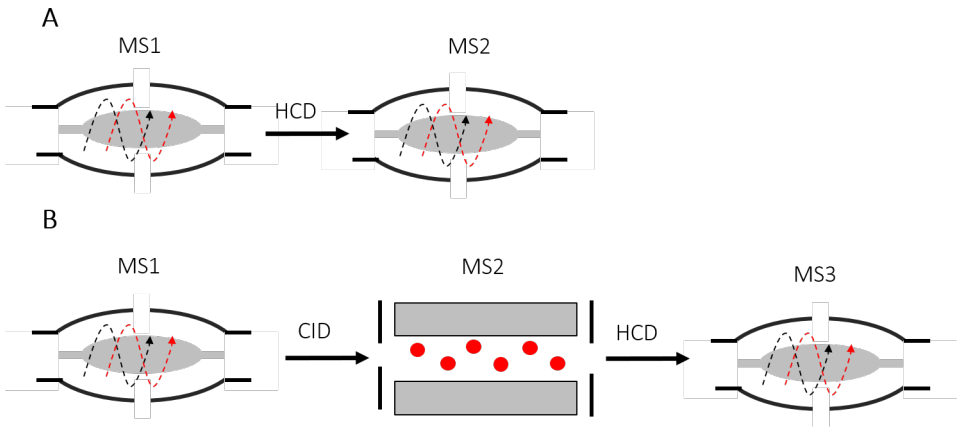

Figure 4.3: (A) MS2 fragmentation of isobaric tags in the Orbitrap Fusion. The MS1 takes place in the Orbitrap, which has high mass accuracy, then the Orbitrap is emptied in order to analyse fragments from the peptides for MS2 analysis. This is because the ion traps mass accuracy is not high enough to differentiate between the reporter ions from the isobaric tags. (B) MS3 fragmentation of isobaric tags in the Orbitrap Fusion. MS1 analysis takes place in the Orbitrap. CID fragmentation will fragment the peptide without breaking off the reporter ion from the isobaric tag, analysis is performed in the ion trap, which loses the bottom third of fragments during analysis, so reporter ions cannot be seen. The ten most intense peptide fragments are chosen for MS3 fragmentation. HCD fragmentation is higher energy and will remove the isobaric tag reporter ions. The ratios of the reporter ions from the ten MS3 scans are averaged to gain accurate quantitative data..

4.1.4 Signalling Mediated by Phosphorylation in *Arabidopsis thaliana*

Organisms utilise post translational modifications (PTMs) for a large number of functions, including transmitting signals and responding to changing stimuli. These PTMs include methylation, ubiquitination, carbonylation, acetylation and phosphorylation (Friso and van Wijk, 2015). These modifications are important in plants because they need to quickly adapt to changes in their environment (Hodges *et al.*, 2013). Protein phosphorylation involves the addition of a phosphate group to specific AAs and, due to protein phosphatases the reaction is reversible (Barford, 1996). Protein phosphorylation plays an essential role in regulating cell function, and biological processes including metabolism, growth, biotic and abiotic stress responses (Hodges *et al.*, 2013). Protein kinases are enzymes which regulate proteins biological activity by phosphorylation of specific AAs (Avendaño and Menéndez, 2008),

it is estimated that there are 1,000 protein kinases in plants (Kersten *et al.*, 2006) and that 30% of proteins are phosphorylated at some point (Cohen, 2000). Protein kinases work by transferring a phosphate group from adenosine triphosphate (ATP) and attaching it via a covalent bond to a free hydroxy group on an AA (Weber, 2010). Mitogen-activated protein kinases (MAPKs) are specific to serine and threonine and respond to a wide range of stimuli including various stresses (Cargnello and Roux, 2011).

There have been many studies of phosphorylation in Arabidopsis mostly looking at phosphoserine, phosphothreonine and phosphotyrosine. Transferases are enzymes which transfer specific functional groups from one molecule to another. Kinases are a form of transferases that catalyse the transfer of phosphate groups from ATP to specific molecules and are involved in cell signalling. Large scale studies of phosphorylation in Arabidopsis have shown that tyrosine phosphorylation mostly happens on proteins that have kinase or transferase activity (Sugiyama *et al.*, 2008). MAPK1 is involved in cell signalling and is known to be become phosphorylated during stress response mechanisms in plants, MAPK1 is therefore involved in plant stress response (Jiang *et al.*, 2017). D-3-phosphoglycerate dehydrogenase is an enzyme which catalysis the transition of 3-phosphoglycerate to 3-phosphohydroxypyruvate which is a step in the L-serine biosynthesis phosphorylated pathway. D-3-phosphoglycerate dehydrogenase has been found to be phosphorylated in Arabidopsis (Lohrig *et al.*, 2009). Triosephosphate isomerase is an enzyme which is important in glycolysis and efficient energy production. It is found to become phosphorylated in Arabidopsis (Lohrig *et al.*, 2009). Casein kinase 2 is a serine/threonine selective protein kinase that is involved in the DNA repair, cell cycle control and regulation of circadian rhythms, and is found to be phosphorylated in Arabidopsis (Lin *et al.*, 2015).

Ten phosphoproteins have been identified in plant chloroplast membranes, but there are thought to be many more (Bennet, 1979). Phosphorylation of chloroplast membranes is thought to control the distribution of excitation energy between PSI and PSII (Staehelin and Arntzen, 1983). The herbicide 3-(3,4-Dichlorophenyl)-1,1-dimethylurea (Diuron) is known to inhibit phosphorylation of PSII, however very little other work has been done of the effect of herbicides on phosphorylation in plants (Bennett, 1979).

4.1.5 Aims & Objectives

The aims of this chapter were to identify proteins which are affected by MV in *Arabidopsis thaliana* and *Zea mays*, to do this, leaves from plants were treated with MV and proteins were extracted fresh so membrane proteins could be separated from soluble proteins. Each sample and replicate were tagged with a different TMT tag for quantitative analysis. TMT labelled samples were then combined and fractionated, this allows more proteins to be identified.

How MV affects phosphorylation of proteins in *Arabidopsis thaliana* and *Zea mays* was also analysed. To do this samples were digested using trypsin and enriched for phosphopeptides using titanium dioxide (TiO_2) beads. There have been many studies into phosphorylation in Arabidopsis particularly, but none looking at the effect of MV on phosphorylation.

4.2 Results

4.2.1 Methyl Viologen Treatment of *Arabidopsis thaliana*

Leaves were cut from Columbia-0 (Col-0) Arabidopsis plants at 6-7 weeks after emergence and placed in Petri dishes with 500 nM of MV under constant light for 16 hours to induce protein changes. So the soluble and membrane proteins could be separated via centrifugation, the leaves were ground fresh on ice. Five replicates were used for each treatment, and proteins were either tagged with tandem mass tag (TMT) or enriched for phosphopeptides then analysed using the Orbitrap Fusion (Figure 4.4).

To determine if the MV treatment induced carbonyl modifications, a western blot was performed on the MV treated soluble fraction of the Arabidopsis leaves using 2,4-dinitrophenylhydrazine (DNPH) which reacts with carbonyl modifications and anti-DNPH (Figure 4.5). An increase in carbonylation levels can be seen in the samples treated with MV. Once it was established that the treatment was causing a change to the proteins, further analysis could go ahead.

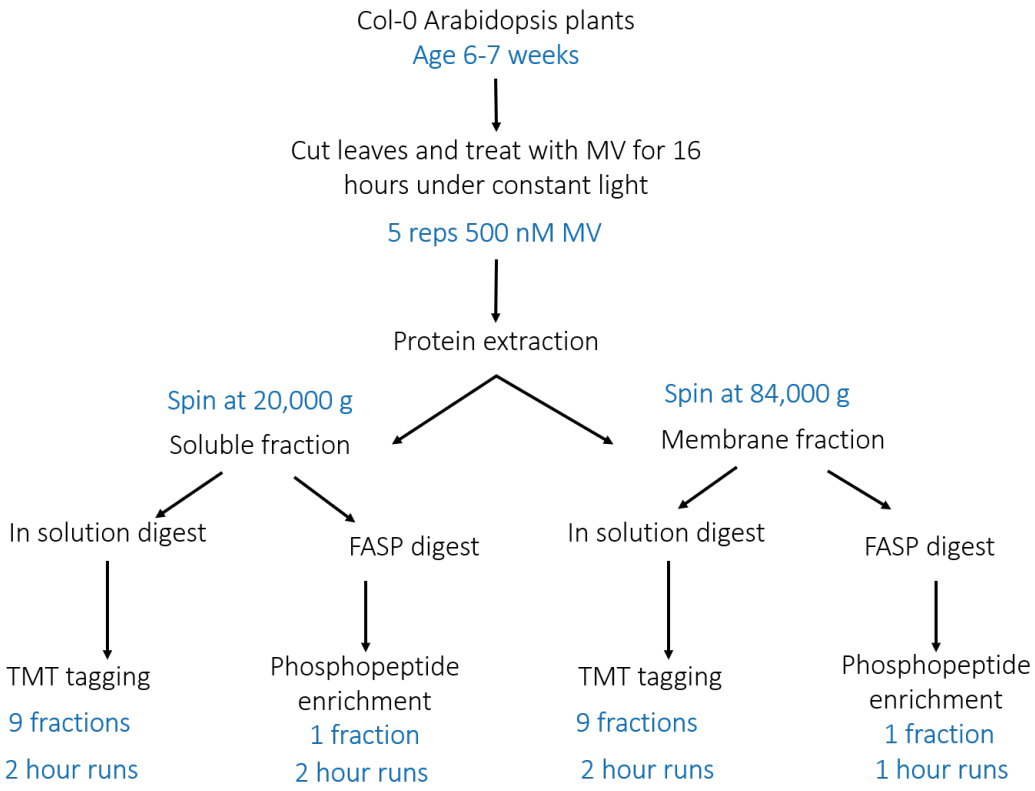

Figure 4.4: Col-0 Arabidopsis plants were grown for 6-7 weeks, then treated in Petri dishes with 500 nM of MV for 16 hours under constant light. Protein was then extracted; samples were spun at 20,000 g to isolate the soluble fraction and 84,000 g to isolate the membrane fraction. An in-solution digest was performed on samples which were tagged with TMT and a FASP digest was performed on samples which were enriched for phosphopeptides.

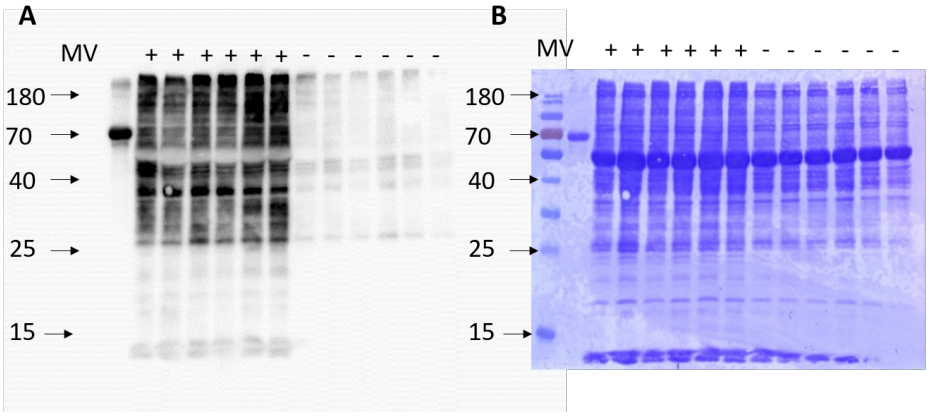

Figure 4.5: (A) Western blot of MV treated Arabidopsis soluble leaf proteins tagged with DNPH, using anti-DNPH conjugated to horse radish peroxidase (HRP). (B) Membrane stained with coomassie. There is an increase in HRP signal in the MV treated samples, showing that MV causes oxidative damage to proteins.

4.2.2 Comparative Quantification of Tandem Mass Tags Using Sequential Fragmentation

To determine the impact of using MS2 or MS3 scans for TMT quantification in the Orbitrap, fraction 4 of the soluble TMT labelled Arabidopsis proteins was analysed using MS2 and MS3 in sequential runs. 377 proteins were identified from Orbitrap analysis using MS3 fragmentation in a 2-hour run, whereas 575 proteins were identified using MS2 fragmentation. MS3 identified 96 significantly changing proteins whereas MS2 identified 178, of which 50 are significant in both (Figure 4.6). Some of the proteins which were identified in both the MS2 and MS3 analysis were found to be significant in one analysis but not the other.

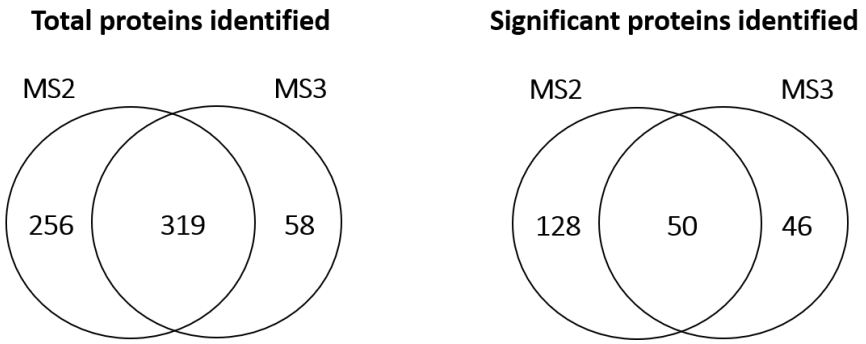

Figure 4.6: Venn diagrams showing the proteins identified in fraction 4 using MS2 and MS3 and the significant proteins identified in both and their overlap. Overall more proteins were identified in the MS2 experiment and more proteins were identified as significant.

There is a trade off when performing MS2 or MS3 analysis. MS2 analysis is much faster than MS3 analysis, so more peptides can be identified, however, significant proteins can be masked, due to ratio suppression which rises from the isolation of peptides within a 1 Da window, also isolating other lower abundant peptides which add to the reporter ion ratios used for quantification. Whilst MS2 analysis may mask some significant proteins, it is unlikely to make proteins which are not significant appear significant. It is for this reason that it was decided that the MS2 method was valid and in order to identify more proteins the MS2 method was continued to be used. Samples were also fractionated to reduce their complexity, making them more suitable for MS2 analysis.

4.2.3 Tandem Mass Tag Quantification of *Arabidopsis thaliana* Soluble & Membrane proteins

Separated soluble and membrane proteins were labelled with TMT, fractionated into 9 fractions and analysed using the Orbitrap Fusion to identify protein changes due to MV treatment. Proteins were identified using MaxQuant (MQ) and statistical differences analysed using Perseus. The principle component analysis (PCA) plot of the soluble fraction shows a difference in the proteins in the MV treatment and control samples, meaning the treatment was effective (Figure 4.7A). In the soluble fractions 1342 proteins were identified (Figure 4.7B), there were 158 proteins identified as significantly increasing in abundance under MV treatment, these proteins were mostly associated with stress response and photosynthesis. Whereas 239 proteins significantly decreased in abundance in the treatment, these were mostly associated with oxidative stress and general stress responses. However, the fold

changes seen in these proteins are small, (mostly a fold change of less than log2 of 1). This is for two reasons, firstly, the ratio supression from the TMT, which will make the proteins appear less significant. Secondly these are soluble proteins and MV attacks the membrane so it might be expected that soluble proteins are less affected by the treatment. To simplify presentation only proteins increasing in abundance with a log2 fold change greater than 0.6 are shown in Table 4.1 and proteins decreasing in abundance with a log2 fold change greater than 0.6 are shown in Table 4.2. A low fold change tolerance was used because the TMT ratio suppression decreases the fold change of the proteins.

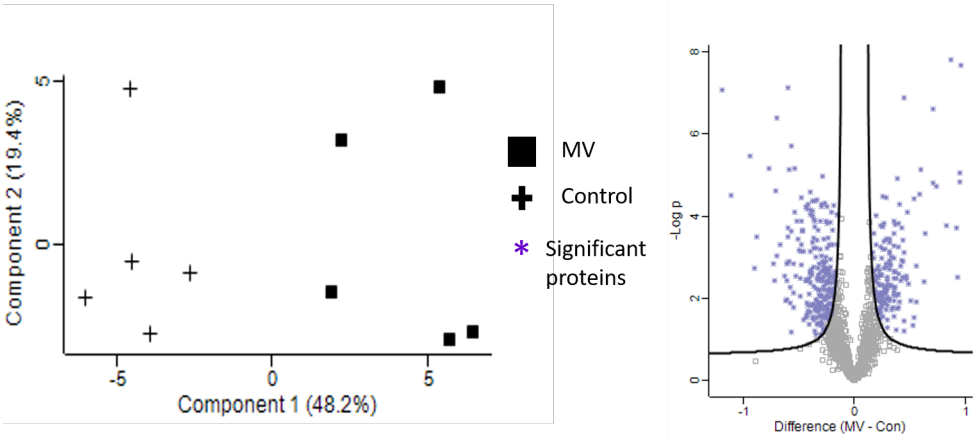

Figure 4.7: (A) PCA plot of the Arabidopsis soluble proteins treated with MV. The control and MV treated samples separate, showing the treatment is changing the protein composition. (B) Volcano plot showing the significantly changed proteins between the control and the treatment. 1342 proteins were identified of which 397 were identified as significantly changed. FDR: 0.05 s0: 0.1.

Mapman was used to assign identified proteins to pathways in Arabidopsis and visualise the location of the changing proteins in the MV treatment (Figure 4.8), all proteins identified and their log2 fold change was used to generate the image. The most dramatic change was seen in the light reaction pathways, which is consistent with the MV mechanism of attack at PSI, and the inhibition of photosynthesis. Therefore the photosynthesis pathway was looked at in more detail (Figure 4.9), which revealed proteins decreasing in abundance in these pathways.

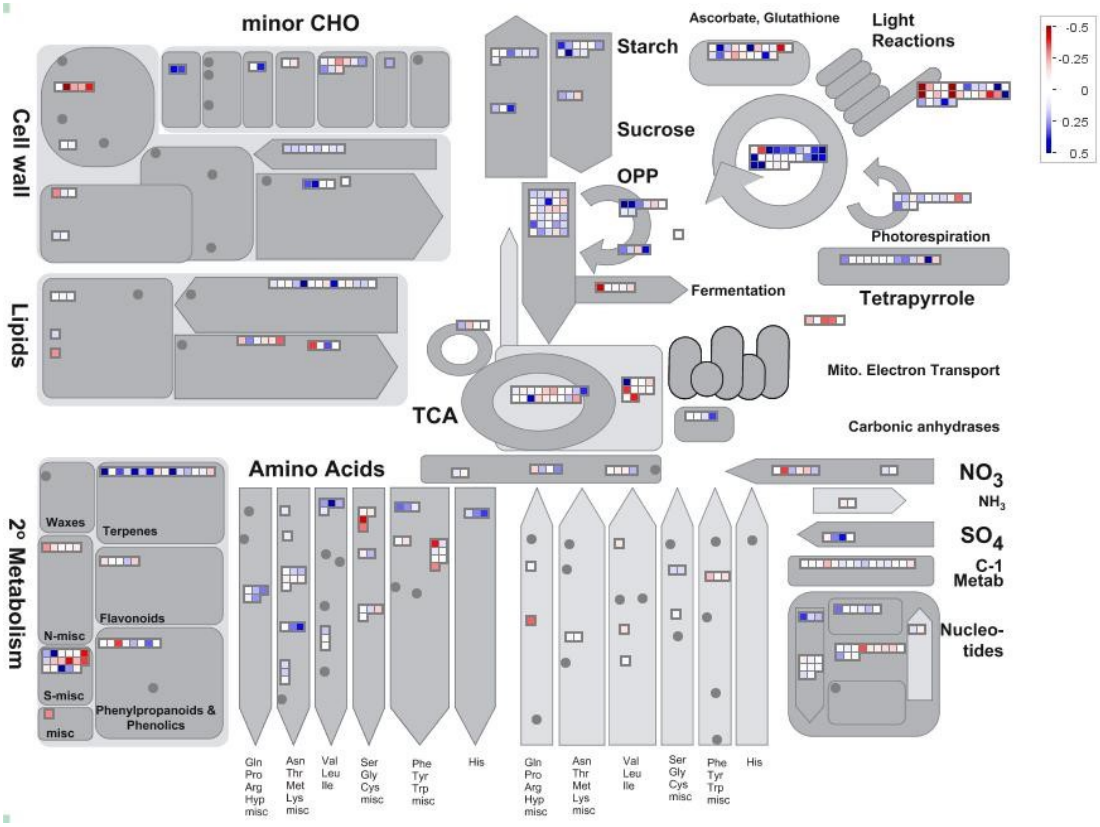

Figure 4.8: An overview of the metabolism pathways from the proteins identified in the MV treated Arabidopsis soluble fraction. The blue colour shows the proteins which increased in abundance under MV treatment, the red shows the proteins which decreased in abundance under MV treatment and the white shows proteins which do not change. We can see proteins associated with the light reaction pathway changing the most, which is consistent with MVs mechanism of attack.

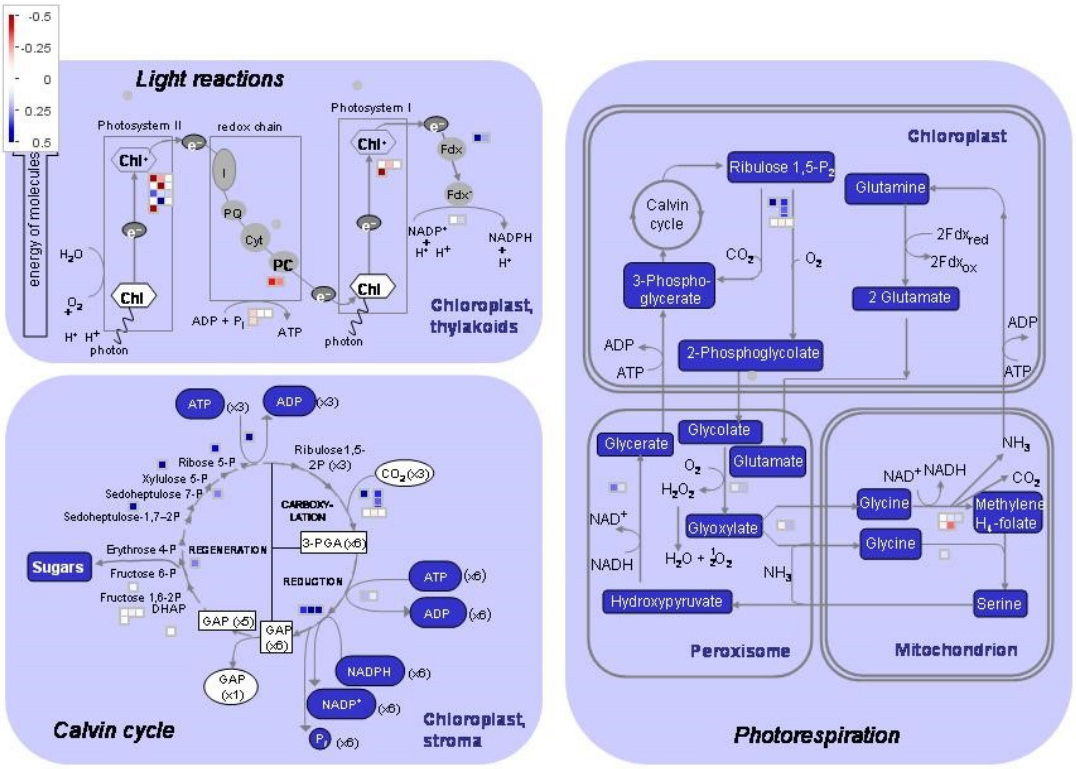

Figure 4.9: An overview of the changing proteins in the photosynthesis pathways of the Arabidopsis soluble proteins. Red are the proteins which decrease in abundance and blue are the proteins which increase in abundance. We can see more proteins decreasing in abundance than increasing, which is consistent with damage caused by the generation of ROS by MV.

Table 4.1: The proteins which significantly increased in abundance identified in the MV treated Arabidopsis soluble fraction with a log2 fold change of more than 0.6.

Protein Name	**Gene Number**	**Log2 Fold Change**	**-Log P Value**	**MQ Score**	**Function/Pathway**
Oxygen-evolving enhancer protein 1-1, chloroplastic (OEE1) (33 kDa subunit of oxygen evolving system of photosystem II)	At5g66570 K1F13.25	0.96	7.69	323.31	Oxygen evolving activity; poly(U) RNA binding
Probable glucan endo-1,3-beta-glucosidase At4g16260 (EC 3.2.1.39)	At4g16260 dl4170c	0.95	4.84	110.67	Glucan endo-1,3-beta-D-glucosidase activity
Protein TIC 62, chloroplastic (Translocon at the inner envelope membrane of chloroplasts 62) (AtTIC62)	At3g18890 MCB22.6	0.95	5.05	56.25	Involved in protein precursor import into chloroplasts. Part of the redox regulon consisting of TIC32, TIC 55 and TIC62. Acts as a membrane anchor of LFNR1 and LFNR2. Has a NADPH-dependent dehydrogenase activity, but only after preincubation with lipids
Histone deacetylase HDT2	At5g22650 MDJ22.7	0.93	2.51	15.34	Histone deacetylase activity

Continued on next page

Table 4.1 – *Continued from previous page*

Protein Name	**Gene Number**	**Log2 Fold Change**	**-Log P Value**	**MQ Score**	**Function/Pathway**
Heat shock protein 90-1 (AtHSP90.1)	At5g52640 F6N7.13	0.92	3.71	219.75	ATP binding; unfolded protein binding
Oxygen-evolving enhancer protein 1-2, chloroplastic (OEE1)	At3g50820 F18B3.100	0.87	7.81	207.56	Oxygen evolving activity; poly(U) RNA binding
Calreticulin-2	At1g09210 T12M4.8	0.83	3.76	61.90	Calcium ion binding; carbohydrate binding; unfolded protein binding
V-type proton ATPase subunit G1 (V-ATPase subunit G1)	At3g01390 T13O15.3	0.73	4.74	70.26	Proton-exporting ATPase activity, phosphorylative mechanism; proton-transporting ATP synthase activity, rotational mechanism
60S acidic ribosomal protein P1-1	At1g01100 T25K16.9	0.71	4.82	31.61	Protein kinase activator activity; ribonucleoprotein complex binding; structural constituent of ribosome
Probable mediator of RNA polymerase II transcription subunit 37c (Heat shock 70 kDa protein 4)	At3g12580 T16H11.7	0.71	6.61	133.88	ATPase activity; ATPase activity, coupled; ATP binding; heat shock protein binding; misfolded protein binding; protein folding chaperone; ubiquitin protein ligase binding; unfolded protein binding
Heat shock protein 90-4 (AtHSP90.4)	At5g56000 MDA7.4	0.64	3.57	12.69	ATP binding; unfolded protein binding

Continued on next page

Table 4.1 – *Continued from previous page*

Protein Name	**Gene Number**	**Log2 Fold Change**	**-Log P Value**	**MQ Score**	**Function/Pathway**
Thioredoxin family protein	At2g47470 T30B22.23	0.63	2.41	60.70	Isomerase activity

Table 4.2: The proteins which significantly decreased in abundance identified in the MV treated Arabidopsis soluble fraction with a log2 fold change of more than 0.6.

Protein Name	**Gene Number**	**Log2 Fold Change**	**-Log P Value**	**MQ Score**	**Function/Pathway**
Alanine–tRNA ligase, chloroplastic/mitochondrial (EC 6.1.1.7)	At5g22800 MRN17.3	-1.19	7.09	90.37	Alanine-tRNA ligase activity; amino acid binding; aminoacyl-tRNA editing activity; ATP binding; tRNA binding; zinc ion binding
Photosystem II repair protein PSB27-H1, chloroplastic (Psb27-H1)	At1g03600 F21B7.14	-1.11	4.51	111.80	
3-isopropylmalate dehydratase large subunit, chloroplastic (EC 4.2.1.33)	At4g13430 T9E8.170	-0.94	5.48	72.72	3-isopropylmalate dehydratase activity; 4 iron, 4 sulfur cluster binding; intramolecular transferase activity, transferring hydroxy groups; metal ion binding
Thylakoid lumenal 29 kDa protein, chloroplastic (TL29)	At4g09010 F23J3.40	-0.90	2.72	103.65	Heme binding; peroxidase activity

Continued on next page

Table 4.2 – *Continued from previous page*

Protein Name	**Gene Number**	**Log2 Fold Change**	**-Log P Value**	**MQ Score**	**Function/Pathway**
Glyceraldehyde-3-phosphate dehydrogenase GAPA1, chloroplastic (EC 1.2.1.13)	At3g26650 MLJ15.4	-0.88	3.49	323.31	Disordered domain specific binding; glyceraldehyde-3-phosphate dehydrogenase (NAD+) (phosphorylating) activity; glyceraldehyde-3-phosphate dehydrogenase (NADP+) (phosphorylating) activity; identical protein binding; NAD binding; NADP binding; protein homodimerization activity
Thiamine thiazole synthase, chloroplastic (EC 2.4.2.60)	At5g54770 MBG8.3	-0.77	5.17	293.81	Iron ion binding; protein domain specific binding; protein homodimerization activity; transferase activity, transferring pentosyl groups; zinc ion binding
Protein IN CHLOROPLAST ATPASE BIOGENESIS, chloroplastic	At4g34090	-0.73	2.84	72.13	Involved in the assembly of the F(1) ATP synthase in chloroplast thylakoid membranes. Functions downstream of the CPN60 chaperones to promote assembly of the catalytically active core of the chloroplast ATP synthase. Assists the assembly of the ATP synthase gamma subunit into the active F(1) core downstream of CPN60-mediated folding, which is critical for the biogenesis of the chloroplast ATP synthase

Continued on next page

Table 4.2 – *Continued from previous page*

Protein Name	**Gene Number**	**Log2 Fold Change**	**-Log P Value**	**MQ Score**	**Function/Pathway**
3-dehydroquinate synthase, chloroplastic (EC 4.2.3.4)	At5g66120 K2A18.20	-0.72	2.43	36.73	3-dehydroquinate synthase activity; metal ion binding
Ribulose-5-phosphate-3-epimerase, chloroplastic (R5P3E) (EC 5.1.3.1)	At5g61410 MFB13.19	-0.71	4.63	201.50	Metal ion binding; ribulose-phosphate 3-epimerase activity
Presequence protease 1, chloroplastic/mitochondrial (AtPreP1) (PreP 1) (EC 3.4.24.-)	At3g19170 MVI11.6	-0.70	6.40	323.31	Metal ion binding; metalloendopeptidase activity
26S proteasome non-ATPase regulatory subunit 12 homolog A	At5g09900 MYH9.11	-0.70	3.03	16.37	Acts as a regulatory subunit of the 26 proteasome which is involved in the ATP-dependent degradation of ubiquitinated proteins. Required for gametogenesis and sporophyte development. Acts redundantly with RPN5B

Continued on next page

Table 4.2 – *Continued from previous page*

Protein Name	**Gene Number**	**Log2 Fold Change**	**-Log P Value**	**MQ Score**	**Function/Pathway**
Serine/threonine-protein phosphatase 2A 65 kDa regulatory subunit A beta isoform	At3g25800 K13N2.14	-0.66	3.31	35.16	Protein phosphatase regulator activity
Glucose-6-phosphate 1-dehydrogenase 1, chloroplastic (AtG6PD1) (G6PDH1) (EC 1.1.1.49)	At5g35790 MIK22.2	-0.63	2.54	24.69	Glucose-6-phosphate dehydrogenase activity; NADP binding
3-oxoacyl-[acyl-carrier-protein] synthase I, chloroplastic (EC 2.3.1.41)	At5g46290 MPL12.7	-0.62	1.93	118.70	3-oxoacyl-[acyl-carrier-protein] synthase activity
Ribulose bisphosphate carboxylase large chain (RuBisCO large subunit) (EC 4.1.1.39)	AtCg00490	-0.61	2.84	323.31	Magnesium ion binding; monooxygenase activity; ribulose-bisphosphate carboxylase activity

Continued on next page

Table 4.2 – *Continued from previous page*

Protein Name	**Gene Number**	**Log2 Fold Change**	**-Log P Value**	**MQ Score**	**Function/Pathway**
Ketose-bisphosphate aldolase class-II family protein	At1g18270 T10O22.24	-0.61	2.42	22.01	Aldehyde-lyase activity; NAD binding; NADP binding; oxidoreductase activity; zinc ion binding
Protein SUPPRESSOR OF QUENCHING 1, chloroplastic (EC 3.1.3.-)	At1g56500 F13N6.21	-0.60	1.96	37.45	Hydrolase activity; metal ion binding; ubiquitin protein ligase activity

The membrane fraction of the MV treated Arabidopsis proteins was also analysed. A PCA plot was produced and shows a change in the proteins between the MV treated and the control in the membrane protein fraction (Figure 4.10A). In the membrane fraction 879 proteins were identified (Figure 4.10B), there were 205 proteins identified as significantly increasing in abundance in the MV treated over the control; these were mostly associated with stress response and photosynthesis. There were 373 proteins found to be significantly decreasing in abundance in the MV treated compared to the control; these were mostly associated with oxidative stress and general stress response. The proteins which significantly increased in abundance with a log2 fold change of more than 1.5 (to keep the table to a manageable size) are shown in Table 4.3, and the less abundant in Table 4.4.

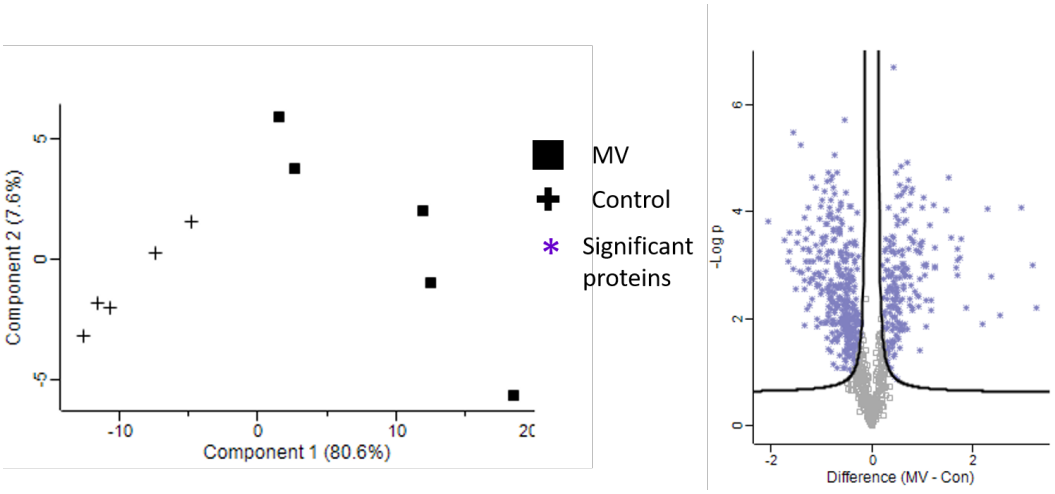

Figure 4.10: (A) PCA plot of the MV treated Arabidopsis membrane fraction proteins treated with MV. The control and MV treated samples separate, showing the treatment is changing the protein composition. (B) Volcano plot showing the proteins significantly changed between the control and the treatment. 879 proteins were identified of which 578 proteins were identified as significantly changed. FDR: 0.05 s0: 0.1.

Mapman was used to assign proteins identified in the membrane fraction to pathways in Arabidopsis (Figure 4.11), identified proteins changing the most in the light response pathway, consistent with the soluble fraction. These observed changes could be expected because MV attacks PSI during photosynthesis. The photosynthesis pathways were also looked at, where proteins that increased in abundance in the Calvin cycle in the soluble fraction, they decrease in abundance in the membrane fraction (Figure 4.12). Proteins increase in abundance in the light reaction pathway, where the photosystems are involved, due to MVs mechanism of attack it would be

expected that proteins in the photosynthesis pathway would decrease in abundance. However, abundance does not equal activity and the plant may be compensating for the damage caused by MV by producing more of the proteins being damaged.

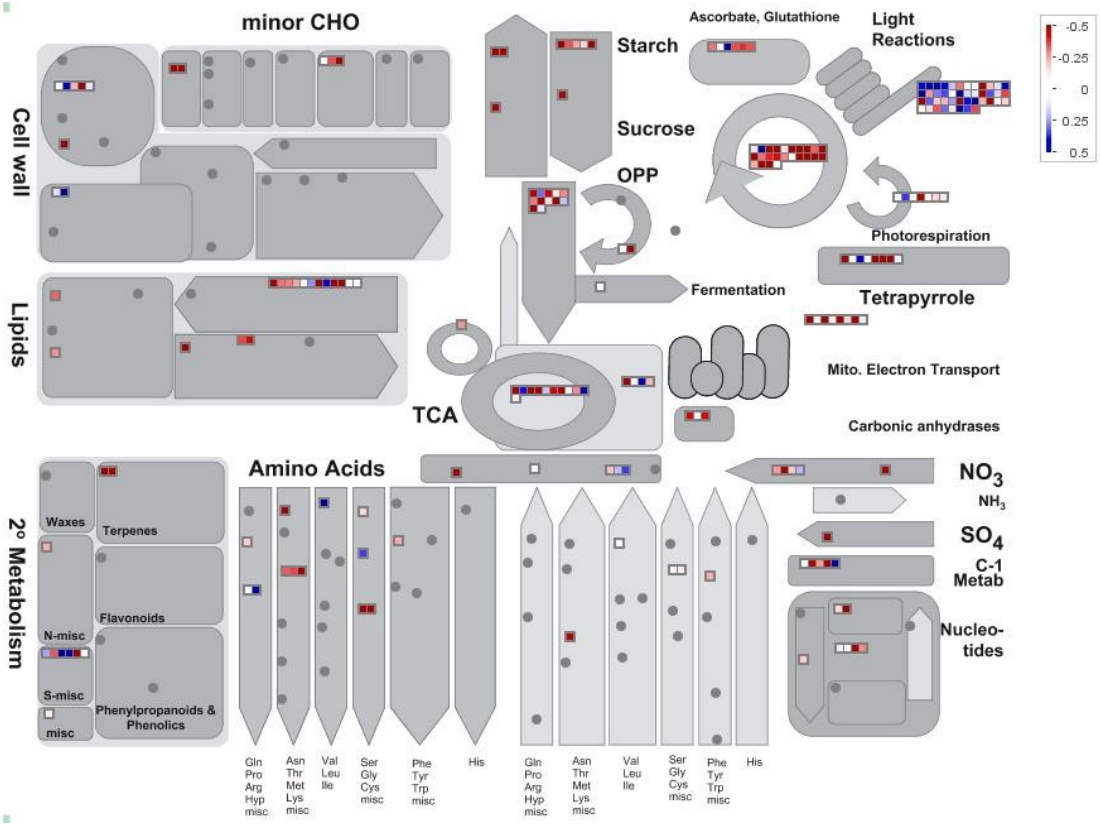

Figure 4.11: An overview of the metabolism pathways from the proteins identified in the MV treated Arabidopsis membrane fraction. The blue colour shows the proteins which increased in abundance under MV treatment, the red shows the proteins which decreased in abundance under MV treatment and the white shows the proteins which don't change in abundance under treatment. We can see proteins associated with the light reaction pathway changing the most, which is consistent with MVs mechanism of attack.

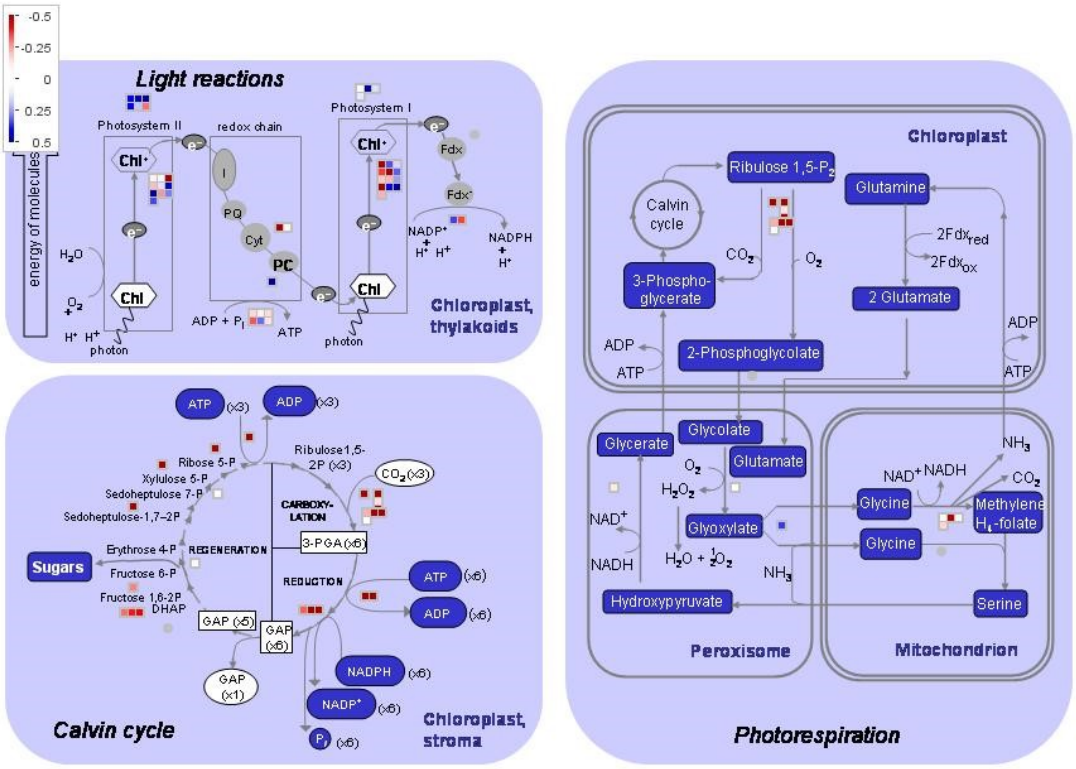

Figure 4.12: An overview of the changing proteins in the photosynthesis pathways of the Arabidopsis membrane proteins. Red are the proteins which decrease in abundance, blue are the proteins which increase in abundance and white are proteins which do not change. We can see proteins in the Calvin cycle decrease in abundance. Proteins associated with the photosystems mostly increase in abundance.

Of the proteins identified in the MV treated Arabidopsis membrane fraction, 32 of the proteins identified as significantly increasing in abundance had a log2 fold change of one or more and 53 proteins identified as significantly decreasing in abundance had a log2 fold change of more than one. This is very different to the soluble data, where none of the protein which increased in abundance had a log2 fold change of more than one, and only two which decreased in abundance had a log2 fold change of one or more, but a more significant fold changes would be expected in the membrane data because MV attacks PSI, which is a membrane protein, so it fits with the MV mechanism of action.

Table 4.3: The proteins which significantly increased in abundance identified in the *Arabidopsis thaliana* membrane fraction with a log2 fold change of more than 1.5.

Protein Name	**Gene Number**	**Log2 Fold Change**	**-Log P Value**	**MQ Score**	**Function/Pathway**
60S ribosomal protein L6-3	At1g74050 F2P9.8	3.27	2.20	17.98	RNA binding; structural constituent of ribosome
60S ribosomal protein L37-3	At3g16080 MSL1.12	3.18	3.01	7.27	Metal ion binding; rRNA binding; structural constituent of ribosome
60S ribosomal protein L29-1	At3g06700 F3E22.16	2.97	4.08	41.44	Structural constituent of ribosome
60S ribosomal protein L29-2	At3g06680 F3E22.18	2.55	2.05	14.49	Structural constituent of ribosome
Photosystem II reaction center protein H (PSII-H)	AtCg00710	2.38	2.79	46.42	Phosphate ion binding
40S ribosomal protein S21-2	At5g27700 T1G16.30	2.31	4.04	113.28	Structural constituent of ribosome
AT2G24420 protein (At2g24420/T28I24.15) (DNA repair ATPase-like protein)	At2g24420 T28I24.15	2.19	1.90	18.85	Endoplasmic reticulum; integral component of membrane; vacuolar membrane; vacuole

Continued on next page

Table 4.3 – *Continued from previous page*

Protein Name	**Gene Number**	**Log2 Fold Change**	**-Log P Value**	**MQ Score**	**Function/Pathway**
Ubiquitin-40S ribosomal protein S27a-3	At3g62250 T17J13.210	1.87	2.19	22.15	Metal ion binding; mRNA binding; protein tag; structural constituent of ribosome; ubiquitin protein ligase binding
Low-density receptor-like protein	At3g02900 F13E7.15	1.77	3.49	38.21	Chloroplast inner membrane; chloroplast thylakoid membrane; integral component of membrane
Adenine nucleotide alpha hydrolases-like superfamily protein	At3g11930	1.74	3.14	14.61	Hydrolase activity
60S ribosomal protein L39-1	At2g25210 T22F11.20	1.71	3.31	50.49	Structural constituent of ribosome
Glycine-rich RNA-binding protein RZ1A (AtRZ-1a)	At3g26420 F20C19.15	1.71	2.80	14.30	DNA binding; mRNA binding; nucleotide binding; RNA binding; zinc ion binding
V-type proton ATPase subunit F	At4g02620 T10P11.25	1.70	3.09	19.77	ATPase-coupled ion transmembrane transporter activity; proton-transporting ATPase activity, rotational mechanism
60S ribosomal protein L35a-3	At1g74270 F1O17.6	1.68	2.96	13.55	Structural constituent of ribosome

Continued on next page

Table 4.3 – *Continued from previous page*

Protein Name	**Gene Number**	**Log2 Fold Change**	**-Log P Value**	**MQ Score**	**Function/Pathway**
40S ribosomal protein S17-4	At5g04800 MUK11.12	1.58	3.51	12.19	mRNA binding; structural constituent of ribosome
Histone deacetylase HDT2	At5g22650 MDJ22.7	1.52	4.63	34.00	Histone deacetylase activity

Table 4.4: The proteins which significantly decreased in abundance identified in the MV treated Arabidopsis membrane fraction with a log2 fold change of more than 1.5.

Protein Name	**Gene Number**	**Log2 Fold Change**	**-Log P Value**	**MQ Score**	**Function/Pathway**
AT5g14910/F2G14_30 (Heavy metal transport/detoxification superfamily protein)	At5g14910 F2G14.30 F2G14_30	-2.06	3.83	41.87	Metal ion binding
Nuclear protein-like (Splicing factor)	At5g64270	-1.74	3.46	10.42	mRNA binding
DExH-box ATP-dependent RNA helicase DExH12 (EC 3.6.4.13)	At1g20960 F9H16.5	-1.66	3.08	21.45	ATP binding; RNA binding; RNA helicase activity
Putative ion channel POLLUX-like 1	At5g02940 F9G14.250	-1.63	3.62	21.47	

Continued on next page

Table 4.4 – *Continued from previous page*

Protein Name	**Gene Number**	**Log2 Fold Change**	**-Log P Value**	**MQ Score**	**Function/Pathway**
Mitochondrial outer membrane protein porin 2 (Voltage-dependent anion-selective channel protein 2)	At5g67500 K9I9.6	-1.63	3.27	26.95	Porin activity; voltage-gated anion channel activity
Protein FATTY ACID EXPORT 2, chloroplastic (At-FAX2)	At3g43520 T18D12.90	-1.56	5.48	50.37	May be involved in free fatty acids export from the plastids
Pyruvate dehydrogenase E1 component subunit beta-3, chloroplastic (EC 1.2.4.1)	At2g34590 T31E10.7	-1.55	2.93	27.88	Pyruvate dehydrogenase (acetyl-transferring) activity; zinc ion binding
Photosystem II stability/assembly factor HCF136, chloroplastic	At5g23120 MYJ24.11	-1.51	2.54	37.83	Essential for photosystem II (PSII) biogenesis; required for assembly of an early intermediate in PSII assembly that includes D2 (psbD) and cytochrome b559. Has been suggested to be required for chlorophyll a binding

4.2.4 Phosphopeptide Analysis of Methyl Viologen Treated *Arabidopsis thaliana*, Soluble & Membrane Proteins

To determine if MV treatment caused differences the protein phosphorylation, samples were enriched for phosphopeptides and analysed using MS. The phosphopeptide data of the MV treated Arabidopsis soluble fraction was analysed using PCA and the treated and control samples separated showing phosphorylation levels in the samples were different (Figure 4.13A). Two samples had to be removed from the analysis, one treated and one control because they had a much lower levels of peptides than the other samples, so were not comparable with other samples in the dataset. 1082 phosphopeptides were identified which mapped to 691 proteins (Figure 4.13B) of which 69 phosphopeptides were significantly increased in abundance in the treated over the control and these mapped to proteins which were mostly associated with stress, photosynthesis and MAPK activity. The phosphopeptides which significantly increased in abundance by more than a log2 fold change of 1 (to keep the table size manageable) are presented Table 4.5. There were 15 phosphopeptides identified as significantly decreasing in abundance in the treated compared to the control and assigned to 15 proteins which were associated with mRNA and DNA binding, ATP binding, actin binding and GTPase activity. The phosphopeptides which significantly decreased in abundance with a log2 fold change of more than two (to keep the table size manageable) can be found in Table 4.6. All significantly changing phosphopeptides are shown in the heat map in Figure 4.14.

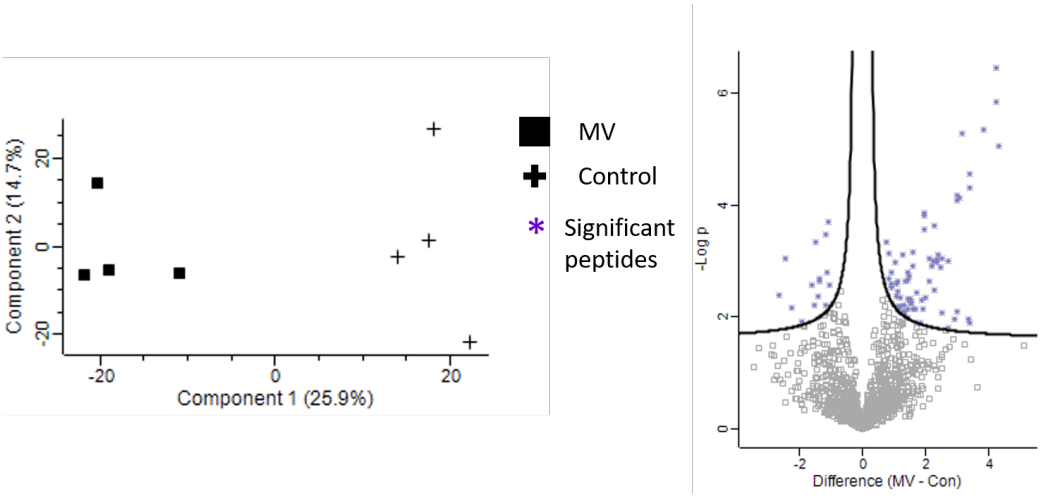

Figure 4.13: (A) PCA plot of the phosphopeptide enrichment of the MV treated Arabidopsis soluble proteins. The control and MV treated samples separate, showing the treatment is changing the phosphorylation sites. (B) Volcano plot showing the significant proteins between the control and the treatment. 1082 phosphopeptides were identified of which 84 were identified as significantly changing between the treatment and the control. FDR: 0.05 s0: 0.1.

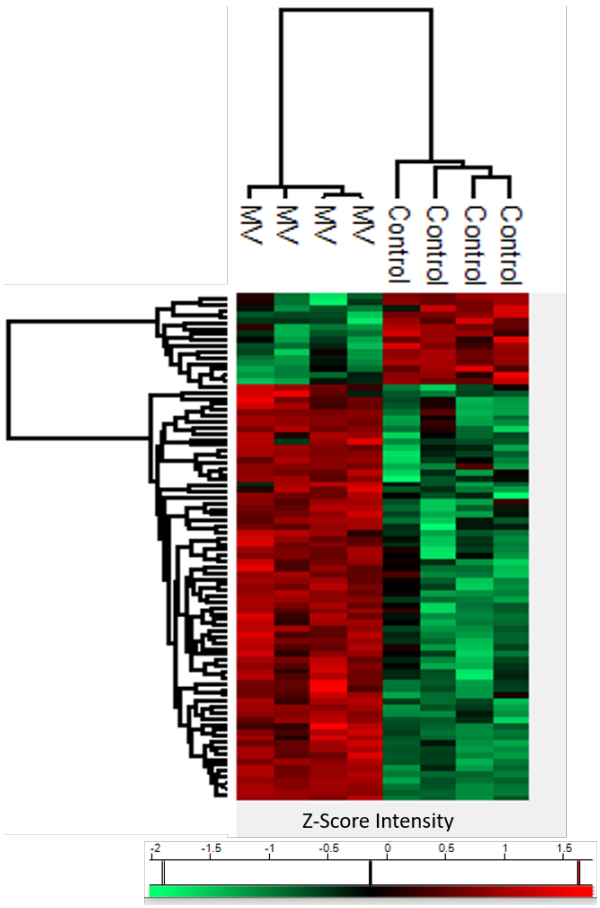

Figure 4.14: A heat map of the significantly changing phosphopeptides in the MV treated Arabidopsis soluble fraction. Significant phosphopeptides log2 fold change values have been z-scored for graphical representation.

In the Arabidopsis soluble data, 81.5% of the phosphosites were phosphoserine, 15.2% were phosphothreonine and 3.3% were phosphotyrosine. 89.4% were mono phosphorylated peptides, 9.0% were doubly phosphorylated and 1.6% were triply phosphorylated. Only 16 phosphopeptides were identified as significantly increasing in abundance in the MV treated over the control. These were mapped to 16 proteins. No proteins were identified as stress response proteins, this could be because the MV treatment is causing oxidative damage rather than phosphorylation.

Table 4.5: The phosphopeptides which significantly increased in abundance in the MV treated Arabidopsis soluble fraction with a log2 fold change of more than 1, mapped to proteins.

Protein Name	**Peptide AA Sequence**	**Gene Number**	**Log2 Fold Change**	**-Log P Value**	**MQ Score**	**Function/Pathway**	**Site & Position**
Fructose-bisphosphate aldolase 8, cytosolic (AtFBA8) (EC 4.1.2.13)	LGDGAAE**S**LHVK	At3g52930 F8J2_100	4.32	5.05	159.58	Copper ion binding; fructose-bisphosphate aldolase activity	S350
Glyceraldehyde-3-phosphate dehydrogenase GAPC1, cytosolic (EC 1.2.1.12)	AA**S**FNIIPSSTGAAK	At3g04120 T6K12.26	4.26	6.45	94.45	Copper ion binding; DNA binding; glyceraldehyde-3-phosphate dehydrogenase (NAD+) (phosphorylating) activity; glyceraldehyde-3-phosphate dehydrogenase (NADP+) (non-phosphorylating) activity; NAD binding; NADP binding	S207

Continued on next page

Table 4.5 – *Continued from previous page*

Protein Name	**Peptide AA Sequence**	**Gene Number**	**Log2 Fold Change**	**-Log P Value**	**MQ Score**	**Function/Pathway**	**Site & Position**
Fructose-bisphosphate aldolase 6, cytosolic (AtFBA6) (EC 4.1.2.13)	LGEGAAE**S**LHVK	At2g36460	4.26	5.84	164.13	Copper ion binding; fructose-bisphosphate aldolase activity	S350
AT4g39150/ T22F8_50 (DNAJ heat shock N-terminal domain-containing protein)	AY**S**RENSLR	At4g39150 T22F8.50	3.86	5.36	93.56	Cytosol; plasma membrane	S320
Calcium-binding EF-hand family protein	RLL**S**NKFEFDK	At4g38810 T9A14.90	3.42	4.30	113.99	Calcium ion binding	S250

Continued on next page

Table 4.5 – *Continued from previous page*

Protein Name	**Peptide AA Sequence**	**Gene Number**	**Log2 Fold Change**	**-Log P Value**	**MQ Score**	**Function/Pathway**	**Site & Position**
DDT domain-containing protein DDR4	KHP**S**PEHPLHR	At1g18950 F14D16.9	3.40	4.56	85.96	Probable transcription regulator	S432
NADPH-dependent aldehyde reductase-like protein, chloroplastic (EC 1.1.1.-)	**S**THSSISQPPLPLAGR S**T**HSSISQPPLPLAGR	At3g03980 T11I18.9	3.40	1.89	253.16	Oxidoreductase activity	S2; T3
Fructose-bisphosphate aldolase 6, cytosolic (AtFBA6) (EC 4.1.2.13)	GILAADESTG**T**IGKR	At2g36460	3.37	1.95	215.09	Copper ion binding; fructose-bisphosphate aldolase activity	T35

Continued on next page

Table 4.5 – *Continued from previous page*

Protein Name	**Peptide AA Sequence**	**Gene Number**	**Log2 Fold Change**	**-Log P Value**	**MQ Score**	**Function/Pathway**	**Site & Position**
Brefeldin A-inhibited guanine nucleotide-exchange protein 3	RNPPL**S**PQGGK	At1g01960 F22M8.9	3.18	5.28	136.24	ARF guanyl-nucleotide exchange factor activity	S1307
Protein PLASTID TRANSCRIPTIONALLY ACTIVE 16, chloroplastic (pTAC16)	QRPS**S**PFASKPK	At3g46780 T6H20.190	3.09	4.12	156.52	Probably involved in the regulation of plastid gene expression	S474

Continued on next page

Table 4.5 – *Continued from previous page*

Protein Name	**Peptide AA Sequence**	**Gene Number**	**Log2 Fold Change**	**-Log P Value**	**MQ Score**	**Function/Pathway**	**Site & Position**
P-loop containing nucleoside triphosphate hydrolases superfamily protein	SFSSVPS**S**PR	At5g61450	3.02	2.08	134.38	Hydrolase activity	S44
Serine/arginine-rich-splicing factor SR34	SR**S**PLPSVQK	At1g02840 F22D16.16	3.00	4.18	158.42	mRNA binding; RNA binding	S273
Patellin-1	TFGSIIT**S**PR	At1g72150 T9N14.1	2.99	4.07	117.14	Lipid binding; protease binding	S428
Methyl-CpG-binding domain-containing protein 10	AT**T**PTPDKEPLLK	At1g15340 F9L1.28	2.92	1.95	131.32	Methyl-CpG binding	T89

Continued on next page

Table 4.5 – *Continued from previous page*

Protein Name	**Peptide AA Sequence**	**Gene Number**	**Log2 Fold Change**	**-Log P Value**	**MQ Score**	**Function/Pathway**	**Site & Position**
Low-temperature-induced 78 kDa protein	FKNSL**T**K	At5g52310 K24M7.4	2.72	3.00	123.21	Involved in responses to abiotic stresses. Regulates probably root elongation in cold conditions	T45
Calcium-binding EF hand family protein (F2D10.25)	HHESEYGTTH**S**EDRSPR	At1g20760 F2D10.25	2.70	1.80	69.26	Calcium ion binding	S769
Protein DNA-DAMAGE INDUCIBLE 1 (EC 3.4.23.-)	RQN**T**SEGPEFEAK	At3g13235 MDC11.6	2.63	1.75	201.72	Aspartic-type endopeptidase activity; polyubiquitin modification-dependent protein binding	T369
Remorin (DNA-binding protein)	ALAVVEKPIEEH**T**PKK	At2g45820 F4I18.20	2.53	3.05	141.34		T58

Continued on next page

Table 4.5 – *Continued from previous page*

Protein Name	**Peptide AA Sequence**	**Gene Number**	**Log2 Fold Change**	**-Log P Value**	**MQ Score**	**Function/Pathway**	**Site & Position**
SNF1-related protein kinase catalytic subunit alpha KIN10 (AKIN10) (EC 2.7.11.1)	MHPAESVA**S**PVSHR	At3g01090 T4P13.22	2.52	2.08	180.85	ATP binding; kinase activity; kinase binding; phosphatase binding; protein serine/threonine kinase activity	S364
Transketolase-1, chloroplastic (TK) (EC 2.2.1.1)	ANSY**S**VHGAALGEK	At3g60750 T4C21_160	2.48	2.89	88.95	Metal ion binding; transketolase activity	S337
AT3G08760 protein (At3g08760) (Protein kinase superfamily protein)	VM**S**APSSIHGAAER	At3g08760	2.38	3.10	101.30	ATP binding; protein kinase activity	S75

Continued on next page

Table 4.5 – *Continued from previous page*

Protein Name	**Peptide AA Sequence**	**Gene Number**	**Log2 Fold Change**	**-Log P Value**	**MQ Score**	**Function/Pathway**	**Site & Position**
Serine/arginine-rich splicing factor RS2Z33 (RS-containing zinc finger protein 33)	IIDG**S**PPPSPK	At2g37340 F3G5.13	2.37	3.03	125.84	RNA binding; zinc ion binding	S185; S189
Probable protein phosphatase 2C 39 (AtPP2C39) (EC 3.1.3.16)	VGLGASASSAD**S**GKGK	At3g15260 K7L4.6	2.37	2.98	189.52	Magnesium-dependent protein serine/threonine phosphatase activity; metal ion binding; protein serine/threonine phosphatase activity	S29
Membrane-associated protein VIPP1, chloroplastic	RK**S**FADNATALK	At1g65260 T8F5.2	2.27	3.63	162.70	Required for plastid vesicle formation and thylakoid membrane biogenesis, but not for functional assembly of thylakoid protein complexes	S167

Continued on next page

Table 4.5 – *Continued from previous page*

Protein Name	**Peptide AA Sequence**	**Gene Number**	**Log2 Fold Change**	**-Log P Value**	**MQ Score**	**Function/Pathway**	**Site & Position**
Dehydrin ERD10 (Low-temperature-induced protein LTI45)	AEEYKNTVPEQE**T**PK	At1g20450 F5M15.21	2.27	2.48	131.48	Actin binding; copper ion binding; nickel cation binding; phosphatidylcholine binding; phosphatidylserine binding	T14
Phosphoenol pyruvate carboxylase 2 (PEPC 2) (EC 4.1.1.31)	MA**S**IDAQLR	At2g42600 F14N22.13	2.26	3.01	128.51	Phosphoenolpyruvate carboxylase activity	S11

Continued on next page

Table 4.5 – *Continued from previous page*

Protein Name	**Peptide AA Sequence**	**Gene Number**	**Log2 Fold Change**	**-Log P Value**	**MQ Score**	**Function/Pathway**	**Site & Position**
DDB1- and CUL4-associated factor homolog 1	QLTFSP**S**FSSQSR	At4g31160 F6E21_80	2.21	2.91	134.68	Component of the CUL4-RBX1-DDB1-DCAF1 E3 ubiquitin-protein ligase complex, DCAF1 may function as the substrate recognition module within this complex. Appears to be required for plant embryogenesis and to affect several other developmental processes including leaf, shoot, and flower development	S1243
Soluble inorganic pyrophosphatase 2 (EC 3.6.1.1)	AEIKDEG**S**AKG**Y**AFPLR	At2g18230 T30D6.26	2.13	3.04	115.00	Inorganic diphosphatase activity; magnesium ion binding	S9; Y13

Continued on next page

Table 4.5 – *Continued from previous page*

Protein Name	**Peptide AA Sequence**	**Gene Number**	**Log2 Fold Change**	**-Log P Value**	**MQ Score**	**Function/Pathway**	**Site & Position**
Serine/arginine-rich splicing factor RS41	GE**S**R**S**PPPYEK	At5g52040 MSG15.12	2.12	2.64	165.51	mRNA binding; RNA binding	S239; S241

Table 4.6: The phosphopeptides which significantly decreased in abundance in the MV treated Arabidopsis soluble fraction leaves with a log2 fold change of more than -2, mapped to proteins.

Protein Name	**Peptide AA Sequence**	**Gene Number**	**Log2 Fold Change**	**-Log P Value**	**MQ Score**	**Function/Pathway**	**Site & Position**
Villin-4	SMSF**S**PDRVR	At4g30160 F6G3.190	-2.63	2.40	86.19	Actin filament binding	S777
Uncharacterized protein At5g39570	RPE**S**GLGSGYGGR	At5g39570 MIJ24_40	-2.43	3.04	83.82	mRNA binding; phosphatidic acid binding	S176
Phospholipase-like protein (PEARLI 4) family protein	N**SS**PPSPFHPAAYK	At4g38550 F20M13.110	-2.24	2.16	117.70	Plasma membrane	S237; S238
COP1-interacting protein-like protein	FSDSEPGSL**S**PLQR	At5g43310	-1.92	1.91	91.31		S761

Continued on next page

Table 4.6 – *Continued from previous page*

Protein Name	**Peptide AA Sequence**	**Gene Number**	**Log2 Fold Change**	**-Log P Value**	**MQ Score**	**Function/Pathway**	**Site & Position**
At3g60670 (PLATZ transcription factor family protein)	ME**S**GEFPAWLEVLLK	At3g60670	-1.58	2.58	62.73		S3
FHA domain-containing protein DDL (Protein DAWDLE)	GG**S**EEPNVEEDSVAR	At3g20550 K10D20.9	-1.52	2.20	164.93	mRNA binding; RNA binding	S133
Disease resistance protein (TIR-NBS-LRR class) family	EASGQVVM**T**IFYKVDPSDVR	At5g40910	-1.49	3.34	45.82	ADP binding	T102
Metal-dependent protein hydrolase	VYSTATSPSP**S**EISVK	At5g41970	-1.40	2.36	77.75	Hydrolase activity	S44

Continued on next page

Table 4.6 – *Continued from previous page*

Protein Name	**Peptide AA Sequence**	**Gene Number**	**Log2 Fold Change**	**-Log P Value**	**MQ Score**	**Function/Pathway**	**Site & Position**
CLIP-associated protein (At-CLASP)	YSGG**S**IDSDSGRK	At2g20190/ At2g20200 T2G17.1	-1.38	2.63	92.06	Microtubule plus-end binding	S1072
Chorismate synthase	**S**IGELSQR	At4g01290 F2N1.34	-1.36	2.68	163.32	mRNA binding	S704
Phosphoribulokinase, chloroplastic (EC 2.7.1.19)	GH**S**LESIK	At1g32060 T12O21.4	-1.17	3.47	160.36	ATP binding; disordered domain specific binding; phosphoribulokinase activity; protein homodimerization activity	S212
Protein PHOX3	SNQVEEK**S**EGEGEDVEPEKK	At5g20360 F5O24.250	-1.15	2.21	56.82	Carboxylate clamp type tetratricopeptide repeat protein that may act as a potential Hsp90/Hsp70 co-chaperone. Contributes to polar growth of root hairs	S298

Continued on next page

Table 4.6 – *Continued from previous page*

Protein Name	**Peptide AA Sequence**	**Gene Number**	**Log2 Fold Change**	**-Log P Value**	**MQ Score**	**Function/Pathway**	**Site & Position**
F3I6.9 protein (Triadin)	SGT**T**AYRSPSHGLK	At1g24160 F3I6.9	-1.12	2.79	84.05	Plasmodesma	T462
Protein PLASTID MOVEMENT IMPAIRED 2	FKGNSEDNGLIN**S**PK	At1g66840 F4N21.22	-1.10	3.71	142.74	Required for the chloroplast avoidance response under high intensity blue light. This avoidance response consists in the relocation of chloroplasts on the anticlinal side of exposed cells. Acts in association with WEB1 to maintain the velocity of chloroplast photorelocation movement via cp-actin filaments regulation	S545

Continued on next page

Table 4.6 – *Continued from previous page*

Protein Name	**Peptide AA Sequence**	**Gene Number**	**Log2 Fold Change**	**-Log P Value**	**MQ Score**	**Function/Pathway**	**Site & Position**
AT1G19000 protein (F14D16.15) (Homeodomain-like superfamily protein)	CV**S**LNNLSDYEK	At1g19000 F14D16.15	-1.06	2.57	142.10	DNA binding; DNA-binding transcription factor activity	S39

Linear motif analysis in Perseus was used to analyse motifs for the significantly changing phosphopeptides. Of the phosphopeptides which significantly increased in abundance 13 contained a MAPK substrate motif including protein plastid transcriptionally active 16 (s474, log2 fold change 3.09) and P-loop containing nucleoside triphosphate hydrolases superfamily protein (S44, log2 fold change 3.02). There were two MAPK substrate motifs identified in the phosphopeptides which significantly decreased in abundance, FHA domain-containing protein DDL (S133, log2 fold change -1.52) and villin-4 (S777, log2 fold change -2.63). Three casein kinase II substrate motifs were also identified on disease resistance protein (T102, log2 fold change -1.49), metal-dependent protein hydrolase (S44, log2 fold change -1.40) and CLIP-associated protein, AtCLASP (S1072, log2 fold change -1.38). Casein kinase is serine/threonine kinase which regulates cell cycle control. There were also six phosphopeptides which contained protein kinase c (PKC) motifs. PKC is a phospholipid depended serine/threonine kinase which is thought to be involved in signal transduction response to hormones and growth factors.

To identify possible kinases a motif analysis using maximal motif finder for phosphopeptides (MMFPH) was performed (Wang *et al.*, 2014). The motif analysis for the phosphopeptides identified in the MV treated Arabidopsis soluble fraction located 13 motifs (Table 4.7), one motif was found to appear in the significantly changing phosphopeptides, sP. Proline directed motifs (sP and tP) were identified, which are known substrates of MAPKs, Sucrose Non-Fermenting Related Protein Kinases (SnRKs), receptor like kinases (RLKs), AGC protein family kinases, cyclin dependent kinases (CDKs), Calcium Dependent Protein Kinases (CDPKs) and STE20 like kinases (SLKs) (van Wijk *et al.*, 2014). The RxxS motif identified in the dataset is a known target for MAPKs (van Wijk *et al.*, 2014). The xSxSx motif identified is also a target for MAPKs, RLKs and CDKs (van Wijk *et al.*, 2014). The motifs identified in the Arabidopsis soluble fraction dataset are shown in Table 4.7.

Table 4.7: Motifs identified by MMFPh in the MV treated Arabidopsis soluble fraction.

Motif	Foreground Matches	Background Matches	Occurrence Threshold	Score
——————SPR————-	60	4120	53	4.57
————-P-SP—————	76	5641	53	4.46
——————SPK————-	53	4143	53	4.39
————-S-SP—————	54	10141	53	3.12
——————RS—————	78	71045	53	0.84
——————TP—————	55	39916	53	2.75
——————S-P————-	99	75455	80	1.10
——K———S—————	96	84726	80	0.89
——————PS—————	84	76496	80	0.84
————-P-S—————	98	72966	80	1.13
————-S-S—————	150	166111	133	0.56
————-R–S—————	193	76375	159	2.05
——————SP—————	395	74628	159	3.11

In the membrane fraction of the MV treated Arabidopsis leaf material, a PCA plot was used to determine if phosphorylation levels are different between the treated and control (Figure 4.15A), and the control and treatment separated. One of the control samples was removed from the analysis because it had fewer peptides than other samples. 761 phosphopeptides were identified which mapped to 543 proteins (Figure 4.15B) of which 36 phosphopeptides were identified as significantly increasing in abundance in the treated than the control, which were assigned to proteins associated with stress, photosynthesis and kinase activity and are shown in Table 4.8. 6 phosphopeptides were identified as significantly decreasing in abundance in the treated compared to the control, these mapped to proteins associated with phospholipase activity, ATP binding and transmembrane transport, proteins with a log2 fold change greater than 2 (to keep the table size manageable) are shown in Table 4.9. All significantly changing phosphopeptides can be seen in the heat map in Figure 4.16.

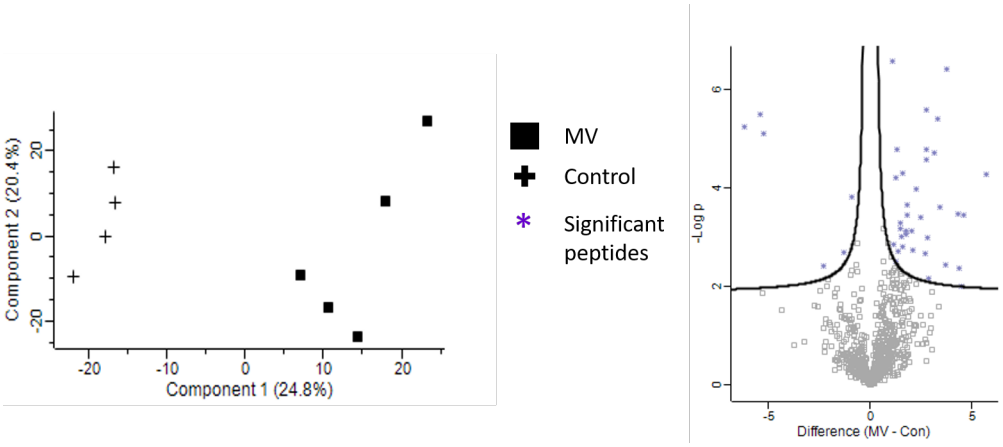

Figure 4.15: (A) PCA plot of the phosphopeptide enrichment of the MV treated Arabidopsis membrane proteins. The control and MV treated samples separate, showing the treatment is changing the phosphorylation sites. (B) Volcano plot showing the significant proteins between the control and the treatment. 761 phosphopeptides were identified of which 42 were identified to be significantly changed. FDR: 0.05 s0: 0.1.

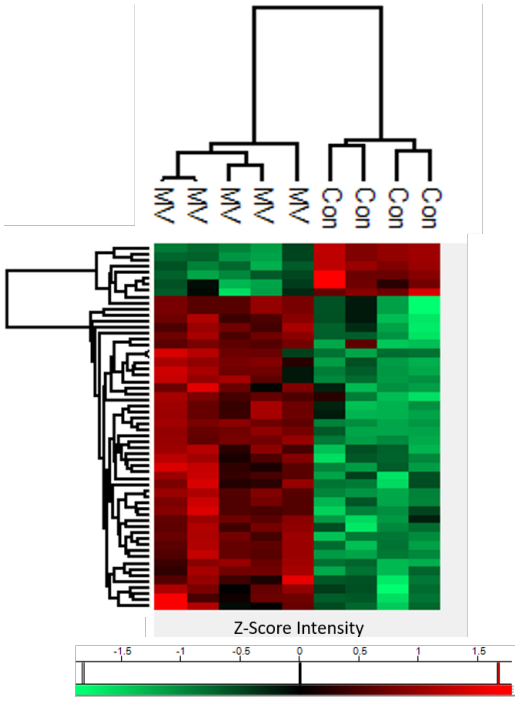

Figure 4.16: A heat map of the significantly changing phosphopeptides in the Arabidopsis MV treated membrane fraction. Significant phosphopeptides log2 fold change values have been z-scored for graphical representation.

For the MV treated Arabidopsis membrane fraction data, 83.6% of sites were phosphoserine, 14.0% were phosphothreonine and 2.4% were phosphotyrosine. 91.7% of peptides were mono phosphorylated, 6.1% were doubly phosphorylated and 2.2% were triply phosphorylated.

Table 4.8: The phosphopeptides which were identified as significantly increasing in abundance in the membrane fraction of the MV treated Arabidopsis leaves, mapped to proteins.

Protein Name	**Peptide AA Sequence**	**Gene Number**	**Log2 Fold Change**	**-Log P Value**	**MQ Score**	**Function/Pathway**	**Site & Position**
Uncharacterized protein At2g11010	KEA**Y**DYMDK	At2g11010 F15K19.8 F15K19_8	5.71	4.28	59.25		Y562
Uncharacterized protein At2g22790	SSSVNPS**S**PVYYK	At2g22790 T30L20.5	4.58	3.45	48.53		S29
AT5g03040/ F15A17_70 (IQ-domain 2)	QSSS**S**PPPALAPR	At5g03040 F15A17.70	4.48	2.00	169.89	Plasma membrane	S49
Acetyl-CoA acetyltransferase, cytosolic 1 (EC 2.3.1.9)	AH**T**SESVNPR AHT**S**ESVNPR	At5g48230 MIF21.12	4.38	2.36	47.89	Acetyl-CoA C-acetyltransferase activity; acetyl-CoA C-acyltransferase activity; metal ion binding	T4; S5
Uncharacterized protein At2g22790	SSSVNPS**S**PVYYK	At2g22790 T30L20.5	4.33	3.47	48.53		S28

Continued on next page

Table 4.8 – *Continued from previous page*

Protein Name	**Peptide AA Sequence**	**Gene Number**	**Log2 Fold Change**	**-Log P Value**	**MQ Score**	**Function/Pathway**	**Site & Position**
Alkaline/neutral invertase CINV1 (EC 3.2.1.26)	HDGIHD**S**PRGR	At1g35580 F15O4.33	3.77	6.40	88.10	Beta-fructofuranosidase activity; glycopeptide alpha-N-acetylgalactosaminidase activity; sucrose alpha-glucosidase activity	S61
Protein kinase superfamily protein	NEVTPYLV**S**R	At3g25840	3.68	2.43	129.42	ATP binding; protein kinase activity	S523
Serine/arginine-rich splicing factor RSZ22	RR**S**PSPPPAR	At4g31580 F28M20.230	3.45	3.59	113.38	mRNA binding; RNA binding; zinc ion binding	S160
Lysine-specific histone demethylase 1 homolog 3	DV**Y**KSIMKK	At4g16310 /At4g16320	3.32	5.39	62.66	DNA binding; oxidoreductase activity	Y1572

Continued on next page

Table 4.8 – *Continued from previous page*

Protein Name	**Peptide AA Sequence**	**Gene Number**	**Log2 Fold Change**	**-Log P Value**	**MQ Score**	**Function/Pathway**	**Site & Position**
At3g16330 (Avr9/Cf-9 rapidly elicited protein)	ST**S**SVRPLR	At3g16330	3.15	4.70	89.03		S153
At4g35785 (RNA-binding (RRM/RBD/RNP motifs) family protein)	RDY**S**PRDER	At4g35785	3.03	1.87	110.31	RNA binding	S197
Glyceraldehyde-3-phosphate dehydrogenase GAPC2, cytosolic (EC 1.2.1.12)	AA**S**FNIIPSSTGAAK	At1g13440 T6J4.17	2.85	2.14	125.33	Copper ion binding; DNA binding; glyceraldehyde-3-phosphate dehydrogenase (NAD+) (phosphorylating) activity; NAD binding; NADP binding; zinc ion binding	S179

Continued on next page

Table 4.8 – *Continued from previous page*

Protein Name	**Peptide AA Sequence**	**Gene Number**	**Log2 Fold Change**	**-Log P Value**	**MQ Score**	**Function/Pathway**	**Site & Position**
Protein TSS (TPR-domain suppressor of STIMPY)	MFVK**S**PLNKK	At4g28080 T13J8.190	2.79	2.97	186.74	Negatively regulates meristematic tissue proliferation by integrating developmental signals with carbon source availability. May act as the scaffold of a protein complex, which sequesters key factors that are required for the G2 to M transition in meristematic tissues	S1320
Serine/arginine-rich SC35-like splicing factor SCL30A	QSR**S**PTPVPR	At3g13570 K20M4.1	2.77	4.56	102.53	mRNA binding; RNA binding	S245
Probable glutathione peroxidase 2 (EC 1.11.1.9)	VLQRY**S**PR	At2g31570 T9H9.9	2.77	4.78	99.79	Glutathione peroxidase activity; peroxidase activity	S148

Continued on next page

Table 4.8 – *Continued from previous page*

Protein Name	**Peptide AA Sequence**	**Gene Number**	**Log2 Fold Change**	**-Log P Value**	**MQ Score**	**Function/Pathway**	**Site & Position**
Phosphoenol pyruvate carboxylase-related / PEP carboxylase-like protein	MA**S**IDAQLR	At3g42628	2.73	5.58	111.82	Phosphoenolpyruvate carboxylase activity	S11
Phosphoenol pyruvate carboxylase 1	MA**S**IDVHLR	At1g53310 F12M16.21	2.69	2.67	101.64	Phosphoenolpyruvate carboxylase activity	S11
Protein CLMP1 (CLUMPED CHLORO-PLASTS 1)	VVLKPVSH**S**PK	At1g62390 F2401.12	2.50	3.39	195.72	Required for plastid separation and partitioning during cell division. Contributes to polar growth of root hairs	S263
ATP-dependent helicase BRM (EC 3.6.4.12)	LHVS**S**PK	At2g46020 T3F17.33	2.27	2.03	114.89	ATP binding; chromatin binding; DNA binding; DNA-dependent ATPase activity; DNA helicase activity	S1856

Continued on next page

Table 4.8 – *Continued from previous page*

Protein Name	**Peptide AA Sequence**	**Gene Number**	**Log2 Fold Change**	**-Log P Value**	**MQ Score**	**Function/Pathway**	**Site & Position**
Syntaxin-71 (AtSYP71)	AT**S**DLKNTNVR	At3g09740 F11F8_33	2.23	3.97	155.47	SNAP receptor activity; SNARE binding	S222
Serine/arginine-rich splicing factor RS2Z33 (RS-containing zinc finger protein 33)	DR**S**PVLDDEGSPK	At2g37340 F3G5.13	2.09	2.73	140.93	RNA binding; zinc ion binding	S170
Elongation factor 2 (EF-2)	FSV**S**PVVR	At1g56070 /At1g56075 T6H22.13	2.04	3.13	82.65	Copper ion binding; GTPase activity; GTP binding; mRNA binding; ribosome binding; translation elongation factor activity	S486

Table 4.9: The phosphopeptides which significantly decreased in abundance in the membrane fraction of the MV treated Arabidopsis leaves, with a log2 fold change of more than -2, mapped to proteins.

Protein Name	**Peptide AA Sequence**	**Gene Number**	**Log2 Fold Change**	**-Log P Value**	**MQ Score**	**Function/Pathway**	**Site & Position**
Phosphoinositide phospholipase C 2 (EC 3.1.4.11)	EVP**S**FIQR	At3g08510 T8G24.4	-6.21	5.23	81.95	Phosphatidylinositol phospholipase C activity; phospholipase C activity	S280
Alkaline/neutral invertase CINV1 (EC 3.2.1.26)	LMNLAEENMSITRPS**S**	At1g35580 F15O4.33	-5.39	5.49	52.00	Beta-fructofuranosidase activity; glycopeptide alpha-N-acetylgalactosaminidase activity; sucrose alpha-glucosidase activity	S700
Alkaline/neutral invertase CINV1 (EC 3.2.1.26)	LMNLAEENMSITRP**S**S	At1g35580 F15O4.33	-5.25	5.09	52.00	Beta-fructofuranosidase activity; glycopeptide alpha-N-acetylgalactosaminidase activity; sucrose alpha-glucosidase activity	S699

Continued on next page

Table 4.9 – *Continued from previous page*

Protein Name	**Peptide AA Sequence**	**Gene Number**	**Log2 Fold Change**	**-Log P Value**	**MQ Score**	**Function/Pathway**	**Site & Position**
Probable inactive receptor kinase At3g02880	LIEEVSHS**S**GSPNPVSD	At3g02880 F13E7.17	-2.29	2.40	78.51	ATP binding; protein kinase activity	S619
Protein PLASTID TRANSCRIPTIONALLY ACTIVE 16, chloroplastic (pTAC16)	VQVA**T**VRGQAK	At3g46780 T6H20.190	-1.28	2.68	150.51	Probably involved in the regulation of plastid gene expression	T451
Protein WALLS ARE THIN 1	APVSRN**S**IK	At1g75500 F10A5.28	-0.92	3.80	99.34	Transmembrane transporter activity	S372

Linear motif analysis in Perseus was used to analyse motifs in the significantly changing phosphopeptides. In the phosphopeptides which significantly increased in abundance four phosphopeptides were found to contain MAPK substrate motifs, including serine/arginine-rich splicing factor RS2Z33 (S170, log2 fold change 2.09) and 3'-phosphoinositide-dependent protein kinase 1 (S29, log2 fold change 1.10). Fifteen were found to contain a casein kinase II substrate motif including acetyl-CoA acetyltransferase, cytosolic 1 (T4 S5, log2 fold change 4.38) and protein kinase superfamily protein (S523, log2 fold change 3.68). Twentynine phosphopeptides contained the PKC substrate motif including alkaline/neutral invertase CINV1 (S61, log2 fold change 3.77), serine/arginine-rich splicing factor RSZ22 (S160, log2 fold change 3.45) and At3g16330 (Avr9/Cf-9 rapidly elicited protein) (S153, log2 fold change 3.15). Of the phosphpeptides which significantly decreased in abundance one phosphopeptide was identified as having a MAPK substrate motif, which was F9K20.7 protein (S78, log2 fold change -2.46). Two phosphopeptides were found to have a casein kinase I substrate motif which were probable inactive receptor kinase (S619, log2 fold change -2.29) and protein walls are thin 1 (S372, log2 fold change -0.92). Five phosphopeptides were identified as containing a PKC substrate motif including alkaline/neutral invertase (S700, log2 fold change -5.39) and alkaline/neutral invertase CINV1 (S699, log2 fold change -5.25).

The motif analysis for the phosphopeptides using MMFPh in the MV treated Arabidopsis membrane fraction identified 22 motifs (Table 4.10), of which two were identified in the significantly changing phosphopeptides, RxxS and sP. Proline directed motifs (sP and tP) were identified, which are known substrates of MAPKs, SnRKs, RLKs, AGC protein family kinases, CDKs, CDPKs and SLKs (van Wijk *et al.*, 2014). The basophilic motifs RxxS and RSxS were identified in the dataset and are known target for MAPKs (van Wijk *et al.*, 2014). The xSxSx motif identified is also a target for MAPKs, RLKs and CDKs (van Wijk *et al.*, 2014). The motifs identified in the Arabidopsis membrane fraction dataset are shown in Table 4.10.

Table 4.10: Motifs identified by MMFPh in the MV treated Arabidopsis membrane fraction.

Motif	Foreground Matches	Background Matches	Occurrence Threshold	Score
——————SPR————-	50	4120	38	4.75
————R–SP—————	44	4204	38	4.54
——————SP—-R———	39	4119	38	4.40
————RS-S—————	45	9324	38	3.42
———R——S—————	75	74770	57	1.16
——————S——R———	76	76072	57	1.15
———R—S—————	73	75505	57	1.10
——————S———R——	69	75164	57	1.03
——————S—-P———-	66	73121	57	1.00
———R——S—————	68	75451	57	1.00
——————S—R———	67	75148	57	0.99
——————S——-R——-	66	74308	57	0.98
——————S—-R———-	65	74681	57	0.95
——————S-K————-	70	81009	57	0.94
—-R———-S—————	66	77561	57	0.92
——————S-P————-	76	75455	76	1.16
———K——S—————	76	86476	76	0.97
——————S-R————-	77	71678	76	1.26
——————S——R———	72	74244	76	1.11
——————SP—————	249	74628	114	2.89
————R–S—————	175	76375	114	2.35
————-S-S—————	117	166111	114	0.65

4.2.5 Tandem Mass Tag Quantification of Methyl Viologen Treated Maize Leaves

Whilst Arabidopsis is the model plant and used for many scientific experiments, it has no economical significance, therefore it was decided that the MV experiment should be repeated in maize. Maize leaves were cut into squares and placed in Petri dishes with 1 μM of MV for 16 hours under constant light (Figure 4.17), the 16 hour treatment was chosen to keep the experiment in line with the Arabidopsis experiment and the 1 μM concentration of MV was chosen because maize has a waxy outer layer which Arabidopsis does not have, so more MV would be needed to penetrate the waxy layer. A wetting agent was also used in the maize experiment which was not used in the Arabidopsis experiment to penetrate the waxy outer layer. However, the anti-DNPH western blot showed no change in oxidative damage in the

treated compared to the control (Figure 4.18). This was further corroborated by the MS analysis, no separation of the control and treated samples can be seen in the PCA plot (Figure 4.19A), and no significant proteins were seen on the volcano plot (Figure 4.19B). Since no significant proteins were identified the samples were not fractionated for further analysis.

The experiment was repeated using 10 mM of MV for 2 hours under constant light (Figure 4.17). The experiment was performed in accordance with Kingston-Smith and Foyer (2000). However, again no change in oxidative damage levels were seen between the control and the MV treated samples using anti-DNPH Western blots (Figure 4.20). Nor were any changes in total protein abundance identified following MS analysis using PCA plot (Figure 4.21A) and the volcano plot showed no significantly changing proteins (Figure 4.21B). Since no significant proteins were identified samples were not fractionated. Due to the short treatment time (2 hours) large protein changes would not be expected, and samples would need to be treated for at least 6 hours in order to see large protein changes, however, the short treatment time was used to see more rapid responses in the phosphopeptides.

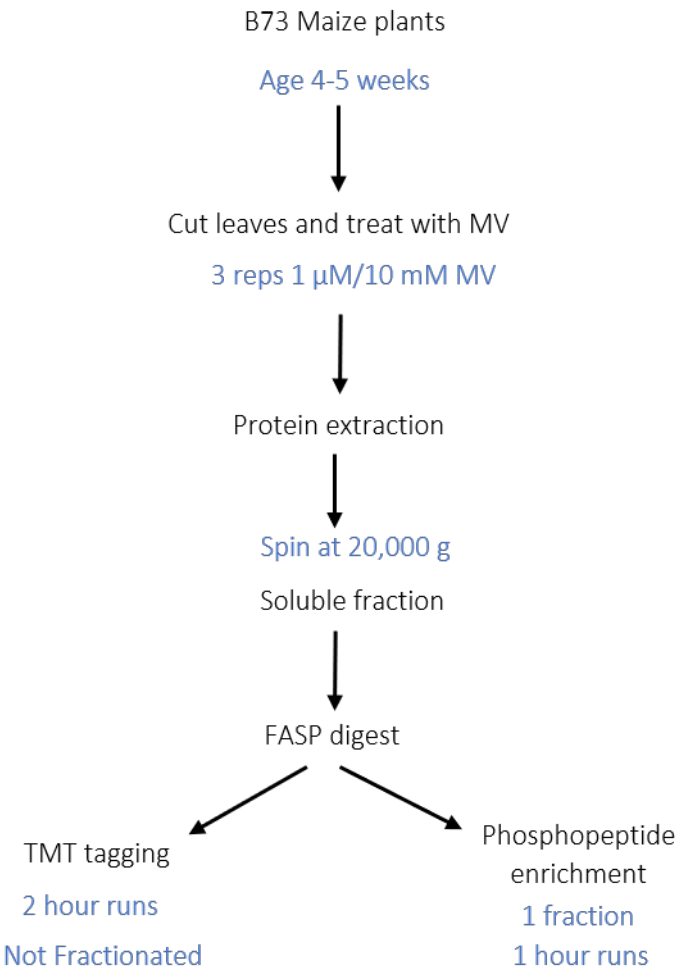

Figure 4.17: Maize plants were grown for 4-5 weeks, then treated with either 1 μM or 10 mM of MV in Petri dishes. The 1 μM treatment was for 16 hours under constant light and the 10 mM treatment was for 2 hours under constant light. Proteins were isolated from the leaves and a FASP digest was performed, some of the sample was tagged with TMT and analysed for 2 hours on the MS, the rest was enriched for phosphopeptides and analysed for 1 hour on the MS.

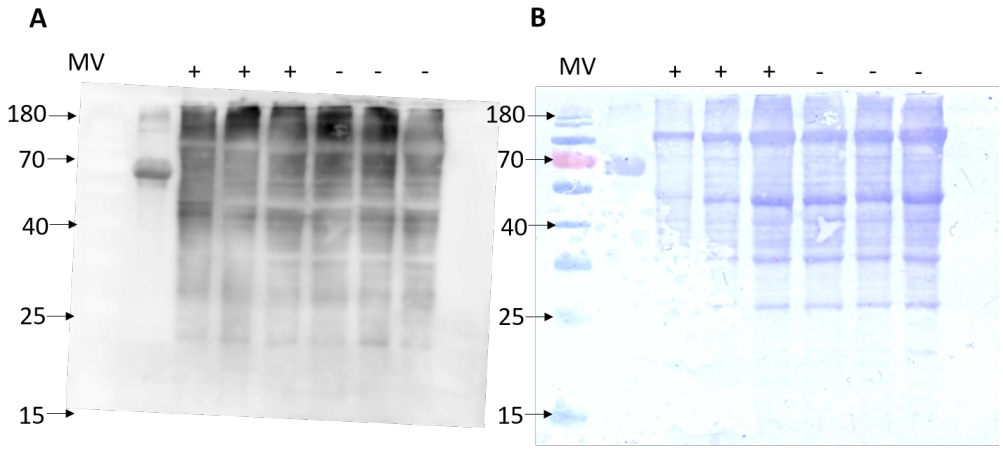

Figure 4.18: (A) Western blot of maize leaves treated with 1μM MV and tagged with DNPH, visualised using anti-DNPH conjugated to HRP. (B) Membrane stained with coomassie. No difference can be seen between the treated and the control.

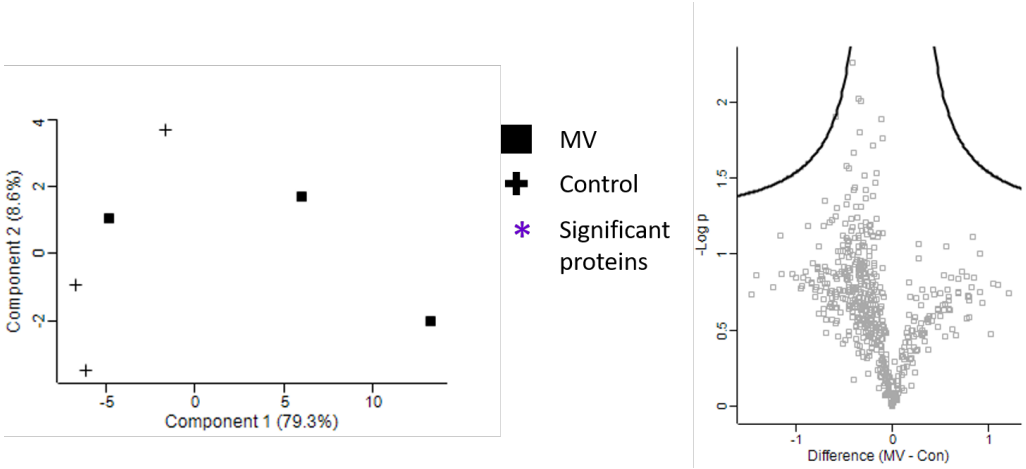

Figure 4.19: (A) PCA plot of the maize treated with 1 μM of MV. The control and MV treated samples do not separate, suggesting the treatment is not doing anything to the proteins. (B) Volcano plot shows no significant changes in proteins between the control and the treatment. 554 proteins were identified in the study. FDR: 0.05 s0: 0.1.

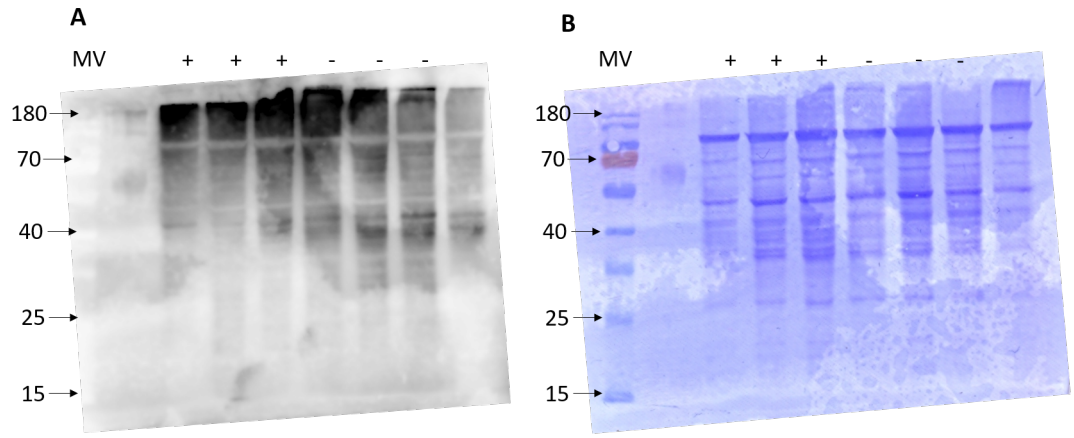

Figure 4.20: (A) Western blot of maize leaves treated with 10 mM MV and tagged with DNPH, visualised using anti-DNPH conjugated to HRP. (B) Membrane stained with coomassie. No difference can be seen between the treated and the control.

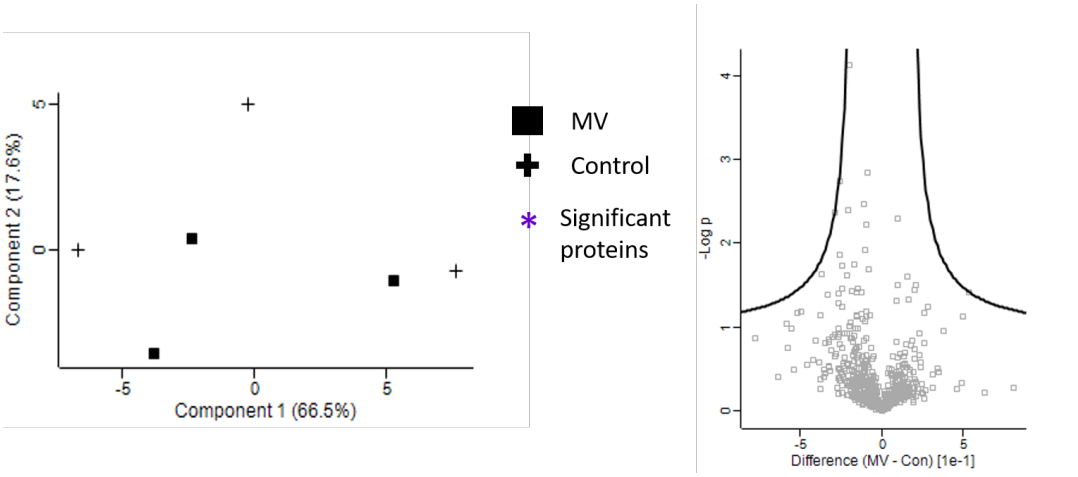

Figure 4.21: (A) PCA plot of the maize treated with 10 mM of MV. The control and MV treated samples do not separate, suggesting that the treatment is not changing the proteins. (B) Volcano plot shows no significant changes in proteins between the control and the treatment. 655 proteins were identified in the study. FDR: 0.05 s0: 0.1.

There were no changes seen in the proteins in the MV treated TMT maize data. The proteins which were identified in the data were associated with photosynthesis, respiration, and other core metabolism proteins. There were some stress response proteins identified however, these were most likely a response to wounding, from when the leaves were cut and put in the Petri dishes for treatment, because these proteins did not significantly change in the MV treated. The lack of changes

in protein abundance would suggest that MV has no affect on monocots, however MV is an unspecific herbicide so should affect maize in a similar way to Arabidopsis (Bromilow, 2003). Whilst there is not an increase in signal seen in the treatment over the control, there is a high signal seen in both, it is therefore possible that the sample prep of cutting the leaves has elevated stress levels which has masked the effect of the MV. Maize has a waxy outer layer on the leaves, which Arabidopsis does not have, for this reason a wetting agent was used in the maize treatment, but the waxy layer could mean that the treatment was not long enough for MV to have an effect.

4.2.6 Phosphopeptide Analysis of Methyl Viologen Treated Maize Leaves

Phosphopeptide analysis was performed on the MV treated maize leaves at both concentrations. For the 1 μM treatment 380 phosphopeptides were identified which mapped to 276 proteins. The PCA plot showed no separation between the control and treatment phosphopeptides (Figure 4.22A). This is also shown in the volcano plot where no significant phosphopeptides are shown (Figure 4.22B). In the 10 mM treatment 1128 phosphopeptides were identified which mapped to 730 proteins. The PCA plot also showed no separation between the control and treatment (Figure 4.23A). However, 19 phosphopeptides were identified as significantly changing between the MV treated and the control (Figure 4.23B). This change in the phosphopeptides can also be seen in the heat map, which shows only the significantly changing phosphopeptides (Figure 4.24). The significantly changing phosphopeptides could be mapped to 18 proteins which are shown in Table 4.11.

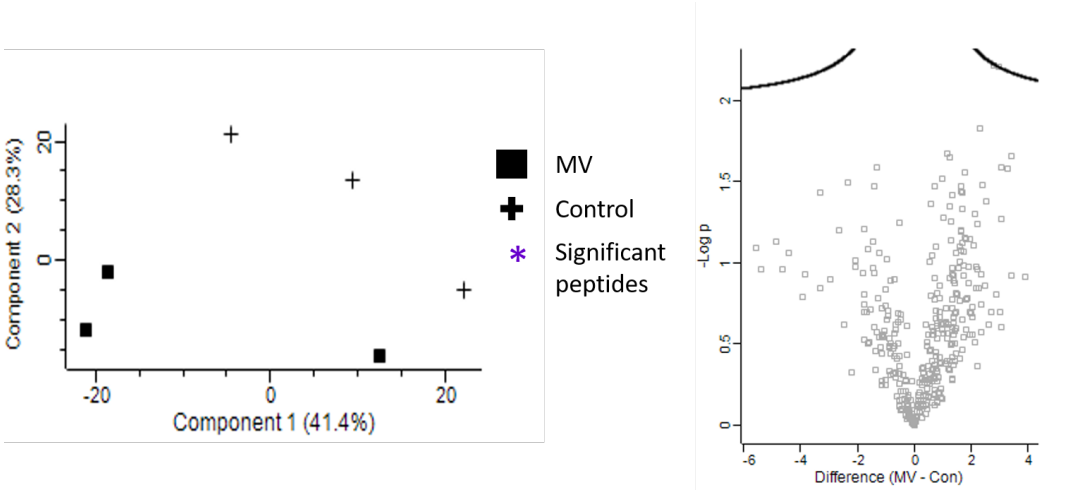

Figure 4.22: (A) PCA plot of the phosphopeptide enrichment of maize treated with 1 μM of MV. The control and MV treated samples separate, showing that there is a change in phosphorylation sites in the treatment. (B) Volcano plot shows no significant changes in proteins between the control and the treatment. FDR: 0.05 s0: 0.1.

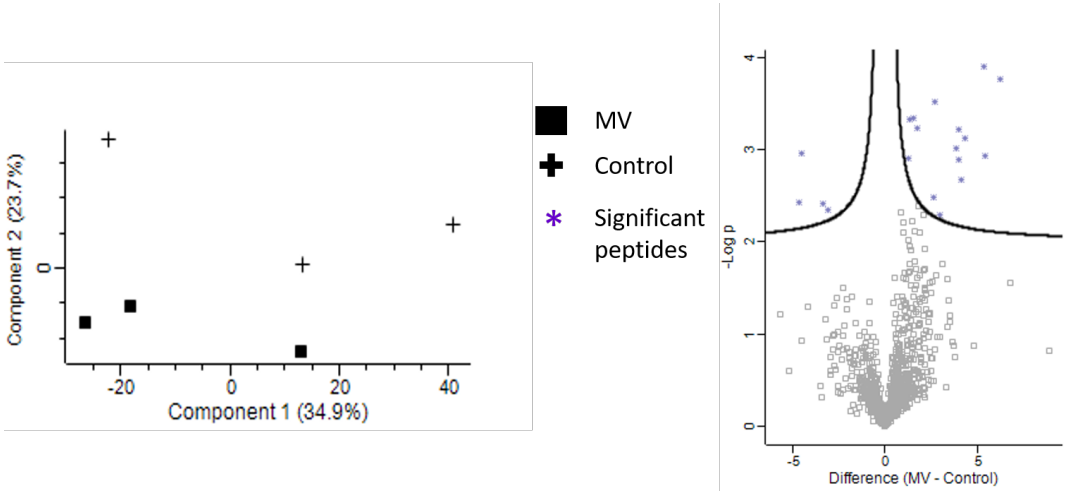

Figure 4.23: (A) PCA plot of the phosphopeptide enrichment of maize treated with 10 mM of MV. The control and MV treated samples separate, showing that there is a change in phosphorylation sites in the treatment. (B) Volcano plot shows significant changes in peptides between the control and the treatment. 1128 phosphopeptides were identified of which 19 phosphopeptides were identified as significantly changed. FDR: 0.05 s0: 0.1.

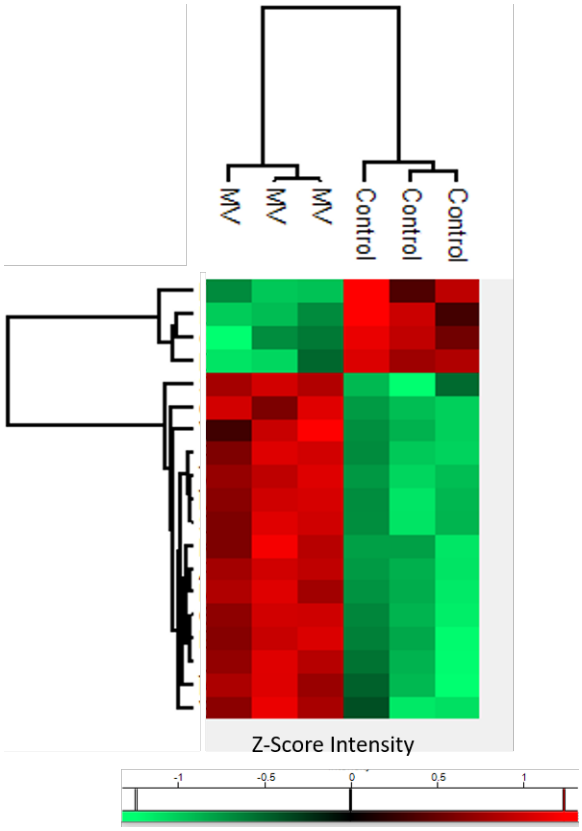

Figure 4.24: A heat map of the significantly changing phosphopeptides in the 10 mM MV treated maize leaves. Significant phosphopeptides log2 fold change values have been z-scored for graphical representation.

The 1 μM MV treated maize leaves showed 81.6% phosphoserine, 17.4% phosphothreonine and 1% phosphotyrosine phosphorylated peptides. 92.9% of phosphopeptides were mono phosphorylated, 6.8% were doubly phosphorylated and 0.3% were triply phosphorylated. The 10 mM MV treated maize leaves showed 85.7% phosphoserine, 14.2% phosphothreonine and 0.1% phosphotyrosine. 90.3% of phosphopeptides were mono phosphorylated, 8.8% were doubly phosphorylated and 0.9% were triply phosphorylated.

Table 4.11: The 19 significantly changing phosphopeptides mapped to 18 phosphoproteins in the 10 mM treated MV maize leaf dataset.

Protein Name	**Peptide AA Sequence**	**Gene Number**	**Log2 Fold Change**	**-Log P Value**	**MQ Score**	**Function/Pathway**	**Site & Position**
Glutathione S-transferase GST 24 (EC 2.5.1.18)	**S**SPQSAAPPVK S**S**PQSAAPPVK	541837 ZEAMMB73_Zm00001d018220	6.22	3.77	79.82	Glutathione transferase activity	S2; S3
Evolutionarily conserved C-terminal region 10	GA**S**SLRSPNGPPEK	100382673 ZEAMMB73_Zm00001d049360	5.42	2.94	134.85	RNA binding	S54
Uncharacterized protein	SVG**S**VGLQPQPQPQPQR	ZEAMMB73_Zm00001d039657	5.37	3.90	191.48		S55
Cyclin-L1-1	ISDLQASKE**S**PAR	ZEAMMB73_Zm00001d019684	4.32	3.13	186.29		S119

Continued on next page

Table 4.11 – *Continued from previous page*

Protein Name	**Peptide AA Sequence**	**Gene Number**	**Log2 Fold Change**	**-Log P Value**	**MQ Score**	**Function/Pathway**	**Site & Position**
BHLH transcription factor (DNA binding protein) (Fragment)	IFGQDL**S**PGGSAR	bHLH57 100284359 ZEAMMB73_Zm00001d043706	4.15	2.68	110.44	Protein dimerization activity	S232
Neutral/alkaline invertase	AS**S**QASLADPDDFDLTR	100281530 ZEAMMB73_Zm00001d051666	4.00	3.23	102.69	Glycopeptide alpha-N-acetylgalactosaminidase activity; sucrose alpha-glucosidase activity	S11
Zinc finger CCCH domain-containing protein 64	AAT**S**PAPAPPR	ZEAMMB73_Zm00001d020242	3.96	2.89	79.20	Integral component of membrane	S5

Continued on next page

Table 4.11 – *Continued from previous page*

Protein Name	**Peptide AA Sequence**	**Gene Number**	**Log2 Fold Change**	**-Log P Value**	**MQ Score**	**Function/Pathway**	**Site & Position**
Glyceraldehyde-3-phosphate dehydrogenase (EC 1.2.1.-)	AAALNIVP**T**STGAAK	542290 ZEAMMB73_Zm00001d027488	3.86	3.02	167.32	Glyceraldehyde-3-phosphate dehydrogenase (NAD+) (phosphorylating) activity; NAD binding; NADP binding	T292
Actin-7 (Actin-97)	DAYVGDEAQ**S**KR	103635981 103629276 ZEAMMB73_Zm00001d011086 ZEAMMB73_Zm00001d011087 ZEAMMB73_Zm00001d035720 ZEAMMB73_Zm00001d035722	2.96	2.30	152.16	ATP binding	S62
Uncharacterized protein	FHGPHSHST**S**T**T**PTGGAAAAAA**S**PR FHGPHSH**S**TST**T**PTGGAAAAA**S**PR	ZEAMMB73_Zm00001d016655	2.70	3.52	101.14		S42; S44; T46; T57

Continued on next page

Table 4.11 – *Continued from previous page*

Protein Name	**Peptide AA Sequence**	**Gene Number**	**Log2 Fold Change**	**-Log P Value**	**MQ Score**	**Function/Pathway**	**Site & Position**
Glyceraldehyde-3-phosphate dehydrogenase (EC 1.2.1.-)	AA**S**FNIIPSSTGAAK	ZEAMMB73_Zm00001d049641	2.66	2.48	188.63	Glyceraldehyde-3-phosphate dehydrogenase (NAD+) (phosphorylating) activity; NAD binding; NADP binding	S205
Multiple stress-responsive zinc-finger protein ISAP1	SP**S**SPTSSSSSLASAASQPR SPS**S**PTSSSSSLASAASQPR	103647538 ZEAMMB73_Zm00001d006016	1.78	3.24	136.17	DNA binding; ubiquitin-protein transferase activity; zinc ion binding	S49; S50
Acetyl-coenzyme A synthetase (EC 6.2.1.1)	HVE**S**MSELPSGAGK	ZEAMMB73_Zm00001d016659	1.53	3.35	227.92	Acetate-CoA ligase activity; AMP binding; ATP binding	S23
ATP-dependent 6-phosphofructokinase 3	NA**S**SVSLADAAYVK	103630633 ZEAMMB73_Zm00001d038775	1.36	3.33	197.06	6-phosphofructokinase activity; ATP binding	S79

Continued on next page

Table 4.11 – *Continued from previous page*

Protein Name	**Peptide AA Sequence**	**Gene Number**	**Log2 Fold Change**	**-Log P Value**	**MQ Score**	**Function/Pathway**	**Site & Position**
S-adenosyl-L-methionine-dependent methyl-transferase superfamily protein	SEYGS**T**LDDDQR	100274302 ZEAMMB73_Zm00001d043827	1.27	2.91	120.55	Methyltransferase activity	T61
Pentatricopeptide repeat (PPR) superfamily protein	HQ**S**YDNIAR	103653005 ZEAMMB73_Zm00001d049408	-3.08	2.34	113.38		S450
RNA binding	WSGSSGGGLGG**S**PPNR	100383162 ZEAMMB73_Zm00001d005281	-3.37	2.42	132.25	RNA binding	S40
Uncharacterized protein	**S**VGSVGLQPQPQPQPQR	ZEAMMB73_Zm00001d039657	-4.50	2.96	170.79		S52

Continued on next page

Table 4.11 – *Continued from previous page*

Protein Name	**Peptide AA Sequence**	**Gene Number**	**Log2 Fold Change**	**-Log P Value**	**MQ Score**	**Function/Pathway**	**Site & Position**
Mitogen-activated protein kinase (EC 2.7.11.24)	TT**S**ETDFMTEYVVTR	541618 ZEAMMB73_Zm00001d045310	-4.60	2.43	127.79	ATP binding; MAP kinase activity	S219

The linear motif analysis in Perseus was used to analyse motifs of the significantly changing phosphopeptides. In the significantly increasing phosphopeptides two contained a MAPK substrate motif, evolutionarily conserved C-terminal region 10 (S45, log2 fold change 5.42) and an uncharacterised protein (S42/S44 T46 S57, log2 fold change 2.70). Five contained a casein kinase II substrate motif, including neutral/alkaline invertase (S11, log2 fold change 4.00) and multiple stress-responsive zinc-finger protein ISAP1 (S49/S50, log2 fold change 1.78). Six contained a PKC motif including cyclin-L1-1 (S119, log2 fold change 4.32) and actin-7 (S62, log2 fold change 2.96). Of the phosphopeptides which significantly decreased in abundance, two contained a casein kinase II substrate motif, which were an uncharacterised protein (S42, log2 fold change -4.50) and mitogen-activated protein kinase (S219, log2 fold change -4.60). Two contained a PKC motif, mitogen-activated protein kinase (S219, log2 fold change -4.60) and pentatricopeptide repeat (PPR) superfamily protein (S450, log2 fold change -3.08).

The motif analysis for the phosphopeptides in the 10 mM MV maize leaf treatment using MMFPh, 17 motifs were identified (Table 4.12), no motifs were identified in the significantly changing phosphopeptides. Proline directed motifs (sP and tP) were identified, which are known substrates of MAPKs, SnRKs, RLKs, AGC protein family kinases, CDKs, CDPKs and SLKs (van Wijk *et al.*, 2014). The basophilic motifs RxxS and RSxS were identified in the dataset and are known target for MAPKs (van Wijk *et al.*, 2014). The xSxSx motif identified is also a target for MAPKs, RLKs and CDKs (van Wijk *et al.*, 2014). The motifs identified in the maize dataset are shown in Table 4.12.

Table 4.12: Motifs identified by MMFPh in the MV treated maize.

Motif	Foreground Matches	Background Matches	Occurrence Threshold	Score
————-P-SP————	81	17636	55	4.19
————SPP————-	65	18341	55	3.82
————SP-P————	55	20654	55	3.41
———-L-R–S————	60	22786	55	3.39
————RS-S————	59	26332	55	3.16
————S—-P———-	113	208776	83	1.11
————S———-R—-	97	213775	83	0.86
————S——P———	91	207310	83	0.81
————S—P————	92	215774	83	0.77
————-P-S————	103	206526	83	0.99
————S–P————	94	218633	83	0.78
————S——P———	97	205579	110	0.91
————GS————	121	268242	110	0.85
————S-P————-	128	214243	110	1.25
————-S-S————	156	410148	138	0.60
————SP————	425	205541	165	3.04
————R–S————	226	217450	165	2.05

4.3 Discussion

Tandem mass tag (TMT) allows more accurate relative quantification between samples, because samples are run together. Quantification using MS2 fragmentation gives rise to ratio supression, because peptides from the MS1 scan are isolated within a 1 Da window, meaning other lower intensity peptides are also isolated and these peptides are also tagged with TMT so contribute to the reporter ion ratios. MS3 negates this issue, however it is much slower and fewer peptides can be identified in the same time period because the Orbitrap needs to be emptied while performing MS3 scans, and therefore cannot do MS1 scans during this time, meanwhile, peptides are still coming off the liquid chromatography (LC) column. Whilst MS3 analysis gives more accurate quantification, there were far fewer peptides identified using MS3 instead of MS2, therefore even though MS2 causes ratio supression, this is more likely to stop significant proteins from being identified as significant, rather than allow proteins which are not significant to be identified as significant, and this is why MS2 quantification was continued rather than switching to MS3 quantification.

The proteins found to be significantly increasing in abundance in the MV treated Arabidopsis soluble fraction included proteins associated with oxidative stress response such as calreticulin-1 (log2 fold change 0.36) and pyridoxal 5'-phosphate synthase subunit (log2 fold change 0.18). L-ascorbate peroxidase 1 (log2 fold change 0.42) and superoxide dismutase (log2 fold change 0.37) are antioxidant enzymes which remove ROS from the cell, so an increase in abundance rather than decrease would be expected, however, in the literature it has been found that in the leaves antioxidant enzymes first increase in abundance then gradually decrease in abundance under MV treatment (Wei *et al.*, 2018). Proteins associated with photosynthesis were identified as some of the most significantly increasing proteins such as oxygen-evolving enhancer protein 1-2 (log2 fold change 0.87) and oxygen-evolving enhancer protein 1-1 (log2 fold change 0.96), which is unexpected because MV attacks at PSI inhibiting photosynthesis, however abundance does not equal activity and there may be more of these proteins being produced because they are being attacked by the MV, one of the ways plants respond to stress is to increase the rate of photosynthesis, which could be the reason for the increase in abundance of these proteins.

The proteins identified as significantly decreasing in abundance in the MV treated Arabidopsis soluble fraction included glycine-rich RNA-binding protein 7 (log2 fold change -0.24) which is known to regulate stomatal closure in response to abiotic stress (Kim *et al.*, 2008), ribonuclease TUDOR 1 (log2 fold change -0.32) and stress-response A/B barrel domain-containing protein HS1 (log2 fold change -0.35) which are all associated with stress response, so would be expected to increase in abundance. However, stomatal closure would not be necessary when the plant is treated with MV because the plant will need to respire more because photosynthesis should be inhibited. There were also proteins associated with oxidative stress response identified such as glyceraldehyde-3-phosphate dehydrogenase (log2 fold change -0.40), which mediates cell death under oxidative stress conditions (Nakajima *et al.*, 2009) and phospholipid hydroperoxide glutathione peroxidase 1 (log2 fold change -0.47). Proteins associated with photosynthesis were also found to decrease in abundance including ribulose bisphosphate carboxylase small chain 1A (log2 fold change -0.32), photosystem II stability/assembly factor (log2 fold change -0.29) and beta carbonic anhydrase 1 (log2 fold change 0.35), the main mechanism of attack for MV is at photosystem I (PSI), so it would be expected that proteins associated with photosynthesis would decrease in abundance however, one of the ways plants respond to stress is to increase the rate of photosynthesis, which could

be the reason for the increase in abundance of these proteins.

The proteins identified as significantly increasing in abundance in the MV treated Arabidopsis membrane fraction included proteins associated with stress such as vesicle-associated membrane protein 721 (log2 fold change 0.37), which is an immune response protein and BURP domain protein RD22 (log2 fold change 0.54). There were also proteins associated with photosynthesis such as chlorophyll a-b binding protein 6 (log2 fold change 0.61) which has been identified as important in response to ABA and stomatal closure (Xu *et al.*, 2012), fumarate hydratase 2 (log2 fold change 1.47) and ferredoxin–NADP reductase, leaf isozyme 2 (log2 fold change 0.35), which is expected to decrease in abundance because MV attacks at PSI. There were several proteins associated with ribosomal structure which were identified as significantly increasing in abundance under MV treatment, 60S ribosomal protein L6-3 (log2 fold change 3.27), 60S ribosomal protein L37-3 (log2 fold change 3.18), 60S ribosomal protein L29-1 (log2 fold change 2.97) and 60S ribosomal protein L29-2 (log2 fold change 2.55), were the four most significantly decreasing proteins. This strongly suggests that MV has an effect on ribosomal structure.

The proteins identified as significantly decreasing in abundance in the MV treated Arabidopsis membrane fraction included proteins associated with oxidative stress response such as L-ascorbate peroxidase 1 (log2 fold change -0.40), which is the primary target of MV in plant leaves (Mano *et al.*, 2001), and probable plastid-lipid-associated protein 2 (log2 fold change -0.42), which is known to accumulate in plant leaves during abiotic stress (Langenkamper *et al.*, 2001). There were also more general stress response proteins identified such as 30S ribosomal protein S1 (log2 fold change -0.47) and heat shock 70 kDa protein 14 (log2 fold change -0.63), which is known to increase in abundance in Arabidopsis during MV treatment (Pulido *et al.*, 2017), so it is odd that it was identified as significantly decreasing in abundance in this dataset. There were also proteins associated with photosynthesis identified as significantly decreasing in abundance such as, protochlorophyllide reductase C (log2 fold change -0.57), which regulates oxidative stress in Arabidopsis (Pattanayak and Tripathy, 2011), beta carbonic anhydrase 1 (log2 fold change -0.44), and photosystem II stability (log2 fold change -1.51) which is an assembly factor for photosystem II (PSII) and is thought to be essential for chlorophyll a binding. It would be expected for photosynthesis proteins to be significantly decreasing in abundance because MV plants attacked at PSI, inhibiting photosynthesis. L-ascorbate peroxidase 1 (log2 fold change -0.34) is an antioxidant enzyme which removes ROS from the

cell and decreases in abundance in this dataset.

The phosphopeptides which significantly increased in abundance in the MV treated Arabidopsis soluble fraction included fructose-bisphosphate aldolase 8 (S350, log2 fold change 4.32), the site identified is a known target of SnRK2 (Wang *et al.*, 2013-2). Phosphopeptides mapped to proteins associated with stress such as serine/arginine-rich splicing factor RS2Z33 (S185 S189, log2 fold change 2.37), heat shock protein 90-1 (S224, log2 fold change 1.59) and La-related protein 1A (S641, log2 fold change 1.85). Two mitogen-activated protein kinases (MAPKs) were also identified: MAPK 17 (T405, log2 fold change 1.20) and MAPK kinase 1 (T29, log2 fold change 1.09). MAPKs are central to many stress responses and are activated by phosphorylation at specific sites (classically the TEY motif on the activation loop) (Cargnello and Roux, 2011). Only three phosphopeptides from photosynthesis proteins were identified, since MV attacks at PSI these proteins are expected to be decreasing in abundance, however, they are membrane proteins, so we do not expect to see them in the soluble fraction, but because a crude extraction process using centrifugation, there is overlap between the proteins in the two datasets.

Of the phosphopeptides which significantly decreased in abundance in the MV treated Arabidopsis soluble fraction, 5 were unique phosphopeptide sites not previously identified in the literature, these were sites on At4g13350 (NSP (Nuclear shuttle protein)-interacting GTPase) (S217, log2 fold change -1.90), At3g60670 (PLATZ transcription factor family protein) (S3, log2 fold change -1.58), disease resistance protein (TIR-NBS-LRR class) family (T102, log2 fold change -1.49), chorismate synthase (S704, log2 fold change -1.36) and F3I6.9 protein (Triadin) (T462, log2 fold change -1.12) in Table 4.5, all other phosphopeptide sites in the table have previously been identified. The phosphopeptide site identified on villin-4 (S777, log2 fold change -2.63) has been identified in the literature as a response to nitrogen deprivation (Menz *et al.*, 2016). The phosphorylation sites identified on the transmembrane protein At5g39570 (S176, log2 fold change -2.43), phospholipase-like protein, COP1-interacting protein-like protein (S761, log2 fold change -1.92), CLIP-associated protein (S1072, log2 fold change -1.38) and phosphoribulokinase (S212, log2 fold change -1.17) have been previously identified as a response to DNA damage (Roitinger *et al.*, 2015). The phosphorylation site identified on protein plastid movement impaired 2 (S545, log2 fold change -1.10) has also been identified in response to stress (Wang *et al.*, 2013-2). The phosphorylation site identified on

FHA domain-containing protein DDL (S133, log2 fold change -1.52) has been previously identified in response to drought and nitrogen deprivation (Menz *et al.*, 2016; Bhaskara *et al.*, 2017), metal-dependent protein hydrolase (S44, log2 fold change -1.40) was also identified in response to drought stress (Bhaskara *et al.*, 2017). The phosphorylation site identified on protein PHOX3 (S298, log2 fold change -1.15) has been previously identified in response to drought (Umezawa *et al.*, 2013). Whilst none of the proteins were directly linked to drought, the phosphopeptide sites were identified in previous studies in response to drought, and therefore could be general stress response phosphorylation sites.

Of the phosphopeptides which significantly increased in abundance in the MV treated Arabidopsis membrane fraction the two proteins which increase in abundance the most are uncharacterised proteins (Y562 S29, log2 fold change 5.71, 4.58) and the phosphopeptide sites identified in this study have not previously been identified. The sites identified on AT5g03040/F15A17_70 (S49, log2 fold change 4.48), acetyl-CoA acetyltransferase (T4/S5, log2 fold change 4.38), At2g22790 (S28, log2 fold change 4.33), protein kinase superfamily protein (S523, log2 fold change 3.68), lysine-specific histone demethylase 1 homolog 3 (Y1572, log2 fold change 3.32), At3g16330 (S153, log2 fold change 3.15), phosphoenolpyruvate carboxylase-related (S153, log2 fold change 3.15) and ATP-dependent helicase BRM (S1856, log2 fold change 2.27) have also not been identified in previous studies. The sites identified in this study on elongation factor 2 (S486, log2 fold change 2.04), serine/arginine-rich splicing factor (S170, log2 fold change 2.09), syntaxin-71 (S222, log2 fold change 2.23) and phosphoenolpyruvate carboxylase 1 (S11, log2 fold change 2.69) were all identified by Reiland *et al.* (2009).

There were only 6 phosphopeptides identified as significantly decreasing in abundance in the MV treated Arabidopsis membrane fraction. These were mapped to 9 proteins. Phosphoinositide phospholipase C 2 (S280, log2 fold change -6.21) is a known target of MAPKs (Rayapuram *et al.*, 2018). Phospholipids are known to be modified by stress (Xue *et al.*, 2009), so it is surprising that this phosphopeptide site decreased in abundance in the MV treated samples. The phosphopeptide site identified in this study has been identified in a number of studies (Rayapuram *et al.*, 2018, 2014; Mattei *et al.*, 2016). Two phosphopeptides identified mapped to a protein associated with stress response, alkaline/neutral invertase CINV1 (S700 and S699, log2 fold change -5.39 and -5.25), and these phosphopeptide sites have not been identified previously. The site identified on kinase with adenine nucleotide

alpha hydrolases-like domain-containing protein (S547, log2 fold change -5.31) has been identified as a known target of MAPKs (Rayapuram *et al.*, 2018). The phosphopeptide site identified on 50S ribosomal protein L12-3 (S144, log2 fold change -2.13) has been identified as a response to stress (Bhaskara *et al.*, 2017). The phosphopeptide site identified on probable receptor-like protein kinase (Y462, log2 fold change -2.07) has not previously been identified, whilst this peptide has previously been identified as phosphorylated, the Y has not previously been identified as phosphorylated. The phosphopeptide site identified on protein plastid transcriptionally active 16 (T451, log2 fold change -1.28) has previously been identified as a response to DNA damage, so could be a more general stress response protein (Roitinger *et al.*, 2015). The phosphopeptide site identified on Protein walls are thin 1 (S372, log2 fold change -0.92) has not previously been identified as phosphorylated in Arabidopsis.

Two MV treatments of maize were used, 1 μM for 16 hours under constant light and 10 mM for 2 hours under constant light. However, neither experiment revealed any significantly changed proteins in the maize soluble fraction. MV is an unspecific herbicide, so should affect both dicots and monocots in a similar way (Bromilow, 2003). However, monocots have a waxy layer on their leaves, which is more difficult to penetrate. Therefore it is possible the MV treatment was not long enough, so a longer treatment of at least 6 hours for the 10 mM treatment may have shown a difference in expressed proteins. The membrane proteins were also isolated but there was no time to analyse them. In the Arabidopsis, there was a larger change in the membrane fraction than the soluble fraction, so whilst no changes in protein expression was seen in the soluble fraction of the maize, a change may have been seen in the membrane fraction.

There were 15 phosphopeptides which significantly increased in abundance. These phosphopeptides mapped to proteins such as multiple stress-responsive zinc-finger protein ISAP1 (S49 S50, log2 fold change 1.78), a stress response protein which is associated with ubiquitin transferase activity. Ubiquitin is involved in cell stress response and activates stress response pathways. Glutathione S-transferases (S2 S3, log2 fold change 6.22) are known to interact with MAPKs for signalling pathways. Glutathione S-transferase is phosphorylated by serine/threonine protein kinases and this enhances metabolic activity (Lo *et al.*, 2004). To the best of my knowledge none of the significantly changing phosphopeptide sites identified in this study have previously been identified in maize (as of February 2020 these modifica-

tions were not in UNIPROT).

In the phosphopeptide enrichment for the 10 mM MV treated maize leaves, four phosphopeptides were identified as significantly decreasing in abundance. The phosphopeptide which decreased the most during MV treatment was MAPK (S219, log2 fold change -4.60), which is known to become phosphorylated under ABA response pathways (Danquah *et al.*, 2014), it would be expected that MAPKs would be more abundant in the dataset. However, typically MAPK are phosphorylated on the TEY activation loop, however in this dataset the phosphorylation site is before the activation loop (TTSETDFMTEYVVTR). According to the MQ analysis there is a small chance the modification is present on this activation loop (0.002/1), but is far more likely to be on the S219 suggested (0.808/1).

It is well established that MV causes oxidative damage, and this was seen in the western blots, however, an increase in oxidative damage modifications was not seen in the treated over the control when an error tolerant search (ETS) was performed on the Arabidopsis samples, to search exhaustively for additional oxidation modifications. This is most likely because like phosphorylation, oxidative damage modifications are in a low abundance, so cannot be seen under natural abundance in the MS, and an enrichment method is needed in order to fully analyse them. Therefore the next step was to develop a method of tagging and enriching carbonyl modifications using bovine serum albumin (BSA) as a standard in Chapter 5.

Chapter 5

Development of a Suitable Proteomic Method for Tagging & Enrichment of Carbonyl Modifications

5.1 Introduction

5.1.1 The Role of Oxidative Damage to Proteins in Biological Systems

Reactive oxygen species (ROS) mediate cell signalling pathways, but the mechanisms which ROS undergo is poorly understood (Wong *et al.*, 2012). ROS also cause significant damage to proteins by producing oxidative modifications on amino acid (AA) residues (Wong *et al.*, 2012). To control ROS levels, cells have antioxidant systems such as, superoxidise dismutase (SOD), which converts superoxide to hydrogen peroxide, peroxisomal catalase (CAT) and glutathione peroxidases (GPx) which degrade hydrogen peroxide to oxygen and water (Fedorova *et al.*, 2014). However, when ROS levels become high under oxidative stress conditions, irreversible damage to proteins is caused. Oxidative modifications to proteins are low in abundance and not very site specific, making them difficult to detect, especially in complex mixtures (Verrastro *et al.*, 2015). The main ROS are the superoxide anion ($\cdot O_2^-$), hydrogen peroxide (H_2O_2) and the hydroxyl radical ($\cdot OH$) which can all be formed under numerous conditions, including various abiotic and biotic stresses (Figure 5.1) (Moller *et al.*, 2007). ROS form in the mitochondria and chloroplasts of cells (Fedorova

et al., 2014). In both systems the reduction of NADP to NADPH causes the production of superoxide which does little damage, because it is relatively unreactive to most biological molecules, only reacting with Fe-S centres (Moller *et al.*, 2017). Continued reduction, however, allows hydrogen peroxide and hydroxyl radicals to form, the latter of which reacts rapidly with lipids, DNA, carbohydrates and proteins (Moller *et al.*, 2017). The damage caused by these ROS to proteins is through the addition of a functional group to AA residues, which changes protein structure which can alter the biological activity leading to a loss or gain in function (Fedorova *et al.*, 2014).

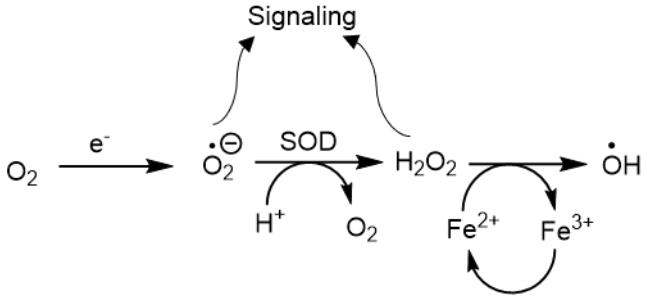

Figure 5.1: Superoxide dismutase activity and production of reactive oxygen species.

There are many different forms of oxidative damage on AAs. Cysteine and methionine are most susceptible to attack by ROS because they contain sulfur atoms which are easily oxidised (Garrison, 1987). Aromatic AAs such as histidine, phenylalanine, tryptophan, and tyrosine are damaged by the addition of an oxygen to their aromatic side chains. Oxidants can directly attack a peptide backbone, causing fragmentation and conformational changes to the secondary and tertiary structure of a protein (Martinaud *et al.*, 1997; Morzel *et al.*, 2006). 4-hydroxynonenal (HNE) is an oxidation modification formed by lipid peroxidation in cells. Including all these variable modifications in sample analysis will increase the search space, leading to an increase in the false discovery rate (FDR), however if not all the modifications are searched for, they will still be present but not picked up in the search, leading to unidentified peptides.

One of the most common forms of oxidative damage is protein carbonylation (Colombo *et al.*, 2016). Due to the relative chemical stability of carbonyl groups, they have been established as a key biomarker for oxidative stress (Fedorova *et al.*, 2014; Bollineni *et al.*, 2011-1). Protein carbonylation can occur via many different routes, the most common of which is metal catalysed oxidation (MCO) (Moller *et al.*, 2011), which occurs when a metal ion such as Fe^{2+} or Cu^{+} reacts with H_2O_2

and is oxidised to Fe^{3+} or Cu^{2+} and the highly reactive ·OH is produced (Moller *et al.*, 2011). During MCO, AA side chains are directly oxidised, the functional group is interconverted to a carbonyl group, and these form primary modifications. Secondary modifications can also form, but they are more prevalent in other mechanisms (Heard *et al.*, 2015). Secondary modifications involve other side reactions after the initial addition of the carbonyl group, creating more complicated products. Glutamic semialdehyde, allysine and 2-amino-3-ketobutyric acid are some of the more common primary modifications produced by MCO (Figure 5.2) (Maisonneuve *et al.*, 2009).

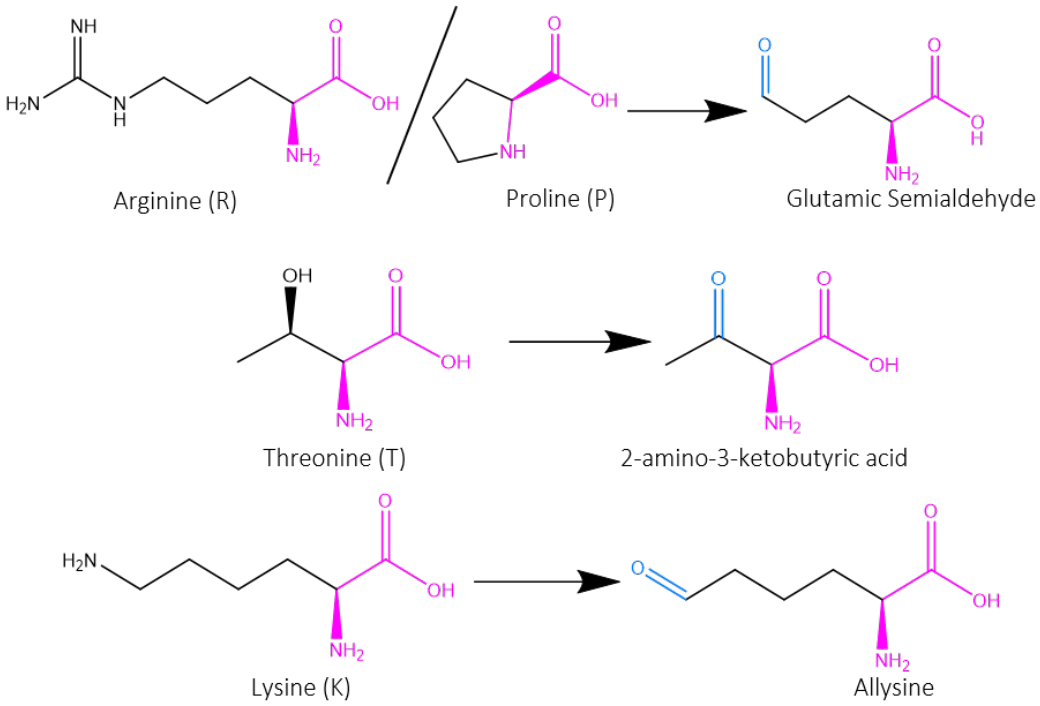

Figure 5.2: The four AAs which are primarily modified by MCO, and the carbonyl modification they form. The AA backbone is highlighted in pink, and the carbonyl modification is highlighted in blue.

One of the biggest problems with identifying carbonylation modifications in cellular systems is their low abundance, making it difficult to identify sites which are susceptible to oxidative stress especially in a complex mixture of proteins. In order to combat the problem of low abundance an effective tagging and enrichment strategy must first be established.

5.1.2 Carbonyl Reactive Tags for Detection & Enrichment

Analysis of carbonylated proteins has traditionally been performed using 2,4-Dinitrophenylhydrazine (DNPH). Due to its absorbance at 360 nm, the standard method of quantifying carbonyl modifications with DNPH is colourimetry (Levine *et al.*, 1990), with the development of specific antibodies, immunoblotting is now also used (Keller *et al.*, 1993; Goto *et al.*, 1999). Additionally, due to DNPH's absorbance at 360 nm, it is able to be used as a matrix for matrix-assisted laser desorption/ionization (MALDI) proteomics. MALDI allows for the enhancement of the desorption and ionisation of DNPH tagged peptides by laser desorption ionisation (LDI) (Peng *et al.*, 2003). However, MALDI studies have been limited to single proteins and have not been performed on complex biological mixtures (Fenaille *et al.*, 2004, 2005; Bollineni *et al.*, 2011-2). Although DNPH is effective at reacting with carbonyl groups, and thereby tagging carbonylated proteins, there are many challenges caused by its use for analysing carbonylated proteins. DNPH is not only reactive to carbonylated proteins but also to carbonylated lipids, nucleic acids and carbohydrates (Luo and Wehr, 2009), possibly causing a wide variation in results obtained from colourimetry and enzyme-linked immunosorbent assay (ELISA) or western blots (Mohanty *et al.*, 2010), and these contaminants cannot be entirely removed. DNPH also causes a side reaction with sulfenic acids, causing oxidation of cysteine resides which will contribute to measured carbonylation levels (Dalle-Donne *et al.*, 2009). DNPH can also affect the isoelectric point and mobility of proteins on sodium dodecyl sulfate polyacrylamide gel electrophoresis (SDS-PAGE) gels, leading to misassignment of proteins when 2D gels are used (Singh *et al.*, 2007; Talent *et al.*, 1998).

Although DNPH has been used extensively to quantify carbonyl modifications, it does have its drawbacks. It has a limited solubility in water and thus solutions of DNPH are often made up in 2 M hydrochloric acid (HCl). Many proteins, however, are insoluble at low pH, making DNPH a difficult reagent to work with (Wehr and Levine, 2012). Other carbonyl reactive tags such as aminoxy tandem mass tag (TMT) and biotin-LC-hydrazide do not have this issue as they are soluble in water and thus easier to use when working with proteins. AminoxyTMT is a derivative of the TMT isobaric labelling reagent, initially developed by Thermo Scientific with an amine reactive group but was modified to contain an alkoxyamine functional group to allow binding to carbonyls instead of amines (Chung *et al.*, 2008; Slade *et al.*, 2011). TMT was originally designed for the purpose of tagging several samples and allowing quantification of those samples by mass spectrometry (MS). Each tag has the same mass and chemical structure, however the placing of various

heavy isotopes at different positions within the molecule allows for different masses when the fragmentation during tandem mass spectrometry (MS2 or MS3) occurs. The mass reporter ion which will be different for each sample is then able to be used to quantitatively measure protein expression during peptide fragmentation (Afiuni-Zadeh *et al.*, 2016). Alkoyamine groups have shown high reactivity with aldehyde groups but lower reactivity to ketones and no reactivity to carbonxylic acids. This is due to the strong higher positive charge residing on carbonyls in aldehydes compared to other groups. The aminoxyTMT forms a covalent bond between the alkoyamine functional group and the carbonyl. The oxime bond (O-N=C) formed is more stable than the hydrazone bond (N-N=C) formed by DNPH and other hydrazide reagents (Kalia and Raines, 2008) (Figure 5.3).

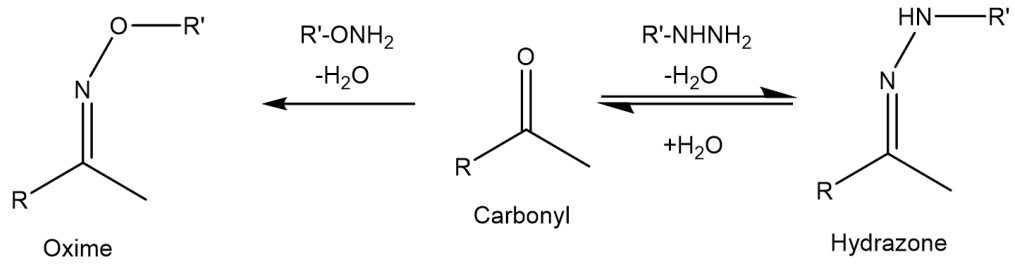

Figure 5.3: The reaction of the carbonyl group with a hydrazine to form a hydrazone bond or an alkoxyamine to form an oxime bond.

Hydrazides can also react with carbonyls, forming a Schiff base, which is then reduced to an amine which is more stable for further analysis. Biotin hydrazides were initially used in gel based proteomic methods in combination with avidin-fluorescein staining to detect protein carbonylation (Yoo and Regnier, 2004). Later (around 2005) affinity chromatography was used to identify carbonylated proteins in MS and their modification sites (Mirzaei, 2005; Mirzaei and Regnier, 2007). More recently, protein enrichment has been used, enriching for carbonylated proteins and then digesting with trypsin, leading to an increased proportion of carbonylated sites (Madian *et al.*, 2011). However, with the low abundance of carbonyl modifications present on proteins, most peptides are still not carbonylated when enrichment at the protein level is performed. Havelund *et al.* (2017) used peptide level enrichment to analyse carbonylated sites on bovine serum albumin (BSA) and were able to identify more carbonylated sites than ever before, though they allowed for an unusually high number of variable modifications in their search (seventeen).

The oxime bond is more stable than the hydrazone bond (Kalia and Raines, 2008). Coffey and Gronert (2016) used an alkoyamine reactive biotin tag with a

cleavable disulphide bond, to allow cleavage from the streptavidin beads with dithiothreitol (DTT). Thus far these methods have only been used on single proteins and not in complex mixtures. Aldehyde reactive probes (ARP) were initially developed to detect and quantify apurinic/apyrimidinic sites on deoxyribonucleic acid (DNA) but have also been used to identify protein carbonylation (Kubo *et al.*, 1992). The oxime bond formed by ARPs is more stable than the hydrazone bond formed by DNPH and biotin hydrazides, and so a reduction step is not required to stabilise the bond. Preliminary studies used SDS-PAGE gels and MS but failed to reveal the carbonylated site or type of carbonylation (Kubo *et al.*, 1992). Later (around 2008) modification sites were able to be identified using tandem mass spectrometry (MS/MS) (Chung *et al.*, 2008). However, under collision induced dissociation (CID) fragmentation, ARPs produce tag specific fragments, increasing the complexity of spectra, making assignment challenging for search engines such as MASCOT and Sequest (Chavez *et al.*, 2010). Coding tools can be used to pick out the spectra with the corresponding reporter ions, this greatly increased assignment rates of proteins and reduced false positive rates (Slade *et al.*, 2011).

Label free quantification (LFQ) has been used to analyse carbonylated peptides in the past (Salvato *et al.*, 2014). However, carbonyl modifications exist in a low abundance, which makes using LFQ without an enrichment process more challenging, as they can be supressed by other more abundant peptides in the proteome unless tagged and enriched for. Carbonyl modifications such as HNE, create a reporter ion fragment in tandem MS, making assignment of the modification and analysis easier (Bolgar *et al.*, 1996).

5.1.3 Mass Spectrometry Analysis of Carbonyl Modifications in Complex Mixtures

The first paper to identify carbonylated sites in a plant-based system using proteomics did not use any tagging or enrichment process. By isolating mitochondria from potato tubers, carbonylated arginine, lysine and threonine were identified (Salvato *et al.*, 2014). However, carbonylated proline could not be identified because the +16 Da mass shift can also be assigned to hydroxylation of proline, so the exact modification is unclear (masses of native modifications shown in Table 5.1). The results of this study by Salvato *et al.* (2014) help to better understand the role post translational modifications (PTMs) play in the function of mitochondria. If a tagging and enrichment strategy had been implemented more of the proteome could have been analysed for carbonyl modifications, not just the mitochondria.

The use of DNPH for tagging and enrichment of carbonyl modifications has been used in many studies with complex mixture to identify carbonylated proteins, however it has never been used to identified carbonylated sites on AA residues in complex mixtures. There have been authors who have used enrichment strategies for DNPH using protein A beads, but due to limitations of MS at the time were able to identify carbonylated proteins but not sites of carbonylation (Kristensen *et al.*, 2004). However, with updated equipment, it is possible that this method can be used to identify carbonylated AA sites. Therefore, the first aim of work in this chapter was to use DNPH to tag carbonyl modifications on BSA, and protein A beads to enrich for carbonyl modifications like Kristensen *et al.* (2004) did, but using a more advanced MS (Orbitrap Fusion, Thermo Scientific) to analyse the enriched samples. Masses of DNPH tagged carbonyl modifications are shown in Table 5.1.

AminoxyTMT was used for tagging and enrichment of carbonyl modifications in complex mixture to compare levels of proteins in obese and lean mice livers (Afiuni-Zadeh *et al.*, 2016). However, since an HNE modification process was used before tagging and enrichment with aminoxyTMT it is unclear if the results were due to an increase in protein expression or an increased susceptibility to HNE modification in the obese mice. The authors did however show that aminoxyTMT can be used for quantitative analysis in complex mixtures and is able to identify specific sites of interest on AAs. No further studies in the literature have been done using aminoxyTMT. Therefore, in aim number two aminoxyTMT was used to tag and enrich for carbonyl modifications on BSA as an alternative to DNPH. Masses of aminoxyTMT tagged carbonyl modifications are shown in Table 5.1.

Carbonylated sites have been identified using ARPs to tag and enrich for carbonyl modifications in legume nodules. Using APRs to enrich for carbonyl modifications threonine has been found to be the most susceptible AA to carbonylation with 25% of carbonyl modifications were found on threonine, 20% on arginine, 20% on lysine and 13% on proline (Matamoros *et al.*, 2018). This shows ARPs are viable tags for identifying carbonylated sites on AAs. Therefore, in aim number three ARPs were used to tag and enrich for carbonyl modifications in BSA. Masses of ARP tagged carbonyl modifications are shown in Table 5.1.

Table 5.1: The mass difference between the main four amino acids and their carbonylated forms with the different carbonyl reactive tags.

Carbonyl Modification	Original (m/z)	DNPH (m/z)	Aminoxy TMT (m/z)	Biotin-LC-hydrazide (m/z)	Alxokyamine-PEG_4-biotin (m/z)	Alkoxyaime-PEG_4-SS-PEG_4-biotin (m/z)
Arginine (R)	-43.0534	136.9749	253.1677	312.1507	357.1371	292.0980
Lysine (K)	-1.0316	178.9967	295.1895	354.1725	399.1589	334.1198
Proline (P)	15.9949	196.0232	312.2161	371.1991	416.1855	351.1464
Threonine (T)	-2.0156	178.0126	294.2055	353.1885	398.1749	332.1280

5.1.4 Error Tolerant & Dependent Peptide Searches

MASCOT (Matrix Science) error tolerant search (ETS) works by first searching all spectra against a database, where peptides are assigned to proteins and identified. Once proteins have been identified as present in the sample a second search is performed to identify additional peptides from that protein with modifications from the database. The ETS includes a large number of modifications, but only using a limited number of protein sequences (from the first search) to prevent the search space from expanding too much. However, if a protein is not assigned in the first round of searches, peptides from that protein cannot be assigned as modified in the second round. In MaxQuant (MQ) the dependent peptide search (DPS) works by assigning spectra to peptides from a protein in the database. DPS looks for patterns in the remaining spectra which correspond to the assigned peptides, and thus assign modified spectra of peptides which have already been assigned. Consequently, if a peptide is not initially found in the samples then it cannot be identified as modified in the second search, regardless of if the protein the peptide is from was identified. Both these techniques prevent the database from becoming too large during the search and reduce the FDR.

In a complex mixture, enrichment at the protein level will give information on the proteins that are carbonylated (Figure 5.4A), but because most of the peptides are not modified it may not give information on the sites which are carbonylated, but rather the overall protein which is modified, because there will be more peptides which are not carbonylated than are in the sample. Enrichment at the peptide level however, will give site specific information as there will be less background of uncarbonylated peptides (Figure 5.4B), but because the sample has been enriched

at the peptide level, a two-peptide tolerance when identifying a protein within the data cannot be used, which increases the possibility of false positives.

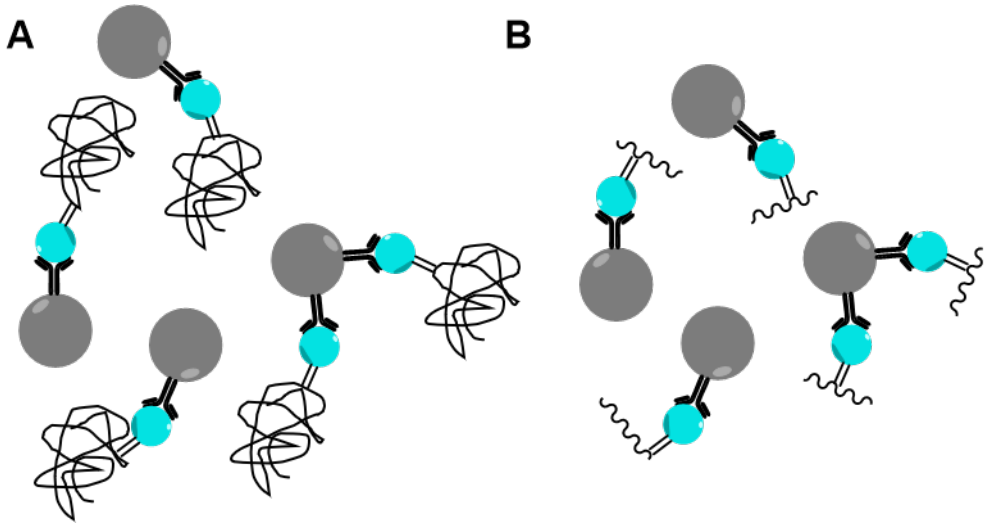

Figure 5.4: (A) Protein level enrichment, proteins are tagged and enriched before digestion. (B) Peptide level enrichment, proteins are tagged and then digested before enrichment of peptides.

5.1.5 Aims & Objectives

The aim of this chapter was to develop a reproducible method for tagging and enriching carbonyl modifications using a standard protein, BSA, at the protein and peptide level which could be used in complex mixtures. To do this four different types of tag were used which use two different chemical tagging techniques, DNPH, aminoxyTMT, biotin hydrazide and ARPs alkoxyamine biotin and alkoxyamine-SS-biotin. BSA was used as a standard protein, and carbonylation was forced using MCO. Work was focussed on the four most common carbonyl modifications, proline and arginine to glutamic semialdehyde, lysine to allysine and threonine to 2-amino-3-ketobutyric acid. To begin with samples were tagged at the protein level for colourimetry and immunoblotting to quantify carbonyl levels before analysis using MS.

After a tagging protocol at the protein level was established, the aim was to move onto peptide level work in plant material. Thus, giving information on the specific sites which are carbonylated in complex mixtures. The overall aim being to identify if there is a link between carbonylation and yield loss in droughted maize.

5.2 Results & Discussion

5.2.1 2,4-Dinitrophenylhydrazine

In order to develop a method of tagging carbonyls, bovine serum albumin (BSA) was used as a standard protein. BSA is a small protein of 66 kDa, and easier to analyse than a complex mixture. A metal catalysed oxidation (MCO) reaction was used to force carbonylation. 2,4-dinitrophenylhydrazine (DNPH) was used to tag carbonyl modifications on proteins and protein A beads were used for enrichment. Colourimetry and western blotting were used to check carbonylation levels, before work moved onto MS analysis at the protein level.

To prove BSA was carbonylated a western blot and a colourimetry assay using DNPH were performed (Figure 5.5). There was a base level of carbonylation in the control, which Bollineni *et al.* (2011-2) also observed, but after MCO treatment carbonylation level of BSA was increased. However, when BSA was left in solution in the freezer, it oxidises to the point where the control had the same level of carbonylation as the MCO treated. Therefore, fresh BSA powder was used for the control in every experiment. The western blot shows a higher level of carbonylation in the MCO treated BSA than the control BSA.

When samples were enriched for carbonylation using anti-DNPH antibodies conjugated to protein A beads, an increased amount of carbonylation was seen in the MCO treated over the control in the western blot. The colourimetry assay further corroborates this, showing higher absorbance in the MCO than the control, 1.05 nmol of carbonylation per milligram of protein in the MCO BSA, and 0.65 nmol of carbonylation per milligram of protein in the fresh BSA. However, the level of enrichment is poor, this could be because the conjugation of the anti-body to the beads may not be complete, some antibodies could be the wrong way around with the active site conjugated to the beads, so proteins would not bind to them, which could possibly be the cause of the ineffective enrichment.

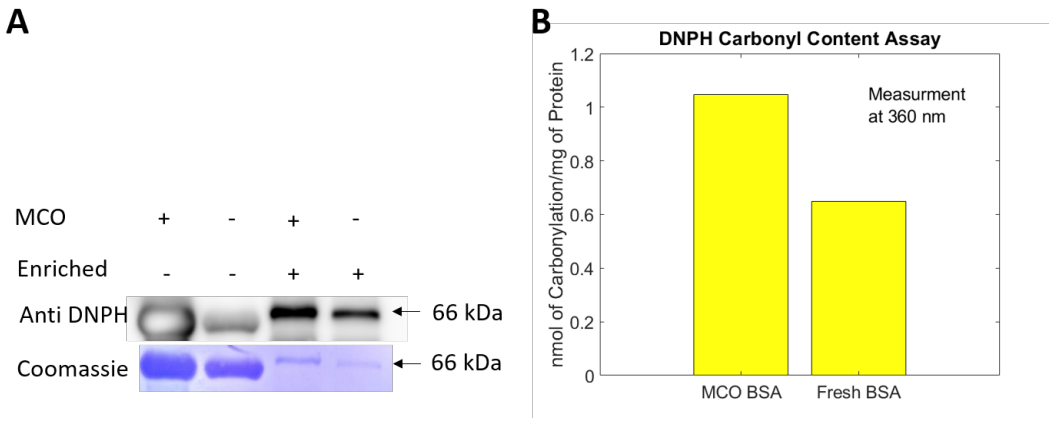

Figure 5.5: (A) DNPH western blot of MCO treated BSA and untreated BSA, input and enriched. There is an increase in carbonylation in the MCO over the control BSA there is also an increase in enrichment. (B) DNPH colourimetry assay. There is an increased absorbance in the MCO BSA than the fresh control BSA showing that the MCO is causing oxidative damage.

MS analysis of the tagged samples was performed, after tryptic digest and liquid chromatography-tandem mass spectrometry (LC-MS/MS) and using Mascot (Matrix Science) excellent coverage of BSA was obtained with 74% percent total coverage and 41 unmodified peptides using standard search criteria (fixed cysteine alkylation and variable oxidation of methionine). Identification of carbonylated peptides proved challenging because many different amino acids (AAs) can be carbonylated and setting multiple modifications as variable modifications in database searches increases the search space, and so increases the false discovery rate (FDR). To combat this, the error tolerant search (ETS) using the algorithm MASCOT (Matrix Science), and the dependent peptide search (DPS) using the Andromeda algorithm in MaxQuant (MQ) was used to analyse the data (Cox *et al.*, 2011).

When the DNPH tagged samples were analysed by ETS 3 low scoring matches to DNPH tagged peptides were found, however after manual inspection of these putative assignments it was concluded that they were false positives. The DPS found no matches to DNPH tagged peptides. However, the hydrazone bond formed between DNPH and a carbonyl is not very stable, so it is possible that this bond had degraded. Therefore, the MASCOT search of the data was repeated using (untagged) original carbonyl modifications and found that the number of carbonyl modifications was similar to the number found in an untagged sample. It is well known that the reaction is reversible and this suggests that the DNPH is being re-

moved and the original carbonyl modification is reforming. Colourimetry assays and western blots tend to be done shortly after samples have been tagged, so there is little time for the reaction to reverse, and the reaction conditions remain the same, so the equilibrium will not easily be pushed in the other direction. When preparing samples for MS however, there are various steps which take more time and more changes in condition which could push the equilibrium back towards the original modifications, the hydrazone bond is less stable under acidic conditions, possibly causing the tag to be removed and not seen in the MS results (Sayre *et al.*, 2006).

Therefore stage tipping samples without any acid was used. The acid helps peptides to stick to the C18-stage tip, and samples are brought down to pH 2 before being stage tipped to stop the digestion reaction. Acid was completely removed from this process and from the loading column on the MS, but acetonitrile and formic acid was still used to elute from the liquid chromatography (LC) column. Electron transfer dissociation (ETD) fragmentation on 3-6+ ions was also performed because Bollineni *et al.* (2013) obtained better spectra with ETD fragmentation than higher-energy collision dissociation (HCD) fragmentation on DNPH tagged peptides. When this data was searched, using the ETS in MASCOT and the DPS in MQ two threonine modifications tagged with DNPH were identified (Figure 5.6) (Table 5.2). Both supporting MS2 spectra showed a good Y ion series providing evidence to suggest the modification was located on the threonine.

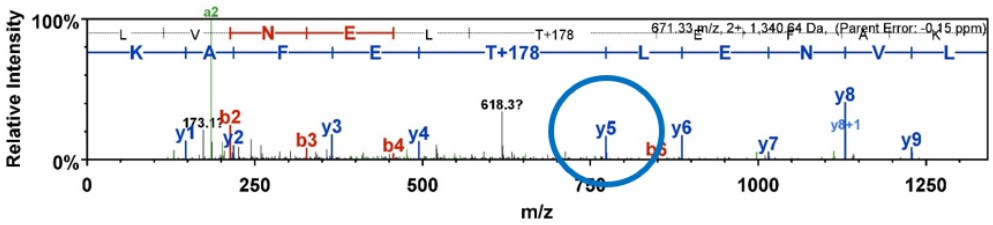

Figure 5.6: A spectrum of a peptide tagged with DNPH at the threonine. The spectrum shows a good Y ion series, with strong evidence to support the presence of the modification on the threonine.

DNPH was effective at tagging the carbonyl modifications, however, the hydrazone bond was unstable especially at low pH, which is the pH of the MS buffers, so the bond would break before MS analysis could be performed and in the first three experiments performed, no peptides tagged with DNPH were identified. When acid was removed from the protocol to help stabilise the hydrazone bond two DNPH tagged peptides were identified (Table 5.2). Therefore, a total of two DNPH tagged

peptides were identified in four experiments using DNPH, they were only identified in input samples and not enriched. Protein A beads used are very sticky and designed to bind to proteins. This means the antibody may not bind the correct way around, so the active site may be conjugated to the beads, making the enrichment less effective. The stickiness of the beads also makes the enrichment unspecific, giving an increase in uncarbonylated proteins in the sample. The yield of enrichment was low and with the acid labile nature likely to be a problem, DNPH is not ideal for working with more complex plant samples, though some western blots were performed with plant samples (shown in Chapter 4), it is not a suitable tag for MS.

5.2.2 Aminoxy Tandem Mass Tag

Aminoxy tandem mass tag (TMT) was designed for tagging glycans but Afiuni-Zadeh *et al.* (2016) used it to tag and enrich 4-hydroxynonenal (HNE) modifications. AminoxyTMT gives diagnostic reporter ions during MS2. AminoxyTMT forms an oxime bond which is more stable than the hydrazone bond. Enrichment of TMT tagged proteins and peptides is possible because Thermo Scientific sell anti-TMT conjugated to beads and anti-TMT elution buffer. After labelling MCO and control BSA samples with aminoxyTMT using a modified protocol from Afiuni-Zadeh *et al.* (2016) to determine tagging efficiency, a western blot was performed using anti-TMT (Figure 5.7). From this blot an increased amount of carbonylation in the MCO treated BSA compared to the control was observed. Whilst there is an increase in signal in the MCO treated samples over the control, there is no difference between the input and the enrichment. Surprisingly the flow-through contained higher signal than the input or enrichment, this suggests that the majority of the carbonylated proteins are not binding to the beads, and the enrichment is ineffective because the beads have a low capacity or low affinity. Scientists at Thermo Scientific were contacted who informed us that the anti-TMT antibody has a low affinity.

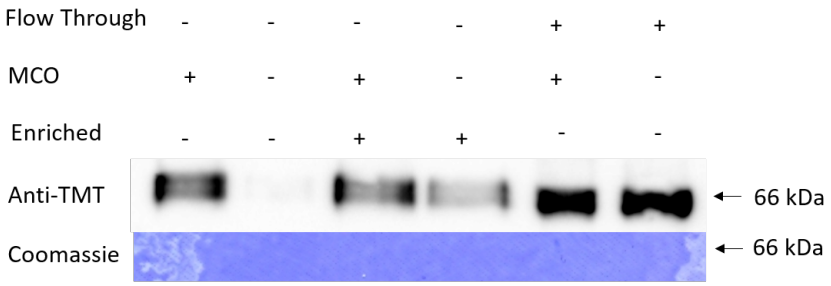

Figure 5.7: Western blot showing MCO and control BSA, input and enriched tagged with aminoxyTMT and the flow through from the beads. There is an increase in signal in the MCO than the control, and an increase in signal in the enriched samples.

Since the western blot showed successful tagging, analysis was continued using MS. Different digestion methods for aminoxyTMT enriched samples were used, on bead, in gel and in solution. Excellent coverage of BSA was obtained with 72% percent total coverage and 37 unmodified peptides using standard search criteria (fixed cysteine alkylation and variable oxidation of methionine). A sample of untagged MCO treated BSA was also analysed for comparison. A carbonylated peptide from an aminoxyTMT tagged sample and an untagged modified sample were compared (Figure 5.8). Both spectra have a strong Y ion series so there is less chance of misassignment. In the spectra of the sample tagged with aminoxyTMT we can see the TMT mass reporter at 126.2 Da which breaks during HCD fragmentation, indicating that the tag is likely to be present. The spectra show that aminoxyTMT is capable of tagging carbonyl modifications, and they can be identified using MS. However, the same tagged modifications were not consistently seen in the MS.

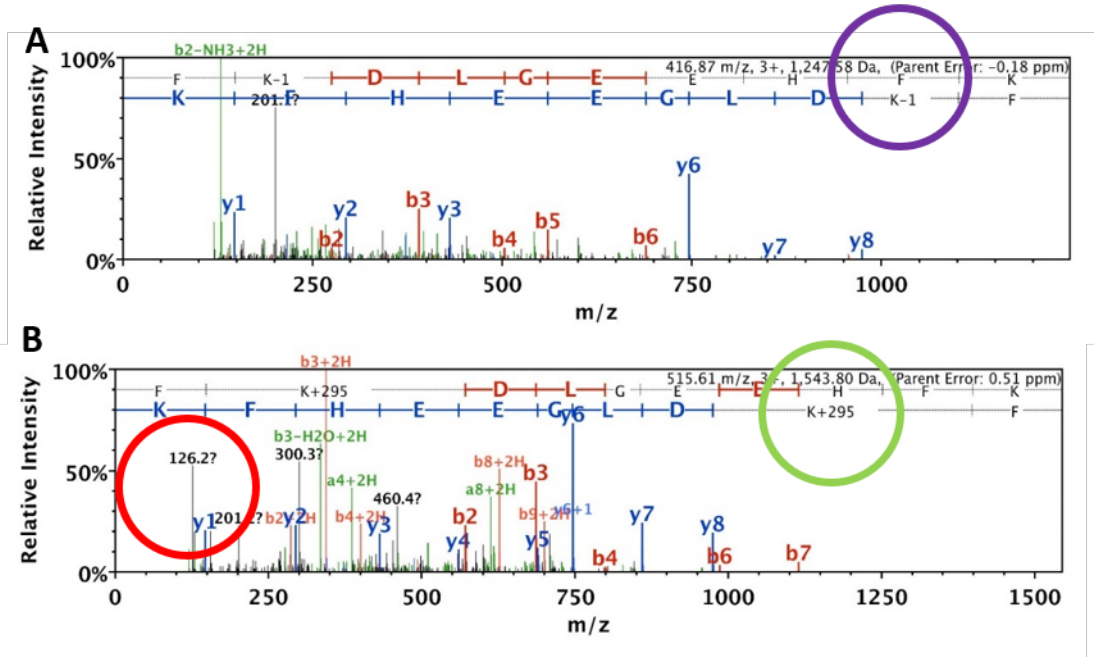

Figure 5.8: (A) A spectrum of peptide FKDLGEEHFK with an allysine modification on the first lysine. (B) A spectrum of the same peptide as A but the modified lysine is tagged with aminoxyTMT. The TMT reporter ion can be seen at 126.2 Da.

Whilst aminoxyTMT showed good tagging of carbonyl modifications, the enrichment was not effective, and the same aminoxyTMT tagged peptides could not consistently be identified between samples. Of the ten experiments performed using aminoxyTMT a total of 36 aminoxyTMT tagged peptides were identified and only 11 of these were identified in enriched samples (Table 5.2).

5.2.3 Biotin Hydrazide

As both DNPH and aminoxyTMT resulted in poor enrichment, work moved onto biotin-LC-hydrazide. Biotin is compatible with MS and so should give good quality MS/MS spectra. The enrichment process for biotin uses streptavidin, which binds with a high affinity to biotin, with a dissociation constant (K_d) of $4*10^{-14}$ M (Green, 1990), so the enrichment should be easily achieved. However, streptavidin is sticky, so will give a lot of background untagged proteins/peptides. The biotin hydrazide forms the hydrazone bond like the DNPH. To overcome the issues observed in DNPH with the reversibility of the hydrazone bond, sodium cyanoborohydride was used to reduce and stabilise the bond and make the reaction irreversible. To begin with, following the protocol established by Havelund *et al.* (2017), spin filtering was used to remove unreacted tag however, this proved ineffective and the beads for enrichment

probably became saturated with unreacted tag, so a methanol chloroform precipitation was used to remove excess tag, which proved more effective. Western blotting showed good labelling with biotin and good enrichment (Figure 5.9). There is an increased level of carbonylation in the MCO BSA over the control according to the biotin blot. However, there is the same band intensity in the MCO enrichment as the control enrichment. This is possibly because the beads reached their maximum capacity. The high binding affinity mentioned above caused issues with removing protein from the beads. Havelund *et al.* (2017) used water heated to 95^{o}C to elute proteins from beads, but this proved ineffective, and western blot analysis showed elution's were blank, but boiled beads showed protein. After this, beads were boiled for western blot analysis and on bead digest was used for MS analysis.

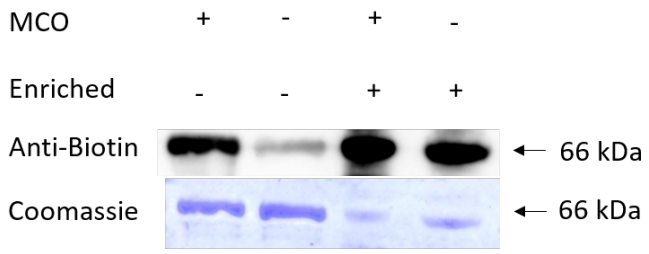

Figure 5.9: Western blot showing MCO and control BSA, input and enriched tagged with biotin-LC-hydrazide. There is an increase in signal in the MCO than the control, and an increase in signal in the enriched samples showing that the enrichment is working.

Work on biotin-LC-hydrazide continued using MS. Enriched samples were digested either on bead or in solution after elution from beads. A 52% coverage of BSA with 38 unmodified peptides was identified, using standard search criteria (fixed cysteine alkylation and variable oxidation of methionine). Biotin-LC-hydrazide has two reporter ions at m/z 227.1350 and m/z 340.1801, which are diagnostic of the tag fragmentation (Figure 5.10A). Therefore, a targeted MS approach was used, observation of these marker ions based on ions in shotgun MS2 then the precursor ion was to be collected again and a higher resolution scan in the Orbitrap was to be used to get a better spectrum. However, BSA has a peptide RHPYFYAPELLYYANK which fragments internally to give a PE fragment (m/z 227.0954) and a PEL fragment (m/z 340.1794) which have the same masses as the reporter ions, so the targeted MS runs mostly picked up this peptide (Figure 5.10B). This is a factor of the RHPYFYAPELLYYANK peptide in BSA and would not be an issue with complex mixtures which do not contain this peptide.

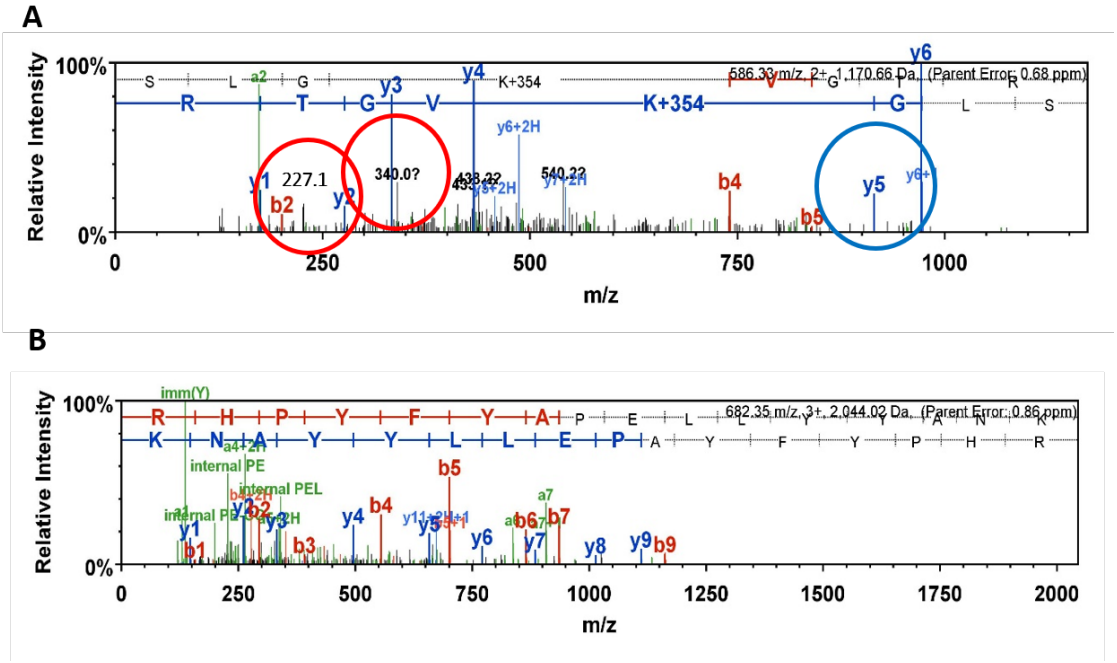

Figure 5.10: (A) A spectrum of the peptide SLGKVGTR with an allysine modification on the lysine and tagged with biotin-LC-hydrazide. The reporter ions can be seen at 227.1 and 340.0 m/z. (B) A spectrum of the peptide RHPYFYAPELLYYANK, this peptide contains the amino acids PEL, which will fragment internally to give a PE fragment of 227.1 m/z and PEL fragment of 340.1 m/z, which interfered with a targeted ion approach.

Despite the reduction of the hydrazone bond to stabilise the affinity tag, the hydrazine reaction does not go to completion, meaning there are still unreduced bonds which reverts back to the native carbonyl modification and the native carbonyl modifications were seen in the samples tagged with biotin-LC-hydrazide. In the experiment where one biotin tagged allysine modification in the MCO enriched sample was identified, 7 native allysine modifications and 15 native 2-amino-3-ketobutyric acid in the MCO input sample were also identified. Therefore stage tipping without any acid and removing acid from the loading column on the LC was performed, as was performed for the DNPH. ETD fragmentation on 3-6+ ions was also performed. However, this proved ineffective and no tagged peptides were identified. In the ten experiments performed using biotin-LC-hydrazide only one tagged peptide was identified (Table 5.2).

The aim was to use the tagging and enrichment process in Arabidopsis and maize to look for protein modification in response to oxidative damage. However,

living organisms including plants contain a certain amount of natural biotin which could interfere with the experiment (Alban *et al.*, 2000). To see if this would affect the enrichment, some *Arabidopsis thaliana* samples which had not been tagged with biotin-LC-hydrazide were run on a western blot, and no signal was observed. It was therefore decided that the levels of naturally occurring biotin would be low enough to not affect the experiments.

5.2.4 Alkoxyamine Biotin

Alkoxyamine-PEG_4-biotin forms the oxime bond, which is more stable than the hydrazone bond. According to Bollineni *et al.* (2013) the reaction is most favourable under low pH, so the reaction was performed at pH 4. Samples were tagged with alkoxyamine-PEG_4-biotin according to the manufacturer's guidelines and enriched with monomeric avidin beads in a spin column. Enrichment was performed at both the protein and the peptide level. The western blot shows good tagging and enrichment of carbonylated proteins (Figure 5.11), with an increase in signal in the MCO treated over the control in the input and the enrichment. A 16^{th} of the enrichment was loaded onto the western blot and the rest was taken to MS.

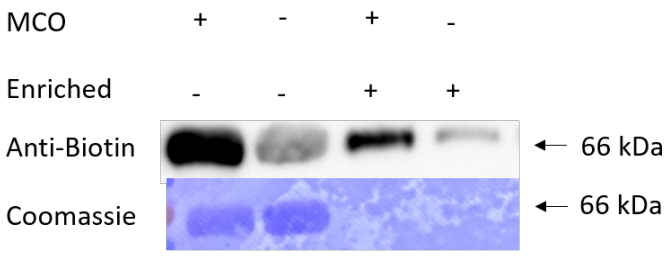

Figure 5.11: Western blot of MCO and control BSA, input and enriched tagged with alkoxyamine-PEG_4-biotin. There is an increased signal in the MCO than the control. $1/16^{th}$ of the enrichment was loaded onto the blot, so there is an increase in signal in the enriched sample, which shows that the enrichment is working.

Alkoxyamine-PEG_4-biotin samples were digested for MS analysis with an in solution digest. 60% coverage of BSA was obtained with 48 unmodified peptides identified, using standard search criteria (fixed cysteine alkylation and variable oxidation of methionine). No peptides tagged with alkoxyamine-PEG_4-biotin were identified using any of our search methods. Stage tipping under high pH conditions was performed, to combat the instability of the tag a low pH, however, this did not lead to the identification of any tagged peptides. In the RAW files the biotin reporter ion could be seen at 227.1 m/z, but these spectra could not be assigned to peptides using MASCOT or MQ and had poor fragmentation patterns when assessed by eye. In the six experiments performed with alkoxyamine-PEG_4-biotin no peptides were identified as being tagged with it.

To facilitate release of tagged proteins and peptides from the avidin beads, the tag alkoxyamine-PEG_4-SS-PEG_4-biotin was also tested, which has a disulfide bond which is easily broken via reduction. This makes it easier to remove the tag from the beads, because it can be removed by breaking the disulfide bond instead of breaking the biotin avidin bond, which is notoriously the strongest non covalent bond found in nature. Due to the removal of this tag by breaking the disulphide bond a western blot could not be performed, as the biotin element would still be attached to the beads and not the protein of interest.

Alkoxyamine-PEG_4-SS-PEG_4-biotin samples were digested for MS via in solution digest. 57% coverage of BSA was obtained with 49 unmodified peptides identified, using standard search criteria (fixed Cysteine alkylation and variable oxidation of methionine). When alkoxyamine-PEG_4-SS-PEG_4-biotin was analysed using MS, only one tagged peptide was identified in the input but no tagged peptides in the enrichment (Table 5.2) (Figure 5.12). The spectrum shows a good Y ion series with clear evidence for the modification being present on the lysine. There is however a high parent ion error of -1.9 ppm, which is within the 5 ppm tolerance of the Orbitrap, but on the high side. In the six experiments performed using alkoxyamine-PEG_4-SS-PEG_4-biotin only one peptide tagged was identified. Unfortunately, due to time constraints, further optimisation of carbonyl enrichment methods was discontinued.

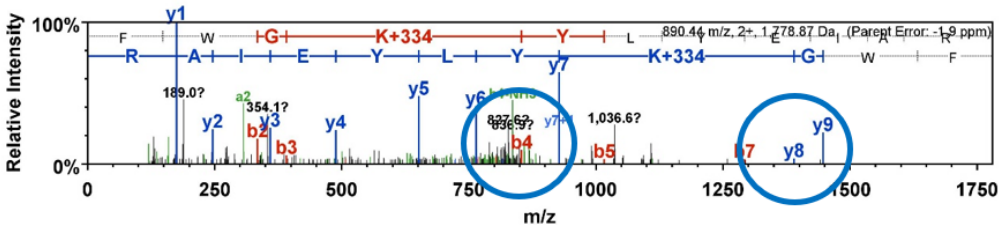

Figure 5.12: Spectrum showing an allysine modification tagged with alkoxyamine-PEG_4-SS-PEG_4-biotin. A clear Y ion series is shown, with good evidence to support the modification being present on the lysine. The modification can also be seen in the B ion series however, it is a much lower peak and is in the noise so could be a misassignment.

5.2.5 Summary of Mass Spectrometry Data for BSA

36 experiments using 5 different carbonyl reactive tags were performed for this chapter, results of all tagged peptides identified are shown below in Table 5.2 along with the tag used, the modification identified and the sample and replicate the results came from.

Table 5.2: Summary of the tagged peptides identified in BSA from all 36 experiments with different tags.

Tag	Modification	Sample Type	Peptide	Position
DNPH	2-amino-3-ketobutyric acid	MCO Input rep4	LVNEL**T**EFAK	71
DNPH	2-amino-3-ketobutyric acid	MCO Input rep4	AEFVEV**T**K	255
AminoxyTMT	Allysine	MCO Enriched rep7	F**K**DLGEEHFK	36
AminoxyTMT	Allysine	MCO Input rep3	F**K**DLGEEHFK	36
AminoxyTMT	Allysine	MCO Input rep6	F**K**DLGEEHFK	36
AminoxyTMT	Allysine	Control Input rep4	L**K**PDPNTLCDEFK	140
AminoxyTMT	Allysine	Control Input rep8	KFWG**K**YLYEIAR	160
AminoxyTMT	Allysine	MCO Input rep6	RHPYFYAPELLYYAN**K**	183
AminoxyTMT	Glutamic Semialdehyde (R)	MCO Input rep1	AWSVA**R**LSQK	241
AminoxyTMT	Allysine	Control Input rep4	FP**K**AEFVEVTK	248
AminoxyTMT	Allysine	Control Input rep5	FP**K**AEFVEVTK	248
AminoxyTMT	Allysine	MCO Enriched rep7	FP**K**AEFVEVTK	248
AminoxyTMT	Allysine	MCO Input rep4	FP**K**AEFVEVTK	248
AminoxyTMT	Allysine	MCO Input rep6	FP**K**AEFVEVTK	248
AminoxyTMT	Allysine	MCO Input rep9	FP**K**AEFVEVTK	248
AminoxyTMT	2-amino-3-ketobutyric acid	MCO Enrichment rep8	AEFVEV**T**K	255
AminoxyTMT	2-amino-3-ketobutyric acid	MCO Input rep4	AEFVEV**T**K	255
AminoxyTMT	Allysine	Control Enrichment rep1	AEFVEVT**K**LVTDLTK	256
AminoxyTMT	Allysine	Control Enrichment rep5	AEFVEVT**K**LVTDLTK	256
AminoxyTMT	Allysine	Control Enrichment rep10	AEFVEVT**K**LVTDLTK	256

Continued on next page

Table 5.2 – *Continued from previous page*

Tag	**Modification**	**Sample Type**	**Peptide**	**Position**
AminoxyTMT	Allysine	MCO Enrichment rep6	AEFVEVT**K**LVTDLTK	256
AminoxyTMT	Allysine	MCO Input rep4	AEFVEVT**K**LVTDLTK	256
AminoxyTMT	Allysine	MCO Input rep6	AEFVEVT**K**LVTDLTK	256
AminoxyTMT	Glutamic Semialdehyde (P)	Control Input rep10	M**P**CTEDYLSLILNR	270
AminoxyTMT	Allysine	Control Enrichment rep10	L**K**HLVDEPQNLIK	401
AminoxyTMT	Allysine	Control Input rep1	L**K**HLVDEPQNLIK	401
AminoxyTMT	Allysine	MCO Enriched rep7	L**K**HLVDEPQNLIK	401
AminoxyTMT	Allysine	MCO Input rep1	L**K**HLVDEPQNLIK	401
AminoxyTMT	Glutamic Semialdehyde (P)	Control Input rep4	HLVDE**P**QNLIK	407
AminoxyTMT	Allysine	Control Enrichment rep3	**K**VPQVSTPTLVEVSR	437
AminoxyTMT	Allysine	Control Input rep4	**K**VPQVSTPTLVEVSR	437
AminoxyTMT	Allysine	MCO Enrichment rep4	**K**VPQVSTPTLVEVSR	437
AminoxyTMT	Allysine	MCO Input rep4	**K**VPQVSTPTLVEVSR	437
AminoxyTMT	Allysine	MCO Input rep9	**K**VPQVSTPTLVEVSR	437
AminoxyTMT	2-amino-3-ketobutyric acid	MCO Input rep4	KVPQVS**T**PTLVEVSR	443
AminoxyTMT	Allysine	MCO Input rep4	**K**QTALVELLK	448
AminoxyTMT	2-amino-3-ketobutyric acid	MCO Enrichment rep8	LVVSTQ**T**ALA	604
AminoxyTMT	2-amino-3-ketobutyric acid	MCO Flow Through rep8	LVVSTQ**T**ALA	604
Biotin-LC-hydrazide	Allysine	MCO Enriched rep3	SLG**K**VGTR	455
Alkoxyamine-PEG_4-SS-PEG_4-biotin	Allysine	Control Input rep6	FWG**K**YLYEIAR	160

5.3 Conclusions

The 2,4-dinitrophenylhydrazine (DNPH) tagged samples showed poor enrichment possibly due to the protein A beads used for enrichment. 2 peptides were seen in the MS tagged with DNPH, this could be because the tag is unstable under low pH and no reduction was performed to stabilise the hydrazone bond, due to time constraints, therefore the hydrazone bond was not reduced with DNPH. Authors such as Kristensen *et al.* (2004) used DNPH to tag carbonyl modifications in a complex mixture and used anti-DNPH conjugated to protein A beads, and were able to successfully enrich for oxidative damage. However, their results could not be replicated in this work.

Aminoxy tandem mass tag (TMT) forms the oxime bond which is more stable than the hydrazone bond and does not require an extra stabilisation step. However, the enrichment was ineffective most likely because of the antibody's low affinity. This was the only tag that was consistently identified in the MS data, though rarely the same peptide in replicates. Whilst aminoxyTMT has previously been used by Afiuni-Zadeh *et al.* (2016) for tagging and enrichment of 4-hydroxynonenal (HNE) modifications, however, samples needed to be treated exogenously with HNE or modifications could not be identified. Whilst the TMT antibody showed effective enrichment, the modifications were in a higher abundance due to the treatment, and not the low abundance they are found in under oxidative stress conditions, making aminoxyTMT unsuitable for further work in complex plant protein mixtures.

Biotin-LC-hydrazide showed a good enrichment, since biotin-LC-hydrazide fragments give reporter ions which could be seen in tandem mass spectrometry (MS/MS), an MS method which would target peptides with the correct fragments could be set up, to collect more of those peptides for fragmentation in the Orbitrap. However, only one peptide tagged with biotin-LC-hydrazide was identified across all MS experiments, and the method set up to target reporter ions, only picked up peptides which had a PEL fragment and not any tagged peptides. Biotin-LC-hydrazide forms the hydrazone bond which is unstable under low pH conditions and whilst a reduction step was performed to stabilise the bond, this reaction does not go to completion. Authors such as Havelund *et al.* (2017) used biotin-LC-hydrazide with streptavidin to enrich for carbonyl modifications, however, they used a large number of modifications in the searches (seventeen), which will have increased their false discovery rate (FDR), they also used a python script to pull out any spectra which

did not contain the biotin reporter ions. Using Hevelunds methods for enrichment and elution with hot water, this method did not effectively elute proteins from the avidin beads, and their results could not be replicated in this study, their FDR is also high, making their results questionable.

Alkoxyamine-PEG_4-biotin showed a good enrichment of carbonyl modifications in the western blot. It forms the oxime bond which is more stable than the hydrazone bond. However, despite several different search parameters the tag could not be seen in the MS, despite being able to see the reporter ions in the RAW files. The use of this tag was discussed with a member of Ralf Holfmann and Maria Federova's groups. They are developing in-house software to identify candidate MS2 spectra, by pulling out spectra with the reporter ions for assignment, but due to time constraints their software could not be used in this study.

Alkoxyamine-PEG_4-SS-PEG_4-biotin showed one tagged peptide, and this was only seen in an input sample not enriched samples, so the enrichment, or the removal of the tag from the beads by reducing the disulphide bond was ineffective. Coffey and Gronert (2016) used alkoxyamine-PEG_4-SS-PEG_4-biotin to tag and enrich for proteins. However, their results could not be reproduced in this study in a single protein, and because the alkoxyamine-PEG_4-SS-PEG_4-biotin uses reduction of the disulfide bond to elute from the beads, using it to enrich for carbonyl modifications at the peptide level is tricky but not unmanageable, because the digestion process involves the reduction and alkylation of cysteine modifications, which would also reduce and alkylate the alkoxyamine-PEG_4-SS-PEG_4-biotin tag. Therefore, the digestion needs to be performed without the reduction and alkylation step which would lead to many missed cleavages, which need to be accounted for in analysis.

Whilst an increase in carbonylation in the metal catalysed oxidation (MCO) treated samples with all tags with the western blots was seen, the enrichments had various levels of success with each tag. However the same tagged peptides were not consistently identified in the MS with any of the five tags used. Therefore a consistent method of tagging and enrichment for carbonyl modifications was not able to be established.

Chapter 6

Discussion

6.0.1 Project Aims & Achievements

The aims of this research were to identify proteins which are affected by different stresses in plant tissues and look at the effect of these stresses on post translational modifications (PTMs). There have been many studies into the effect of drought on protein abundance in the crop plants wheat, rice, maize and barley. In the drought maize leaf dataset (Chapter 3), 1114 proteins were identified and quantified, of which 271 proteins significantly changed under the drought stress conditions, 94 proteins significantly increased in abundance under drought stress and 177 proteins were significantly decreased in abundance under drought stress. In the drought silk dataset (Chapter 3), 1338 proteins were identified, of which 405 were significantly different between the drought and the control, 215 proteins significantly increased in abundance and 190 were significantly decreased in abundance under drought conditions. The effect of drought stress on protein abundance and phosphorylation in maize was examined. Abscisic acid (ABA) response proteins are important for drought response and were both prominent in the literature and this dataset (Zhao *et al.*, 2016-1; Riccardi *et al.*, 1998; Zhao *et al.*, 2016-2). Late embryogenesis abundant (LEA) proteins are key biomarker for drought stress and increase stress tolerance by decreasing aggregation of proteins, LEA proteins were identified that decreasing in abundance in the silks data but in the literature they were prominent in other tissues (Mostafa *et al.*, 2010; Yang *et al.*, 2014; Ghatak *et al.*, 2016). As their name suggests, heat shock proteins (HSPs) are often reported to increase in abundance due to drought stress (Benesova *et al.*, 2012; Hajheidari *et al.*, 2006; Alvarez *et al.*, 2014) HSPs were observed as significantly increasing in abundance in the leaf and silk datasets. Adenosine triphosphate (ATP) synthase has also been shown to increase in abundance during drought stress (Faghani *et al.*, 2015; Ji *et al.*, 2012; Ashoub

et al., 2013), however in this dataset ATP synthase remained constant. Proteins which significantly changed in abundance were identified, not previously observed in the literature as responses to drought stress such as OSIGBa0147B06.5 protein, tryptophan aminotransferase-related protein 4 and methionine–tRNA ligase chloroplastic/mitochondrial which are involved in signalling, carbon sulfur lyase activity and respiration respectively.

Drought stress induces protein modifications, therefore the effect of drought stress on phosphorylation levels in maize were analysed. In the drought leaf phosphopeptide dataset (Chapter 3), 589 phosphopeptides were identified which mapped to 387 proteins, of which 61 phosphopeptides had statistically significant differences between the drought and the control. In the drought silk dataset (Chapter 3), 1553 phosphopeptides were identified that mapped to 981 proteins, of which 130 phosphopeptides were statistically significant between the drought and the control. The phosphopeptides identified as significantly changing in abundance to the best of my knowledge have not previously been identified in maize, however there are many similar phosphoproteins which have previously been identified in studies in other plants. Phosphoenolpyruvate carboxykinase proteins were prominent in this dataset and have previously been identified as phosphorylated in droughted maize (Zhengdan 958) (Hu *et al.*, 2015-1). Vu *et al.* (2016) looked at phosphorylation caused by drought stress in maize (B104) leaves however, similar phosphoproteins to them were not identified in the leaf dataset. Mitogen-activated protein kinases (MAPKs) are known to become phosphorylated during drought stress response, possibly phosphorylated by sucrose non-fermenting related protein kinase 2 (SnRK2) (Matsuoka *et al.*, 2015; Mitula *et al.*, 2015). In the droughted silk dataset mitogen-activated protein kinase kinase kinase (MAPKKK) protein were identified which increased in abundance and one which decreased in abundance, the latter contradicts data in the literature. MAPKs phosphorylation levels are known to increase in abundance during drought stress, because MAPKs are involved in drought response pathways and improve tolerance to drought (Ma *et al.*, 2017).

The herbicide methyl viologens (MV) effect on protein abundance in *Arabidopsis thaliana* and maize and the effect of MV on phosphorylation modifications was analysed. In the MV treated Arabidopsis soluble fraction dataset (Chapter 4), 1342 proteins were identified of which 158 proteins were identified as significantly increasing in abundance and 239 proteins significantly decreased in abundance during MV treatment. The most notable changes were the proteins associated with

oxidative stress response and antioxidant enzymes which significantly increased in abundance. It would be expected that proteins associated with oxidative stress to increase in abundance because MV kills plants by increasing reactive oxygen species (ROS) abundance and causing oxidative damage (Lascano *et al.*, 2012).

In the MV treated Arabidopsis membrane fraction dataset (Chapter 4), 879 proteins were identified of which 205 proteins significantly increased in abundance and 373 proteins significantly decreased in abundance during MV treatment. The most notable protein abundance changes were oxidative stress response proteins which significantly decreased in abundance, MV kills plants by causing oxidative damage (Lascano *et al.*, 2012), so it would be expected that these proteins would increase in abundance, however MV blocks antioxidant enzyme production, which could be causing a decrease in antioxidant abundance (Wei *et al.*, 2018). Proteins associated with photosynthesis were found to decrease in abundance in the dataset, since MVs mode of action is at photosystem I (PSI) during photosynthesis (Lascano *et al.*, 2012), it would be expected that proteins associated with photosynthesis would decrease in abundance. The data in this study suggests MV has an impact on ribosomal structure, as four of the most significantly increasing in abundance proteins were associated with ribosomal structure.

In the MV treated Arabidopsis soluble fraction (Chapter 4) 1082 phosphopeptides were identified of which 84 significantly changed in abundance. The phosphopeptides which significantly increased in abundance included fructose-bisphosphate aldolase 8 and the site identified is a known target of SnRKs (Wang *et al.*, 2013-2). MAPK 17 (T405, log2 fold change 1.20) and MAPK kinase 1 (T29, log2 fold change 1.09) were found to be increased in abundance under MV treatment, MAPKs are important in stress response pathways. Five phosphopeptide sites were identified which significantly decreased in abundance which to the best of my knowledge had not previously been identified, these were At4g13350 (NSP (nuclear shuttle protein)-interacting GTPase) (S217, log2 fold change -1.90), At3g60670 (PLATZ transcription factor family protein) (S3, log2 fold change -1.58), disease resistance protein (TIR-NBS-LRR class) family (T102, log2 fold change -1.49), chorismate synthase (S704, log2 fold change -1.36) and F3I6.9 protein (triadin) (T462, log2 fold change -1.12). The other phosphopeptide sites identified as stress responses were previously identified as response to nitrogen deprivation, DNA damage and response to drought stress (Roitinger *et al.*, 2015; Wang *et al.*, 2013-2; Bhaskara *et al.*, 2017; Umezawa *et al.*, 2013).

In the MV treated Arabidopsis membrane fraction (Chapter 4) 761 phosphopeptides were identified of which 42 significantly changed in abundance. Of the phosphopeptides which significantly increased in abundance ten were unique phosphopeptide sites not previously identified in the literature. Four phosphopeptide sites were identified which significantly decreased in abundance which to the best of my knowledge had not previously been identified, these were probable receptor-like protein kinase (Y462, log2 fold change -2.07), protein walls are thin 1 (S372, log2 fold change -0.92) and alkaline/neutral invertase CINV1 (S700 and S699, log2 fold change -5.39 and -5.25). The phosphopeptides which significantly decreased in abundance included phosphoinositide phospholipase C 2 (S280, log2 fold change -6.21) which is a known target of MAPKs (Rayapuram *et al.*, 2018), and phospholipids are known to be involved in signalling pathways and modified by stress (Xue *et al.*, 2009), and this site has previously been identified in a number of studies (Rayapuram *et al.*, 2018, 2014; Mattei *et al.*, 2016). The site identified on kinase with adenine nucleotide alpha hydrolases-like domain-containing protein (S547, log2 fold change -5.31) has been identified as a known target of MAPKs (Rayapuram *et al.*, 2018). Two phosphopeptides identified have been previously identified in response to stress (Roitinger *et al.*, 2015; Bhaskara *et al.*, 2017).

MV had a minimal effect on maize in this work (Chapter 4). This is most likely due to the waxy cuticles on maize leaves, which protects the plant, and the short treatment time. 1128 phosphopeptides were identified which mapped to 730 proteins in the 10 mM MV maize treatment, of which 19 phosphopeptides were found to significantly change during MV treatment. Whilst to the best of my knowledge none of the significantly changing phosphosites identified have previously been identified in the literature, the most notable phosphoproteins identified were MAPK (S219, log2 fold change -4.60), which is known to become phosphorylated under stress and ABA response pathways (Danquah *et al.*, 2014), and glutathione S-transferase (S2 S3, log2 fold change 6.22) which is known to be involved metabolic processing in cells and is a phosphorylation target of MAPKs (Lo *et al.*, 2004).

MV is known to cause oxidative damage, and in this work, western blots of Arabidopsis showed an increase in oxidative damage, as measured by protein carbonylation detected using the hydrazine 2,4-dinitrophenylhydrazine (DNPH). However, the mass spectrometry (MS) results showed the same levels of carbonyl modifications in the treated as the control. Therefore an attempt to develop a method

for tagging and enriching carbonylation in complex mixtures was made (Chapter 5). A method for tagging and enrichment of carbonyl modifications was attempted in bovine serum albumin (BSA), using five different tags, using both the hydrazone and oxime bond, which have different chemistries. This approach encountered problems including the tag stability, the hydrazone bond is unstable at low pH, which meant the tag was removed by the low pH buffers used for MS. Whilst the oxime bond was more stable, the enrichment efficiency still posed problems with antibody affinity and removing tags from beads and the same tagged peptides were not consistently identified in the MS. An effective tagging and enrichment strategy was not able to be established during this project.

6.0.2 Carbonyl Detection Using Mass Spectrometry

Carbonyl modifications could not be reliably identified on BSA using MS. Other groups have used in house scripts to pull out spectra containing reporter ions for tags, and then searching those spectra against a database using MASCOT, MaxQuant (MQ) or Sequest (Havelund *et al.*, 2017). This decreases the search space and allows more tagged peptides to be assigned. Some published algorithms were tried on the datasets but, due to time constraints, was not able to make them work with this data.

Peptides will fragment in different ways depending on the size of the peptide, the amino acid (AA) sequence and the fragmentation method used. Modifications and tags also affect the way a peptide fragments, changing both the mass to charge ratio (m/z) and intensity of fragments. Modifications can be added to databases to combat the change in m/z however, conventual algorithms cannot combat the change in fragment intensity caused by the addition of tags, leading to misassignment of peptides (Barton and Whittaker, 2009). Data driven tools such as MS^2 Peak Intensity Prediction (MS^2PIP) have been developed to predict fragment ion intensities (Degroeve and Martens, 2013). MS^2PIP uses all data available in the Proteomics Identifications Database (PRIDE) archive and applies machine learning to predict peptide fragment intensities. Tools like MS^2PIP give more accurate fragmentation data, allowing for more accurate assignment of modified and tagged peptides. More recently MS^2PIPs algorithm has been updated to improve assignment of tandem mass tag (TMT) tagged peptides, because isobaric tags such as isobaric tag for absolute and relative quantification (iTRAQ) and TMT heavily alter fragmentation patterns and ion intensities of peptides (Gabriels *et al.*, 2019). The tags used in the carbonylation experiments will also have altered fragmentation patterns, and tools such as MS^2PIP could help to better assign tagged peptides.

6.0.3 Conclusions & Further Work

If there had been more time on this project, to test the functional roles of some of the proteins identified, overexpression and knockout lines of proteins could have been used. Knock out and overexpressing line of proteins known to be affected by the stress treatments could have been used to see how the plant responds to stress responses with the overexpression and knock out of these proteins. This would give a better insight into how important the protein is to the plants stress response.

In the drought stressed maize plants knockout lines of SnRK2 and protein phosphatase 2C (PP2C) could have been used if there was more time. Without SnRK2 the plants should be unable to close stomata in response to stress, making the plant less tolerant to drought stress. An overexpressing line of SnRK2 would also theoretically make the plant more tolerant to drought stress. Song *et al.* (2016) used an overexpressing SnRK2 line in Arabidopsis to look at salt stress tolerance, and found that overexpression enhanced stress tolerance. To the best of my knowledge, SnRK2 knockout lines have not been experimented on in maize. However, SnRK2s are affected by an upstream pathway, PP2C binds to SnRK2, preventing SnRK2s autophosphorylation. Under drought stress conditions PP2C binds to ABA receptors, freeing SnRK2 and allowing downstream signalling causing stomatal closure. A knockout line of PP2C could cause SnRK2 to phosphorylate without drought stress signalling, showing the importance of PP2C in the drought response signalling. An overexpressing line of PP2C could also lead to SnRK2 not being released under drought stress conditions, leading to stomata remaining open during drought stress or oversensitivity to drought stress. Brock *et al.* (2010) used a PP2C knockout line in Arabidopsis and found knocking out PP2C caused stomatal closure under non stress conditions, however, the PP2C overexpression line was unstable, so they were not able to analyse it. Sugimoto *et al.* (2014) used an overexpressing line of PP2C in Arabidopsis and found this made plants more sensitive to drought stress. To the best of my knowledge PP2C knockout or overexpression lines have not been established in maize.

To expand the phosphopeptide work noncanonical phosphorylation sites could have been analysed. Hardman *et al.* (2017) used strong anion exchange (SAX) chromatography (UPAX) to enrich for phosphorylation sites on histidine, arginine, lysine, aspartate, glutamate and cysteine. These sites are acid labile, meaning the conventional enrichment techniques using acidic conditions to bind to the titanium dioxide (TiO_2) beads is not suitable for these phosphorylation sites. UPAX has

been used to analyse noncanonical phosphorylation sites in human proteins (Hardman *et al.*, 2019), but to the best of my knowledge no work has been done in plants.

Carbonylation is an important biomarker for oxidative damage, but detecting it using MS cased many problems during this project. If a tagging and enrichment method could have been established in BSA, work could have moved to more complex mixtures, to pull out carbonyl modifications in MV treated Arabidopsis, which is known to cause oxidative damage, and then used the method to analyse oxidative damage in drought treated maize, to see if a link could be established between carbonylation, drought stress and yield loss. In the literature antioxidants were found to increase in abundance during drought, which could indicate an increase in oxidative damage during drought (Ford *et al.*, 2011; Qin *et al.*, 2014; Vitamvas *et al.*, 2015), however an increase in antioxidant enzymes during drought was not seen in this data.

Bibliography

Abas, L. and Luschnig, C. (2010), 'Maximum yields of microsomal-type membranes from small amounts of plant material without requiring ultracentrifugation', *Analytical Biochemistry* **401**(2), 217–227.

Aebersold, R., Agar, J. N., Amster, I. J., Baker, M. S., Bertozzi, C. R., Boja, E. S., Costello, C. E., Cravatt, B. F., Fenselau, C., Garcia, B. A., Ge, Y., Gunawardena, J., Hendrickson, R. C., Hergenrother, P. J., Huber, C. G., Ivanov, A. R., Jensen, O. N., Jewett, M. C., Kelleher, N. L., Kiessling, L. L., Krogan, N. J., Larsen, M. R., Loo, J. A., Ogorzalek Loo, R. R., Lundberg, E., MacCoss, M. J., Mallick, P., Mootha, V. K., Mrksich, M., Muir, T. W., Patrie, S. M., Pesavento, J. J., Pitteri, S. J., Rodriguez, H., Saghatelian, A., Sandoval, W., Schluter, H., Sechi, S., Slavoff, S. A., Smith, L. M., Snyder, M. P., Thomas, P. M., Uhlen, M., Van Eyk, J. E., Vidal, M., Walt, D. R., White, F. M., Williams, E. R., Wohlschlager, T., Wysocki, V. H., Yates, N. A., Young, N. L. and Zhang, B. (2018), 'How many human proteoforms are there?', *Nat Chem Biol* **14**(3), 206–214.

Afiuni-Zadeh, S., Rogers, J. C., Snovida, S. I., Bomgarden, R. D. and Griffin, T. J. (2016), 'Aminoxytmt: A novel multi-functional reagent for characterization of protein carbonylation', *Biotechniques* **60**(4), 186–196.

Agrawal, L., Gupta, S., Mishra, S. K., Pandey, G., Kumar, S., Chauhan, P. S., Chakrabarty, D. and Nautiyal, C. S. (2016), 'Elucidation of complex nature of peg induced drought-stress response in rice root using comparative proteomics approach', *Front Plant Sci* **7**, 1466–1484.

Alban, C., Job, D. and Douce, R. (2000), 'Biotin metabolism in plants', *Annual review of plant biology* **51**(1), 17–47.

Alexandersson, E., Saalbach, G., Larsson, C. and Kjellbom, P. (2004), 'Arabidopsis plasma membrane proteomics identifies components of transport, signal transduction and membrane trafficking', *Plant Cell Physiol* **45**(11), 1543–1556.

Ali, G. M. and Komatsu, S. (2006), 'Proteomic analysis of rice leaf sheath during drought stress', *Journal of Proteome Research* **5**(2), 396–403.

Alqurashi, M., Chiapello, M., Bianchet, C., Paolocci, F., Lilley, K. S. and Gehring, C. (2018), 'Early responses to severe drought stress in the arabidopsis thaliana cell suspension culture proteome', *Proteomes* **6**(4), 38–55.

Alvarez, S., Roy Choudhury, S. and Pandey, S. (2014), 'Comparative quantitative proteomics analysis of the aba response of roots of drought-sensitive and drought-tolerant wheat varieties identifies proteomic signatures of drought adaptability', *J Proteome Res* **13**(3), 1688–701.

Andolfo, G. and Ercolano, M. R. (2015), 'Plant innate immunity multicomponent model', *Front Plant Sci* **6**, 987–993.

Apel, K. and Hirt, H. (2004), 'Reactive oxygen species: metabolism, oxidative stress, and signal transduction', *Annu Rev Plant Biol* **55**, 373–99.

Appel, R. D. and Bairoch, A. (2004), 'Post-translational modifications: A challenge for proteomics and bioinformatics', *Protemics* **4**(6), 1525–1526.

Ardito, F., Giuliani, M., Perrone, D., Troiano, G. and Lo Muzio, L. (2017), 'The crucial role of protein phosphorylation in cell signaling and its use as targeted therapy (review)', *Int J Mol Med* **40**(2), 271–280.

Asada, K. (1999), 'The water-water cycle in chloroplasts: Scavenging of active oxygens and dissipation of excess photons', *Annu Rev Plant Physiol Plant Mol Biol* **50**(1), 601–39.

Ashoub, A., Beckhaus, T., Berberich, T., Karas, M. and Bruggemann, W. (2013), 'Comparative analysis of barley leaf proteome as affected by drought stress', *Planta* **237**(3), 771–81.

Ashraf, M. and Foolad, M. R. (2007), 'Roles of glycine betaine and proline in improving plant abiotic stress resistance', *Environmental and Experimental Botany* **59**(2), 206–216.

Atkinson, N. J. and Urwin, P. E. (2012), 'The interaction of plant biotic and abiotic stresses: from genes to the field', *J Exp Bot* **63**(10), 3523–43.

Avendaño, C. and Menéndez, J. C. (2008), 'Chapter 9 - drugs that inhibit signalling pathways for tumor cell growth and proliferation', *Medical Chemistry of Anticancer Drugs* pp. 251–305.

Avramova, V., AbdElgawad, H., Zhang, Z., Fotschki, B., Casadevall, R., Vergauwen, L., Knapen, D., Taleisnik, E., Guisez, Y., Asard, H. and Beemster, G. T. (2015), 'Drought induces distinct growth response, protection, and recovery mechanisms in the maize leaf growth zone', *Plant Physiol* **169**(2), 1382–96.

Bachor, R., Waliczek, M., Stefanowicz, P. and Szewczuk, Z. (2019), 'Trends in the design of new isobaric labeling reagents for quantitative proteomics', *Molecules* **24**(4), 701–720.

Bantscheff, M., Lemeer, S., Savitski, M. M. and Kuster, B. (2012), 'Quantitative mass spectrometry in proteomics: critical review update from 2007 to the present', *Anal Bioanal Chem* **404**(4), 939–65.

Barber, K. W. and Rinehart, J. (2018), 'The abcs of ptms', *Nat Chem Biol* **14**(3), 188–192.

Barford, D. (1996), 'Molecular mechanisms of the protein serine/threonine phosphatases', *Trends in Biochemical Sciences* **21**(11), 407–412.

Barlow, K. M., Christy, B. P., O'Leary, G. J., Riffkin, P. A. and Nuttall, J. G. (2015), 'Simulating the impact of extreme heat and frost events on wheat crop production: A review', *Field Crops Research* **171**, 109–119.

Barton, S. J. and Whittaker, J. C. (2009), 'Review of factors that influence the abundance of ions produced in a tandem mass spectrometer and statistical methods for discovering these factors', *Mass Spectrometry Reviews* **28**(1), 177–187.

Benesova, M., Hola, D., Fischer, L., Jedelsky, P. L., Hnilicka, F., Wilhelmova, N., Rothova, O., Kocova, M., Prochazkova, D., Honnerova, J., Fridrichova, L. and Hnilickova, H. (2012), 'The physiology and proteomics of drought tolerance in maize: early stomatal closure as a cause of lower tolerance to short-term dehydration?', *PLoS One* **7**(6), 1–17.

Benjamini, Y. and Hochberg, Y. (1995), 'Controlling the false discovery rate: a practical and powerful approach to multiple testing', *J R Stat Soc Series B* **57**(1), 289–300.

Bennet, J. (1979), 'Chloroplast phosphoproteins: Phosphorylation of polypeptides of the light-harvesting chlorophyll protein complex', *J Biol Chem* **99**(1), 133–137.

Bennett, J. (1979), 'Chloroplast phosphoproteins. the protein kinase of thylakoid membranes is light-dependent', *FEBS Letters* **103**(2), 342–344.

Benschop, J. J., Mohammed, S., O'Flaherty, M., Heck, A. J., Slijper, M. and Menke, F. L. (2007), 'Quantitative phosphoproteomics of early elicitor signaling in arabidopsis', *Mol Cell Proteomics* **6**(7), 1198–214.

Besant, P. G. and Attwood, P. V. (2012), 'Histone h4 histidine phosphorylation: kinases, phosphatases, liver regeneration and cancer', *Biochem Soc Trans* **40**(1), 290–3.

Bhaskara, G. B., Wen, T. N., Nguyen, T. T. and Verslues, P. E. (2017), 'Protein phosphatase 2cs and microtubule-associated stress protein 1 control microtubule stability, plant growth, and drought response', *Plant Cell* **29**(1), 169–191.

Biringer, R. G., Horner, J. A., Viner, R., Hühmer, A. F. R. and Specht, A. (2011), 'Quantitation of tmt-labeled peptides using higher-energy collisional dissociation on the velos pro ion trap mass spectrometer'.

Bohan, D. A., Boffey, C. W., Brooks, D. R., Clark, S. J., Dewar, A. M., Firbank, L. G., Haughton, A. J., Hawes, C., Heard, M. S., May, M. J., Osborne, J. L., Perry, J. N., Rothery, P., Roy, D. B., Scott, R. J., Squire, G. R., Woiwod, I. P. and Champion, G. T. (2005), 'Effects on weed and invertebrate abundance and diversity of herbicide management in genetically modified herbicide-tolerant winter-sown oilseed rape', *Proc Biol Sci* **272**(1562), 463–74.

Bolgar, M., Yang, C. and Gaskell, S. (1996), 'First direct evidence for lipid/protein conjugation in oxidized human low density lipoprotein', *J Biol Chem* **271**(45), 27999–28001.

Bollineni, R. C., Fedorova, M. and Hoffmann, R. (2013), 'Qualitative and quantitative evaluation of derivatization reagents for different types of protein-bound carbonyl groups', *Analyst* **138**(17), 5081–8.

Bollineni, R., Fedorova, M. and Hoffmann, R. (2011-2), 'Identification of carbonylated peptides by tandem mass spectrometry using a precursor ion-like scan in negative ion mode', *J Proteomics* **74**(11), 2351–9.

Bollineni, R., Hoffmann, R. and Fedorova, M. (2011-1), 'Identification of protein carbonylation sites by two-dimensional liquid chromatography in combination with maldi- and esi-ms', *J Proteomics* **74**(11), 2338–50.

Boudsocq, M., Droillard, M. J., Barbier-Brygoo, H. and Lauriere, C. (2007), 'Different phosphorylation mechanisms are involved in the activation of sucrose non-

fermenting 1 related protein kinases 2 by osmotic stresses and abscisic acid', *Plant Mol Biol* **63**(4), 491–503.

Bradford, M. M. (1976), 'A rapid and sensitive method for the quantitation of microgram quantities of protein utilizing the principle of protein-dye binding', *Anal Biochem* **72**(1-2), 248–254.

Brock, A. K., Willmann, R., Kolb, D., Grefen, L., Lajunen, H. M., Bethke, G., Lee, J., Nurnberger, T. and Gust, A. A. (2010), 'The arabidopsis mitogen-activated protein kinase phosphatase pp2c5 affects seed germination, stomatal aperture, and abscisic acid-inducible gene expression', *Plant Physiol* **153**(3), 1098–111.

Bromilow, R. H. (2003), 'Paraquat and sustainable agriculture', *Pest Manag Sci* **60**, 340–349.

Budak, H., Akpinar, B. A., Unver, T. and Turktas, M. (2013), 'Proteome changes in wild and modern wheat leaves upon drought stress by two-dimensional electrophoresis and nanolc-esi–ms/ms', *Plant Molecular Biology* **83**(1), 89–103.

Buhler, D. D., Swisher, B. A. and Burnside, O. C. (1985), 'Behavior of 14c-haloxyfop-methyl in intact plants and cell cultures', *Weed Science* **33**(3), 291–299.

Burton, J., Gronwald, J., Somers, D., Connelly, J., Gengenbach, B. and Wyse, D. (1987), 'Inhibition of plant acetyl-coenzyme a carboxylase by the herbicides sethoxydim and haloxyfop', *Biochem Biophys Res Commun* **148**(3), 1039–1044.

Cargnello, M. and Roux, P. P. (2011), 'Activation and function of the mapks and their substrates, the mapk-activated protein kinases', *Microbiology and Molecular Biology Reviews* **75**(1), 50–83.

Carter, M. and Shieh, J. (2015), *Biochemical Assays and Intracellular Signaling*, Guide to Research Techniques in Neuroscience, Academic Press.

Caruso, G., Cavaliere, C., Foglia, P., Gubbiotti, R., Samperi, R. and Laganà, A. (2009), 'Analysis of drought responsive proteins in wheat (triticum durum) by 2d-page and maldi-tof mass spectrometry', *Plant Science* **177**(6), 570–576.

Cello, F. D., Bevivino, A., Chiarini, L., Fani, R., Paffetti, D., Tabacchioni, S. and Dalmastri, C. (1997), 'Biodiversity of a burkholderia cepacia population isolated from the maize rhizosphere at different plant growth stages', *Appl Environ Microbiol.* **63**(11), 4485–4493.

Chang, I. F., Hsu, J. L., Hsu, P. H., Sheng, W. A., Lai, S. J., Lee, C., Chen, C. W., Hsu, J. C., Wang, S. Y., Wang, L. Y. and Chen, C. C. (2012), 'Comparative phosphoproteomic analysis of microsomal fractions of arabidopsis thaliana and oryza sativa subjected to high salinity', *Plant Sci* **185**, 131–142.

Chaves, M. M., Flexas, J. and Pinheiro, C. (2009), 'Photosynthesis under drought and salt stress: regulation mechanisms from whole plant to cell', *Ann Bot* **103**(4), 551–60.

Chavez, J. D., Bisson, W. H. and Maier, C. S. (2010), 'A targeted mass spectrometry-based approach for the identification and characterization of proteins containing alpha-aminoadipic and gamma-glutamic semialdehyde residues', *Anal Bioanal Chem* **398**(7), 2905–14.

Chavez, J., Wu, J., Han, B., Chung, W.-G. and Maier, C. S. (2006), 'New role for an old probe: Affinity labeling of oxylipid protein conjugates by n′-aminooxymethylcarbonylhydrazino d-biotin', *Anal Chem* **78**(19), 6847–6854.

Chen, Y., Zhang, J., Xing, G. and Zhao, Y. (2009), 'Mascot-derived false positive peptide identifications revealed by manual analysis of tandem mass spectra', *J Proteome Res* **8**(6), 3141–7.

Cheng, L., Pisitkun, T., Knepper, M. A. and Hoffert, J. D. (2016), 'Peptide labeling using isobaric tagging reagents for quantitative phosphoproteomics', *Methods Mol Biol* **1355**, 53–70.

Cheng, Z., Dong, K., Ge, P., Bian, Y., Dong, L., Deng, X., Li, X. and Yan, Y. (2015), 'Identification of leaf proteins differentially accumulated between wheat cultivars distinct in their levels of drought tolerance', *PLoS One* **10**(5), 1–20.

Chinnusamy, V., Zhu, J. and Zhu, J. K. (2007), 'Cold stress regulation of gene expression in plants', *Trends Plant Sci* **12**(10), 444–51.

Chung, W. G., Miranda, C. L. and Maier, C. S. (2008), 'Detection of carbonyl-modified proteins in interfibrillar rat mitochondria using n'-aminooxymethylcarbonylhydrazino-d-biotin as an aldehyde/keto-reactive probe in combination with western blot analysis and tandem mass spectrometry', *Electrophoresis* **29**(6), 1317–24.

Coffey, C. M. and Gronert, S. (2016), 'A cleavable biotin tagging reagent that enables the enrichment and identification of carbonylation sites in proteins', *Anal Bioanal Chem* **408**(3), 865–74.

Cohen, P. (2000), 'The regulation of protein function by multisite phosphorylation–a 25 year update.', *Trends in Biochemical Sciences* **25**(12), 596–601.

Cohen, P. (2002), 'The origins of protein phosphorylation', *Nat. Cell Biol* **4**(5), 127–30.

Colombo, G., Clerici, M., Garavaglia, M. E., Giustarini, D., Rossi, R., Milzani, A. and Dalle-Donne, I. (2016), 'A step-by-step protocol for assaying protein carbonylation in biological samples', *J Chromatogr B Analyt Technol Biomed Life Sci* **1019**, 178–90.

Comisarow, M. B. and Marshall, A. G. (1974), 'Fourier transform ion cyclotron resonance spectroscopy', *Chem. Phys. Lett* **25**(2), 282–283.

Cox, J., Hein, M. Y., Luber, C. A., Paron, I., Nagaraj, N. and Mann, M. (2014), 'Accurate proteome-wide label-free quantification by delayed normalization and maximal peptide ratio extraction, termed maxlfq', *Mol Cell Proteomics* **13**(9), 2513–26.

Cox, J. and Mann, M. (2008), 'Maxquant enables high peptide identification rates, individualized p.p.b.-range mass accuracies and proteome-wide protein quantification', *Nat Biotechnol* **26**(12), 1367–72.

Cox, J. and Mann, M. (2012), '1d and 2d annotation enrichment: a statistical method integrating quantitative proteomics with complementary high-throughput data', *BMC Bioinformatics* **13**(16), 12–23.

Cox, J., Neuhauser, N., Michalski, A., Scheltema, R. A., Olsen, J. V. and Mann, M. (2011), 'Andromeda: a peptide search engine integrated into the maxquant environment', *J Proteome Res* **10**(4), 1794–805.

Creasy, D. M. and Cottrell, J. S. (2002), 'Error tolerant searching of uninterpreted tandem mass spectrometry data', *Proteomics* **2**(10), 1426–1434.

Cui, F., Brosché, M., Shapiguzov, A., He, X.-Q., Vainonen, J. P., Leppälä, J., Trotta, A., Kangasjärvi, S., Salojärvi, J., Kangasjärvi, J. and Overmyer, K. (2018), 'Methyl viologen can affect mitochondrial function in arabidopsis', *BioRxiv* p. 436543.

Cutler, S. R., Rodriguez, P. L., Finkelstein, R. R. and Abrams, S. R. (2010), 'Abscisic acid: emergence of a core signaling network', *Annu Rev Plant Biol* **61**, 651–79.

Cvetesic, N., Semanjski, M., Soufi, B., Krug, K., Gruic-Sovulj, I. and Macek, B. (2016), 'Proteome-wide measurement of non-canonical bacterial mistranslation by quantitative mass spectrometry of protein modifications', *Sci Rep* **6**, 28631–28644.

Dalle-Donne, I., Carini, M., Orioli, M., Vistoli, G., Regazzoni, L., Colombo, G., Rossi, R., Milzani, A. and Aldini, G. (2009), 'Protein carbonylation: 2,4-dinitrophenylhydrazine reacts with both aldehydes/ketones and sulfenic acids', *Free Radic Biol Med* **46**(10), 1411–9.

Dami, I. and Hughes, H. G. (1997), 'Effects of peg-induced water stress on in vitro hardening of 'valiant' grape', *Plant Cell* **42**(2), 97–101.

Danquah, A., de Zelicourt, A., Colcombet, J. and Hirt, H. (2014), 'The role of aba and mapk signaling pathways in plant abiotic stress responses', *Biotechnol Adv* **32**(1), 40–52.

Darling, A. L. and Uversky, V. N. (2018), 'Intrinsic disorder and posttranslational modifications: The darker side of the biological dark matter', *Front Genet* **9**, 158–176.

Davletova, S., Schlauch, K., Coutu, J. and Mittler, R. (2005), 'The zinc-finger protein zat12 plays a central role in reactive oxygen and abiotic stress signaling in arabidopsis', *Plant Physiol* **139**(2), 847–56.

Davy, A. and Perrow, M. (2002), 'Establishment and manipulation of plant populations and communities in terrestrial systems', *Handbook of ecological restoration. Volume 1: Principles of restoration Cambridge University Press, Cambridge, United Kingdom.* p. 223–241.

Debska, K., Krasuska, U., Budnicka, K., Bogatek, R. and Gniazdowska, A. (2013), 'Dormancy removal of apple seeds by cold stratification is associated with fluctuation in h2o2, no production and protein carbonylation level', *J Plant Physiol* **170**(5), 480–8.

Degroeve, S. and Martens, L. (2013), 'Ms2pip: a tool for ms/ms peak intensity prediction', *Bioinformatics* **29**(24), 3199–203.

Demirevska, K., Zasheva, D., Dimitrov, R., Simova-Stoilova, L., Stamenova, M. and Feller, U. (2009), 'Drought stress effects on rubisco in wheat: changes in the rubisco large subunit', *Acta Physiologiae Plantarum* **31**(6), 1129–1138.

Dephoure, N., Gould, K. L., Gygi, S. P. and Kellogg, D. R. (2013), 'Mapping and analysis of phosphorylation sites: a quick guide for cell biologists', *Mol Biol Cell* **24**(5), 535–42.

Ding, Z. S., Sun, X. F., Huang, S. H., Zhou, B. Y. and Zhao, M. (2015), 'Response of photosynthesis to short-term drought stress in rice seedlings overexpressing c4 phosphoenolpyruvate carboxylase from maize and millet', *Photosynthetica* **53**(4), 481–488.

Doorenbos, J., K. A. (1979), 'Yield response to water', *Irrigation and Drainage Paper 33. FAO, United Nations, Rome* p. 176.

Drabik, A., Bodzoń-Kułakowska, A. and Silberring, J. (2016), *Gel Electrophoresis*, Elsevier, pp. 115–143.

Du, W., Lin, H., Chen, S., Wu, Y., Zhang, J., Fuglsang, A. T., Palmgren, M. G., Wu, W. and Guo, Y. (2011), 'Phosphorylation of sos3-like calcium-binding proteins by their interacting sos2-like protein kinases is a common regulatory mechanism in arabidopsis', *Plant Physiology* **156**(4), 2235–2243.

Duan, G. and Walther, D. (2015), 'The roles of post-translational modifications in the context of protein interaction networks', *PLoS Comput Biol* **11**(2), 1–23.

Duke, S. O. (1990), 'Overview of herbicide mechanisms of action', *Environmental Health Perspectives* **87**, 263–271.

Duke, S. O. and Abbas, H. K. (1995), 'Natural products with potential use as herbicides', *ACS Symposium Series* **582**, 348–362.

Duke, S. O. and Kenyon, W. H. (1988), 'Polycyclic alkanoic acids', *Herbicides – Chemistry, Degradation, and Mode of Action* **3**, 71–116.

Easterling, D. R., Meehl, G. A., Parmesan, C., Changnon, S. A., Karl, T. R. and Mearns, L. O. (2000), 'Climate extremes: Observations, modeling, and impacts', *Science* **289**(5487), 2068–2074.

Ephritikhine, G., Ferro, M. and Rolland, N. (2004), 'Plant membrane proteomics', *Plant Physiol Biochem* **42**(12), 943–62.

Faghani, E., Gharechahi, J., Komatsu, S., Mirzaei, M., Khavarinejad, R. A., Najafi, F., Farsad, L. K. and Salekdeh, G. H. (2015), 'Comparative physiology and proteomic analysis of two wheat genotypes contrasting in drought tolerance', *J Proteomics* **114**, 1–15.

Fan, F., Williams, H. J., Boyer, J. G., Graham, T. L., Zhao, H., Lehr, R., Qi, H., Schwartz, B., Raushel, F. M. and Meek, T. D. (2012), 'On the catalytic mechanism of human atp citrate lyase', *Biochemistry* **51**(25), 5198–211.

Fan, S., Meng, Y., Song, M., Pang, C., Wei, H., Liu, J., Zhan, X., Lan, J., Feng, C., Zhang, S. and Yu, S. (2014), 'Quantitative phosphoproteomics analysis of nitric oxide-responsive phosphoproteins in cotton leaf', *PLoS One* **9**(4), 1–13.

Fan, X., Xu, J., Lavoie, M., Peijnenburg, W., Zhu, Y., Lu, T., Fu, Z., Zhu, T. and Qian, H. (2018), 'Multiwall carbon nanotubes modulate paraquat toxicity in arabidopsis thaliana', *Environ Pollut* **233**, 633–641.

Fedorova, M., Bollineni, R. C. and Hoffmann, R. (2014), 'Protein carbonylation as a major hallmark of oxidative damage: update of analytical strategies', *Mass Spectrom Rev* **33**(2), 79–97.

Fedtke, C. and Trebst, A. (1987), 'Advances in understanding herbicide modes of action. in: Pesticide science and biotechnology', *Blackwell Scientific Publications* pp. 161–168.

Fenaille, F., Parisod, V., Tabet, J. C. and Guy, P. A. (2005), 'Carbonylation of milk powder proteins as a consequence of processing conditions', *Proteomics* **5**(12), 3097–104.

Fenaille, F., Tabet, J. and Guy, P. (2004), 'Identification of 4-hydroxy-2-nonenal-modified peptides within unfractionated digests using matrix-assisted laser desorption/ionization time-of-flight mass spectrometry', *Anal Chem* **76**(4), 867–873.

Fenn, J., Mann, M., Meng, C., Wong, S. and Whitehouse, C. (1989), 'Electrospray ionization for mass spectrometry of large biomolecules', *Science* **246**(4926), 64–71.

Ferries, S., Perkins, S., Brownridge, P. J., Campbell, A., Eyers, P. A., Jones, A. R. and Eyers, C. E. (2017), 'Evaluation of parameters for confident phosphorylation site localization using an orbitrap fusion tribrid mass spectrometer', *J Proteome Res* **16**(9), 3448–3459.

Ficarro, S., McCleland, M., Stukenberg, P., Burke, D., Ross, M., Shabanowitz, J., Hunt, D. and White, F. (2002), 'Phosphoproteome analysis by mass spectrometry and its application to saccharomyces cerevisiae', *Nat Biotechnol* **20**(3), 301–305.

Fitzgerald, T. L., Waters, D. L. and Henry, R. J. (2009), 'Betaine aldehyde dehydrogenase in plants', *Plant Biol (Stuttg)* **11**(2), 119–30.

Ford, K. L., Cassin, A. and Bacic, A. (2011), 'Quantitative proteomic analysis of wheat cultivars with differing drought stress tolerance', *Front Plant Sci* **2**, 44–55.

Frese, C. K., Altelaar, A. F., Hennrich, M. L., Nolting, D., Zeller, M., Griep-Raming, J., Heck, A. J. and Mohammed, S. (2011), 'Improved peptide identification by targeted fragmentation using cid, hcd and etd on an ltq-orbitrap velos', *J Proteome Res* **10**(5), 2377–88.

Friso, G. and van Wijk, K. J. (2015), 'Posttranslational protein modifications in plant metabolism', *Plant Physiol* **169**(3), 1469–87.

Gabriels, R., Martens, L. and Degroeve, S. (2019), 'Updated ms(2)pip web server delivers fast and accurate ms(2) peak intensity prediction for multiple fragmentation methods, instruments and labeling techniques', *Nucleic Acids Res* **47**(W1), W295–W299.

Gargallo-Garriga, A., Sardans, J., Perez-Trujillo, M., Rivas-Ubach, A., Oravec, M., Vecerova, K., Urban, O., Jentsch, A., Kreyling, J., Beierkuhnlein, C., Parella, T. and Penuelas, J. (2014), 'Opposite metabolic responses of shoots and roots to drought', *Sci Rep* **4**, 6829.

Garrison, W. M. (1987), 'Reaction mechanisms in the radiolysis of peptides, polypeptides, and proteins', *Chem Rev* **87**(2), 381–398.

Gauvrit, C. and Gaillardon, P. (1991), 'Effect of low temperatures on 2,4-d behaviour in maize plants', *Weed Research* **31**(3), 135–142.

Ghatak, A., Chaturvedi, P., Nagler, M., Roustan, V., Lyon, D., Bachmann, G., Postl, W., Schrofl, A., Desai, N., Varshney, R. K. and Weckwerth, W. (2016), 'Comprehensive tissue-specific proteome analysis of drought stress responses in pennisetum glaucum (l.) r. br. (pearl millet)', *J Proteomics* **143**, 122–135.

Gill, B. S., Appels, R., Botha-Oberholster, A. M., Buell, C. R., Bennetzen, J. L., Chalhoub, B., Chumley, F., Dvorak, J., Iwanaga, M., Keller, B., Li, W., McCombie, W. R., Ogihara, Y., Quetier, F. and Sasaki, T. (2004), 'A workshop report on wheat genome sequencing: International genome research on wheat consortium', *Genetics* **168**(2), 1087–96.

Gokce, E., Shuford, C. M., Franck, W. L., Dean, R. A. and Muddiman, D. C. (2011), 'Evaluation of normalization methods on gelc-ms/ms label-free spectral counting data to correct for variation during proteomic workflows', *J Am Soc Mass Spectrom* **22**(12), 2199–208.

Goodman, J. K., Zampronio, C. G., Jones, A. M. E. and Hernandez-Fernaud, J. R. (2018), 'Updates of the in-gel digestion method for protein analysis by mass spectrometry', *Proteomics* **18**(23), e1800236.

Goto, S., Nakamura, A., Radak, Z., Nakamoto, H., Takahashi, R., Yasuda, K., Sakurai, Y. and Ishii, N. (1999), 'Carbonylated proteins in aging and exercise: immunoblot approaches', *Mechanisms of ageing and development* **107**(3).

Graham, J., Ford, T. and Rickwood, D. (1994), 'The preparation of subcellular organelles from mouse liver in self-generated gradients of iodixanol.', *Anal Biochem* **220**(2), 367–373.

Graves, P. R. and Haystead, T. A. (2002), 'Molecular biologist's guide to proteomics', *Microbiol Mol Biol Rev* **66**(1), 39–63.

Green, N. M. (1990), *[5] Avidin and streptavidin*, Vol. 184 of *Methods in enzymology*, Academic Press.

Gull, A., Lone, A. and Wani, N. U. I. (2019), *Biotic and Abiotic Stresses in Plants*, Biotic and Abiotic Stresses in Plants, IntechOpen.

Gururani, M. A., Venkatesh, J. and Tran, L. S. (2015), 'Regulation of photosynthesis during abiotic stress-induced photoinhibition', *Mol Plant* **8**(9), 1304–20.

Gygi, S., Rist, B., Gerber, S., Turecek, F., Gelb, M. and Aebersold, R. (1999), 'Quantitative analysis of complex protein mixtures using isotope-coded affinity tags', *Nat Biotechnol* **17**(10), 994–999.

Hajheidari, M., Eivazi, A., Buchanan, B., Wong, J., Majidi, I. and Salekdeh, G. (2006), 'Proteomics uncovers a role for redox in drought tolerance in wheat', *J Proteome Res* **6**(4), 1451–1460.

Han, G., Ye, M. and Zou, H. (2008), 'Development of phosphopeptide enrichment techniques for phosphoproteome analysis', *The Analyst* **133**(9), 1128–1139.

Han, H. J., Peng, R. H., Zhu, B., Fu, X. Y., Zhao, W., Shi, B. and Yao, Q. H. (2014), 'Gene expression profiles of arabidopsis under the stress of methyl viologen: a microarray analysis', *Mol Biol Rep* **41**(11), 7089–102.

Han, K. and Martinage, A. (1992), 'Post-translational chemical modification(s) of proteins', *Int J Biochem* **24**(1), 19–28.

Hanin, M., Brini, F., Ebel, C., Toda, Y., Takeda, S. and Masmoudi, K. (2011), 'Plant dehydrins and stress tolerance: versatile proteins for complex mechanisms', *Plant Signal Behav* **6**(10), 1503–9.

Hao, P., Zhu, J., Gu, A., Lv, D., Ge, P., Chen, G., Li, X. and Yan, Y. (2015), 'An integrative proteome analysis of different seedling organs in tolerant and sensitive wheat cultivars under drought stress and recovery', *Proteomics* **15**(9), 1544–63.

Harb, A., Krishnan, A., Ambavaram, M. M. and Pereira, A. (2010), 'Molecular and physiological analysis of drought stress in arabidopsis reveals early responses leading to acclimation in plant growth', *Plant Physiol* **154**(3), 1254–71.

Hardie, D. G., Schaffer, B. E. and Brunet, A. (2016), 'Ampk: An energy-sensing pathway with multiple inputs and outputs', *Trends Cell Biol* **26**(3), 190–201.

Hardman, G., Perkins, S., Brownridge, P. J., Clarke, C. J., Byrne, D. P., Campbell, A. E., Kalyuzhnyy, A., Myall, A., Eyers, P. A., Jones, A. R. and Eyers, C. E. (2019), 'Strong anion exchange-mediated phosphoproteomics reveals extensive human non-canonical phosphorylation', *EMBO J* **38**(21), 1–22.

Hardman, G., Perkins, S., Ruan, Z., Kannan, N., Brownridge, P., Byrne, D. P., Eyers, P. A., Jones, A. R. and Eyers, C. E. (2017), 'Extensive non-canonical phosphorylation in human cells revealed using strong-anion exchange-mediated phosphoproteomics', *bioRxiv* pp. 1–24.

Havelund, J. F., Wojdyla, K., Davies, M. J., Jensen, O. N., Moller, I. M. and Rogowska-Wrzesinska, A. (2017), 'A biotin enrichment strategy identifies novel carbonylated amino acids in proteins from human plasma', *J Proteomics* **156**, 40–51.

Heard, W., Sklenar, J., Tome, D. F. A., Robatzek, S. and Jones, A. M. E. (2015), 'Identification of regulatory and cargo proteins of endosomal and secretory pathways in arabidopsis thaliana by proteomic dissection.', *Molecular and Cellular Proteomics* **14**(7), 1796–1813.

Heazlewood, J. L., Durek, P., Hummel, J., Selbig, J., Weckwerth, W., Walther, D. and Schulze, W. X. (2008), 'Phosphat: a database of phosphorylation sites in arabidopsis thaliana and a plant-specific phosphorylation site predictor', *Nucleic Acids Res* **36**, 1015–1021.

Hendley, P., Dicks, J. W., Monaco, T. J., Slyfield, S. M., Tummon, O. J. and Barrett, J. C. (1985), 'Translocation and metabolism of pyridinyloxyphenoxypropionate herbicides in rhizomatous quackgrass (agropyron repens)', *Weed Science* **33**(1), 11–24.

Herrero, M. and Johnson, R. (1981), 'Drought stress and its effects on maize reproductive systems', *Crop Science* **21**(1), 105–110.

Hess, F. D. (1987), 'Herbicide effects on the cell cycle of meristematic plant cells', *Rev. Weed Sci.* **3**, 183–203.

Ho, C., Lam, C., Chan, M., Cheung, R., Law, L., Lit, L., Ng, K., Suen, M. and Tai, H. (2003), 'Electrospray ionisation mass spectrometry: Principles and clinical applications', *Clin Biochem Rev* **24**(1), 3–12.

Hodges, M., Jossier, M., Boex-Fontvieille, E. and Tcherkez, G. (2013), 'Protein phosphorylation and photorespiration', *Plant Biol (Stuttg)* **15**(4), 694–706.

Hohl, M. and Schopfer, P. (1991), 'Water relations of growing maize coleoptiles', *Plant Physiol* **95**(3), 716–22.

Horie, T., Kaneko, T., Sugimoto, G., Sasano, S., Panda, S. K., Shibasaka, M. and Katsuhara, M. (2011), 'Mechanisms of water transport mediated by pip aquaporins and their regulation via phosphorylation events under salinity stress in barley roots', *Plant Cell Physiol* **52**(4), 663–75.

Hu, Q., Noll, R. J., Li, H., Makarov, A., Hardman, M. and Graham Cooks, R. (2005), 'The orbitrap: a new mass spectrometer', *J Mass Spectrom* **40**(4), 430–43.

Hu, X., Li, N., Wu, L., Li, C., Li, C., Zhang, L., Liu, T. and Wang, W. (2015-2), 'Quantitative itraq-based proteomic analysis of phosphoproteins and aba-regulated phosphoproteins in maize leaves under osmotic stress', *Sci Rep* **5**, 15626.

Hu, X., Wu, L., Zhao, F., Zhang, D., Li, N., Zhu, G., Li, C. and Wang, W. (2015-1), 'Phosphoproteomic analysis of the response of maize leaves to drought, heat and their combination stress', *Front Plant Sci* **6**, 298.

Huang, H., Moller, I. M. and Song, S. Q. (2012), 'Proteomics of desiccation tolerance during development and germination of maize embryos', *J Proteomics* **75**(4), 1247–62.

Hunt, D., Coon, J., Syka, J. and Marto, J. (2014), *Electron transfer dissociation for biopolymer sequence analysis*, Patent No. 8,692,187, USA.

Hunter, T. (2012), 'Why nature chose phosphate to modify proteins', *Philos Trans R Soc Lond B Biol Sci* **367**(1602), 2513–6.

Isayenkov, S. V. and Maathuis, F. J. M. (2019), 'Plant salinity stress: Many unanswered questions remain', *Front Plant Sci* **10**, 1–11.

Itzhak, D. N., Davies, C., Tyanova, S., Mishra, A., Williamson, J., Antrobus, R., Cox, J., Weekes, M. P. and Borner, G. H. H. (2017), 'A mass spectrometry-based approach for mapping protein subcellular localization reveals the spatial proteome of mouse primary neurons', *Cell Rep* **20**(11), 2706–2718.

Jaleel, C., Manivannan, P., Wahid, A., Farooq, M., Al-Juburi, H., Somasundaram, R., Panneerselvam, R., Wahid, P. and Al-Azzawi, H. (2009), 'Drought stress in plants: A review on morphological characteristics and pigments composition', *International Journal of Agriculture and Biology* **11**(1), 100–105.

Jedrychowski, M. P., Huttlin, E. L., Haas, W., Sowa, M. E., Rad, R. and Gygi, S. P. (2011), 'Evaluation of hcd- and cid-type fragmentation within their respective detection platforms for murine phosphoproteomics', *Mol Cell Proteomics* **10**(12), 1–9.

Ji, K., Wang, Y., Sun, W., Lou, Q., Mei, H., Shen, S. and Chen, H. (2012), 'Drought-responsive mechanisms in rice genotypes with contrasting drought tolerance during reproductive stage', *J Plant Physiol* **169**(4), 336–44.

Jiang, L., Anderson, J. C., Gonzalez Besteiro, M. A. and Peck, S. C. (2017), 'Phosphorylation of arabidopsis map kinase phosphatase 1 (mkp1) is required for pamp responses and resistance against bacteria', *Plant Physiol* **175**(4), 1839–1852.

Jiang, S. S., Liang, X. N., Li, X., Wang, S. L., Lv, D. W., Ma, C. Y., Li, X. H., Ma, W. J. and Yan, Y. M. (2012), 'Wheat drought-responsive grain proteome analysis by linear and nonlinear 2-de and maldi-tof mass spectrometry', *Int J Mol Sci* **13**(12), 16065–83.

Johansson, E., Olsson, O. and Nystrom, T. (2004), 'Progression and specificity of protein oxidation in the life cycle of arabidopsis thaliana', *J Biol Chem* **279**(21), 22204–8.

Jung, T. and Grune, T. (2008), 'The proteasome and its role in the degradation of oxidized proteins', *IUBMB Life* **60**(11), 743–52.

Juretic, D., Zucic, D., Luclic, B. and Trinajstic, N. (1998), 'Preference functions for prediction of membrane-buried helices in integral membrane proteins', *Computers and Chemistry* **22**(4), 279–294.

Kalia, J. and Raines, R. (2008), 'Hydrolytic stability of hydrazones and oximes', *Angewandte Chemie International Edition* **47**(39), 7523–7526.

Karas, M. and Hillenkamp, F. (1988), 'Laser desorption ionization of proteins with molecular masses exceeding 10,000 daltons', *Anal Chem* **60**(20), 2299–2301.

Karpievitch, Y. V., Polpitiya, A. D., Anderson, G. A., Smith, R. D. and Dabney, A. R. (2010), 'Liquid chromatography mass spectrometry-based proteomics: Biological and technological aspects', *Ann Appl Stat* **4**(4), 1797–1823.

Kaul, S., Koo, H., Jenkins, J., Rizzo, M., Rooney, T., Tallon, L., Feldblyum, T., Nierman, W., Benito, M., Lin, X. and Stiekema, W. (2000), 'Analysis of the genome sequence of the flowering plant arabidopsis thaliana', *Nature* **408**, 796–815.

Kausar, R., Arshad, M., Shahzad, A. and Komatsu, S. (2013), 'Proteomics analysis of sensitive and tolerant barley genotypes under drought stress', *Amino Acids* **44**(2), 345–59.

Ke, Y., Han, G., He, H. and Li, J. (2009), 'Differential regulation of proteins and phosphoproteins in rice under drought stress', *Biochem Biophys Res Commun* **379**(1), 133–8.

Keller, R., Halmes, N., Hinson, J. and Pumford, N. (1993), 'Immunochemical detection of oxidized proteins', *Chem Res Toxicol* **6**(4), 430–3.

Kelley, K. B. and Riechers, D. E. (2007), 'Recent developments in auxin biology and new opportunities for auxinic herbicide research', *Pesticide Biochemistry and Physiology* **89**(1), 1–11.

Kersten, B., Agrawal, G. K., Iwahashi, H. and Rakwal, R. (2006), 'Plant phosphoproteomics: a long road ahead', *Proteomics* **6**(20), 5517–28.

Keryer, E., Collin, V., Lavergne, D., Lemaire, S. and Issakidis-Bourguet, E. (2004), 'Characterization of arabidopsis mutants for the variable subunit of ferredoxin:thioredoxin reductase', *Photosynthesis Research* **79**(3), 265–274.

Kim, J. S., Jung, H. J., Lee, H. J., Kim, K. A., Goh, C. H., Woo, Y., Oh, S. H., Han, Y. S. and Kang, H. (2008), 'Glycine-rich rna-binding protein 7 affects abiotic stress

responses by regulating stomata opening and closing in arabidopsis thaliana', *Plant J* **55**(3), 455–66.

Kim, M. S. and Pandey, A. (2012), 'Electron transfer dissociation mass spectrometry in proteomics', *Proteomics* **12**(1), 530–542.

Kingston-Smith, A. and Foyer, C. (2000), 'Bundle sheath proteins are more sensitive to oxidative damage than those of the mesophyll in maize leaves exposed to paraquat or low temperatures', *Journal of Experimental Botany* **51**(342), 123–130.

Koag, M. C., Fenton, R. D., Wilkens, S. and Close, T. J. (2003), 'The binding of maize dhn1 to lipid vesicles. gain of structure and lipid specificity', *Plant Physiol* **131**(1), 309–16.

Kohlbacher, O., Reinert, K., Gropl, C., Lange, E., Pfeifer, N., Schulz-Trieglaff, O. and Sturm, M. (2007), 'Topp–the openms proteomics pipeline', *Bioinformatics* **23**(2), 191–197.

Koller, A., Washburn, M. P., Lange, M., Andon, N. L., Deciu, C., Haynes, P. A., Hays, L., Schieltz, D., Ulaszek, R., Wei, J., Wolters, D. and III, J. R. Y. (2002), 'Proteomic survey of metabolic pathways in rice', *PNAS* **99**(18), 11969–11974.

Koussevitzky, S., Suzuki, N., Huntington, S., Armijo, L., Sha, W., Cortes, D., Shulaev, V. and Mittler, R. (2008), 'Ascorbate peroxidase 1 plays a key role in the response of arabidopsis thaliana to stress combination', *J Biol Chem* **283**(49), 34197–203.

Kristensen, B. K., Askerlund, P., Bykova, N. V., Egsgaard, H. and Moller, I. M. (2004), 'Identification of oxidised proteins in the matrix of rice leaf mitochondria by immunoprecipitation and two-dimensional liquid chromatography-tandem mass spectrometry', *Phytochemistry* **65**(12), 1839–51.

Kröncke, K.-D. and Kolb-Bachofen, V. (1996), 'Detection of nitric oxide interaction with zinc finger proteins', *Methods in Enzymology* **269**, 279–284.

Kubo, K., Ide, H., Wallace, S. and Kow, Y. (1992), 'A novel, sensitive, and specific assay for abasic sites, the most commonly produced dna lesion', *Biochem J* **31**(14), 3703–8.

Kulik, A., Wawer, I., Krzywinska, E., Bucholc, M. and Dobrowolska, G. (2011), 'Snrk2 protein kinases–key regulators of plant response to abiotic stresses', *OMICS* **15**(12), 859–72.

Kweon, H. K. and Håkansson, K. (2006), 'Selective zirconium dioxide-based enrichment of phosphorylated peptides for mass spectrometric analysis', *Anal Chem* **78**(6), 1743–1749.

Lai, X., Wang, L., Tang, H. and Witzmann, F. A. (2011), 'A novel alignment method and multiple filters for exclusion of unqualified peptides to enhance label-free quantification using peptide intensity in lc-ms/ms', *J Proteome Res* **10**(10), 4799–812.

Lai, X., Wang, L. and Witzmann, F. A. (2013), 'Issues and applications in label-free quantitative mass spectrometry', *Int J Proteomics* **2013**, 1–13.

Langenkamper, G., Manac'h, N., Broin, M., Cuine, S., Becuwe, N., Kuntz, M. and Rey, P. (2001), 'Accumulation of plastid lipid-associated proteins (fibrillin/cdsp34) upon oxidative stress, ageing and biotic stress in solanaceae and in response to drought in other species', *Journal of Experimental Botany* **52**(360), 1545–1554.

Lascano, R., Munoz, N., Robert, G., Rodriguez, M., Melchiorre, M., Trippi, V. and Quero, G. (2012), *Paraquat: An Oxidative Stress Inducer*, Herbicides-properties, synthesis and control of weeds, IntechOpen, Argentina.

Lee, S., Young, N. L., Whetstone, P. A., Cheal, S. M., Benner, W. H., Lebrilla, C. B. and Meares, C. F. (2006), 'Method to site-specifically identify and quantitate carbonyl end products of protein oxidation using oxidation-dependent element coded affinity tags (o-ecat) and nanoliquid chromatography fourier transform mass spectrometry', *Journal of Proteome Research* **539**(5), 539–547.

Levine, R. L., Garland, D., Oliver, C. N., Amici, A., Climent, I., Lenz, A.-G., Ahn, B.-W., Shaltiel, S. and Stadtman, E. R. (1990), 'Determination of carbonyl content in oxidatively modified proteins', *Methods in Enzymology* **186**, 464–478.

Lilley, K. S., Razzaq, A. and Dupree, P. (2002), 'Two-dimensional gel electrophoresis: recent advances in sample preparation, detection and quantitation', *Current Opinion in Chemical Biology* **6**(1), 46–50.

Lin, L. L., Hsu, C. L., Hu, C. W., Ko, S. Y., Hsieh, H. L., Huang, H. C. and Juan, H. F. (2015), 'Integrating phosphoproteomics and bioinformatics to study brassinosteroid-regulated phosphorylation dynamics in arabidopsis', *BMC Genomics* **16**(1), 533–550.

Liu, H., Sultan, M. A., Liu, X. L., Zhang, J., Yu, F. and Zhao, H. X. (2015), 'Physiological and comparative proteomic analysis reveals different drought responses in roots and leaves of drought-tolerant wild wheat (triticum boeoticum)', *PLoS One* **10**(4), 1–29.

Liu, Y. (2012), 'Roles of mitogen-activated protein kinase cascades in aba signaling', *Plant Cell Rep* **31**(1), 1–12.

Lo, H.-W., Antoun, G. R. and Ali-Osman, F. (2004), 'The human glutathione s-transferase p1 protein is phosphorylated and its metabolic function enhanced by the ser/thr protein kinases, camp-dependent protein kinase and protein kinase c, in glioblastoma cells', **64**, 9131–9138.

Lodish, H., Berk, A., Zipursky, S. L., Matsudaira, P., Baltimore, D. and Darnell, J. (2000), *Membrane Proteins*, Vol. 4 of *Molecular Cell Biology*, W. H. Freeman, New York.

Lohrig, K., Muller, B., Davydova, J., Leister, D. and Wolters, D. A. (2009), 'Phosphorylation site mapping of soluble proteins: bioinformatical filtering reveals potential plastidic phosphoproteins in arabidopsis thaliana', *Planta* **229**(5), 1123–34.

Luo, S. and Wehr, N. B. (2009), 'Protein carbonylation: avoiding pitfalls in the 2,4-dinitrophenylhydrazine assay', *Redox Rep* **14**(4), 159–66.

Lv, D. W., Zhu, G. R., Zhu, D., Bian, Y. W., Liang, X. N., Cheng, Z. W., Deng, X. and Yan, Y. M. (2016), 'Proteomic and phosphoproteomic analysis reveals the response and defense mechanism in leaves of diploid wheat t. monococcum under salt stress and recovery', *J Proteomics* **143**, 93–105.

Ma, H., Chen, J., Zhang, Z., Ma, L., Yang, Z., Zhang, Q., Li, X., Xiao, J. and Wang, S. (2017), 'Mapk kinase 10.2 promotes disease resistance and drought tolerance by activating different mapks in rice', *Plant J* **92**(4), 557–570.

Ma, Y., Dai, X., Xu, Y., Luo, W., Zheng, X., Zeng, D., Pan, Y., Lin, X., Liu, H., Zhang, D., Xiao, J., Guo, X., Xu, S., Niu, Y., Jin, J., Zhang, H., Xu, X., Li, L., Wang, W., Qian, Q., Ge, S. and Chong, K. (2015), 'Cold1 confers chilling tolerance in rice', *Cell* **160**(6), 1209–21.

Maas, E. V. and Grattan, S. R. (1999), *Crop Yields as Affected by Salinity*, Vol. 38 of *Agricultural Drainage*, American Society of Agronomy.

Madian, A. G., Myracle, A. D., Diaz-Maldonado, N., Rochelle, N. S., Janle, E. M. and Regnier, F. E. (2011), 'Differential carbonylation of proteins as a function of in vivo oxidative stress', *J Proteome Res* **10**(9), 3959–72.

Madian, A. G. and Regnier, F. E. (2006), 'Proteomic identification of carbonylated proteins and their oxidation sites', *Journal of Proteome Research* **9**(8), 3766–3780.

Maisonneuve, E., Ducret, A., Khoueiry, P., Lignon, S., Longhi, S., Talla, E. and Dukan, S. (2009), 'Rules governing selective protein carbonylation', *PLoS One* **4**(10), 1–12.

Makarov, A. (2000), 'Electrostatic axially harmonic orbital trapping: A high-performance technique of mass analysis', *Anal Chem* **72**(6), 1156–1162.

Makarov, A., Denisov, E., Kholomeev, A., Balschun, W., Lange, O., Strupat, K. and Horning, S. (2006), 'Performance evaluation of a hybrid linear ion trap/orbitrap mass spectrometer', *Anal Chem* **78**(7), 2113–2120.

Maksymiec, W. (2011), 'Effects of jasmonate and some other signalling factors on bean and onion growth during the initial phase of cadmium action', *Biologia Plantarum* **55**(1), 112–118.

Mann, M. and Jensen, O. N. (2003), 'Proteomic analysis of post-translational modifications', *nature biotechnology* **21**, 255–261.

Mano, J., Ohno, C., Domae, Y. and Asada, K. (2001), 'Chloroplastic ascorbate peroxidase is the primary target of methylviologen-induced photooxidative stress in spinach leaves: its relevance to monodehydroascorbate radical detected with in vivo esr', *Biochimica et Biophysica Acta (BBA) - Bioenergetics* **1504**(3), 275–287.

March, R. E., Hughes, R. J. and Todd, J. F. J. (1989), *Quadrupole storage mass spectrometry*, Wiley, Toronto.

Marcon, C., Malik, W. A., Walley, J. W., Shen, Z., Paschold, A., Smith, L. G., Piepho, H. P., Briggs, S. P. and Hochholdinger, F. (2015), 'A high-resolution tissue-specific proteome and phosphoproteome atlas of maize primary roots reveals functional gradients along the root axes', *Plant Physiol* **168**(1), 233–46.

Martinaud, A., Mercier, Y., Marinova, P., Tassy, C., Gatellier, P. and Renerre, M. (1997), 'Comparison of oxidative processes on myofibrillar proteins from beef during maturation and by different model oxidation systems', *J. Agric. Food Chem.* **45**(7), 2481-2487.

Matamoros, M. A., Kim, A., Penuelas, M., Ihling, C., Griesser, E., Hoffmann, R., Fedorova, M., Frolov, A. and Becana, M. (2018), 'Protein carbonylation and glycation in legume nodules', *Plant Physiol* **177**(4), 1510–1528.

Matsuoka, D., Yasufuku, T., Furuya, T. and Nanmori, T. (2015), 'An abscisic acid inducible arabidopsis mapkkk, mapkkk18 regulates leaf senescence via its kinase activity', *Plant Mol Biol* **87**(6), 565–75.

Mattei, B., Spinelli, F., Pontiggia, D. and De Lorenzo, G. (2016), 'Comprehensive analysis of the membrane phosphoproteome regulated by oligogalacturonides in arabidopsis thaliana', *Front Plant Sci* **7**, 1107.

McSteen, P. (2010), 'Auxin and monocot development', *Cold Spring Harb Perspect Biol* **2**(3), 001479.

Medzihradszky, K. F. (2005), *In-Solution Digestion of Proteins for Mass Spectrometry*, Vol. 405 of *Methods in Enzymology*.

Menz, J., Li, Z., Schulze, W. X. and Ludewig, U. (2016), 'Early nitrogen-deprivation responses in arabidopsis roots reveal distinct differences on transcriptome and (phospho-) proteome levels between nitrate and ammonium nutrition', *Plant J* **88**(5), 717–734.

Mirzaei, H. Regnier, F. (2005), 'Affinity chromatographic selection of carbonylated proteins followed by identification of oxidation sites using tandem mass spectrometry', *Anal Chem* **77**(8), 2386–2392.

Mirzaei, H. and Regnier, F. (2006), 'Enrichment of carbonylated peptides using girard p reagent and strong cation exchange chromatography', *Anal Chem* **78**(3), 770–778.

Mirzaei, H. and Regnier, F. (2007), 'Identification of yeast oxidized proteins: chromatographic top-down approach for identification of carbonylated, fragmented and cross-linked proteins in yeast', *J Chromatogr A* **1141**(1), 22–31.

Mirzaei, M., Soltani, N., Sarhadi, E., George, I. S., Neilson, K. A., Pascovici, D., Shahbazian, S., Haynes, P. A., Atwell, B. J. and Salekdeh, G. H. (2014), 'Manipulating root water supply elicits major shifts in the shoot proteome', *J Proteome Res* **13**(2), 517–26.

Mirzaei, M., Soltani, N., Sarhadi, E., Pascovici, D., Keighley, T., Salekdeh, G. H., Haynes, P. A. and Atwell, B. J. (2012), 'Shotgun proteomic analysis of long-distance drought signaling in rice roots', *J Proteome Res* **11**(1), 348–58.

Mitula, F., Tajdel, M., Ciesla, A., Kasprowicz-Maluski, A., Kulik, A., Babula-Skowronska, D., Michalak, M., Dobrowolska, G., Sadowski, J. and Ludwikow, A. (2015), 'Arabidopsis aba-activated kinase mapkkk18 is regulated by protein phosphatase 2c abi1 and the ubiquitin-proteasome pathway', *Plant Cell Physiol* **56**(12), 2351–67.

Mohanty, J. G., Bhamidipaty, S., Evans, M. K. and Rifkind, J. M. (2010), 'A fluorimetric semi-microplate format assay of protein carbonyls in blood plasma', *Anal Biochem* **400**(2), 289–94.

Moller, I. M. (2001), 'Plant mitochondria and oxidative stress: Electron transport, nadph turnover, and metabolism of reactive oxygen species', *Annu Rev Plant Physiol Plant Mol Biol* **52**, 561–591.

Moller, I. M., Havelund, J. F. and Rogowska-Wrzesinska, A. (2017), 'Protein carbonylation in plants', *Principles, Analysis, and Biological Implications* pp. 321–339.

Moller, I. M., Jensen, P. E. and Hansson, A. (2007), 'Oxidative modifications to cellular components in plants', *Annu Rev Plant Biol* **58**, 459–81.

Moller, I. M., Rogowska-Wrzesinska, A. and Rao, R. S. (2011), 'Protein carbonylation and metal-catalyzed protein oxidation in a cellular perspective', *J Proteomics* **74**(11), 2228–42.

Monaco, T., Weller, S. and Ashton, F. (2002), *Weed Science, Principles and Practices*, Vol. 4 of *Weed Science, Principles and Practices*, Wiley-Blackwell, New York.

Montgomery, S. and Brown, C. (2008), 'Field crop manual: Maize a guide to upland production in cambodia', *NSW Department of Primary Industries* pp. 1–43.

Morzel, M., Gatellier, P., Sayd, T., Renerre, M. and Laville, E. (2006), 'Chemical oxidation decreases proteolytic susceptibility of skeletal muscle myofibrillar proteins', *Meat Sci* **73**(3), 536–43.

Mostafa, K. A. H., Ki-Hyun, K., Kwang-Hyun, S., Jong-Soon, C., Byung-Kee, B., Hisashi, T., Young, H. H., Chul-Soo, P. and Sun-Hee, W. (2010), 'Abiotic stress responsive proteins of wheat grain determined using proteomics technique', *Australian Journal of Crop Science* **4**(3), 196–208.

Moustaka, J., Tanou, G., Adamakis, I. D., Eleftheriou, E. P. and Moustakas, M. (2015), 'Leaf age-dependent photoprotective and antioxidative response mechanisms to paraquat-induced oxidative stress in arabidopsis thaliana', *Int J Mol Sci* **16**(6), 13989–4006.

Mueller, L. N., Rinner, O., Schmidt, A., Letarte, S., Bodenmiller, B., Brusniak, M. Y., Vitek, O., Aebersold, R. and Muller, M. (2007), 'Superhirn - a novel tool for high resolution lc-ms-based peptide/protein profiling', *Proteomics* **7**(19), 3470–80.

Nakajima, H., Amano, W., Kubo, T., Fukuhara, A., Ihara, H., Azuma, Y. T., Tajima, H., Inui, T., Sawa, A. and Takeuchi, T. (2009), 'Glyceraldehyde-3-phosphate dehydrogenase aggregate formation participates in oxidative stress-induced cell death', *J Biol Chem* **284**(49), 34331–41.

Ndimba, B. K., Chivasa, S., Simon, W. J. and Slabas, A. R. (2005), 'Identification of arabidopsis salt and osmotic stress responsive proteins using two-dimensional difference gel electrophoresis and mass spectrometry', *Proteomics* **5**(16), 4185–96.

Nelson, T. and Dengler, N. (1997), 'Leaf vascular pattern formation', *Plant Cell* **9**(7), 1121–1135.

Nguyen, A. T. and Donaldson, R. P. (2005), 'Metal-catalyzed oxidation induces carbonylation of peroxisomal proteins and loss of enzymatic activities', *Arch Biochem Biophys* **439**(1), 25–31.

Nievola, C. C., Carvalho, C. P., Carvalho, V. and Rodrigues, E. (2017), 'Rapid responses of plants to temperature changes', *Temperature (Austin)* **4**(4), 371–405.

Okazawa, H., Hu, L., Huang, T., Liu, X.-J. and Cai, Y.-D. (2011), 'Predicting protein phenotypes based on protein-protein interaction network', *PLoS ONE* **6**(3), 1–8.

Olsen, J. V., Ong, S. E. and Mann, M. (2004), 'Trypsin cleaves exclusively c-terminal to arginine and lysine residues', *Mol Cell Proteomics* **3**(6), 608–14.

Osakabe, Y., Osakabe, K., Shinozaki, K. and Tran, L. S. (2014), 'Response of plants to water stress', *Front Plant Sci* **5**, 86–94.

Osmolovskaya, N., Shumilina, J., Kim, A., Didio, A., Grishina, T., Bilova, T., Keltsieva, O. A., Zhukov, V., Tikhonovich, I., Tarakhovskaya, E., Frolov, A. and Wessjohann, L. A. (2018), 'Methodology of drought stress research: Experimental setup and physiological characterization', *Int J Mol Sci* **19**(12), 4089–5002.

Otter, D. (2003), 'Protein — determination and characterization', *Encyclopedia of Food Sciences and Nutrition* **2**, 4824–4830.

Ozols, J. (1990), *[17] Preparation of membrane fractions*, Vol. 182 of *Methods Enzymol*, Academic Press.

Pandey, A., Rajamani, U., Verma, J., Subba, P., Chakraborty, N., Datta, A., Chakraborty, S. and Chakraborty, N. (2009), 'Identification of extracellular matrix proteins of rice (oryza sativa l.) involved in dehydration-responsive network: a proteomic approach.', *J Proteome Res* **9**(7), 3443–3464.

Pastore, D., Trono, D., Laus, M. N., Di Fonzo, N. and Flagella, Z. (2007), 'Possible plant mitochondria involvement in cell adaptation to drought stress. a case study: durum wheat mitochondria', *J Exp Bot* **58**(2), 195–210.

Pattanayak, G. K. and Tripathy, B. C. (2011), 'Overexpression of protochlorophyllide oxidoreductase c regulates oxidative stress in arabidopsis', *PLoS One* **6**(10), 26532.

Paul, W. and Steinwedel, H. (1953), 'Ein neues massenspektrometer ohne magnetfeld', *Zeitschrift für Naturforschung A* **8**(7), 448–450.

Peng, J., Schmidt, B., Figura, K. v. and Dierks, T. (2003), 'Identification of formylglycine in sulfatases by matrix-assisted laser desorption/ionization time-of-flight mass spectrometry', *J Mass Spectrom* **38**(1), 80–6.

Peremarti, A., Marè, C., Aprile, A., Roncaglia, E., Cattivelli, L., Villegas, D. and Royo, C. (2014), 'Transcriptomic and proteomic analyses of a pale-green durum wheat mutant shows variations in photosystem components and metabolic deficiencies under drought stress', *BMC Genomics* **15**, 125–152.

Perkins, D., Pappin, D., Creasy, D. and Cottrell, J. (1999), 'Probability-based protein identification by searching sequence databases using mass spectrometry data.', *Electrophoresis* **20**(18), 3551–67.

Pulido, P., Llamas, E. and Rodriguez-Concepcion, M. (2017), 'Both hsp70 chaperone and clp protease plastidial systems are required for protection against oxidative stress', *Plant Signal Behav* **12**(3), 1290039.

Qin, Y., Song, W., Xiao, S., Yin, G., Zhu, Y., Yan, Y. and Hu, Y. (2014), 'Stress-related genes distinctly expressed in unfertilized wheat ovaries under both normal and water deficit conditions whereas differed in fertilized ovaries', *J Proteomics* **102**, 11–27.

Rabello, A. R., Guimaraes, C. M., Rangel, P. H., da Silva, F. R., Seixas, D., de Souza, E., Brasileiro, A. C., Spehar, C. R., Ferreira, M. E. and Mehta, A. (2008), 'Identification of drought-responsive genes in roots of upland rice (oryza sativa l)', *BMC Genomics* **9**(1), 485–498.

Raghavendra, A. S., Reumann, S. and Heldt, H. W. (1998), 'Participation of mitochondrial metabolism in photorespiration', *Plant Physiol* **116**(4), 1333–1337.

Rappsilber, J., Mann, M. and Ishihama, Y. (2007), 'Protocol for micro-purification, enrichment, pre-fractionation and storage of peptides for proteomics using stagetips', *Nat Protoc* **2**(8), 1896–906.

Rauniyar, N. and Yates, J. R., . (2014), 'Isobaric labeling-based relative quantification in shotgun proteomics', *J Proteome Res* **13**(12), 5293–309.

Rayapuram, N., Bigeard, J., Alhoraibi, H., Bonhomme, L., Hesse, A. M., Vinh, J., Hirt, H. and Pflieger, D. (2018), 'Quantitative phosphoproteomic analysis reveals shared and specific targets of arabidopsis mitogen-activated protein kinases (mapks) mpk3, mpk4, and mpk6', *Mol Cell Proteomics* **17**(1), 61–80.

Rayapuram, N., Bonhomme, L., Bigeard, J., Haddadou, K., Przybylski, C., Hirt, H. and Pflieger, D. (2014), 'Identification of novel pamp-triggered phosphorylation and dephosphorylation events in arabidopsis thaliana by quantitative phosphoproteomic analysis', *J Proteome Res* **13**(4), 2137–51.

Reeves, G. A., Talavera, D. and Thornton, J. M. (2009), 'Genome and proteome annotation: organization, interpretation and integration', *J R Soc Interface* **6**(31), 129–47.

Reid, E. and Williamson, R. (1974), '[73] centrifugation', *Methods in enzymology* **31**, 713–733.

Reiland, S., Messerli, G., Baerenfaller, K., Gerrits, B., Endler, A., Grossmann, J., Gruissem, W. and Baginsky, S. (2009), 'Large-scale arabidopsis phosphoproteome profiling reveals novel chloroplast kinase substrates and phosphorylation networks', *Plant Physiol* **150**(2), 889–903.

Rejeb, I. B., Pastor, V. and Mauch-Mani, B. (2014), 'Plant responses to simultaneous biotic and abiotic stress: Molecular mechanisms', *Plants (Basel)* **3**(4), 458–75.

Riccardi, F., Gazeau, P., Jacquemot, M. P., Vincent, D. and Zivy, M. (2004), 'Deciphering genetic variations of proteome responses to water deficit in maize leaves', *Plant Physiol Biochem* **42**(12), 1003–11.

Riccardi, F., Gazeau, P., Vienne, D. d. and Zivy, M. (1998), 'Protein changes in response to progressive water deficit in maize', *Plant Physiol* **117**, 1253–1263.

Richard;, D., Sebastien;, D., Marie;, H., Asif;, I., Scott;, M., Aude-Sophie;, R., Jason;, R. and Esha., Z. (2017), *Uncharted Waters : The New Economics of Water Scarcity and Variability.*, World Bank, Washington, DC.

Rodrigues, S. M., Andrade, M. O., Gomes, A. P., Damatta, F. M., Baracat-Pereira, M. C. and Fontes, E. P. (2006), 'Arabidopsis and tobacco plants ectopically expressing the soybean antiquitin-like aldh7 gene display enhanced tolerance to drought, salinity, and oxidative stress', *J Exp Bot* **57**(9), 1909–18.

Roitinger, E., Hofer, M., Kocher, T., Pichler, P., Novatchkova, M., Yang, J., Schlogelhofer, P. and Mechtler, K. (2015), 'Quantitative phosphoproteomics of the ataxia telangiectasia-mutated (atm) and ataxia telangiectasia-mutated and rad3-related (atr) dependent dna damage response in arabidopsis thaliana', *Mol Cell Proteomics* **14**(3), 556–71.

Rollins, J. A., Habte, E., Templer, S. E., Colby, T., Schmidt, J. and von Korff, M. (2013), 'Leaf proteome alterations in the context of physiological and morphological responses to drought and heat stress in barley (hordeum vulgare l.)', *J Exp Bot* **64**(11), 3201–12.

Romero-Puertas, M., Palma, J., Gomez, M., Río, L. D. and Sandalio, L. (2002), 'Cadmium causes the oxidative modification of proteins in pea plants', *Plant, Cell and Environment* **25**(5), 677–686.

Rosegrant, M., Ringler, C., Sulser, T., Ewing, M., Palazzo, A., Zhu, T., Nelson, G., Koo, J., Robertson, R., Msangi, S. and Batka, M. (2009), *Agriculture and food security under global change: Prospects for 2025/2050*, International Food Policy Research Institute, Washington, DC.

Rosentrater, K. A. and Evers, A. D. (2018), *Chemical components and nutrition*, pp. 267–368.

Rossi, C. and Chopineau, J. (2007), 'Biomimetic tethered lipid membranes designed for membrane-protein interaction studies', *Eur Biophys J* **36**(8), 955–65.

Rudall, P. J. and Bateman, R. M. (2004), 'Evolution of zygomorphy in monocot flowers: iterative patterns and developmental constraints', *New Phytologist* **162**(1), 25–44.

Salvador, R. and Pearce, R. (1995), 'Proposed standard system of nomenclature for maize grain filling events and concepts.', *Maydica* **40**, 141–146.

Salvato, F., Havelund, J. F., Chen, M., Rao, R. S., Rogowska-Wrzesinska, A., Jensen, O. N., Gang, D. R., Thelen, J. J. and Moller, I. M. (2014), 'The potato tuber mitochondrial proteome', *Plant Physiol* **164**(2), 637–53.

Sangwan, V., Orvar, B. L., Beyerly, J., Hirt, H. and Dhindsa, R. S. (2002), 'Opposite changes in membrane fluidity mimic cold and heat stress activation of distinct plant map kinase pathways', *The Plant Journal* **31**(5), 629–638.

Santoni, V. (2007), *Plant Plasma Membrane Protein Extraction and Solubilization for Proteomic Analysis*, Plant Proteomics Methods and Protocols, Humana Press, UMR de Génétique Végétale, La Ferme du Moulon, Gif-sur-Yvette, France.

Saraswathy, N. and Ramalingam, P. (2011), *Protein Identification by Peptide Mass Fingerprinting (PMF)*, Elsevier, pp. 185–192.

Savitski, M. M., Mathieson, T., Zinn, N., Sweetman, G., Doce, C., Becher, I., Pachl, F., Kuster, B. and Bantscheff, M. (2013), 'Measuring and managing ratio compression for accurate itraq/tmt quantification', *J Proteome Res* **12**(8), 3586–98.

Sayre, L. M., Lin, D., Yuan, Q., Zhu, X. and Tang, X. (2006), 'Protein adducts generated from products of lipid oxidation: focus on hne and one', *Drug Metab Rev* **38**(4), 651–675.

Scarpella, E. and Meijer, A. H. (2004), 'Pattern formation in the vascular system of monocot and dicot plant species', *New Phytologist* **164**(2), 209–242.

Schnable, P., Ware, D., Fulton, R., Stein, J., Wei, F., Pasternak, S., Liang, C., Zhang, J., Fulton, L., Graves, T., Minx, P., Reily, A., Courtney, L., Kruchowski, S., Tomlinson, C., Strong, C., Delehaunty, K., Fronick, C., Courtney, B., Rock, S., Belter, E., Du, F., Kim, K., Abbott, R., Cotton, M., Levy, A., Marchetto, P., Ochoa, K., Jackson, S., Gillam, B., Chen, W., Yan, L., Higginbotham, J., Cardenas, M., Waligorski, J., Applebaum, E., Phelps, L., Falcone, J., Kanchi, K., Thane, T., Scimone, A., Thane, N., Henke, J., Wang, T., Ruppert, J., Shah, N., Rotter, K., Hodges, J., Ingenthron, E., Cordes, M., Kohlberg, S., Sgro, J., Delgado, B., Mead, K., Chinwalla, A., Leonard, S., Crouse, K., Collura, K., Kudrna, D., Currie, J., He, R., Angelova, A., Rajasekar, S., Mueller, T., Lomeli, R., Scara, G., Ko, A., Delaney, K., Wissotski, M., Lopez, G., Campos, D., Braidotti, M.,

Ashley, E., Golser, W., Kim, H., Lee, S., Lin, J., Dujmic, Z., Kim, W., Talag, J., Zuccolo, A., Fan, C., Sebastian, A., Kramer, M., Spiegel, L., Nascimento, L., Zutavern, T., Miller, B., Ambroise, C., Muller, S., Spooner, W., Narechania, A., Ren, L., Wei, S., Kumari, S., Faga, B., Levy, M., McMahan, L., Buren, P. V., Vaughn, M. *et al.* (2009), 'The b73 maize genome: Complexity, diversity, and dynamics', *Science* **326**(5956), 1112–1115.

Seki, M., Narusaka, M., Ishida, J., Nanjo, T., Fujita, M., Oono, Y., Kamiya, A., Nakajima, M., Enju, A., Sakurai, T., Satou, M., Akiyama, K., Taji, T., Yamaguchi-Shinozaki, K., Carninci, P., Kawai, J., Hayashizaki, Y. and Shinozaki, K. (2002), 'Monitoring the expression pro®les of 7000 arabidopsis genes under drought, cold and high-salinity stresses using a full-length cdna microarray', *Plant Journal* **31**(3), 279–292.

Shiferaw, B., Prasanna, B. M., Hellin, J. and Banziger, M. (2011), 'Crops that feed the world 6. past successes and future challenges to the role played by maize in global food security', *Food Security* **3**(3), 307–327.

Shire, S. J. (2015), *Analytical tools used in the formulation and assessment of stability of monoclonal antibodies (mAbs)*, pp. 17–44.

Shu, L., Lou, Q., Ma, C., Ding, W., Zhou, J., Wu, J., Feng, F., Lu, X., Luo, L., Xu, G. and Mei, H. (2011), 'Genetic, proteomic and metabolic analysis of the regulation of energy storage in rice seedlings in response to drought', *Proteomics* **11**(21), 4122–38.

Sinclair, J. and Timms, J. F. (2011), 'Quantitative profiling of serum samples using tmt protein labelling, fractionation and lc–ms/ms', *Methods* **54**(4), 361–369.

Singh, N. R., Rondeau, P., Hoareau, L. and Bourdon, E. (2007), 'Identification of preferential protein targets for carbonylation in human mature adipocytes treated with native or glycated albumin', *Free Radic Res* **41**(10), 1078–1088.

Slade, P., Williams, M., Chiang, A., Iffrig, E., Tannenbaum, S. and Wishnok, J. (2011), 'A filtered database search algorithm for endogenous serum protein carbonyl modifications in a mouse model of inflammation', *Molecular and Cellular Proteomics* **10**(10), 1–45.

Song, X., Yu, X., Hori, C., Demura, T., Ohtani, M. and Zhuge, Q. (2016), 'Heterologous overexpression of poplar snrk2 genes enhanced salt stress tolerance in arabidopsis thaliana', *Front Plant Sci* **7**, 612.

Sonjaroon, W., Jutamanee, K., Khamsuk, O., Thussagunpanit, J., Kaveeta, L. and Suksamrarn, A. (2018), 'Impact of brassinosteroid mimic on photosynthesis, carbohydrate content and rice seed set at reproductive stage under heat stress', *Agriculture and Natural Resources* **52**(3), 234–240.

Sonnett, M., Yeung, E. and Wuhr, M. (2018), 'Accurate, sensitive, and precise multiplexed proteomics using the complement reporter ion cluster', *Anal Chem* **90**(8), 5032–5039.

Stadtman, E. R. and Levine, R. L. (2003), 'Free radical-mediated oxidation of free amino acids and amino acid residues in proteins', *Amino Acids* **25**(3-4), 207–218.

Staehelin, L. A. and Arntzen, C. J. (1983), 'Regulation of chloroplast membrane function: protein phosphorylation changes the spatial organization of membrane components', *J Cell Biol* **97**(5 Pt 1), 1327–37.

Stecker, E. K., Minkoff, B. B. and Sussman, M. R. (2014), 'Phosphoproteomic analyses reveal early signaling events in the osmotic stress response', *Plant Physiol* **165**(3), 1171–1187.

Steen, H. and Mann, M. (2004), 'The abc's (and xyz's) of peptide sequencing', *Nat Rev Mol Cell Biol* **5**(9), 699–711.

Stephans, W. E. (1946), 'A pulsed mass spectrometer with time dispersion', *Bull Am Phys Soc* **21**(2), 22.

Stiti, N., Missihoun, T. D., Kotchoni, S. O., Kirch, H. H. and Bartels, D. (2011), 'Aldehyde dehydrogenases in arabidopsis thaliana: Biochemical requirements, metabolic pathways, and functional analysis', *Front Plant Sci* **2**, 65–76.

Sugimoto, H., Kondo, S., Tanaka, T., Imamura, C., Muramoto, N., Hattori, E., Ogawa, K., Mitsukawa, N. and Ohto, C. (2014), 'Overexpression of a novel arabidopsis pp2c isoform, atpp2cf1, enhances plant biomass production by increasing inflorescence stem growth', *J Exp Bot* **65**(18), 5385–400.

Sugiyama, N., Nakagami, H., Mochida, K., Daudi, A., Tomita, M., Shirasu, K. and Ishihama, Y. (2008), 'Large-scale phosphorylation mapping reveals the extent of tyrosine phosphorylation in arabidopsis', *Molecular Systems Biology* **4**(1), 1–7.

Swisher, B. A. and Corbin, F. T. (1982), 'Behavior of bas-9052 oh in soybean (glycine max) and johnsongrass (sorghum halepense) plant and cell cultures', *Weed Science* **30**(6), 640–650.

Syka, J., Coon, J., Schroeder, M., Shabanowitz, J. and Hunt, D. (2004), 'Peptide and protein sequence analysis by electron transfer dissociation mass spectrometry', *Proc Natl Acad Sci U S A* **101**(26), 9528–33.

Talent, J., Kong, Y. and Gracy, R. (1998), 'A double stain for total and oxidized proteins from two-dimensional fingerprints', *Anal Biochem* **263**(1), 31–38.

Tamburino, R., Vitale, M., Ruggiero, A., Sassi, M., Sannino, L., Arena, S., Costa, A., Batelli, G., Zambrano, N., Scaloni, A., Grillo, S. and Scotti, N. (2017), 'Chloroplast proteome response to drought stress and recovery in tomato (solanum lycopersicum l.)', *BMC Plant Biology* **17**(1), 40–54.

Thao, N. P., Khan, M. I., Thu, N. B., Hoang, X. L., Asgher, M., Khan, N. A. and Tran, L. S. (2015), 'Role of ethylene and its cross talk with other signaling molecules in plant responses to heavy metal stress', *Plant Physiol* **169**(1), 73–84.

Thimm, O., Blasing, O., Gibon, Y., Nagel, A., Meyer, S., Kruger, P., Selbig, J., Muller, L. A., Rhee, S. Y. and Stitt, M. (2004), 'Mapman: a user-driven tool to display genomics data sets onto diagrams of metabolic pathways and other biological processes', *Plant J* **37**(6), 914–39.

Thompson, A., Schafer, J., Kuhn, K., Kienle, S., Schwarz, J., Schmidt, G., Neumann, T., Johnstone, R., Mohammed, A. and Hamon, C. (2003), 'Tandem mass tags: A novel quantification strategy for comparative analysis of complex protein mixtures by ms/ms', *Anal Chem* **75**(8), 1895–1904.

Thomson, J. J. (1913), *Rays of positive electricity and their application to chemical analyses*, Vol. 42, Longmans, Green and Co., London.

Ting, L., Rad, R., Gygi, S. P. and Haas, W. (2011), 'Ms3 eliminates ratio distortion in isobaric multiplexed quantitative proteomics', *Nat Methods* **8**(11), 937–40.

Tusher, V. G., Tibshirani, R. and Chu, G. (2001), 'Significance analysis of microarrays applied to the ionizing radiation response', *PNAS* **98**(9), 5116–5121.

Tyanova, S. and Cox, J. (2018), *Perseus: A Bioinformatics Platform for Integrative Analysis of Proteomics Data in Cancer Research*, Springer New York, New York, NY, pp. 133–148.

Tyanova, S., Temu, T., Sinitcyn, P., Carlson, A., Hein, M. Y., Geiger, T., Mann, M. and Cox, J. (2016), 'The perseus computational platform for comprehensive analysis of (prote)omics data', *Nat Methods* **13**(9), 731–40.

Ulintz, P. J., Yocum, A. K., Bodenmiller, B., Aebersold, R., Andrews, P. C. and Nesvizhskii, A. I. (2009), 'Comparison of ms(2)-only, msa, and ms(2)/ms(3) methodologies for phosphopeptide identification', *J Proteome Res* **8**(2), 887–99.

Umezawa, T., Sugiyama, N., Takahashi, F., Anderson, J., Ishihama, Y., Peck, S. and Shinozaki, K. (2013), 'Genetics and phosphoproteomics reveal a protein phosphorylation network in the abscisic acid signaling pathway in arabidopsis thaliana', *Sci Signal* **6**(270), 1–13.

Urban, P. L. (2016), 'Quantitative mass spectrometry: an overview', *Philos Trans A Math Phys Eng Sci* **374**(2079), 1–5.

Usadel, B., Nagel, A., Thimm, O., Redestig, H., Blaesing, O. E., Palacios-Rojas, N., Selbig, J., Hannemann, J., Piques, M. C., Steinhauser, D., Scheible, W. R., Gibon, Y., Morcuende, R., Weicht, D., Meyer, S. and Stitt, M. (2005), 'Extension of the visualization tool mapman to allow statistical analysis of arrays, display of corresponding genes, and comparison with known responses', *Plant Physiol* **138**(3), 1195–204.

van Wijk, K. J., Friso, G., Walther, D. and Schulze, W. X. (2014), 'Meta-analysis of arabidopsis thaliana phospho-proteomics data reveals compartmentalization of phosphorylation motifs', *Plant Cell* **26**(6), 2367–2389.

Verma, S., Nizam, S. and Verma, P. K. (2013), *Biotic and Abiotic Stress Signaling in Plants*, Vol. 1, Springer, New York, book section Chapter 2, pp. 25–49.

Verrastro, I., Pasha, S., Jensen, K. T., Pitt, A. R. and Spickett, C. M. (2015), 'Mass spectrometry-based methods for identifying oxidized proteins in disease: advances and challenges', *Biomolecules* **5**(2), 378–411.

Vitamvas, P., Urban, M. O., Skodacek, Z., Kosova, K., Pitelkova, I., Vitamvas, J., Renaut, J. and Prasil, I. T. (2015), 'Quantitative analysis of proteome extracted from barley crowns grown under different drought conditions', *Front Plant Sci* **6**, 479–497.

Vu, L. D., Stes, E., Van Bel, M., Nelissen, H., Maddelein, D., Inze, D., Coppens, F., Martens, L., Gevaert, K. and De Smet, I. (2016), 'Up-to-date workflow for plant (phospho)proteomics identifies differential drought-responsive phosphorylation events in maize leaves', *J Proteome Res* **15**(12), 4304–4317.

Wagner, V. and Nelson, C. R. (2014), 'Herbicides can negatively affect seed performance in native plants', *Restoration Ecology* **22**(3), 288–291.

Wallace, J. (2000), 'Increasing agricultural water use efficiency to meet future food production', *Agriculture, Ecosystems and Environment* **82**(1-3), 105–119.

Wang, D., Heckathorn, S., Mainali, K. and Tripathee, R. (2016-2), 'Timing effects of heat-stress on plant ecophysiological characteristics and growth', *Front Plant Sci* **7**, 1629–1640.

Wang, D., Portis, A. R., Moose, S. P. and Long, S. P. (2008), 'Cool c4 photosynthesis: Pyruvate pi dikinase expression and activity corresponds to the exceptional cold tolerance of carbon assimilation in miscanthus × giganteus', *Plant Physiology* **148**(1), 557–567.

Wang, N., Zhao, J., He, X., Sun, H., Zhang, G. and Wu, F. (2015), 'Comparative proteomic analysis of drought tolerance in the two contrasting tibetan wild genotypes and cultivated genotype', *BMC Genomics* **16**(1), 432–451.

Wang, P., Xue, L., Batelli, G., Lee, S., Hou, Y. J., Van Oosten, M. J., Zhang, H., Tao, W. A. and Zhu, J. K. (2013-2), 'Quantitative phosphoproteomics identifies snrk2 protein kinase substrates and reveals the effectors of abscisic acid action', *Proc Natl Acad Sci U S A* **110**(27), 11205–10.

Wang, X., Cai, X., Xu, C., Wang, Q. and Dai, S. (2016-1), 'Drought-responsive mechanisms in plant leaves revealed by proteomics', *Int J Mol Sci* **17**(10), 1706–1736.

Wang, X., Pattison, J. S. and Su, H. (2013-1), 'Posttranslational modification and quality control', *Circ Res* **112**(2), 367–81.

Wang, X., Vignjevic, M., Jiang, D., Jacobsen, S. and Wollenweber, B. (2014), 'Improved tolerance to drought stress after anthesis due to priming before anthesis in wheat (triticum aestivum l.) var. vinjett', *J Exp Bot* **65**(22), 6441–56.

Wang, Z., Li, G., Sun, H., Ma, L., Guo, Y., Zhao, Z., Gao, H. and Mei, L. (2018), 'Effects of drought stress on photosynthesis and photosynthetic electron transport chain in young apple tree leaves', *Biol Open* **7**(11), 1–9.

Weber, T. (2010), '2.24 - protein kinases', *Comprehensive Toxicology (Second Edition)* **2**, 473–493.

Wehr, N. B. and Levine, R. L. (2012), 'Quantitation of protein carbonylation by dot blot', *Anal Biochem* **423**(2), 241–5.

Wei, Z., Gao, T., Liang, B., Zhao, Q., Ma, F. and Li, C. (2018), 'Effects of exogenous melatonin on methyl viologen-mediated oxidative stress in apple leaf', *International Journal of Molecular Sciences* **19**(1), 316–330.

White, P. J. and Broadley, M. R. (2003), 'Calcium in plants', *Ann Bot* **92**(4), 487–511.

Wijk, K. J. v. (2001), 'Challenges and prospects of plant proteomics', *Plant Physiol* **126**(2), 501–508.

Wilkins, M. R., Sanchez, J. C., Gooley, A. A., Appel, R. D., Humphery-Smith, I., Hochstrasser, D. F. and Williams, K. L. (1996), 'Progress with proteome projects: why all proteins expressed by a genome should be identified and how to do it', *Biotechnol Genet Eng Rev* **13**, 19–50.

Wilkinson, R. E. (1988), 'Carbamothioates.', *Herbicides – Chemistry, Degradation, and Mode of Action* **3**, 245–300.

Wisniewski, J. R., Zougman, A., Nagaraj, N. and Mann, M. (2009), 'Universal sample preparation method for proteome analysis', *Nat Methods* **6**(5), 359–62.

Wong, C. M., Bansal, G., Marcocci, L. and Suzuki, Y. J. (2012), 'Proposed role of primary protein carbonylation in cell signaling', *Redox Rep* **17**(2), 90–4.

Wu, L., Hu, X., Wang, S., Tian, L., Pang, Y., Han, Z., Wu, L. and Chen, Y. (2015), 'Quantitative analysis of changes in the phosphoproteome of maize induced by the plant hormone salicylic acid', *Sci Rep* **5**(1), 1–16.

Xiang, J., Chen, X., Hu, W., Xiang, Y., Yan, M. and Wang, J. (2018), 'Overexpressing heat-shock protein oshsp50.2 improves drought tolerance in rice', *Plant Cell Reports* **37**(11), 1585–1595.

Xu, J., Tian, Y. S., Xing, X. J., Peng, R. H., Zhu, B., Gao, J. J. and Yao, Q. H. (2016), 'Over-expression of atgstu19 provides tolerance to salt, drought and methyl viologen stresses in arabidopsis', *Physiol Plant* **156**(2), 164–175.

Xu, Y. H., Liu, R., Yan, L., Liu, Z. Q., Jiang, S. C., Shen, Y. Y., Wang, X. F. and Zhang, D. P. (2012), 'Light-harvesting chlorophyll a/b-binding proteins are required for stomatal response to abscisic acid in arabidopsis', *J Exp Bot* **63**(3), 1095–106.

Xue, H. W., Chen, X. and Mei, Y. (2009), 'Function and regulation of phospholipid signalling in plants', *Biochem J* **421**(2), 145–56.

Yan, W., Zheng, S., Zhong, Y. and Shangguan, Z. (2017), 'Contrasting dynamics of leaf potential and gas exchange during progressive drought cycles and recovery in amorpha fruticosa and robinia pseudoacacia', *Sci Rep* **7**(1), 1–12.

Yanagihara, N., Suwa, M. and Mitaku, S. (1989), 'A theoretical method for distinguishing between soluble and membrane proteins', *Biophysical Chemistry* **34**(1), 69–77.

Yang, F., Jorgensen, A. D., Li, H., Sondergaard, I., Finnie, C., Svensson, B., Jiang, D., Wollenweber, B. and Jacobsen, S. (2011), 'Implications of high-temperature events and water deficits on protein profiles in wheat (triticum aestivum l. cv. vinjett) grain', *Proteomics* **11**(9), 1684–95.

Yang, F., Melo-Braga, M. N., Larsen, M. R., Jorgensen, H. J. and Palmisano, G. (2013), 'Battle through signaling between wheat and the fungal pathogen septoria tritici revealed by proteomics and phosphoproteomics', *Mol Cell Proteomics* **12**(9), 2497–508.

Yang, L., Jiang, T., Fountain, J. C., Scully, B. T., Lee, R. D., Kemerait, R. C., Chen, S. and Guo, B. (2014), 'Protein profiles reveal diverse responsive signaling pathways in kernels of two maize inbred lines with contrasting drought sensitivity', *Int J Mol Sci* **15**(10), 18892–918.

Yoo, B. S. and Regnier, F. E. (2004), 'Proteomic analysis of carbonylated proteins in two-dimensional gel electrophoresis using avidin-fluorescein affinity staining', *Electrophoresis* **25**(9), 1334–41.

Yoo, Y. H., Hong, W. J. and Jung, K. H. (2019), 'A systematic view exploring the role of chloroplasts in plant abiotic stress responses', *Biomed Res Int* **2019**, 1–14.

Yost, R. A. and Enke, C. G. (1978), 'Selected ion fragmentation with a tandem quadrupole mass spectrometer', *J. Am. Chem. Soc.* **100**(7), 2274–2275.

Yuan, F., Yang, H., Xue, Y., Kong, D., Ye, R., Li, C., Zhang, J., Theprungsirikul, L., Shrift, T., Krichilsky, B., Johnson, D. M., Swift, G. B., He, Y., Siedow, J. N. and Pei, Z. M. (2014), 'Osca1 mediates osmotic-stress-evoked ca2+ increases vital for osmosensing in arabidopsis', *Nature* **514**(7522), 367–71.

Zhao, F., Zhang, D., Zhao, Y., Wang, W., Yang, H., Tai, F., Li, C. and Hu, X. (2016-2), 'The difference of physiological and proteomic changes in maize leaves adaptation to drought, heat, and combined both stresses', *Front Plant Sci* **7**, 1471.

Zhao, Y., Wang, Y., Yang, H., Wang, W., Wu, J. and Hu, X. (2016-1), 'Quantitative proteomic analyses identify aba-related proteins and signal pathways in maize leaves under drought conditions', *Front Plant Sci* **7**, 1827–1850.

Zhu, J. K. (2002), 'Salt and drought stress signal transduction in plants', *Annu Rev Plant Biol* **53**, 247–73.

Zhu, J. K. (2016), 'Abiotic stress signaling and responses in plants', *Cell* **167**(2), 313–324.

Zhu, W., Smith, J. W. and Huang, C. M. (2009), 'Mass spectrometry-based label-free quantitative proteomics', *BioMed Research International* **2010**, 1–6.

Zimmermann, R. and Werr, W. (2005), 'Pattern formation in the monocot embryo as revealed by nam and cuc3 orthologues from zea mays l', *Plant Mol Biol* **58**(5), 669–85.